Department of Neurology
Faculty2: Medicine Clinical Medicine
Saarland University Medical Center, Homburg/Saar

Modulation of Alzheimer's Disease Brain Pathology in Mice by Gut Bacterial Deletion: The Role of IL-17a

Dissertation for the degree of
Doctor of Medicine and Natural Sciences (MD/PhD)
Faculty of Medicine

SAARLAND UNIVERSITY

2025

Submitted by Wenlin Hao
Born in August 1975 in Beijing, P. R. China

Aus der Klinik für Neurologie
Klinische Medizin der Medizinischen Fakultät
Universitätsklinikum des Saarlandes (UKS), Homburg/Saar

Modulation der Pathologie im Mausgehirn des Alzheimer-Krankheitsmodells durch Depletion der Darmbakteria: Die Rolle des IL-17a

Dissertation zur Erlangung des Grades eines
Doktors der Medizin und der Naturwissenschaften (MD/PhD)
der Medizinischen Fakultät

der UNIVERSITÄT DES SAARLANDES

2025

vorgelegt von Wenlin Hao
Geb. im August 1975 in Beijing, V. R. China

To

Alex

Declaration

I hereby declare that this thesis is my own original work and effort. All experiments, except for those specified, were exclusively performed by me. Except for the publications written by myself listed in the publication list, the data presented here have not been submitted anywhere else for any award. Where other sources of information and help have been used, they have been indicated and acknowledged.

Homburg/Saar,

_____

Wenlin Hao

ABBREVIATIONS

% (v/v)	Volume/volume percentage solution
% (w/v)	Weight/volume percentage solution
ABC	ATP-binding cassette
ABCB	ATP Binding Cassette Subfamily B Member
AD	Alzheimer's disease
ADEs	amyloid-degrading enzymes
AMP	antimicrobial peptide
APOE	Apolipoprotein E
APP	Amyloid precursor protein
AQP4	Aquaporin 4
AVs	autophagic vacuoles
Aβ	Amyloid β-peptide
BACE-1	B-site APP-cleaving enzyme
BBB	Blood-brain barrier
BCSFB	blood cerebrospinal fluid barrier
BDNF	Brain-derived neurotrophic factor
BSA	Bovine serum albumin
CAA	cerebral amyloid angiopathy
CD	Cluster of differentiation
CNS	Central nervous system
COVID-19	Coronavirus disease 2019
CSF	Cerebrospinal fluid
CSF1R	colony stimulating factor 1 receptor
Ct	Threshold cycle
CTF	C-terminal fragment
CTLA8	cytotoxic T lymphocyte-associated antigen 8
CX3CL1	C-X3-C Motif Chemokine Ligand 1
CX3CR1	C-X3-C Motif Chemokine Receptor 1
DAM	Disease-associated microglia
DAPI	4',6-diamidino-2-phenylindole
DMSO	Dimethyl sulfoxide
DNA	Deoxyribonucleic acid
dsDNA	Double-strand deoxyribonucleic acid
dsRNA	Double-strand ribonucleic acid
DTT	Dithiothreitol
e.g.	*Exempli gratia*, for example
EAE	Experimental autoimmune Encephalomyelitis
EDTA	Ethylenediaminetetraacetic acid
ELISA	Enzyme-linked immunosorbent assay
ELN	Endosomal-lysosomal Network
EOAD	Early-onset Alzheimer's disease
ETEC	Enterotoxigenic *Escherichia coli*
FAD	Familial AD
FBS	Fetal bovine serum
FSC	Forward-scatter
g	Gram
G	*Gravity*
GABA	Gamma-aminobutyric acid
Gau-HCl	Guanidine chloride buffer

GF	Germ-free
GFP	Green fluorescence protein
GI	gastrointestinal
GPCRs	G protein-coupled receptors
GPER	G protein-coupled estrogen receptor
H_2O_2	Hydrogen peroxide
HBSS	Hanks Balanced Salt Solution
HBV	hepatitis B virus
HEPES	N-2-Hydroxyethylpiperazine-N-2-Ethane Sulfonic Acid
HRP	Horseradish Peroxidase
Iba1	Ionized calcium-binding adaptor molecule 1
IDE	Insulin-degrading enzyme
IF	Immunofluorescence
IFN	Interferon
IGF	Insulin-like growth factor
IgG	Immunoglobulin G
IL	Interleukin
ILC	innate lymphocytes
iNKT	invariant natural killer T
iNOS	Inducible nitric oxide synthase
IRF	Interferon regulatory factor
IPAD	intramural periarterial drainage
ISF	Interstitial fluid
kb	Kilo base pairs
KBs	Ketone bodies
kDa	Kilodalton
KO/ko	Knockout
LANDO	LC3-associated endocytosis
LOAD	Late-onset Alzheimer's disease
LPS	Lipopolysaccharide
LRP1	Low-density lipoprotein-related protein 1
M	Molar/L
MAPK	Mitogen-activated protein kinase
MCI	Mild cognitive impairment
MeXO4	Methoxy-XO4
mFI	Mean fluorescence intensity
Min	Minute
MMP	Matrix-Metalloproteinase
MyD88	Myeloid differentiation primary response 88
NEP	Neprilysin
O.D.	Optical density
PAGE	Polyacrylamide gel electrophoresis
PBS	Phosphate-Buffered Saline
PCR	Polymerase chain reaction
PFA	Paraformaldehyde
PVC	Polyvinyl chloride
PVDF	Polyvinylidene difluoride
RNA	Ribonucleic acid
RNA-seq	Single-cell RNA sequencing
ROS	Reactive oxygen
rpm	Revolutions per minute
RPMI	Roswell Park Memorial Institute
RT-RCR	Real-time reverse transcription polymerase chain reaction

s	Second
sAPPα	Soluble ectodomain of APP
sAPPβ	Soluble APPβ fragment
SCFA	Short chain fatty acid
SDS	Sodium dodecyl sulfate
SFB	*Segmented filamentous bacteria*
SEM	Standard Error of Mean
sLRP1	Soluble low-density lipoprotein-related protein 1
SPF	Specific pathogen-free
SSC	Side-scatter
TBS	Tris buffer with salt
TCR	T-cell receptor
TEMED	N, N, N′, N′-Tetramethyl ethylenediamine
TGFβ	Transforming growth factor β
TLR	Toll-like receptor
TNF	Tumor necrosis factor
TREM2	Triggering receptors expressed on myeloid cells 2
Tris	Tris(hydroxymethyl)aminomethane
U	Unit
UPS	Ubiquitin-proteasome system
V	Volt
WB	Western blot
WT/wt	Wildtype
α2M	α2-Macroglobulin

CONTENT

1 ABSTRACT

Alzheimer's disease (AD) is the most common cause of dementia in the elderly. It is pathologically characterised by extracellular deposition of amyloid-β peptides (Aβ), intracellular neurofibrillary tangles primarily composed of hyperphosphorylated tau protein, and microglial activation in the brain parenchyma. Recent studies have also shown that the composition of bacteria in the gut of AD patients and animals changes in correlation with inflammatory status in the blood and the severity of AD pathology in the brain; however, the molecular mechanisms mediating the pathogenic effects of gut bacteria in AD remains unclear.

Interleukin-17a (IL-17a) is an important cytokine in the gut, which interacts with gut bacteria and protects the host from microbial invasion under physiological conditions; however, dysregulation of IL-17a may also lead to inflammatory disorders in the host by pathological conditions, for example, multiple sclerosis. Our previous study has indicated that IL-17a expression increases in CD4-positive spleen cells in APP-transgenic mice. We hypothesize that IL-17a mediates the effects of gut bacteria on AD pathology in AD mice.

We crossed APP-transgenic mice with *Il-17a*-knockout mice to create IL-17a-deficient and wild-type AD models. Three-month-old APP-transgenic female mice with different expression of IL-17a were depleted or not of intestinal bacteria by drinking antibiotics-supplemented or normal water for two months. The gut microbiome was analysed by sequencing the bacterial 16S DNA V3-V4 regions, the amount of bacterial DNA in the brain tissue was detected by real-time PCR, and IL-17a-expressing T lymphocytes in the gut were quantified by flow cytometry and in the spleen by quantitative RT-PCR. AD-associated pathologies, i.e., neuroinflammation, Aβ pathology, and neurodegeneration, were investigated by immunohistochemistry, ELISA, Western blot and molecular biology approaches. To further investigate the pathogenic mechanisms, microglial morphology, microglial transcription of disease-associated microglia signature genes, microglial phagocytosis of Aβ, β- and γ-secretase activity, transcription of Aβ-degrading enzyme

genes *Neprilysin* and *Insulin-degrading enzyme*, and protein levels of Aβ-transporting proteins LRP1 and ABCB1 in the isolated capillaries, were determined.

We have obtained the following major results:

1) The antibiotic treatment eradicated almost all intestinal bacteria, and led to a reduction in bacterial DNA in the brain tissues of both IL-17a-deficient and wild-type APP-transgenic mice;
2) Depletion of gut bacteria reduced IL-17a-expressing CD4-positive T lymphocytes in the spleen and gut in APP-transgenic mice;
3) Depletion of gut bacteria inhibited inflammatory activation in both brain tissue and individual microglia, which were reversed by knockout of *Il-17a* gene;
4) Depletion of gut bacteria decreased Aβ levels in IL-17a wild-type, but not IL-17a-deficient APP-transgenic mice;
5) Depletion of gut bacteria promoted transcription of *Arc* gene in the brain of IL-17a wild-type, but not IL-17a-deficient APP-transgenic mice. Arc expression is associated with the improvement of cognitive function.

To further identify possible mechanisms, through which depletion of gut bacteria regulates Aβ pathology, we have the following findings:

1) Depletion of gut bacteria inhibited the β-secretase activity in the brain of IL-17a wild-type, but not IL-17a-deficient APP-transgenic mice, which potentially led to reduced Aβ production;
2) Depletion of gut bacteria increased the expression of ABCB1 and LRP1 in the brain or at the BBB of IL-17a wild-type, but not IL-17a-deficient APP-transgenic mice. ABCB1 and LRP1 are responsible for the Aβ efflux through the blood-brain barrier;
3) Interestingly, knockout of *Il-17a* gene already increased ABCB1 and LRP1 expression at the blood-brain barrier;
4) Depletion of gut bacteria did not increase microglial Aβ phagocytosis and extracellular Aβ degradation in the brain of APP-transgenic mice.

In conclusion, depletion of gut bacteria attenuates inflammatory activation and amyloid pathology in APP-transgenic mice via IL-17a-involved signalling pathways. Our study

contributes to a better understanding of the gut-brain axis in AD pathophysiology and highlights the therapeutic potential of IL-17a inhibition or specific depletion of gut bacteria that stimulate the development of IL-17a-expressing T cells.

2 ZUSAMMENFASSUNG

Die Alzheimer-Krankheit (AD) ist die häufigste Ursache für Demenz bei älteren Menschen. Sie ist pathologisch gekennzeichnet durch extrazelluläre Ablagerungen von Amyloid-β-Peptiden (Aβ), intrazelluläre neurofibrilläre Tangles, die hauptsächlich aus hyperphosphoryliertem Tau-Protein bestehen, und mikrogliale Aktivierung im Gehirnparenchym. Jüngste Studien haben auch gezeigt, dass sich die Zusammensetzung der Bakterien im Darm von AD-Patienten und Tieren in Korrelation mit dem Entzündungsstatus im Blut und dem Schweregrad der Alzheimer-Pathologie im Gehirn verändert; die molekularen Mechanismen, die die pathogenen Wirkungen der Darmbakterien bei AD vermitteln, sind jedoch noch unklar.

Interleukin-17a (IL-17a) ist ein wichtiges Zytokin im Darm, das mit Darmbakterien interagiert und den Host unter physiologischen Bedingungen vor mikrobieller Invasion schützt; eine Dysregulation von IL-17a kann jedoch auch zu entzündlichen Störungen im Host unter pathologischen Bedingungen führen, z. B. bei Multipler Sklerose. Unsere frühere Studie hat gezeigt, dass die Expression von IL-17a in CD4-positiven Milzzellen bei APP-transgenen Mäusen zunimmt. Wir stellen die Hypothese auf, dass IL-17a die Auswirkungen von Darmbakterien auf die AD-Pathologie in AD-Mäusen vermittelt.

Wir kreuzten APP-transgene Mäuse mit *Il-17a*-Knockout-Mäusen, um IL-17a-defiziente und Wildtyp-AD-Modelle zu schaffen. Drei Monate alten APP-transgenen weiblichen Darmbakterien in Mäusen mit unterschiedlicher Expression von IL-17a wurden zwei Monate lang durch das Trinken von mit Antibiotika angereichertem oder normalem Wasser entzogen oder nicht. Das Darmmikrobiom wurde durch Sequenzierung der bakteriellen 16S-DNA-V3-V4-Regionen analysiert, die Menge der bakteriellen DNA im Hirngewebe wurde durch Realtime-PCR nachgewiesen, und IL-17a-exprimierende T-Lymphozyten im Darm wurden durch Durchflusszytometrie und in der Milz durch quantitative Realtime-PCR quantifiziert. AD-assoziierte Pathologien, d. h. Neuroinflammation, Aβ-Pathologie und Neurodegeneration, wurden durch Immunhistochemie, ELISA, Western Blot und molekularbiologische Ansätze untersucht. Um die pathogenen Mechanismen weiter zu untersuchen, wurden die Mikroglia-

Morphologie, die mikrogliale Transkription von krankheitsassoziierten Mikroglia-Signaturgenen, die mikrogliale Phagozytose von Aβ, die β- und γ-Sekretaseaktivität, die Transkription der Aβ-abbauenden Enzymgene *Neprilysin* und *Insulin-abbauendes Enzym* sowie die Proteinkonzentrationen der Aβ-transportierenden Proteine LRP1 und ABCB1 in den isolierten Kapillaren bestimmt.

Wir haben die folgenden wichtigen Ergebnisse erzielt:

1) Die Antibiotikabehandlung löschte fast alle Darmbakterien aus, was zu einer Verringerung der bakteriellen DNA im Gehirngewebe sowohl von IL-17a-defizienten als auch von Wildtyp-APP-transgenen Mäusen führte;
2) Die Depletion von Darmbakterien reduzierte die IL-17a-exprimierenden CD4-positiven T-Lymphozyten in Milz und Darm von APP-transgenen Mäusen;
3) Die Depletion von Darmbakterien hemmte die entzündliche Aktivierung sowohl im Hirngewebe als auch in einzelnen Mikroglia, was durch Knockout des *Il-17a-Gens* umgekehrt wurde;
4) Die Depletion von Darmbakterien verringerte den Aβ-Spiegel in IL-17a-Wildtyp-Mäusen, aber nicht in IL-17a-defizienten APP-transgenen Mäusen;
5) Die Depletion von Darmbakterien förderte die Transkription des *Arc-Gens* im Gehirn von IL-17a-Wildtyp-, aber nicht von IL-17a-defizienten APP-transgenen Mäusen. Die Arc-Expression wird mit der Verbesserung der kognitiven Funktion in Verbindung gebracht.

Zur weiteren Identifizierung möglicher Mechanismen, durch die die Depletion von Darmbakterien die Aβ-Pathologie reguliert, haben wir die folgenden Ergebnisse:

1) Die Depletion von Darmbakterien hemmte die β-Sekretase-Aktivität im Gehirn von IL-17a-Wildtyp-, aber nicht von IL-17a-defizienten APP-transgenen Mäusen, was möglicherweise zu einer verringerten Aβ-Produktion führte;
2) Die Depletion von Darmbakterien erhöhte die Expression von ABCB1 und LRP1 im Gehirn oder an der BHS von IL-17a-Wildtyp-, aber nicht IL-17a-defizienten APP-transgenen Mäusen. ABCB1 und LRP1 sind für den Aβ-Efflux durch die Blut-Hirn-Schranke verantwortlich;
3) Interessanterweise erhöhte bereits der Knockout des *Il-17a-Gens* die ABCB1- und LRP1-Expression an der Blut-Hirn-Schranke;

4) Die Depletion von Darmbakterien erhöhte nicht die mikrogliale Aβ-Phagozytose und den extrazellulären Aβ-Abbau im Gehirn von APP-transgenen Mäusen.

Zusammenfassend lässt sich sagen, dass die Depletion von Darmbakterien die entzündliche Aktivierung und die Amyloid-Pathologie in APP-transgenen Mäusen über IL-17a-beteiligte Signalwege abschwächt. Unsere Studie trägt zu einem besseren Verständnis der Darm-Hirn-Achse in der Pathophysiologie der Alzheimer-Krankheit bei und unterstreicht das therapeutische Potenzial einer IL-17a-Hemmung oder einer spezifischen Depletion von Darmbakterien, die die Entwicklung von IL-17a-exprimierenden T-Zellen stimulieren.

3 INTRODUCTION

3.1 Alzheimer's Disease

3.1.1 Epidemiology of Alzheimer's disease

Alzheimer's disease (AD) is the most prevalent dementia described by short-term memory loss, language and orientation confusion, mood alteration, motivation loss, and self-care and behavioral issues (Fabi 2024). AD affects more than 27 million people and accounts for 60–70% of all dementia cases (Silva, Loures et al. 2019). The 2024 report from the Alzheimer's Association estimated that 6.9 million adults > 65 years in the US are currently living with AD. Modeling studies predict that this number will double by 2050 (Parums 2024). In a European, memory clinic-based cohort, median survival time was 6 years after a diagnosis of AD dementia (median 6.2 years [range 6·0–6·5]) (Scheltens, De Strooper et al. 2021). The strongest risk factors for AD are advanced age (older than 65 years, although this is not a fixed definition) and carrying at least one APOE ε4 allele. Moreover, women are more likely to develop AD than are men, especially after the age of 80 years (Scheltens, De Strooper et al. 2021).

3.1.2 Pathophysiology of AD

The pathology of canonical AD dementia involves Aβ-containing extracellular senile plaques that are found in a widespread distribution throughout the cerebral cortex and tau-containing neurofibrillary tangles that occur initially in the medial temporal lobe, followed by the isocortical regions of the temporal, parietal and frontal lobes (Knopman, Amieva et al. 2021).

Aβ is a 40-42 amino acid peptide (~4 kDa) derived from the sequential proteolytic cleavage of the amyloid precursor protein (APP) (Haass and Selkoe 2007). APP is available in a variety of sizes ranging from 677 to 770 amino acids, with APP695 being the most abundant in the brain und mainly generated by neurons. APP family members have important physiological functions in the peripheral and central nervous systems (Muller, Deller et al. 2017). There are two major processing pathways of APP degradation: nonamyloidogenic und amyloidogenic pathways. In the nonamyloidogenic

pathway α-secretase cleaves APP at the cell surface, releasing soluble ectodomain of APP (sAPP-α) and a membrane-retained C-terminal fragment (CTF-α). The resulting CTF-α is also cleaved by γ-secretase to produce a truncated version of Aβ called p3 (Haass and Willem 2019). These fragments do not form oligomers and appear to be benign. Some of them may even have neuropretective effects (Haass and Willem 2019). In contrast, through the amyloidogenic processing APP is first cleaved by β-secretase within its ectodomain. This releases sAPP-β and generates CTF-β. CTF-β is then cleaved by γ-secretase, which finally releases Aβ into the extracellular space as a monomer (Thinakaran and Koo 2008). Owing to its sequence, Aβ (particularly Aβ 42) has a high propensity to aggregate, which occurs in a concentration-dependent manner (Knopman, Amieva et al. 2021). Only aggregated or oligomeric Aβ, but not the monomeric Aβ, is neurotoxic and causes neuronal hyperactivity within the neighborhood of amyloid plaques (Busche, Eichhoff et al. 2008). Following reports of weak associations between senile plaque counts and cognitive impairment in AD patients and the finding that Aβ oligomers rather than fibrillar Aβ may be the most neurotoxic Aβ conformation, the hypothesis was revised to suggest that Aβ oligomers may initiate AD pathology (Loeffler 2024).

Synaptic loss is strongly correlated with cognition in patients with AD (DeKosky and Scheff 1990). Aβ plaques are surrounded by a ring of soluble oligomeric Aβ and decreased synaptic content that extends for ~50 μm, marked by both a loss of presynaptic and postsynaptic markers; given the large number of cortical plaques in patients with AD, this amounts to a substantial number of lost synapses. Moreover, in animal models of plaque deposition in which there is little neuronal loss, an additional 25% loss of synaptic content in the neuropil between plaques can be observed; it is likely that a similar phenomenon occurs in humans. These data suggest a strong interaction between the oligomeric Aβ species thought to surround plaques and the neuropil and synaptic toxicity (Spires, Meyer-Luehmann et al. 2005, Spires-Jones and Hyman 2014, Arbel-Ornath, Hudry et al. 2017).

3.1.3 Aβ clearance mechanisms

Aβ concentrations are increased in the brain in both early onset and late onset AD. In early onset AD (EOAD), cerebral Aβ production is increased and its clearance is decreased (Loeffler 2024). In late-onset AD (LOAD), which accounts for 90– 95% of AD cases, the increase in cerebral Aβ has been attributed to impaired removal of Aβ (Loeffler 2024). Aβ is cleared from the brain by extracellular enzyme-mediated degradation and the intracellular degredation through the endosomal-lysosomal system, the ubiquitin-proteasome system, and autophagy (Ji, Cheng et al. 2018). Additional mechanisms through which soluble Aβ can leave the brain include its efflux across the blood brain barrier (BBB) and blood cerebrospinal fluid (CSF) barrier (BCSFB), glymphatic drainage, and intramural periarterial drainage (IPAD) (Loeffler 2024).

3.1.3.1 Extracellular enzyme-mediated degradation

Aβ is degredated extracellular by secreted or membrane-bound proteases. More than 20 enzymes possessing Aβ-degrading ability have been reported (Nalivaeva, Belyaev et al. 2014). Among the amyloid-degrading enzymes (ADEs), neprilysin (NEP) and insulin-degrading enzyme (IDE) are the most studied proteases.

One of the first ADEs in the brain to be identified was a cell-surface, zinc metallopeptidase now known as NEP. The major activity of the enzyme degrading both Aβ40 and Aβ42 in the brain was shown by examining Aβ degradation in NEP-deficient mice and through the use of potent NEP inhibitors such as thiorphan (Iwata, Tsubuki et al. 2001, Shirotani, Tsubuki et al. 2001). Viral gene delivery of NEP to the brain of AD transgenic mice also was shown to reduce amyloid pathology (Marr, Rockenstein et al. 2003). Functional profiling of several ADEs in elderly and AD patients' brains has provided additional support for NEP as the major protease involved in Aβ degradation (Wang, Wang et al. 2010). NEP expression are altered in mild cognitive impairment (MCI) subjects relative to non-impaired subjects in AD-susceptible regions (Huang, Hafez et al. 2012). Reduced NEP mRNA levels were reported in the hippocampus and temporal gyrus of AD patients suggesting a relationship between NEP activity and deficient degradation of Aβ peptide leading to high number of senile plaques in these brain areas (Yasojima, Akiyama et al. 2001). Studies on rat brain demonstrated that NEP

mRNA and protein levels in the cortex and hippocampus significantly declined with age and was being the highest in the first month of animal life when development of the nervous system and its neuronal networks was the most active. On the contrary, in the striatum, which is less affected by plaque pathology, NEP expression remained at a relatively high level during advanced age (Nalivaevaa, Fisk et al. 2004, Nalivaeva, Belyaev et al. 2012).

Another zinc metallopeptidase, insulin- degrading enzyme (IDE), also plays a significant role in Aβ degradation in the brain. The secreted IDE is functional in extracellular Aβ degradation and it appears to be routed via detergent-resistant membrane complexes into exosomes for secretion, along with Aβ (Bulloj, Leal et al. 2010). Similarly to NEP, reduced IDE levels were reported in the hippocampus of AD patients bearing the APOE-ε4 allele (Cook, Leverenz et al. 2003). It was also shown that IDE declined with age in human cortex and hippocampus and was more oxidized in the hippocampus of AD patients compared to the cerebellum (Caccamo, Oddo et al. 2005). The McGill-Thyl-APP transgenic mouse model of AD demonstrated significant down-regulation of IDE at the preclinical early stage of AD pathology (Ferretti et al., 2011). Partial loss-of-function mutation of the IDE gene in vivo impaired neuronal regulation of Aβ and increased Aβ levels (Farris, Mansourian et al. 2004). Overexpression of IDE in neurons significnatly reduced brain Aβ levels and retarded amyloid plaque accumulations in APP transgenic mice (Leissring, Farris et al. 2003).

3.1.3.2 Intracellular degradation

Cells utilize different degradation strategies, including the ubiquitin–proteasome system (UPS), autophagy, and the endosomal–lysosomal system (ELS), to prevent the accumulation of misfolded or abnormal proteins, and to create a dynamic balance between protein clearance and renewal or production. Dysfunction in these degradation systems results in the accumulation of protein aggregates, which cause cellular dysfunction, cognitive impairments, and cell death in the brain. Studies have suggested that accumulation of Aβ in the AD brain results from a dysfunction in these cellular clearance systems (Ji, Cheng et al. 2018).

The ubiquitin- proteasome system (UPS) degrades unwanted or damaged proteins in the cytoplasm. Ubiquitination first acts as a signal for protein degradation, mediated by three different enzymes: the ubiquitin-activating enzyme (E1), the ubiquitin-conjugating enzyme (E2), and the ubiquitin-ligase enzyme (E3). Then ubiquitin-tagged proteins are directed to the 26S proteasome for degradation (Zhang, Li et al. 2023). In the AD brain the activity of the proteasome was significantly decreased in hippocampal gyrus, superior and middel temporal gyri, and interior parietal lobe (Keller, Hanni et al. 2000, Zhang, Chen et al. 2017). Several studies have also shown that Aβ oligomers impair proteasome activity and impede the function of the UPS (Tseng, Green et al. 2008).

Autophagy is essential for the removel of larger proteins and aggregates, and typically proteins with long half-lives (>10 h) (Chung, Hernandez et al. 2019). One prominent feature of AD is neuronal loss accompanied by the presence of autophagic vacuoles (AVs) within neuronal processes, including in synaptic regions. AVs have been observed in human AD brains and in transgenic mice expressing mutant P301L Tau and are considered as late-stage autophagic remnants, suggesting an impaired autophagic pathway at the lysosomal degradation stage. Further, the expression of crucial autophagy protein Beclin-1 declines in the brain of AD patients (Caponio, Veverova et al. 2022). Genetic ablation of mTOR in Tg2576 mice promoted autophagy and rescued memory deficits (Caccamo, De Pinto et al. 2014).

The endosomal–lysosomal network (ELN) is involved in memory and cognition in the context of normal brain health. Aβ and the CTF-β peptide arising from the β-secretase cleavage of APP are generated mainly within endosomes, which are the first neuronal organelles known to exhibit AD-specific neuropathology. Lysosomes are the principal sites for the clearance of intracellular Aβ and CTF-β. In AD, Aβ and CTF-β accumulate abnormally in ELN compartments. Furthermore, APOE ε4 carriage has allele-specific effects at every ELN level, from accelerating and accentuating endosome dysfunction and impeding exosome release131 to causing lysosomal expansion and lysosomal membrane permeabilization (Knopman, Amieva et al. 2021).

3.1.3.3 Aβ efflux through BBB, BCSFB, glymphatic drainage, and IPAD

The BBB consists of capillary endothelial cells separated by tight junctions, adherens junctions, and gap junctions (Stamatovic, Johnson et al. 2016). The BBB is supported by astrocytes, pericytes, and extracellular matrix components (Loeffler 2024). The percentage of Aβ cleared by the BBB was estimated by Qosa et al. to be 62% (Qosa, Abuasal et al. 2014) and by Goulay et al. to be 85% (Goulay, Mena Romo et al. 2020). In AD, BBB clearance of Aβ is decreased by approximately 30% (Krohn, Lange et al. 2011). The length and conformation of Aβ influence its BBB clearance. Aβ 42 is cleared via the BBB more slowly than Aβ 40 (Bell, Sagare et al. 2007) and BBB clearance of aggregated Aβ has been suggested to be less effective than clearance of monomeric Aβ (Ito, Ohtsuki et al. 2007). Low-density lipoprotein receptor-related protein 1 (LRP1) and ATP-binding cassette sub-family B member 1 (ABCB1, also known as P-glycoprotein 1) have been suggested to be key transporters in BBB clearance of cerebral Aβ (Storck, Hartz et al. 2018). LRP1 is expressed on the abluminal surface of the BBB while ABCB1 is expressed on its luminal surface. The expression of these transporters on the BBB decreases during normal aging (Osgood, Miller et al. 2017) and AD (Kang, Pietrzik et al. 2000, Wijesuriya, Bullock et al. 2010).

The term BCSFB (blood-CSF-barrier) refers to the barrier posed by the tight junctions between choroid epithelial cells to passage of solutes between CSF and blood (Loeffler 2024). The choroid plexus is a major component of the BCSFB (Redzic, Preston et al. 2005). The choroid plexus has an extensive capacity for taking up Aβ from CSF (Crossgrove, Li et al. 2005). Active transfer of Aβ between CSF and peripheral blood occurs in both directions across the choroid plexus, although movement of Aβ from CSF to peripheral blood predominates (Crossgrove, Li et al. 2005). Impaired functioning of the choroid plexus was suggested to be an early pathogenic event in late onset AD, possibly preceding deposition of cerebral Aβ (Krzyzanowska and Carro 2012). The age-related structural changes in the BCSFB are exacerbated in AD (Serot, Bene et al. 2000). Functional changes in the BCSFB also occur in AD, e.g. increases of pro-inflammatory gene expression (Kant, Stopa et al. 2018) and decreases of CSF production (Fishman 2002). CSF turnover is also reduced to about 40% (Silverberg, Mayo et al. 2003), which

may contribute to the development of AD due to slower clearance of cerebral waste products (Damkier, Brown et al. 2013).

The glymphatic System, in reference to glial-associated lymphatic drainage, was first in 2012 from Iliff et al. described als a pathway for cerebral clearance of Aβ and other solutes via the paravascular space (Iliff, Wang et al. 2012). In the glymphatic system, CSF enters the brain through para-arterial spaces (Rennels, Gregory et al. 1985). After mixing with the brain interstitial fluid (ISF) CSF leaves the brain through paravenous spaces (Iliff, Wang et al. 2012). Movement of CSF from the subarachnoid space into the brain, as well as efflux of ISF from the brain, has been suggested to be driven by bulk flow rather than diffusion (Loeffler 2024). Iliff et al. observed that cerebral clearance of radiolabeled Aβ 40, after its intrastrial injection, was decreased by 55% in mice lacking the water channel protein aquaporin-4 (AQP4) compared to its clearance in wildtype mice (Iliff, Wang et al. 2012). This finding suggested that drainage via the paravascular space may play an important role in Aβ clearance from the brain. Altered AQP4 expression and localization in reactive astrocytes under neuropathological conditions may contribute to deranged interstitial bulk flow and a resulting failure in the clearance of neurotoxic solutes such as Aβ (Hamby and Sofroniew 2010, Iliff, Wang et al. 2012). Notably, reduction in glymphatic drainage of Aβ in APP/PS1 mouse model of AD was detected in 3-4-month old mice, prior to the development of extensive Aβ pathology (Loeffler 2024).

Through the IPAD the drainage of solutes from brain parenchyma occurrs along basement membranes of capillaries and arteries und in the opposite direction to the flow of blood (Carare, Bernardes-Silva et al. 2008). The solutes draining from the brain is emptied into cervical lymph nodes via dural lymphatic vessels (Aspelund, Antila et al. 2015). Studies in mice with intracerebrally injected Aβ have shown that its drainage follows the same pattern as tracer dyes (Morris, Carare et al. 2014). A similar pattern of deposition of Aβ along cerebral arteries and capillaries is found in cerebral amyloid angiopathy (CAA), reflecting failure of Aβ to be cleared from these vessels (Preston, Steart et al. 2003, Morris, Carare et al. 2014). Blockage of lymphatic drainage of ISF and solutes from the brain by CAA may result in loss of homeostasis of the neuronal environment that may contribute to neuronal malfunction and dementia (Weller, Djuanda et al. 2009).

3.2 Microglia

Microglia are innate immune cells in the central nervous system (CNS) und are essential in maintainung neural health and homeostasis. They play an important role in the early brain development, synaptic prunning and responding to injury or disease.

3.2.1 Microgia physiology

Microglia are derived from the yolk sac myeloid precursors, which are then transported to the embryonic head with blood flow and later migrate to the developing brain using specific matrix metalloproteinases (Kierdorf, Erny et al. 2013). Maintenance of the microglial population following this migration is mostly independent of bone marrow-produced circulating monocytes and relies on the self-renewal of microglia. Similarly to other tissue-resident macrophages, microglial populations are replenished exclusively from brain-resident cells through an IL-1α-dependent pathway (Bruttger, Karram et al. 2015).

Microglial activity is believed to synchronize with the development, maturation and senescence of the CNS throughout life via the adoption of different regulatory networks and has important roles in developmental synaptic pruning, neuronal apoptosis, maintenance of synaptic plasticity and immune surveillance (Salter and Stevens 2017, Leng and Edison 2021).

Microglia have highly dynamic processes and continually survey their local environment. It is estimated that resident microglia scan the entire volume of the brain over the course of a few hours, suggesting that they have homeostatic functions in the healthy brain. The fine processes of microglia continuously contact neurons, axons, and dendritic spines. Moreover, process motility can change dramatically in response to extracellular stimuli, including neuronal activity and neurotransmitters (Salter and Stevens 2017). In the presence of an endogenous or exogenous pathological insult, classes of microglial surface receptors, termed damage-associated molecular patterns and pathogen-associated molecular patterns, can recognize pathogens, cell debris or abnormal proteins (including Aβ species) and induce a microglial response (Leng and Edison 2021). Activated microglia internalize the pathogenic species via pinocytosis, phagocytosis or receptor-

mediated endocytosis and try to degrade them through various endocytic pathways as well as by activating the expression of relevant gene modules, including chemokine receptors and interferons, which are major components of the neuroinflammatory process (Leng and Edison 2021).

Numerous studies suggest that microglia are crucial regulators of activity-triggered synaptic plasticity, adult neurogenesis, and learning and memory. Changes in microglial number or function during development, for example, through the deletion of transforming growth factor (TGF)-β in the CNS or by knocking out CX3CR1, results in aberrations in neuroplasticity in adulthood. But more importantly, eliminating microglia in the adult or blocking the cells' ability to make brain-derived neurotrophic factor (BDNF) leads to impaired synaptic plasticity, and learning and memory (Salter and Stevens 2017).

3.2.2 Microglia in the pathology of AD

A prominante pathological feature of AD brain is the activation und recruitment of microglial cells to amyloid plaques. Systems-level analyses of gene regulatory networks in postmortem human LOAD brain specimens have identified the immune/microglial molecular network as most highly associated with pathophysiology in LOAD (Zhang, Gaiteri et al. 2013). A detailed morphological analysis of microglial activation state in brain specimens from two cohorts of cognitive aging found that the proportion of activated microglia strongly correlated with presence of pathologic AD (Long and Holtzman 2019).

Due to their close association with Aβ plaques, microglia have been suggested to be causally involved in various steps of Aβ plaque formation, including plaque seeding, plaque compaction, and plaque isolation (Fruhwurth, Zetterberg et al. 2024). In 5xFAD mice, efficient depletion of microglia using colony stimulating factor 1 receptor (CSF1R) inhibitors before AD onset reduced Aβ plaque seeding, in particular the formation of dense-core plaques within cortical regions (Spangenberg, Severson et al. 2019). Another study has found that microglia depletion before plaque deposition enhanced neuritic dystrophy and increased diffuse-like plaques while fewer compact-like plaques was

observed (Casali, MacPherson et al. 2020). Microglial repopulation led to subsequent plaque remodeling, resulting in more compact plaques predominating microglia-repopulated regions (Casali, MacPherson et al. 2020). The clustering of microglia around plaques has been suggested to exert a barrier function that increases plaque compaction while decreasing neuritic dystrophy (Condello, Yuan et al. 2015, Fruhwurth, Zetterberg et al. 2024). Inhibition of microglial proliferation in APP/PS1 mice resulted in an improved performance in memory and behavioural tasks and a prevention of synaptic degeneration, although these changes were not correlated with a change in the number of Aβ plaques (Olmos-Alonso, Schetters et al. 2016). These studies suggest that microglia might be involved in the different steps of Aβ accumulation in mice, and that the exact role of microglia might depend on the disease stage.

Microglial Aβ phagocytosis is a critical mechanism for Aβ clearance but is impaired with the progression of AD. By using 2-photon intravital imaging in live mice, it was showed that the formation of Aβ plaques rapidly recruits microglia that actively participate in phagocytosis (Wang and Colonna 2019). Larger plaques were associated with larger microglia, and the size of some plaques increased or decreased over time in parallel with the volume of associated microglia (Wang and Colonna 2019). In mice, genetic defects in different receptors or proteins involved in phagocytosis result in neurodegeneration and may be responsible for increased amyloidosis in mouse models of AD (Lucin, O'Brien et al. 2013). Conversely, driving microglial activation towards a more phagocytic phenotype reduces Aβ pathology in mouse models of AD (Lucin, O'Brien et al. 2013). The genome-wide association studies suggest that microglial phagocytic receptors may have a critical role in AD. TREM2 protein is expressed on microglia, promotes microglial phagocytosis, modulates inflammatory signaling and promotes microglial survival (Long and Holtzman 2019). Rare variants in TREM2 triple the risk of developing AD and represent one of the strongest known risk factors (Lucin, O'Brien et al. 2013). Microglia that express TREM2 have an enhanced ability to bind to and phagocytose Aβ aggregate; however, loss of TREM2 function results in reduced phagocytosis of Aβ, exacerbating plaque accumulation and contributing to increased neuroinflammation and neurodegeneration (Shi, Gutierrez et al. 2024). TREM2 also directly interacts with Aβ, influencing the trafficking and internalization of Aβ aggregates into microglia (Shi, Gutierrez et al. 2024). The autophagy protein beclin 1 is required for efficient

phagocytosis in vitro and in mouse brains. Beclin 1-mediated impairments in phagocytosis are associated with impaired recycling of phagocytic receptors CD36 and TREM2 (Lucin, O'Brien et al. 2013). LC3-associated endocytosis (LANDO) is required for the recycling of putative Aβ receptors (CD36, TREM2, and TLR4) from internalized endosomes to the plasma membrane. In 5xFAD AD mouse model microglia-specific deletion of the LANDO related genes resulted in exacerbated Aβ deposition and plaque formation, reactive microgliosis, tau hyperphosphorylation, and neuronal cell death and dysfunction, leading to significant memory impairment (Heckmann, Teubner et al. 2019).

Microglia are the principal mediators of inflammation in response to Aβ accumulation, and their contribution to neuroinflammation is highly correlated to the progression of neurodegeneration (Heckmann, Teubner et al. 2019). Microglia are traditionally believed to adopt two distinctive microglial phenotypes, namely, the M1 (neurotoxic) and M2 (neuroprotective) subtypes (Xu, Au et al. 2022). M1 microglia express pro-inflammatory cytokines such as IL-1β, IL-6 and TNF-α, ROS and nitric oxide (NO), whereas M2 microglial phenotype is characterized by the production of anti-inflammatory cytokines (IL-4, IL-10, IL-13, and TGF-β), neurotrophic factors (IGF-1) and increased expression of inflammatory mediators that promote phagocytosis of cellular debris and misfolded proteins, neuronal survival, tissue repair and wound healing processes (Chi3l3, FIZZ1, and Arg-1) (Xu, Au et al. 2022). During AD pathogenesis, the phagocytic activity of microglia seems to decline, while the production of proinflammatory cytokines and neurotoxic molecules escalates (Wang and Colonna 2019). Quantitative PCR analysis of freshly isolated microglia revealed that microglia from old APP/PS1 mice, but not from younger mice, had a 2- to 5-fold decrease in expression of the Aβ-binding scavenger receptors A, CD36, and receptor for advanced-glycosylation endproducts, and the Aβ-degrading enzymes IDE, neprilysin, and MMP9, compared with their littermate controls. In contrast, APP/PS1 microglia had a 2.5-fold increase in the proinflammatory cytokines IL-1β and TNFα (Hickman, Allison et al. 2008). However, recent molecular analyses suggest that the M1 and M2 states are oversimplified and that microglial activation mechanisms may produce a variety of microglial subtypes (Shi, Gutierrez et al. 2024). Transcriptomic analysis at single-cell resolution identified functionally and phenotypic distinct microglial subtypes that closely associate with the pathogenesis of AD, namely the disease-associated microglia (DAM). Before the disease onset, homeostatic microglia

expressed high levels of microglia-specific marker genes including *P2ry12*, *Cx3cr1*, and *Tmem119*, and the expression was gradually declined when microglia were activated during the disease progression (Xu, Au et al. 2022). Two sequential but distinct stages in DAM activation were identified in 5xFAD mice. The first step, which is Trem2-independent, involves activation of a set of genes, including the Trem2-signaling adaptor Tyrobp, Apoe, and B2m, concomitantly with downregulation of microglia homeostatic factors (e.g., Cx3cr1 and P2ry12/P2ry13). The second phase of DAM activation, including induction of lipid metabolism and phagocytic pathways (e.g., Lpl, Cst7, and CD9), was found to be Trem2-dependent (Keren-Shaul, Spinrad et al. 2017). Immunostaining of DAM-specific genes together with Aβ plaques identified enhanced phagocytic activity of DAM cells and their functional conservation in both mice and human AD brains (Keren-Shaul, Spinrad et al. 2017).

Microglia have been shown to be both beneficial and detrimental during the onset and progression of AD. It is proposed, that early microglial recruitment promotes Aβ clearance and is neuroprotective in AD, as disease progresses, proinflammatory cytokines produced in response to Aβ deposition downregulate genes involved in Aβ clearance and promote Aβ accumulation (Hickman, Allison et al. 2008, Wang and Colonna 2019).

3.3 Gut microbiota

The intestinal microbiota has significant functions in various aspects, such as the immune system modulation (development and maturation), the maintenance of the intestinal barrier integrity, the modulation of neuromuscular functions in the intestine, and the facilitation of essential metabolic functions for both the microbiota and the host (Fabi 2024). Not only has the gut microbiota been invoked as a contributor to, if not the cause of, every gastrointestinal ailment but its influence has been extended far afield to impinge on the lungs, joints, endocrine organs, vascular system, and the nervous system (Quigley 2017).

3.3.1 The origin and composition of the gut microbiota

The human microbiota begins to form in the intrauterine period via the bloodstream. At birth the type of delivery is an essential factor in the installation of the newborn's

microbiota (Fabi 2024). Vaginally delivered infants acquired bacterial communities resembling their own mother's vaginal microbiota, dominated by *Lactobacillus, Prevotella*, or *Sneathia* spp., and Cesarean section-delivered infants harbored bacterial communities similar to those found on the skin surface, dominated by *Staphylococcus, Corynebacterium*, and *Propionibacterium* spp. (Dominguez-Bello, Costello et al. 2010). Breast milk is the primary modulator of the gut microbiota. Breastfed children have higher amounts of *Lactobacillus* and *Bifidobacterium* in the stool (Fabi 2024). The maturation of the gut microbiota occurs up to 3 years of age, however, colonization can be altered by factors such as lifestyle, exposure to medications, environmental factors, aging, body changes, and comorbidities (Fabi 2024).

It is estimated that 10^{14} microorganisms reside in the adult gastrointestinal (GI) tract which amounts to 10 times the number of human cells in the body, the majority of which are comprised of bacteria from 500 to 1000 different species that vary in stability, diversity, and number throughout development and across different human populations (Burokas, Moloney et al. 2015). The most populous bacterial phyla, constituting more than 90% of the intestinal microbiota, are Bacteriodetes and Firmicutes, with Bacteroidaceae and Prevotellaceae being the most abundant families of Bacteriodetes and Ruminococcuceae of Firmicutes (Fabi 2024). Important physiological conditions like pH, bile content, and transit time vary along the GI tract and contribute to distinct microbial communities inhabiting the upper and lower GI tract (Ruan, Engevik et al. 2020). The small intestine is dominated by rapidly dividing facultative anaerobes such as *Proteobacteria* and *Lactobacillales* because of the metabolism, which favors simple sugar and amino acid metabolism (Ruan, Engevik et al. 2020). The great diversity of microorganisms is found in the colon due to the fermentation of complex carbohydrates (Fabi 2024). The predominant colonic bacterial phyla in the healthy human are *Bacteroidetes*, *Firmicutes*, *Verrucomicrobia*, *Proteobacteria*, and *Actinobacteria* (Ruan, Engevik et al. 2020). Several studies have attempted to define a human intestinal core microbiota. Longitudinal analysis and cross-sectional comparisons of fecal 16S rRNA have revealed that a significant fraction of bacterial phylotypes is continuously present and thus comprises a stable microbial core. These core microbes include *Bacteroides*, *Eubacterium*, *Faecalibacterium*, *Alistipes*, *Ruminococcus*, *Clostridium*, *Roseburia*, and *Blautia*; with *Faecalibacterium prausnitzii*, *Oscillospira*

guillermondii, and *Ruminococcus obeum* as the top three taxa shared by all adults (Ruan, Engevik et al. 2020).

3.3.2 Microbiota-gut-brain axis and the gut microbiota metabolites

The gut-brain axis is a bidirectional channel of communication between the "big brain" in the cranium and the "little brain" (i.e., the enteric nervous system) in the abdomen linked by neurons of the sympathetic and parasympathetic nervous systems, as well as by circulating hormones and other neuromodulatory molecules (Quigley 2017). This axis has now been extended to include the microbiota (the microbiota-gut-brain axis) and building on indications suggest that the resident bacteria in the GI tract influence the CNS (Quigley 2017). The interactions between the gut microbiota, the parasympathetic nervous system, the immune system and the different cells located in the gut can occur by direct contact or indirectly through the secretion of a plenty of specific products and metabolites (Ortega, Alvarez-Mon et al. 2023). The microbiota is suggested to produce and metabolize neurotransmitters such as GABA, tryptophan, polyamines, and histamine. The gut microbiota also produce short-chain free fatty acids (SCFAs, i.e., acetate, butyrate and propionate) that promote the maturation of microglia, innate immune responses and energy metabolism in a homeostatic state (Erny, Dokalis et al. 2021). Dietary SCFA supplementations in AD mice reshaped the homeostasis of microbiota and alleviated the cognitive impairment by reducing Aβ deposition and tau hyperphosphorylation (Sun, Zhang et al. 2023).

3.3.3 Gut bacteria in the pathogenesis of AD

The microbial composition in the gut undergoes alterations in both AD patients and mouse models (Vogt, Kerby et al. 2017, Dunham, McNair et al. 2022, Meyer, Lulla et al. 2022, Zhang, Gao et al. 2023). A prospective study of cognitively healthy individuals revealed that a decrease in butyrate-producing bacterial species (e.g., *Roseburia inulinivorans* and *R. faecis*) or an increase in pro-inflammatory bacteria (e.g., *Veillonella dispar* and *V. atypica*) correlates with subjective cognitive decline over a follow-up period of 2 to 4 years (Ma, Li et al. 2023). Transplantation of gut bacteria from AD patients to gut bacteria-depleted rats results in impaired neurogenesis and cognitive function (Grabrucker, Marizzoni et al. 2023). Gut bacteria-free APP-transgenic or App^{NL-}

$^{G\text{-}F}$ knock-in AD mice also exhibit reduced Aβ deposition and microgliosis in the brain (Minter, Zhang et al. 2016, Harach, Marungruang et al. 2017, Minter, Hinterleitner et al. 2017, Dodiya, Kuntz et al. 2019, Kaur, Nookala et al. 2021). Consequently, gut bacteria play an important role in AD pathogenesis, though the mechanism of how gut bacteria impact brain pathology in AD remains to be investigated.

However, the specific profile of intestinal bacteria associated with AD has not yet been defined. There is often a decrease in bacterial abundance in *Firmicutes* phylum, an increase in *Proteobacteria* phylum, and both a decrease and an increase in the proportion of *Bacteroidetes* bacteria (Vogt, Kerby et al. 2017, Liu, Wu et al. 2019, Murray, Kemp et al. 2022, Zhang, Gao et al. 2023). At the family and genus levels, the variability of results regarding AD-specific bacterial changes is even greater across different studies. For example, a consistent decrease in bacteria of the genus *Butyricicoccus* or *Coprococcus* or an increase in the genera *Escherichia/Shigella* (three genera are not changed in the same study) in AD patients is only found in two out of twenty independent studies (Zhang, Gao et al. 2023). *Butyricicoccus* and *Coprococcus* produce butyrate, which prevents excessive inflammation in the gut (Cattaneo, Cattane et al. 2017, Vital, Karch et al. 2017), while *Escherichia/Shigella* releases toxins and promotes inflammatory activation in the human body (Cattaneo, Cattane et al. 2017). The variability in research findings also exists in AD animals (Zhang, Gao et al. 2023). It is a challenge to investigate the precise role of different bacterial taxa in AD pathogenesis. Germ-free or broad-spectrum antibiotic-treated mice are still often used to study the molecular mechanisms by which gut bacteria influence brain pathology in AD.

An important mechanism mediating the gut-brain axis is that gut bacteria produce SCFAs. Administration of SCFAs to germ-free or antibiotic-treated AD mice restores microglial proliferation and inflammatory activation; however, the effects on Aβ phagocytosis and Aβ accumulation in the brain are inconsistent between different studies (Colombo, Sadler et al. 2021, Erny, Dokalis et al. 2021, Xie, Bruggeman et al. 2023). Whether SCFAs act directly on microglia also remains unclear. We found that SCFA receptors, G protein-coupled receptor (Gpr) 41 and Gpr43 are absent in murine microglia (Quan, Luo et al. 2021); however, deficiency of Gpr41 and Gpr43 likely inhibits microglial maturation under physiological conditions (Erny, Hrabe de Angelis et al. 2015) and increases

microglial density and Aβ deposits in the brain of APP-transgenic mice (Zhou, Xie et al. 2023). Deficiency of the butyrate receptor Gpr109a, which is highly expressed in microglia (Quan, Luo et al. 2021), has limited effects on microglial activation (Zhou, Xie et al. 2023). Since the SCFAs produced by intestinal bacteria activate Gpr41, Gpr43 and Gpr109a, promote anti-inflammatory properties and regulate the development of interleukin (Il)-17a or Il-10 producing T cells in the gut (Singh, Gurav et al. 2014, Dupraz, Magniez et al. 2021, Zhou, Xie et al. 2023) we hypothesized that gut bacteria alter microglial activation (Erny, Hrabe de Angelis et al. 2015) and brain pathology through circulating T lymphocytes.

Intestinal bacteria may also release structural components into the blood and bacteria themselves may even spread in the brain, both of which can directly activate microglia. Blood concentrations of lipopolysaccharide (LPS) together with inflammatory cytokines, e.g., IL-1β and tumor necrosis factor (TNF)-α, are increased in AD patients compared to non-AD individuals with and without cognitive impairment (Marizzoni, Mirabelli et al. 2023). Components of *Porphyromonas gingivalis*, a bacterium often existing in chronic periodontitis, were found in the brains of AD patients (Dominy, Lynch et al. 2019). We have observed that bacterial receptors CD14 and Toll-like receptor (TLR)-2 are receptors for aggregated Aβ (Fassbender, Walter et al. 2004, Liu, Walter et al. 2005, Liu, Liu et al. 2012), implying that Aβ and bacterial components share receptors on microglia in the brain. MyD88 is an adaptor protein that is down-stream of most TLRs (O'Neill, Golenbock et al. 2013). Our previous studies showed that deficiency of CD14, TLR2, TLR4, or MyD88 inhibits inflammatory activation of microglia, reduces cerebral Aβ and improves cognitive function in APP-transgenic mice (Liu, Walter et al. 2005, Walter, Letiembre et al. 2007, Hao, Liu et al. 2011, Liu, Liu et al. 2012, Quan, Luo et al. 2021). Antibiotic therapy for AD patients has attracted interest (Panza, Lozupone et al. 2019). A large cohort study suggests that sporadic use of antibiotics in older adults may decrease the risk of dementia (Rakusa, Fink et al. 2023).

3.4 Interleukin-17

Interleukin-17 (IL-17) cytokine family members have diverse biological functions, promoting protective immunity against many pathogens but also driving inflammatory

pathology during infection and autoimmunity (Mills 2023). IL-17 has also been revealed to have a strong association with neuroinflammation and the microbiota–gut–brain axis (Lu, Zhang et al. 2023). Therefore IL-17 may be important in the pathogenesis of AD. The precise correlations require further explorations.

3.4.1 Physiological functions of IL-17

The IL-17 family comprises six members (IL-17A to IL-17F) that mediate their biological functions through the IL-17 receptors (IL-17RA to IL-17RE) (Mills 2023). The most studied IL-17 family member, IL-17A, was firstly identified in 1993 from a T cell hybridoma and was initially named cytotoxic T lymphocyte-associated antigen 8 (CTLA8) (Rouvier, Luciani et al. 1993). Its encoding protein was 57% homologous to the putative protein encoded by the ORF13 gene of herpesvirus Saimiri, a T lymphotropic virus (Rouvier, Luciani et al. 1993). IL-17B to IL-17F were identified based on homology with IL-17A (Mills 2023).

IL-17 is mainly derived from $CD4^+$ T helper 17 (Th17) cells and is the main effector cytokine of Th17 cells. However, studies indicated that other lymphocytes involved in innate or adaptive immunity can also secrete IL-17A, such as γδ-T cells, αβ-T cells, invariant natural killer T (iNKT) cells, CD8+ T cells [cytotoxic T cells 17 (Tc17)], and type 3 innate lymphocytes (ILC3) (Lu, Zhang et al. 2023). Additionally, astrocytes and microglia of the CNS also express IL-17 (Amatya, Garg et al. 2017).

IL-17-mediated inflammation is crucial for microbial clearance by rapidly mediating the chemokine recruitment of neutrophil and promoting antimicrobial peptide (AMP) production in acute inflammation (Lu, Zhang et al. 2023). IL-17-secreting cells play a central role in protective immunity to *Candida* and other fungal pathogens (Mills 2023). Individuals with inborn defects in IL-17 immunity display severe and chronic skin and mucosal candidiasis (Puel, Cypowyj et al. 2011). Patients treated with anti-IL-17 monoantibodies have an increased risk of developing oropharyngeal, oesophageal and cutaneous candidiasis (Davidson, van den Reek et al. 2022). Studies in mouse models showed enhanced fungal burden post challenge in mice lacking IL-17 or its receptor. Dramatically increaced fungal burden in the kidney und substantially reduced survival

after systemic challenge with Candida albicansin in IL-17AR knockout mice was associated with impaired mobilization of peripheral neutrophils and their influx to infected organs (Huang, Na et al. 2004). Studies in mouse models with bacterial infektions showed that IL-17 can not only promote indirect recruitment of neutrophils by inducing chemokine production, but also directly activate bacterial killing by neutrophils and macrophages (Mills 2023). The role of IL-17 in immunity to viruses is still unclear. IL-17 secreting cells may be protective in influenza A infection bei promoting neutrophil influx into the lung. The blocking antibody to IL-17 increases weight loss and reduces survival (Hamada, Garcia-Hernandez Mde et al. 2009).

In addition to its protective role, IL-17 can also promote detrimental inflammation in response to infection. In a mouse model of Infection with *Cryptococcus deneoformans*, an opportunistic intracellular growth fungal pathogen, IL-17A was quickly produced by γδT cells at an innate immune phase in infected lung and suppressed the protective Th1 cell responses required for fungal clearance (Sato, Yamamoto et al. 2020). In sepsis models, IL-17 was associated with abscess formation following *Bacteroides fragilis* challenge in T_H2-impaired *Stat6*$^{-/-}$ mice and treatment with anti-IL-17 mAbs prevented abscess formation after bacterial challege (Chung, Kasper et al. 2003). IL-17 can also promote inflammatory pathology during viral infection. In patients with different chronic hepatitis B virus (HBV)-related diseases the expression of IL-17 is significantly increased, and the level of IL-17 is strongly correlated with the degree of liver fibrosis (Wang, Chen et al. 2011). In COVID-19 patients with pulmonary sequelae Th17 cells are expanded und activated even if one year after discharge (Wu, Tang et al. 2021).

By dysregulation IL-17 responses can drive the pathology in autoimmune und inflammatory diseases. IL-17 has a well-established role in the pathology of psoriasis, psoriatic arthritis and ankylosing spondylitis. A range of highly effective therapeutics that target the IL-23–IL-17 pathway are in widespread clinical use (Mills 2023). IL-17 expression is increased in the mucosa und serum in patients with active ulcerative colitis or Crohn's disease but is not detected in samples from normal colonic mucosa, infectious colitis, or ischaemic colitis (Fujino, Andoh et al. 2003). Studies in the experimental autoimmune encephalomyelitis (EAE) mouse model of multiple sclerosis (MS) have provided convincing evidence that IL-17 is a key pathogenic cytokine (Mills 2023).

3.4.2 IL-17 and microbiota-gut-brain axis

IL-17 has been shown to transduce inflammatory signals through the microbiota–gut–brain axis (Lu, Zhang et al. 2023). Growing evidences have demonstrated that gut microbiota modulate immune responses to gastrointestinal resident bacteria in IL-17A-dependent manner and gut microbiota-induced IL-17A play positive roles on the normal immune cell maintenance and homeostasis in intestinal mucosal immunity (Douzandeh-Mobarrez and Kariminik 2019). *Segmented filamentous bacteria* (SFB), a relatively low-abundance microbial population in the ileum, can induce the generation of RORγt^{+}Th17 cells in the tissue-associated lymph nodes in the gut, although the excessive activation of RORγt^{+}Th17 cells might lead to autoimmune diseases (Wang, Yuan et al. 2024). Studies in mice lacking IL-17R, particularly on intestinal epithelial cells, demonstrated a delicate balance between IL-17 and the microbiota: IL-17 routinely regulates bacterial growth, potentially leading to intestinal ecological dysregulation, which in turn drives the activation of Th17 cells, resulting in increased IL-17 secretion (Lu, Zhang et al. 2023). IL-17A and IL-17F are considered to be the modulators of the intestinal microbiota. In mice deficient for IL-17A and IL-17F alterations of the intestinal microbiota were correlated with EAE resistance. Moreover, through experimental manipulation of the IL-17–sensitive microbiota, the EAE susceptibility in IL-17–deficient mice could be reestablisched (Regen, Isaac et al. 2021). Although no epidemiological data linking intestinal microbiota to stroke risk or stroke outcome are yet available, inflammatory bowel disease and Crohn's disease, which have been linked to altered gut flora and increased intestinal IL-17 production, have been identified as risk factors for stroke (Benakis, Brea et al. 2016). IL-17 and IL-17 inucing gut microbiota contribute to degree of lesion severity following ischemic stroke (Majumder and McGeachy 2021). Conversely, by regulating gut microbiota, IL-17 can alter systemic microbial products that are increasingly thought to affect mental health, and Th17 cells were increased and promoted depression-like symptoms in mouse models (Majumder and McGeachy 2021).

In addition, some neurotransmitters in the microbiota-gut-brain axis can interact with IL-17. Gamma-aminobutyric acid (GABA) is the most abundant inhibitory neurotransmitter and is widely distributed in the mammalian brain. It has already been stated the production of GABA by some bacteria present in the gut microbiota, thus demonstrating gut

microbiota modulation can influence the levels of circulating GABA (Fabi 2024). Enterotoxigenic *Escherichia coli* (ETEC) infection induced expression of intestinal IL-17 and dysbiosis of intestinal microbiota, increasing abundance of GABA-producing *Lactococcus lactis* subsp. *lactis*. Antibiotics treatment in mice lowered the expression of intestinal IL-17 during ETEC infection, while GABA or *L. lactis* subsp. *lactis* administration restored the expression of intestinal IL-17 (Ren, Yin et al. 2016).

3.4.3 IL-17 in AD

Several emerging studies have suggested a pivotal role for the IL-17 cytokine family in the neurodegenerative diseases such as AD. However the precise effect of IL-17 in ameliorating or exacerbating the neuropathogenesis of AD remains unclear. Current understandings have highlighted that IL-17 may contribute in the progression and worsening of pathophysiology of AD by activating glial cells. An increased population of circulating Th17 cells and its enhanced infiltration into brain is reported in patients with mild cognitive impairment and in AD models (Gautam, Pulivarthi et al. 2023). In an animal study, Injection of $A\beta_{1-42}$ bilaterally into hippocampus of rats resulted in disruption of BBB und infiltration of Th17 cells into brain parenchyma. The expression of IL-17 and IL-22 was increased in the hippocampus, and concentrations of the two cytokines were elevated in both the CSF and the serum in AD occurence and development (Zhang, Ke et al. 2013). In contrast, overexpression of IL-17A in an AD mouse model did not exacerbate neuroinflammation, but decreased the level of soluble Aβ in the CSF and hippocampus as well as improved the metabolism of glucose (Yang, Zeng et al. 2019). In several reports, serum levels of IL-17 in AD patients was elevated and significant higher concentration of IL-17 was observed in females (Doecke, Laws et al. 2012, Chen, Jiang et al. 2014). However, two distinct human cohort studies reported that the IL-17A level was decreased in AD patients compared to healthy controls (Chen, Liu et al. 2020).

In recent years, the microbiota–gut–brain axis has received expanding interest in the pathogenesis of AD, and patients with AD can exhibit alterations in both the gut microbiota and blood proinflammatory cytokine profiles (Lu, Zhang et al. 2023). It has been reported that microbiota-derived SCFAs, particularly propionate, reduce IL-17 and

IL-22 production by intestinal γδ T cells in mice; moreover, the production of IL-17 by human IL-17-producing γδ T cells from patients with inflammatory bowel disease is regulated by propionate (Dupraz, Magniez et al. 2021). In AD mice treatment with 27-hydroxycholesterol resulted in further excerbation of cognitive deficits, which was associated with elevated levels of IL-17 in serum and intestinal plasma, and decreased levels of SCFAs such as propionate and butyrate (Wang, An et al. 2020). Long-term antibiotic exposure reduces Th17 cells in the gut (Drummond, Desai et al. 2022). The question arises as to whether inhibition of IL-17a signaling mediates the efficacy of potential antibiotic therapy in AD.

Germ-free mice generate fewer Il-17a-producing CD4(+) T help (Th17) lymphocytes but more CD4(+)CD25(+)Foxp3(+) regulatory T (Treg) cells in the gut and spinal cord, which is associated with resistance to EAE in mice (Lee, Menezes et al. 2011). Depletion of intestinal bacteria by antibiotics reduces the accumulation of Il-17a-producing γδ T cells in the leptomeninges and ameliorates brain injury in a stroke mouse model (Benakis, Brea et al. 2016). In APP-transgenic mice, reductions in cerebral Aβ deposition and microglia after gut antibiotic treatments correlate with increased levels of Foxp3+ Treg cells in blood and brain (Minter, Hinterleitner et al. 2017). However, transient depletion of Treg cells was shown to regulate microglia or/and infiltrated macrophages with differential effects on Aβ clearance and cognitive protection in two studies (Baruch, Rosenzweig et al. 2015, Dansokho, Ait Ahmed et al. 2016). Our recent study showed that deficiency of p38α-MAPK in peripheral myeloid cells decreases Th17 cells, which possibly increases microglial activation and Aβ clearance in AD mice (Luo, Schnoder et al. 2022).

Taken together, recent findings have highlighted the involvement of IL-17 in the AD pathophysiology both in AD patient and in animal model. However, the role of IL-17 in regulation of the AD pathogenesis is controversal discussed. Changes of IL-17 level or Th17 cells have been shown in animal models treated with microbiota-derived component or antibiotics. Therefore, we asked whether Il-17a-expressing cells mediate the effects of gut bacteria on AD pathology. This may contribute to a better understanding of IL-17 and its related signaling pathways in the AD pathogenesis and may be helpful in exploring therapeutic approaches targeting IL-17.

4 AIM OF THIS WORK

As we described in the introduction, gut bacteria change in AD patients and in animal models and influence AD pathology. However, it remains unclear how gut bacteria alter AD pathology in the brain. There is growing evidence that gut bacteria impact the brain GABA via the vagus nerve and indirectly through the release of bacterial metabolites and the retraining of immune cells, i.e. T lymphocytes. However, it is largely unknown which molecules link the gut and brain and mediate the development of AD.

In this project, we aimed to answer the following questions:

1) How does depletion of gut bacteria (establishment of germ-free status) regulate brain pathology in APP-transgenic mice, in particular, what changes are there in inflammatory signature of microglia and in Aβ pathology?
2) Which mechanisms mediate the changes in Aβ pathology, in particular with a focus on β- and γ-secretases-mediated Aβ production, microglial internalization of Aβ, extracellular degradation of Aβ and Aβ efflux from the brain to the circulation across the blood-brain barrier?
3) How does depletion of gut bacteria regulate the development of T lymphocytes, in particular IL-17a-expressing Th17 cells, in APP-transgenic mice?
4) Do gut bacteria translocate from the gut to the brain in APP-transgenic mice?
5) Do IL-17a-expressing cells mediate the effects of gut bacteria on AD-associated pathology in APP-transgenic mice?

5 MATERIALS AND METHODS

5.1 Materials

5.1.1 Instruments

Instruments	Company
7500 Fast Real-Time PCR System	Applied Biosystems (Darmstadt, Germany)
Accu jet Pipettes Control	BrandTech Scientific (Essex, CT, USA)
Autoclave 3870 ELV	Systec (Wettenberg, Germany)
Autoclave V-150	Systec (Wettenberg, Germany)
Axiovert 25 invetiertes Microscope	Carl Zeiss Microscopy (Jena, Germany)
Axiovert 40 CFL Microscope	Carl Zeiss Microscopy (Jena, Germany)
Biofuge 13 Centrifuge	Heraeus (Hanau, Germany)
Biowizard KR-200 Bench	Kojair Tech Oy (Vilppula, Finland)
Coolbox KB 1001	Liebherr (Lindau, Germany)
Drying cabinet	Heraeus (Hanau, Germany)
Eclipse TS100 Invetiertes Microscop	Nikon Instruments (Melville, NY, USA)
Eclipse E600 Fluorescence Microscopy	Nikon Instruments (Melville, NY, USA)
FACSCanto II Flow Cytometer	BD Biosciences (Heidelberg, Germany)
Freezer Premium no frost	Liebherr (Lindau, Germany)
Freezer UF75-110 T	Colora (Frankfurt, Germany)
General Rotator STR4	Stuart Scientific (Staffordshire, UK)
HERAcell CO_2 Incubators	Heraeus (Hanau, Germany)
HERAcell 150i CO_2 Incubators	Thermo Scientific (Langenselbold, Germany)
HERAsafe HS 12 biological safety cabinet	Heraeus (Hanau, Germany)
Ice Machine	Eurfrigor Ice Makers Srl (Lainate, Italy)
Incubations hood TH-30	Edmund Bühler GmbH (Hechingen, Germany)
InoLab pH 720 pH-meter	WTW (Weilheim, Germany)
Jouan B4i Centrifuge	Thermo Scientific (Langenselbold, Germany)
Laboshaker	Gerhardt Analytical Systems (Königswinter, Germany)
Liquid Nitrogen Container	KGW-Isotherm (Karlsruhe, Germany)
Microwelle HF 26521	Siemens (München, Germany)
Mini-PROTEAN 3 Electrophoresis system	Bio-Rad Laboratories (München, Germany)
Mini Trans-Blot Cell	Bio-Rad Laboratories (München, Germany)
Multipette Plus	Eppendorf (Hamburg, Germany)
Nalgene Mr. Frosty Freezing Container	A. Hartenstein (Würzburg, Germany)
Nanodrop ND-1000 Spectrophotometer	PEQLAB Biotechlonogie (Erlangen, Germany)
Optima Max Ultracentrifuge	Beckman Coulter (Krefeld, Germany)
Perfection V700 Photoscanner	Epson (Meerbusch, Germany)
Pipette PIPETMAN	Gilson (Middleton, WI, USA)
Pipette Single-Channel	Eppendorf (Hamburg, Germany
Pipette Pipetus	Hirschmann (Eberstadt, Germany)

PowerPac 200 Power Supply	Bio-Rad Laboratories (München, Germany)
Precision Balance scale 770	Kern & Sohn (Balingen, Germany)
Precision Balance scale CP 42023	Sartorius (Göttingen, Germany)
PS250 Power Supply	Hybaid (Heidelberg, Germany)
PTC 200 DNA Engine Thermal Cycler	MJ Research (St. Bruno, Canada)
PURELAB Ultra Water Purification system	Elga (Celle, Germany)
QuadroMACS™ Separator	Miltenyi Biotec(Bergisch Gladbach,Germany)
Refrigerated Laboratory Centrifuge	Eppendorf (Hamburg, Germany)
Refrigerator KG39VVI30	Siemens (München, Germany)
Refrigerator Premium	Liebherr (Lindau, Germany)
Refrigerator V.I.P. Series -86 °C Freezer	Sanyo (Wood Dale, IL, USA)
Rocky 3D	Labortechnik Frübel (Lindau, Germany)
Savant SpeedVac DNA 110	Thermo Scientific (Langenselbold, Germany)
Shakers SM-30	Edmund Bühler (Hechingen, Germany)
SmartSpec 3000 Spectralphotometer	Bio-Rad Laboratories (München, Germany)
Sunrise Microtiter plate reader	Tecan (Männedorf, Schweiz)
Tabletop Centrifuge 4K10	Sigma Laborzentrifugen (Osterode am Harz, Germany)
Tabletop Centrifuge 4K15C	Sigma Laborzentrifugen (Osterode am Harz, Germany)
Tecan Infinite M200 microplate reader	Männedorf, Switzerland
Thermoblock TDB-120	BioSan (Riga, Latvia)
Thermomixer comfort	Eppendorf (Hamburg, Germany)
TLA-55 Rotor Package, Fixed Angle	Beckman Coulter (Krefeld, Germany)
Transsonic Ultrasonic Cleaning Units	Elma (Singen, Germany)
Ultrospec 3100 pro Spectralphotometer	Amersham Biosciences (München, Germany)
Vortex Genie 2	Scientific Industries (Bohemia, NY, USA)
Vortex Shaker REAX 2000	Heidolph (Schwabach, Germany)
Water bath	Köttermann (Hänigsen, Germany)
XCell SureLock Mini-Cell Electrophoreses system	Invitrogen (Darmstadt, Germany)

5.1.2 General experimental materials und consumables

Products	**Company**
Amersham Hyperfilm ECL	GE Healthcare (Buckinghamshire, UK)
Beackers	VWR (Darmstadt, Germany)
Biosphere Filter Tips (10 µl, 200 µl, 1000 µl)	Sarstedt (Nümbrecht, Germany)
Blotting Paper Grade GB003	Whatman (Dassel, Germany)
Cell Scrapers	TPP (Trasadingen, Schweiz)
Centrifugentubes (15 ml, 50 ml)	Sarstedt (Nümbrecht, Germany)
Combitips Plus (5 ml, 10 ml)	Eppendorf (Hamburg, Germany)
CryoPure tubes 1.8 ml	Sarstedt (Nümbrecht, Germany)
Cuvettes	Sarstedt (Nümbrecht, Germany)
Erlenmeyer Flasks	Schott (Mainz, Germany)

Falcon Multiwell Cell Culture Plates	BD Biosciences (Heidelberg, Germany)
Falcon Round bottom test tubes 5 ml	BD Biosciences (Heidelberg, Germany)
Filtropur Cell Strainer	Sarstedt (Nümbrecht, Germany)
Filtropur Syringe Filter	Sarstedt (Nümbrecht, Germany)
Glass Bottles	Fisher Scientific (Schwerte, Germany)
Gloves, Latex	VWR (Darmstadt, Germany)
Gloves, Nitril	VWR (Darmstadt, Germany)
Hemocytometer	Brand (Wertheim, Germany)
LS Columns	Miltenyi Biotec (Bergisch Gladbach, Germany)
MicroAmp Optical 96-Well Reaction Plate	Applied Biosystems (Darmstadt, Germany)
MicroAmp Optical Adhesive Film	Applied Biosystems (Darmstadt, Germany)
Microlance™ needles	BD Biosciences (Heidelberg, Germany)
Microlon 600 96-Well Microplate	Greiner Bio-One (Frickenhausen, Germany)
Microscopic cover glasses 12x12 mm	R. Langenbrinck (Emmendingen, Germany)
Microtestplate 96-Well	Sarstedt (Nümbrecht, Germany)
Mini-PROTEAN 3 Short Plates	Bio-Rad Laboratories (München, Germany)
Mini-PROTEAN 3 Spacer Plates 1,5 mm	Bio-Rad Laboratories (München, Germany)
Mini-PROTEAN Comb (15 Wells, 1,5 mm)	Bio-Rad Laboratories (München, Germany)
Myelin Removal Beads II	Miltenyi Biotec (Bergisch Gladbach, Germany)
Nunc MaxiSorp 96-Well Plate, black	Thermo Scientific (Langenselbold, Germany)
Overhead Transparencies	R. Langenbrinck (Emmendingen, Germany)
Pasteur Pipettes	VWR (Darmstadt, Germany)
PCR Soft Tube 0.2 ml	Biozym Scientific (Oldendorf, Germany)
Pipette Tips (10 µl, 200 µl, 1000 µl)	Sarstedt (Nümbrecht, Germany)
Polyallomer Tube, 1.5 ml, Snap-On Cap	Beckman Coulter (Krefeld, Germany)
Precision Wipes Kimtech Science	Kimberly-Clark (Koblenz, Germany)
Pro-Gel 10-20% Tris-Tricin-Gel	Anamed Elektrophorese (Groß-Bieberau/Rodau, Germany)
Protran Nitrocellulose Transfermembranes	Whatman (Dassel, Germany)
PVDF Western Blotting Membranes	Roche (Mannheim, Germany)
Safe-Lock Tubes (0.5 ml, 1 ml, 2 ml)	Eppendorf (Hamburg, Germany)
Scalpel Blades	B. Braun (Melsungen, Germany)
Serological Pipettes (5 ml, 10 ml, 25 ml)	Sarstedt (Nümbrecht, Germany)
Slide Box	neoLab (Heidelberg, Germany)
Standing Cylinders	VWR (Darmstadt, Germany)
Syringes	B. Braun (Melsungen, Germany)
Tissue Culture Dish	Sarstedt (Nümbrecht, Germany)
Tissue Culture Flask	Sarstedt (Nümbrecht, Germany)
UV Quartz cuvette 10 mm	Hellma (Müllheim, Germany)

5.1.3 Chemicals, reagents, Kits, Antibodies

5.1.3.1 General chemicals und reagents

Chemicals and Reagents	Company
0.05% Trypsin/EDTA (1x)	Invitrogen (Darmstadt, Germany)
(3-Aminopropyl) triethoxysilane	Sigma Aldrich (Taufkirchen, Germany)
β-Mercaptoethanol	Sigma Aldrich (Taufkirchen, Germany)
β-Secretase Substrate IV, Fluorogenic	Merck (Darmstadt, Germany)
γ-Secretase Substrate, Fluorogenic	Merck (Darmstadt, Germany)
Agarose	Biozym (Oldendorf, Germany)
Ammoniumpersulfat (APS)	Sigma Aldrich (Taufkirchen, Germany)
Antibiotic-Antimycotic 100x	Invitrogen (Darmstadt, Germany)
Bovine Serum Albumin (BSA)	Sigma Aldrich (Taufkirchen, Germany)
Borat	VWR (Darmstadt, Germany)
Bromphenol blue	Sigma Aldrich (Taufkirchen, Germany)
Casein	Fluka (Buchs, Switzerland)
Chloroform	Applichem (Darmstadt, Germany)
Citrate acid	Serva (Heidelberg, Germany)
Congo red	Sigma Aldrich (Taufkirchen, Germany)
Collagen Coating Solution	Sigma-Aldrich (Taufkirchen, Germany)
Cx3Cr1 antagonist 18a: AZD 8797	Axon Medchem BV (Groningen, Netherlands)
Cy3- labelled Streptavidin	Sigma-Aldrich (Taufkirchen, Germany)
Dimethylsulfoxid (DMSO)	Sigma Aldrich (Taufkirchen, Germany)
Diaminobenzidin-Hydrochlorid (DAB)	Sigma Aldrich (Taufkirchen, Germany)
DNA Ladder (100 bp, 1 kb)	New England Biolabs (Frankfurt am Main, Germany)
dNTP Mix	Roche (Mannheim, Germany)
Dithiothreitol (DTT)	Sigma Aldrich (Taufkirchen, Germany)
Digest-All 3 (Pepsin)	Thermo Fisher Scientific (Mannheim, Germany)
Dulbecco's Modified Eagle Medium (DMEM)	Invitrogen (Darmstadt, Germany)
Entellan®mouting media	VWR (Darmstadt, Germany)
Ethidiumbromid	Carl Roth (Karlsruhe, Germany)
Ethanol	Sigma Aldrich (Taufkirchen, Germany)
Ethylendiaminetetraacetat acid (EDTA)	Sigma Aldrich (Taufkirchen, Germany)
Ethylene glycol tetraacetic acid (EGTA)	Sigma Aldrich (Taufkirchen, Germany)
Fetal Bovine Serum (FBS)	Invitrogen (Darmstadt, Germany)
Glycine	Carl Roth (Karlsruhe, Germany)
Glycerol	Sigma Aldrich (Taufkirchen, Germany)
Guanidine Hydrochloride	Sigma Aldrich (Taufkirchen, Germany)
H_2O_2	Otto Fishar (Saarbrueken, Germany)
H_2SO_4	Fluka (Buchs, Switzerland)

HCl	Sigma Aldrich (Taufkirchen, Germany)
Ham's F-12 Medium	Invitrogen (Darmstadt, Germany)
Hank's Buffered Salt Solution (HBSS)	Sigma Aldrich (Taufkirchen, Germany)
Hexamer Random Primer	Invitrogen (Darmstadt, Germany)
HiLyte Fluor™ 488-conjugated Aβ42	AnaSpec(Fremont, USA)
Isoflurane	Baxter (Unterschleißheim, Germany)
Isopropanol	Carl Roth (Karlsruhe, Germany)
$KHCO_3$	Merck (Darmstadt, Germany)
KCl	Merck (Darmstadt, Germany)
Lipopolysaccharide (LPS)	Axxora (Lörrach, Germany)
$MgCl_2$	Fluka (Buchs, Switzerland)
$MgSO_4$	Fluka (Buchs, Switzerland)
Methoxy-XO4	Bio-Techne GmbH
Methanol	Sigma Aldrich (Taufkirchen, Germany)
MCC950	Sigma Aldrich (Taufkirchen, Germany)
Milk powder	Carl Roth (Karlsruhe, Germany)
NaCl	Merck (Darmstadt, Germany)
NaF	Merck (Darmstadt, Germany)
Na_2HPO_4	Carl Roth (Karlsruhe, Germany)
NaH_2PO_4 x H_2O	Merck (Darmstadt, Germany)
$Na_4P_2O_7$	Sigma Aldrich (Taufkirchen, Germany)
Na_3VO_4	Sigma Aldrich (Taufkirchen, Germany)
NH_4Cl	Sigma Aldrich (Taufkirchen, Germany)
Niacin	Sigma Aldrich (Taufkirchen, Germany)
Okadic acid	Sigma Aldrich (Taufkirchen, Germany)
Orange G	Merck (Darmstadt, Germany)
PageRuler Prestained Protein Ladder	Invitrogen (Darmstadt, Germany)
Paraformaldehyd (PFA)	Merck (Darmstadt, Germany)
Protease inhibitor Cocktail	Roche (Mannheim, Germany)
Penicillin-streptomycin	Sciencell Research Laboratories (Carlsbad, CA, USA)
Rotiphorese Gel 30	Carl Roth (Karlsruhe, Germany)
RPMI 1640	Invitrogen (Darmstadt, Germany)
Recombinant human IL-1β	R&D Systems (Wiesbaden, Germany)
Sodium actate	Merck (Darmstadt, Germany)
Sodium dedecylsulfat (SDS)	Carl Roth (Karlsruhe, Germany)
Sucrose	VWR (Darmstadt, Germany)
Tetramethylethylendiamin (TEMED)	Serva (Heidelberg, Germany)
Tricine	Carl Roth (Karlsruhe, Germany)
Trizma®base	Sigma Aldrich (Taufkirchen, Germany)
Triton X-100	Sigma Aldrich (Taufkirchen, Germany)
TRizol	Sigma Aldrich (Taufkirchen, Germany)

Tween 20	Sigma Aldrich (Taufkirchen, Germany)
Western Lightning ECL Substrate	Perkin Elmer (Rodgau, Germany)
Xylene	Otto Fischar (Saarbrücken, Germany)
Xylene cyanol	Molekula (München, Germany)

5.1.3.2 Kits

Products	**Company**
Bio-Rad Protein Assay	Bio-Rad Laboratories (Feldkirchen, Germany)
QIAamp Fast DNA Stool Mini Kit	Qiagen (Hilden, Germany)
DyNAmo™ Flash probe qPCR Kit	Thermo Scientific (Bonn, Germany)
DyNAmo™ Flash SYBR Green qPCR Kit	Thermo Scientific (Bonn, Germany)
Human Aβ40 ELISA Kit	Invitrogen (Darmstadt, Germany)
Human Aβ42 ELISA Kit	Invitrogen (Darmstadt, Germany)
Mouse TNF-alpha DuoSet® ELISA	R&D Systems (Wiesbaden, Germany)
Mouse IL-1β DuoSet® ELISA	R&D Systems (Wiesbaden, Germany)
Spleen Dissociation Kit (mouse)	Miltenyi Biotec (B.V. & Co. KG, Bergisch Gladbach, Germany)
Neural Tissue Dissociation Kit (papain-based)	Miltenyi Biotec (B.V. & Co. KG, Bergisch Gladbach, Germany)
OptEIA™ TMB Substrate Reagent Set	BD Bioscience (Heidelberg, Germany)
RNeasy® Plus Mini Kit	Qiagen (Hilden, Germany)
RQ1 RNase-free DNase	Promega (Mannheim, Germany)
Maxima Reverse Transcriptase	Thermo Scientific (Bonn, Germany)
VectaStain Elite ABC-HRP kit	Vector Laboratorie (Burlingame, USA)

5.1.3.3 Antibodies

Antibody	**Company**
rabbit polyclonal anti α-tubulin, Cat.No. 2144	Cell Signaling Technology (Europe)
rabbit monoclonall anti β-actin, clone: 13E5	Cell Signaling Technology (Europe)
rabbit monoclonal anti Amyloid β, clone: D12B2	Cell Signaling Technology (Europe)
rat monoclonal anti CD16/CD32, clone:2.4G2	BioXCell (West Lebanon, NH)
Microbeads-conjugated CD11b, clone: M1/70	Miltenyi Biotec
Dynabeads™ Mouse CD4 (L3T4)	Thermo Scientific (Bonn, Germany)
PE-Cy5-conjugated CD11b, clone: M1/70	Thermo Scientific (Bonn, Germany)
APC-conjugated rat monoclonal anti-CD4, clone: GK1.5	Thermo Scientific (Bonn, Germany)
rabbit polyclonal anti Iba1	Wako (Neuss, Germany)
rabbit monoclonal anti ABCB1, clone: E1Y7S	Cell Signaling Technology (Europe)
rabbit polyclonal anti LRP-1	Cell Signaling Technology (Europe)
rabbit polyclonal anti claudin-5, Cat. No. GTX 49370	GeneTex, Hsinchu, China

rabbit anti CD68, clone:E307V	Cell Signaling Technology (Europe)
Cy3-conjugated goat anti-rabbit IgG	*Jackson ImmunoResearch Ltd. (Europe)*

5.1.4 Buffer

Recipe	Chemicals	Amount	Concentration
10x Citric buffer	Citric acid	2.014g Up to1 Liter	10mM
10x PBS	NaCl KCl Na_2HPO_4 NaH_2PO_4 x H_2O dest. H_2O Adjust to pH 7.4	400 g 10 g 71 g 69 g Up to5 Liter	1.37 M 27 mM 100 mM 100 mM
10x TBS	Tris NaCl dest. H_2O Adjust to pH 7.4	302.5 g 425 g Up to 5 Liter	500 mM 1.45 M
5x DNA-Loading buffer	Bromphenol blue Xylene cyanol Orange G Sucrose 0.5 M EDTA [pH 8.0] dest. H_2O	1 mg 2 mg 2 mg 500 mg 2 µl Up to 1 ml	0.1% 0.2% 0.2% 50% 1 mM
5x TBE	Tris Borat 0.5 M EDTA [pH 8.0] dest. H_2O	270 g 137.5 g 100 ml Up to 5 Liter	446 mM 446 mM 10 mM
3x SDS-PAGE Loading buffer	1 M Tris/HCl [pH 6.8] 20% SDS Glycerol β-Mercaptoethanol 3% Bromphenol blue (w/v) dest. H_2O	187.5 µl 300 µl 300 µl 150 µl 10 µl Up to 1 ml	187.5 mM 6% 30% 15% 0.03%
10x SDS-Tris-Glycine Running buffer	Tris Glycine SDS dest. H_2O	151.5 g 720.5 g 50 g Up to 5 Liter	250 mM 1.92 M 1% (w/v)
10x SDS-Tris-Tricine running buffer	Tris Tricine	121 g 171 g	1 M 1 M

	SDS	10 g	1% (w/v)
	dest. H_2O	Up to1 Liter	
10x Transfer buffer*	Tris	30 g	248 mM
	Glycine	138 g	1.84 M
	dest. H_2O	Up to 1 Liter	
* for use, mix 100 mL 10X Transfer buffer with 200 mL methanol and 700 mL dest. H_2O			
Western blot Blocking buffer	Nonfatty milk	5g	10%
	1x PBS	Up to 50 ml	
DMEM media*	Dulbecco's Modifed Eagle Medium (DMEM)(High Glucose)	445 ml	89%
	Fetal bovine serum	50 ml	10%
	Antibiotic-antimycotic(100x)	5 m	1%
* Fetal bovine serum should be inactivated in 56°C water bath for 30 min.			
RPMI media*	RPMI 1640 Medium	445 ml	89%
	Fetal bovine serum	50 ml	10%
	Antibiotic-antimycotic(100x)	5 ml	1%
* Fetal bovine serum should be inactivated in 56°C water bath for 30 min.			
SDS-Cell lysis buffer	1 M Tris/HCl [pH 7.5]	2.5 ml	50 mM
	0.5 M EDTA [pH 8.0]	200 µl	2 mM
	0.5 M EGTA [pH 8.0]	200 µl	2 mM
	Protease inhibitor Cocktail	1 Tablet	1x
	20 µM Okadic acid	125 µl	50 mM
	0.25 M $Na_4P_2O_7$	1 ml	5 mM
	1 M Na_3VO_4	100 µl	100 µM
	1 M DTT	50 µl	1 mM
	1 M NaF	2.5 ml	50 mM
	20% SDS	5 ml	2%
	dest. H_2O	Up to 50 ml	

5.2 Animal models and cross-breeding

APP/PS1-transgenic mice (APP^{tg}) over-expressing human mutated APP (KM670/671NL) and PS1 (L166P) under Thy-1 promoters (Radde, Bolmont et al. 2006) were gifts from M. Jucker, Hertie Institute for Clinical Brain Research, Tübingen, Germany. *Il-17a* knockout ($Il17a^{-/-}$) mice were kindly provided by Y. Iwakura, Tokyo University of Science, Japan (Nakae, Komiyama et al. 2002). IL-17a-deficient AD mice were created by cross-breeding APP/PS1-transgenic mice and $Il17a^{-/-}$ mice to obtain $APP^{tg}/Il17a^{-/-}$ genotype in our previous study (Luo, Schnoder et al. 2022). APP/PS1-transgenic mice were also cross-bred with IL-17a-eGFP reporter mice ($Il17a^{GFP/GFP}$;

kindly provided by R. Flavell, Yale University, USA) to get $APP^{tg}/Il17a^{GFP/wt}$ of genotype, in which eGFP is expressed under the control of endogenous *Il-17a* gene promoter (Esplugues, Huber et al. 2011). All mice used in this project were on C57BL/6 genetic background. Because of the difference in the prevalence of AD between women and men we used only female mice in this study.

5.3 Methods

5.3.1 Depletion of intestinal bacteria with antibiotics in drinking water

Sisters of IL-17a-deficient or wildtype APP-transgenic mice from each litter (≥ 2 mice per genotype) were randomly separated. IL-17a-deficient and wild-type female mice were cohoused and treated with and without vancomycin (500mg/L), ampicillin (1g/L), neomycin sulfate (1g/L), streptomycin (1g/L), and metronidazole (1g/L) (all antibiotics were purchased from Sigma-Aldrich Chemie GmbH, Taufkirchen, Germany) in drinking water from 3 months of age for 2 months to remove gut bacteria according to a published protocol (Liu, da Cunha et al. 2016). As controls, 3 or 22-month-old C57BL/6J female mice were treated in the same way. The water with antibiotics was changed every 7 days. In order to examine the off-target effects of oral antibiotics on neuroinflammation, we injected 5-month-old APP-transgenic mice via the peritoneal cavity daily for 7 days with 1.5 mg/kg/day vancomycin, 3 mg/kg/day ampicillin, neomycin and streptomycin according to the published protocol (Bercik, Denou et al. 2011) and 30 mg/kg/day metronidazole, as it has a high oral bioavailability (Jensen and Gugler 1983). Animal experiments were conducted in accordance with national rules and ARRIVE guidelines, and authorized by Landesamt für Verbraucherschutz, Saarland, Germany (registration numbers: 56/2015, 46/2017 and 34/2019) and Nanchang University, China.

5.3.2 Tissue collection

Animals were euthanized at 5 months of age by inhalation of overdose isoflurane or by *i.p.* injection of ketamine (100 mg/kg) / xylazine (10 mg/kg). After intracardial perfusion with ice-cold PBS, the brain was removed and divided along the anterior-posterior axis. The left hemisphere was immediately fixed in 4% paraformaldehyde (Sigma-Aldrich) in PBS and embedded in paraffin for immunohistochemistry. The olfactory bulb was first

removed from the right hemisphere, and the cortex and hippocampus were carefully separated from the brainstem, thalamus and striatum under microscope. A roughly 0.5-mm thick sagittal section of tissue was cut from the medial side of the tissue and homogenized in TRIzol (Thermo Fisher Scientific, Darmstadt, Germany) for RNA and DNA isolation. The remainder of the right hemisphere was snap-frozen in liquid nitrogen and stored at -80°C until biochemical analysis. The appendix together with a 0.5-cm-long segment of the neighboring colon was also collected, snap-frozen and stored at -80°C for isolation of intestinal bacteria.

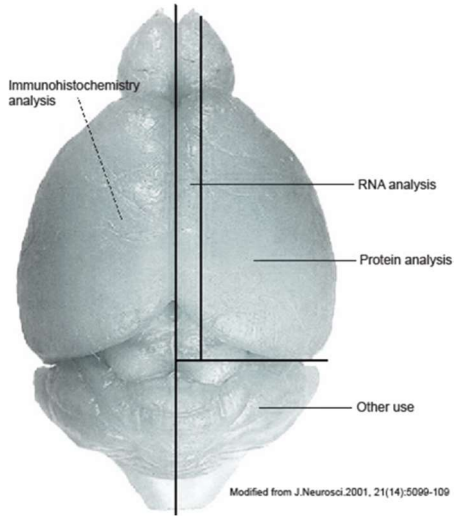

Fig. 5.3.2, Schematic diagram of the preparation of brain sample sections. The brain is divided into 4 parts. The left half of the brain was immediately fixed in 4% PFA and stored at 4°C for the immunohistochemical procedure. A 0.5 mm thick piece of brain tissue was sagittally cut from the right half of the brain and homogenized in Trizol for RNA isolation. The remainder of the right hemisphere was snap frozen in liquid nitrogen for biochemical analysis. The remaining portion was also frozen in liquid nitrogen.

5.3.3 Isolation of blood vessels

To isolate brain blood vessels, the cortex and hippocampus from 5-month-old APP-transgenic mice were carefully dissected and brain vessel fragments were isolated according to our published protocol (Quan, Luo et al. 2021). Briefly, brain tissues were homogenized in HEPES-contained Hanks' balanced salt solution (HBSS) and centrifuged at 4,400g in HEPES-HBSS buffer supplemented with dextran from *Leuconostoc spp*. (molecular weight ~70,000; Sigma-Aldrich) to delete myelin. The vessel pellet was re-

suspended in HEPES-HBSS buffer supplemented with 1% bovine serum albumin (Sigma-Aldrich) and filtered with 20 μm-mesh. The blood vessel fragments were collected on the top of filter and stored at -80°C for biochemical analysis.

The steps are as follows:

a) Solution preparation: B1, 5 ml of HEPES 1M in 500 ml of HBSS; B2, 0.9 g of Dextran 7000 in 5 ml of B1 (per hemisphere); B3, 5 g of BSA in 500 ml of B1.
b) The brain tissue was collected as described above, and the right hemisphere tissue was placed in a 15 ml tube containing 3 ml of cold B1 solution
c) Manual mincing of brain tissue in B1 solution using ophthalmic shears, followed by obtaining small pieces of approximately 2 mm.
d) Homogenize brain tissue using an automatic Dounce homogenizer with 20 strokes at 400 rpm. Always keep the glass tube on ice. Ensure the upper half of the douncer is kept in solution when moving up und down to aboud the production of air bubbles.If more than on sample is prepared, wash the douncer with ionized water between each homogenization.
e) Transfer the homogenate to a 15 ml polypropylene tube and centrifuge for 10 minutes at 4 °C at 2,000 g. A massive white interface (mainly myelin) will emerge on the top of the vessel pellet.
f) Discard the supernatant. The white interface and the vessel pellet will remain contained. Add 5 ml of ice-cold B2 solution to each tube and aggressively shake it for 1 minute.
g) Centrifuge again at 4,400 g for 15 minutes at 4 °C. The myelin will now form a dence white layer on the surface of the supernatant.
h) Hold the tube and slowly rotate it so that the supernatant passes along the tube wall, carefully separating the myelin layer from the tube wall. The supernatant is removed along with the myelin sheath and the particles containing the brain vessel attached to the bottom of the tube.
i) Blot the inside of the tube with absorbent paper wrapped around a 5 ml plastic pipette and remove any residual liquid, avoiding contact with the container particles. Place the tube upside down on the absorbent paper to drain the residual liquid.

j) Suspend the pellet in 1 ml of ice-cold B3 soultion by pipetting up and down with low-binding tips, keeping the tube on ice, then adding another 5 ml of B3 solution. Make sure that the vessels are dispersed as much as possible and do not form aggeregates.
k) Assembling the filter set, then place a 20 µm-mesh filter on the filter set on the top of a becker flask and equilibrate by applying 10 ml of ice-cold B3 solution.
l) Prepare a beaker on ice with 30 ml of ice-cold B3 solution. Cover with parafilm to avoid air contamination.
m) Rinse the membrane repeatly with 40 ml ice-cold B3 solution in a beaker, and pour the beaker content in a 50 ml plastic tube and centrifuge at 2,000 g for 10 minutes at 4 °C.
n) Add 1 ml of B3 solution to the tube to resuspend the precipitate, transfer to a 1.5 ml tube, centrifuge again at 2,00 g for 5 minutes 4 °C.
o) 50 µl of RIPA solution is added to the vessel precipitates and treated with an ultrasonic cracker for 1 minute. Protein levels of ABCB1, LRP1 and claudin-5 are detected by Westen blot.

5.3.4 Intestinal bacterial collection and 16S rRNA sequencing

Bacterial DNA was extracted from intestinal bacteria (100 mg) in the frozen cecum and colon with QIAamp Fast DNA Stool Mini Kit (Qiagen, Hilden, Germany). The amount of bacteria was evaluated by quantifying 16S rRNA with SYBR Green-based real-time PCR using the universal bacterial r16S gene primers (16S-V2-101F: 5-AGYGGCGIACGGGTGAGTAA-3, and 16S-V2-361R: 5-CYIACTGCTGCCTCCCGTAG-3) as it was conducted in a published study (Benakis, Brea et al. 2016). The V3 -V4 region of the 16S rRNA-encoding gene was then amplified with the barcode fusion primers (338F: 5-ACTCCTACGGGAGGCAGCAG-3, and 806R: 5-GGACTACHVGGGTWTCTAAT-3). After purification, PCR products were used for constructing libraries and sequenced on the Illumina MiSeq platform at Majorbio Co. Ltd. (Shanghai, China). The raw data was processed on Qiime2 (https://qiime2.org/), reducing sequencing and PCR errors, and denoising to get the operational taxonomic unit (OTU) consensus sequences, which were mapped to the 16S Mothur-Silva SEED r119 database (http://www.mothur.org/). Alpha diversity including Sobs, Shannon, Ace, Chao and Simpson indexes were used for the analysis of bacterial richness and diversity in a

single mouse. Principal coordinate analysis (PCoA) and analysis of similarity (ANOSIM) were used for β-diversity analysis to compare bacterial compositions on genus level between APP-transgenic mice with and without antibiotic treatments. The difference of bacterial compositions on genus level between these two groups were also compared with Wilcoxon rink sum test. All the analysis was performed using cloud-based tools with default analysis parameters (https://cloud.majorbio.com/page/tools.html).

5.3.5 Quantification of bacterial DNA in the brain tissue

DNA was extracted from the brain tissue using TRIzol (Thermo Fisher Scientific) according to the protocol provided by the company. To assess the presence and extent of bacterial dissemination into the brain, real-time PCR was conducted using universal bacterial 16S rRNA gene primers (16S-V2-101F and 16S-V2-361R), and primers targeted mouse *Gapdh* gene (sense, 5'-*ACAACTTTGGCATTGTGGAA*-3' and antisense, 5'-*GATGCAGGGATGATGTTCTG*-3') as an internal control.

The steps to isolate total DNA from brain tissue are as follows, according to the protocol provided by the company:

(1) 0.5-mm-thick tissue slide sagittally excised from the right hemisphere (see above in Tissue Preparation section 5.3.2) was homogenized in 1 ml of TRIzol in a 2-ml tube.
(2) For complete dissociation of the nucleoprotein complex, the homogenized sample was first incubated for 5 minutes ar toom temperature. Chloroform, 0.2 ml per ml TRIzol used, was added into the tube, which was the closed tightly and shaked vigorously ba hand for 15 seconds. The sample was then incubated at room temperature for 3 minutes. The resulting mixture was centrifuged at 12,000 g for 15 minutes at 4 °C. The sample mixture was separated into 3 phases: a lower red oraganic phase (containing protein), an interphase (containing DNA), and a upper colourless aqueous phase (containing RNA).
(3) The colourless aqueous phase was totally discharged. 300 µl of 100% ethanol was added per 1 ml TRIzol Reagent used before. The mixture was allowed to stand at room temperature for 2-3 minutes and centrifuged at 2,000 g for 5 minutes at 4 °C. The DNA was precipitated to a gel-like pellet on the bottom of the tube.

(4) The supernatant was thoroughly removed and the DNA pellet was resuspended in 1 ml of 0.1 M sodium citrate in 10% ethanol, pH 8.5 and incubated for 30 minutes at room temperature. The mixture centrifuged at 2,000 g for 5 minutes at 4 °C. The supernatant was removed and this step was repeated once.
(5) The DNA pellet was washed by adding 1 ml 75% ethanol and incubating for 15 minutes. After that the mixture was centrifuged at 2,000 g for 5 minutes at 4 °C.
(6) The supernatant was agein thoroughly removed. The DNA pellet was air dryed, and then resuspended in 0.3 ml of 8 mM NaOH by pipetting up and down. The mixture was centrifuged at 12,000 g for 10 minutes at 4 °C.
(7) The supernatant was collected in a new tube und pH was adjusted with HEPES to 7-8. The DNA was ready to use in realtime-PCR.

5.3.6 Positive selection of CD11b-positive and CD4-positive cells from the brain and spleen, respectively

The brain tissue (hippocampus and cortex) and spleen of 5-month-old APP-transgenic mice with and without treatments with antibiotics were prepared for single-cell suspensions using Neural Tissue Dissociation Kit (papain-based) and Spleen Dissociation Kit (mouse), respectively (Miltenyi Biotec GmbH, Bergisch Gladbach, Germany). After blocking with 50 µg/ml CD16/CD32 antibody (clone 2.4G2; BioXCell, Lebanon, USA), CD11b-positive brain cells were selected from the brain with microbeads-conjugated CD11b antibody (clone M1/70.15.11.5; Miltenyi Biotec) and CD4-positive spleen cells from the spleen with Dynabeads® magnetic beads-conjugated mouse CD4 antibody (clone L3T4; Thermo Fisher Scientific). Lysis buffer was immediately added to selected cells and total RNA was isolated using RNeasy Plus Mini Kit (Qiagen).

The steps for isolation CD11b-positive cells from the brain are as follows:
(1) Enzymatic Neural Tissue Dissociation
   a) Enzyme mix 1 and 2 were prepared for one brain tissue (upto 400 mg) as follows:
      i. Enzyme mixture 1 (for digestion): Enzyme P 50 µl + Buffer X 1900 ul
      ii. Enzyme mixture 2 (for dissolution of DNA)): Enzyme A 10 µl + Buffer Y 20 ul
   b) Enzyme mixture 1 was prewarmed in a 37 °C water bath for 10 minutes before use.

c) The weight of the brain tissue was measured in 1 ml of cold HBSS to ensure that the weight did not exceed 400 mg per digestion.
d) The meninges were removed. The brain tissue was minced into small pieces on a petri disch to facilitate enzyme dissociation.
e) The brain tissue pieces were transferred to a 15 ml tube containing 1950 ul prewarmed enzyme mixture 1 and incubated in a 37 °C water bath for 10 minutes under continuous rotation.
f) 30 µl enzyme mixture 2 was added to the sample, which was gently inverted und incubated at 37 °C water bath for another 10 minutes under slow, continuous rotation.
g) The digested tissue was filtered through a 70 µm strainer into a 50 ml tube and the filter was rinsed with 10 ml of HBSS. Ther filtered solution was then centrifuged at 700 g for 10 minutes at 4 °C.
h) The supernatant was removed and the pellet was resuspended in HBSS to obtain a concentration of 10^7 nucleated cells/ 80 µl for later use.

(2) Magnetic isolation of CD11b-positive cells

a) To reduce Fc receptor-mediated binding by antibody of CD11b, the cell suspension was incubated with 50 µg/ml CD16/CD32 antibody at 4 °C for 30 minutes, 10% fetal bovine serum (FBS) was added to prevent non-specific binding.
b) Microbeads-conjugated CD11b antibody was added to the cell suspension to obtain a final dilution volume accommodating 1:5. The mixture was then incubated at 4 °C for 15 minutes.
c) The cell suspension was washed 3 times with HBSS and finally resuspended up to 10^8 cells in 500 µl HBSS.
d) The tube containing the cell suspension was placed in the magnetic field of the MACS separater for 2 minutes. The unlabeled cells were discharged and the attached cells were rinsed 3 times.
e) The tube was removed from the MACS separater. Lysis buffer was immediately added to selected cells and total RNA was isolated using RNeasy Plus Mini Kit (Qiagen).

The steps for isolation CD4-positive cells from the spleen are as follows:

(1) Spleen Dissociation

a) Enzyme mixture was prepared by adding 50 µL of Enzyme D, and 15 µL of Enzyme A to 2.4 mL of 1× Buffer S.

b) Enzyme mixture 1 was prewarmed in a 37 °C water bath for 10 minutes before use.

c) The spleen was minced into small pieces on a petri disch to facilitate enzyme dissociation.

d) The spleen pieces were transferred to a tube containing the enzyme mixture and incubated in a 37 °C water bath for 30 minutes under continuous rotation.

e) The digested tissue was filtered through a 30 µm strainer into a 15 ml tube and the filter was rinsed with 2,5 ml of Buffer S. The filtered solution was then centrifuged at 300 g for 10 minutes at 4 °C.

f) The supernatant was removed and the pellet was resuspended in HBSS to obtain a concentration of 10^7 nucleated cells/ ml for later use.

(2) Magnetic isolation of CD4-positive cells

a) To reduce Fc receptor-mediated binding by antibody of CD4, the cell suspension was incubated with 50 µg/ml CD16/CD32 antibody at 4 °C for 30 minutes, 10% fetal bovine serum (FBS) was added to prevent non-specific binding.

b) Dynabeads® mouse CD4 antibody was added to the cell suspension to obtain a final dilution volume accommodating 1:40. The mixture was then incubated at 4 °C for 15 minutes.

c) The cell suspension was washed 3 times with HBSS and finally resuspended up to 10^8 cells in 500 µl HBSS.

d) The tube containing the cell suspension was placed in the magnetic field of the MACS separater for 2 minutes. The unlabeled cells were discharged and the attached cells were rinsed 3 times.

e) The tube was removed from the MACS separater. Lysis buffer was immediately added to selected cells and total RNA was isolated using RNeasy Plus Mini Kit (Qiagen).

5.3.7 Microglial Aβ phagocytosis assay

Methoxy-XO4 (Bio-Techne GmbH, Wiesbaden-Nordenstadt, Germany) can penetrate the blood-brain barrier and binds to β-sheet secondary structure of Aβ aggregates. If microglia engulf amyloid plaques actively, MeX04 will be internalized along with Aβ. Five-month-old APP-transgenic mice received an intraperitoneal injection after treatment with and without antibiotics according to a published protocol (Lau, Wu et al. 2021). Three hours later, a single cell suspension from the hippocampus and cortex was prepared using Neural Tissue Dissociation Kit (papain-based) (Miltenyi Biotec GmbH). After blocking with CD16/CD32 antibody (clone 2.4G2; BioXCell) and subsequent staining with PE-Cy5-conjugated CD11b antibody (clone M1/70; Thermo Fisher Scientific), fibrillar Aβ-containing CD11b-positive brain cells were detected by BD FACSVerse™ flow cytometry (BD Biosciences; Heidelberg, Germany).

The steps are as follows:

(1) In vivo labelling of amyloid plaques
   Methoxy-XO4 solution (2 mg/ml in a 1:1 mixture of DMSO and 0.9% NaCl [pH 12] (v/v)) was intraperitoneal injected at a weight adapted dose of 10 mg/kg.
(2) Brain dissociation and microglia staining
   a) Brain dissociation war performed as described in section 5.3.6
   b) To reduce Fc receptor-mediated binding by antibody of CD11b, the cell suspension was incubated with 50 µg/ml CD16/CD32 antibody at 4 °C for 30 minutes, 10% fetal bovine serum (FBS) was added to prevent non-specific binding.
   c) PE-Cy5-conjugated CD11b antibody was added to the cell suspension to obtain a concentration of 1.25 µg/ml. The mixture was then incubated at 4 °C for 60 minutes under gentle rotation.
   d) AD transgenic mice was used as unstained controls. Non-transgenic wild-type mice were used as flurescence-minus-one controls.
(3) Flow cytometry protocol according to our previous study (Luo, Schnoder et al. 2022)
   a) The following diagram were created in the template:
      i. Side-scatter (SSC) versus forward-scatter (FCS) to identify cell populations

ii. Pulse width trigger versus FSC to identify singlets
iii. PB660 versus FSC-A to identify CD11b signal
iv. PB450 versus PB660 to identify Methoxy-XO4 signal

b) A negative signal was set for Methoxy-XO4 using a non-transgenic mouse brain sample and a negative signal for CD11b using an unstained control sample.
c) Each sample was sequentially performed and Methoxy-XO4 signals were recorded for 10,000 microglia using BD Trucount absolute counting tubes (BD Biosciences).
d) Using FlowJo to analyze the data, the following information was obtained:
   i. Proportion of Methoxy-XO4 positive microglia= proportion of Aβ phagaocytotic microglia
   ii. Mean fluorescence intensity of Methoxy-XO4= Aβ phagocytic capacity

5.3.8 Flow cytometric detection of IL-17a-eGFP reporter in intestinal cells

A published protocol (Couter and Surana 2016) was used to prepare single cell suspensions from both lamina propria and Peyer's patches of the small intestine of 5-month-old $APP^{tg}/Il17a^{GFP/wt}$ mice with and without two months of antibiotic treatment. After staining with APC-conjugated rat anti-CD4 monoclonal antibody (clone: GK1.5; Thermo Fisher Scientific), eGFP-expressing CD4-positive cells were detected by BD FACSCanto™ II flow cytometry (BD Biosciences).

The steps for isolation the intestinal cells are as follows:

(1) Preparation of Solutions
   a) Extraction media (per small intestine): 30 ml RPMI + 93 µl 5% (w/v) dithiothreitol (DTT) + 60 µl 0.5 M EDTA + 500 µl FBS. Add the DTT immediately before use.
   b) Digestion media (per small intestine): 25 ml RPMI + 12.5 mg dispase + 37.5 mg collagenase II + 300 µl FBS. Add the dispase and collagenase immediately before use.
   c) For all incubations performed at 37 °C, prewarm solutions to 37 °C.
(2) Preparing a single cell suspension from the small intestinal lamina propria
   a) Mice were euthanized by inhalation of isoflurane followed by cervical dislocation.

b) The abdominal cavity was exposed by an incision along the midline of the abdomen with scissors and the small intestine and stomach were separated at the pyloric sphincter. Then the small intestine was gently removed in sequence and incised again at the ileo-cecum junction. Place the isolated small intestine in a 4 °C RPMI with 10% FBS.
c) The small intestine was placed on a paper towel moistended with RPMI and the fat was removed from the tissue with a blunt knife to remove residual fat.
d) Gently flush the intestine with 15-20 ml of cold PBS using a syringe with a 18g needle to remove the intestinal contents.
e) Peyer's patches were excised with scissors and collected in cold RPMI containing 5% FBS. Peyer's patches are located on the antimesenteric side of the small intestine and appeared as multilobed white masses.
f) Cut the small intestine into 6-8 cm pieces.
g) Insert a corved forceps into the intestinal fragment, grasp the distal end of the tissue and turn the tissue inside out.
h) Tissue pieces were incubated in a 50 ml tube containing 30 mil of extractions medium und stirred at 500 rpm for 15 minutes at 37 °C on a shaker.
i) After incubation, the tissue pieces were collected with a steel strainer. Then the tissue pieces were placed on a dry paper towel und turned over several times to facilitate removal of residual mucus.
j) Tissue fragments were placed in 1.5 ml tubes containing 600 µl of digestion medium and chopped with scissors until the fragments no longer adhered to the scissors to facilitate the digestion.
k) The minced small intestine was transferred into a 50 ml tube containing 25 ml of digestion medium, stirred at 500 rpm for 30 minutes at 37 °C on a shaker.
l) The digested tissues were filtered through a 100 µm strainer into a 50 ml tube and the filter was rinsed with 20 ml of RPMI containing 10% FBS. Ther filtered solution was centrifuged at 700 g for 10 minutes at 4 °C.
m) The supernatant was removed and the pellet was resuspended in 1 ml of RPMI containing 10% FBS.
n) The suspended cells were filtered into a 50 ml tube through a 40 µm cell strainer and the filter was rinsed with 20 ml of RPMI containing 10% FBS. Ther filtered solution was centrifuged at 700 g for 10 minutes at 4 °C.

o) The supernatant was carefully decanted and the pellet was resuspended in 1 ml of RPMI containing 2% FBS for later use.

(3) Preparing a single cell suspension from Peyer's patches

a) Peyer's patches were transferred to a 15 ml tube containing 2 ml of digestion medium and stirred at 500 rpm for 10 minutes at 37 °C on a shaker.

b) The digested Peyer's patches were then filtered into a 50 ml tube using a 40 µm cell strainer and the filter was rinsed with 10 ml of RPMI containing 10% FBS. Ther filtered solution was centrifuged at 700 g for 10 minutes at 4 °C.

c) The supernatant was carefully decanted and the pellet was resuspended in 1 ml of RPMI containing 2% FBS for later use.

5.3.9 Histological analysis

Serial 50-µm-thick sagittal sections were cut from the paraffin-embedded hemisphere. Four neighboring sections with 300 µm of interval were deparaffinized, labeled with rabbit anti-ionized calcium-binding adapter molecule (Iba)-1 antibody (Wako Chemicals, Neuss, Germany) and VectaStain *Elite* ABC-HRP kit (Cat.-No.: PK-6100, Vector Laboratories, Burlingame, USA), and visualized with diaminobenzidine (Sigma-Aldrich). Iba-1-positive microglia/brain macrophages were counted with Optical Fractionator in the hippocampus on a Zeiss AxioImager.Z2 microscope (Carl Zeiss Microscopy GmbH, Göttingen, Germany) equipped with a Stereo Investigator system (MBF Bioscience, Williston), as we did previously (Liu, Liu et al. 2014).

To evaluate the cerebral Aβ level, after deparaffinization, 4 serial brain sections from each animal were stained with rabbit anti-human Aβ antibody (clone D12B2; Cell Signaling Technology Europe, Frankfurt am Main, Germany) and Cy3-conjuagted goat anti-rabbit IgG (Jackson ImmunoResearch Europe Ltd. Cambridge, UK), or with methoxy-XO4 (Bio-Techne GmbH). After mounting, the whole section including hippocampus and cortex was imaged with Microlucida (MBF Bioscience) and merged. The positive staining and brain region analyzed were measured for the area with Image J tool "Analyse Particles" (https://imagej.nih.gov/ij/). The threshold for all compared samples was manually set and kept constantly. The percentage of Aβ coverage in the brain was calculated.

To determine the density of CD68-positive microglia, serial brain sections were stained with rabbit anti-CD68 antibody (clone E3O7V; Cell Signaling Technology Europe) and Cy3-conjugated goat anti-rabbit IgG (Jackson ImmunoResearch Europe Ltd.). Since the single CD68-positive cell could not be clearly recognized (see Fig. 6.7) and reliably counted, the percentage of CD68 coverage in the brain was calculated as for Aβ.

The steps for immunostaining are as follows:

(1) Paraffin-embedded slides deparaffinazation and rehydration

Paraffin-embedded brain tissue blocks were cut into 50 µm sentions. The slides were dryed at 37 °C overnight und 60 °C for 60 minutes before use. The slides were deparaffinised sequentially in the solutions: 2x 10 minutes xylene, 2x10 minutes 100% ethanol, 5 minutes 96% ethanol, 5 minutes 70% ethanol and 5 minutes 50% ethanol. Then the slides were re-hydrated by rinsing in distilled water for 30 seconds, repeated 3 times.

(2) Antigen retrieval

The slides were put in citrate buffer (10mM Sodium Citrate, pH=6,0) und cooked in a steamer for 30 minutes.

(3) Blocking of endogenous peroxidase by using the HRP conjugate for detection

After cooling to roome temperature the slides were rinsed 3 times with distilled water und incubated for 30 minutes in a mixture of H_2O_2 and methanol with the final concentration of 0.3% H_2O_2 and 17% methanol. The slides were then rinsed 3 times with distilled water.

(4) Immunostaining

a) To minimize the cross-react with endogeneous immunglobuline in the tissue, the slides were incubated in the blocking buffer (0.2% casein (w/v) + 0.1% Tween 20 + 0.1% Triton X in PBS) at room temperature for 60 minutes.

b) The slides were then incubated sequentially in the primary antibody at 4 °C overnight und und secondary antibody at room temperature for 60 minutes, diluted as following in diluting buffer (0.02% casein (w/v) + 0.01% Tween 20 + 0.01% Triton X in PBS), respectively. The slides were rinsed in PBST 10 minutes x 3 times after each incubation.

Primary antibody	Secondary antibody
Rabbit anti Iba (Wako Chemicals, Neuss, Germany) Dilution v/v: 1:500	Cy3-conjuagted goat anti-rabbit IgG (Jackson ImmunoResearch Europe Ltd. Cambridge, UK) Dilution v/v: 1:200
Rabbit anti-human Aβ antibody (clone D12B2; Cell Signaling Technology Europe, Frankfurt am Main, Germany) Dilution v/v: 1:1600	Cy3-conjuagted goat anti-rabbit IgG (Jackson ImmunoResearch Europe Ltd. Cambridge, UK) Dilution v/v: 1:200
Rabbit anti-CD68 antibody (clone E3O7V; Cell Signaling Technology Europe) Dilution v/v: 1:200	Cy3-conjugated goat anti-rabbit IgG (Jackson ImmunoResearch Europe Ltd. Cambridge, UK) Dilution v/v: 1:200

c) The slides incubated with Iba-Antibody were visualized with the VectaStain *Elite* ABC-HRP kit (Cat.-No.: PK-6100, Vector Laboratories, Burlingame, USA), using the protocol provides by the company. The slides were counter-staine with hematoxylin. Then they were de-hydrated by passing a sery of 50% ethanol, 70% ethanol, 95% ethanol, 100% ethano x 2 times and 100% xylene x 2times. Finaly they were mounted in Entlan, covered with coverslip and ready to be analysized.

d) The slides incubated with anti-human Aβ antibody or anti-CD68 antibody were mounted with Moviol with DAPI, covered with coverslip and ready to be analysized.

The steps for Methoxy-X40 staining are as follows:

(1) The stock solution of Methoxy-X40 was prepared by dissolve Methoxy-X40 powder in DMSO at a concentration of 10 mM and stored at -20 °C. The working solution was prepared before use by diluting the stock solution 1:1000 (v/v) with a 1:1 (v/v) mixture of DMSO and 0,9% NaCl solution.

(2) The slides were de-paraffinized und re-hydrated as described. The antigen retrieval was processed by cooking the slides in citrate buffer (10mM Sodium Citrate, pH=6.0) in a steamer for 60 minutes.

(3) The slides were incubated in the Methoxy-X40 working solution for 20 minutes.

(4) After rinsing in PBST for 10 minutes x 3 times the slides were mounted with Moviol with DAPI, covered with coverslip and ready to be analysized.

5.3.10 Analysis of microglial morphology

For the analysis of microglial morphology, our established protocol and Fiji Image J were used (Luo, Schnoder et al. 2022). Paraffin-embedded 50-µm sagittal brain sections were used as described above. After fluorescent co-staining with Iba-1 and Aβ antibodies, total 10 Aβ plaques/mouse were randomly selected from the cortex dorsal to hippocampus and imaged under 40× objective with Z-stack scanning with 1 µm of interval. The serial images were Z-projected with maximal intensity, 8-bit grayscale transformed, Unsharp-Mask filter and despeckle-treated, and binarized to obtain a black and white image. The cells with complete nucleus and branches and without overlapping with neighboring cells were chosen for analysis. The single-pixel background noise was eliminated and the gaps along processes were filled under the view of the original image of the cell. The processed image was skeletonized and analyzed with the plugin Analyze Skeleton (2D/3D) (http://imagej.net/AnalyzeSkeleton) for the total number of primary branches, length of all branches, and the number of branch endpoints of each microglia. The whole analysis was done blinded to genotypes.

5.3.11 β- and γ-secretase activity assays

(1) Purification of membrane components

Membrane components were purified from mouse brains according to our previous studies (Hao, Liu et al. 2011, Xie, Liu et al. 2013). Briefly, brain tissue was homogenized in sucrose buffer (10 mM Tris/HCl, pH 7.4, 1 mM EDTA, 200 mM sucrose) by 10 subsequent passages through 24- and 27-gauge needles. Cell nuclei were removed by centrifugation at 1000*g* at 4 °C for 10 minutes. The supernatant was transferred to a new tube and centrifuged again at 10,000*g* at 4 °C for 10 minutes. Finally, the resulting supernatant was centrifuged at 187,000*g* at 4 °C for 75 minutes in an Optima MAX Ultracentrifuge (Beckman Coulter, Krefeld, Germany). The supernatant was discharged and the pellet containing the crude membrane fraction was stored at −80 °C until use.

(2) β- and γ-secretase activity assays

β- and γ-Secretase activities were measured by incubating the crude membrane fraction with secretase-specific substrates based on fluorescence resonance energy transfer according to our previous study (Xie, Liu et al. 2013). At 37 °C and in buffers with different pH values, both secretases cleaved the fluorogenic substrates resulting in continuous accumulation of fluorescence signals that were quantified by measurements obtained using a Tecan Infinite M200 microplate reader (Männedorf, Switzerland).

For measurement of β-secretase activity, the crude membrane fraction was resuspended in 500-µL β-secretase assay buffer (0.1 M sodium acetate, pH 4.5). The protein concentration of each sample was determined using the Bio-Rad Protein Assay (Bio-Rad Laboratories). The final concentrations for the β-secretase assay were: 0.1 mg/mL membrane protein (125 µg protein per well in 96-well plates), 10% dimethyl sulfoxide, and 8 µM β-secretase substrate IV (Calbiochem, Darmstadt, Germany). Excitation wavelength was set at 350 nm (9 nm of bandwidth) and emission wavelength at 490 nm (bandwidth 20 nm).

For measurement of γ-secretase activity, the crude membrane fraction was resuspended in 500 µL γ-secretase assay buffer (50 mM Tris/HCl, pH 6.8, 2 mM EDTA). Protein concentration was determined as already described herein. Final concentrations for the γ-secretase assay were: 1 mg/mL membrane protein (1250 µg protein per well in 96-well plates) and 8 µM γ-secretase substrate (Calbiochem). Excitation wavelength was set at 355 nm (9 nm of bandwidth) and emission wavelength at 440 nm (bandwidth 20 nm).

For both secretase assays, kinetics were performed at 37 °C and fluorescence intensity in each well was measured for 73 cycles with intervals of 5 minutes. Fluorescence intensity of the first cycle was considered as background and subtracted for each well.

5.3.12 Western blot analysis

Frozen brain tissues and blood vessel isolates were homogenized on ice in radioimmunoprecipitation assay buffer (RIPA buffer consistend of 50mM Tris [pH 8.0], 150 mM NaCl, 0.1% SDS, 0.5% sodiumdeoxy-cholate, 1% NP-40, and 5mM EDTA) supplemented with protease inhibitor cocktail (Roche Applied Science, Mannheim, Germany). The proteins were separated by 10% or 12% Tris-glycine SDS/PAGE. Before loading on PAGE gel, vessel preparations were sonicated. Western blots were performed using rabbit monoclonal antibody against ABCB1 (clone E1Y7S) and rabbit polyclonal antibody against LRP1 (Cat.-No.: 64099) (both antibodies were bought from Cell Signaling Technology), as well as rabbit polyclonal antibody against claudin-5 (Cat.-No.: GTX49370; GeneTex, Hsinchu, China). The detected proteins were visualized via the Plus-ECL method (PerkinElmer, Waltham, USA). To quantify proteins of interest, rabbit monoclonal antibody against β-actin (clone 13E5) or rabbit polyclonal antibody against α-tubulin (Cat.-No.: 2144) (both antibodies were from Cell Signaling Technology) was used as a protein loading control. Densitometric analysis of band densities was performed with Image-Pro Plus software version 6.0.0.260 (Media Cybernetics, Rockville, MD). For each sample, the protein level was calculated as a ratio of target protein/loading control per sample.

The detailed steps are as follows, according to our previous study (Luo, Schnoder et al. 2022):

(1) Sample preparation

Frozen brain tissues were homogenized on ice in radioimmunoprecipitation assay buffer (RIPA buffer consistend of 50mM Tris [pH 8.0], 150 mM NaCl, 0.1% SDS, 0.5% sodiumdeoxy-cholate, 1% NP-40, and 5mM EDTA) supplemented with protease inhibitor cocktail (Roche Applied Science, Mannheim, Germany), and then centrifuged ar 16,000 g for 30 minutes at 4°C to collect the supernatant ccontaining the protein mixture. Isolated blood vessels were directly lysed in 2x sodium dodecyl sulfate-polyacrylamide gel electrophoresis (SDS-PAGE) sample loading buffer dontaining 4% SDS and ultrasonically lysed on ice for 1 minutes before loading. The protein concentrations were messured using the Bio-Rad assay, ensuring consistent concentrations between samples and adding about 30 µg of total protein to each well.

Samples were diluted at 1:2 (v/v) in 3x SDS-PAGE loading buffer and heated at 96°C for 5 minutes.

(2) Electrophoretic separation of proteins bei SDS-PAGE

a) Gel preparation

The electrophoretic separation of proteins is mot generally carried out in polyacrylamide gels. These gels are cast between glass plates by polymerizing the acrylamide monomer solution into polyacrylamide chains and simultaneously cross-linking the chains into a semisolid matrix. A completed gel consists of a lower separating gel and an upper stacking gel. By varying the concentrations of polyacrylamide and crosslinker, the pore size of the separating gel may be altered. 10% or 12% separating gel and 5% stacking gel were used in our study.

b) Electrophoresis

The SDS-PAGE system used in our study was the Mini-PROTEAN®3 Cell electrophoresis system (Bio-Rad). The first step was to place the prepared gel into the electrophoresis spparatus, then to pour the electrophoresis buffer intro the electrophorator, and to make sure the buffer completely covered the gel. After carefully removing the comb the marker (5 µl) or sample (20 µl) were loaded into each well separately. The electrophoresis was firstly run at 80 V for 30 minutes, then at 120 V until the bromophenol blue flew away from the gel.

c) Electrotransfer

The gel was first equilibrated in transfer buffer, cushioned by a pad and then compacted together by a support grid in a 'transfer sandwich' (filter paper-gel-membrane-filter paper). In our study, we used polyvinylidene fluoride (PVDF) membrane (soaked in methanol for 1 minutes before use) with 0.2 µm or 0.4 µm pore size depending on the size of the target protein. The sandwich was placed vertically in the transfer apparatus in a transfer chamber, filled with transfer buffer (pre-cooled at 4°C). The transfer was performed at 250 mA for 90 to 120 minutes.

(3) Western blot

a) The membrane with immobilized proteins was blocked the 10% skimmed milk powder (w/v) in PBS for 60 minutes at room temperature to seal the non-specific bindung sites.

b) The membrane was incubated with the primary antibody diluted in 1% skimmed mikl powder (w/v) overnight at 4°C on a shaker. The primary antibodies were

rabbit monoclonal antibody against ABCB1 (clone E1Y7S, Cell Signaling Technology) and rabbit polyclonal antibody against LRP1 (Cat.-No.: 64099, Cell Signaling Technology), as well as rabbit polyclonal antibody against claudin-5 (Cat.-No.: GTX49370; GeneTex, Hsinchu, China). Rabbit monoclonal antibody against β-actin (clone 13E5, Cell Signaling Technology) or rabbit polyclonal antibody against α-tubulin (Cat.-No.: 2144, Cell Signaling Technology) was used as a protein loading control.

c) On the following day, the membrane was washed with 3x 10 minutes in TBS + 0.05% Tween 20 to remove the residual primary antibody.
d) The membrane was the incubated with a secondary antibody diluted in PBS + 1% skimmed milk powder (w/v) at room temperature for 2 hours.
e) The membrane was washed with 3x 10 minutes in TBS + 0.05% Tween 20 to remove the residual secondary antibody.
f) The membrane was then developed by using the Plus-ECL method (PerkinElmer, Waltham, USA), according to the instructions provided by the company.

5.3.13 Brain homogenates and ELISA assays of Aβ and Il-1β and Tnf-α

The frozen brain hemispheres were homogenized and extracted serially in Tris-buffered saline (TBS), TBS plus 1% Triton X-100 (TBS-T), guanidine buffer (5 M guanidine HCl/50 mM Tris, pH 8.0) as described in our previous study (Liu, Liu et al. 2014). Aβ concentrations in three separate fractions of brain homogenates were determined by Invitrogen™ Amyloid β 42 and 40 Human ELISA kits (Cat.-No.: KHB3441 and KHB3481, respectively; both from Thermo Fisher Scientific). Results were normalized on the basis of the sample's protein concentration.

We measured concentrations of Il-1β and Tnf-α in TBS-soluble brain homogenates with ELISA kits (Cat.-No.: DY401 and DY410, respectively, from R&D systems, Minneapolis, USA). The results were also adjusted by the protein concentration in the same sample.

The detailed steps for extraction of Aβ into TBS-soluble, TBS-T-soluble and guanidine-soluble fractions are as follows:

(1) TBS-soluble fraction

a) The TBS extraction buffer was prepared by adding one tab of protease inhibitor cocktail to 10 ml steril 1x TBS.
b) The frozen brain tissue was weight and kept on ice until homogenization.
c) Ice-cold TBS extraction buffer was added as four brain volumes (4 µl/mg brain tissue) into a 2 ml Porter Elvehjem (PE) homogenizer containing the brain tissue.
d) The brain tissue was bounce-homogenized in the TBS extraction buffer and then centrifuged at 16,000 g for 30 minutes at 4 °C.
e) The supernatant was collected as the TBS-soluble fraction and stored at -80 °C for the ELISA assays.

(2) TBS-T-soluble fraction

a) The pellet was re-suspended with four volumes (based on the initial weight) ice-cold TBS-T.
b) The remaining residue was lysed by sonication for 5 minutes in a 4 °C water bath.
c) The mixture was centrifuged at 16,000 g for 30 minutes at 4 °C.
d) The supernatant was collected as the TBS-T-soluble fraction and stored at -80 °C for the ELISA assays.

(3) Guanidine-soluble fraction

a) The guanidine buffer was prepared by dissolving guanidine hydrochloride in 50 mM Tris-solution to obtain a final concentration of 0.5 M and the pH was adjusted to 8.0.
b) The pellet was extracted using four volumes of ice-cold guanidine buffer und lysing bei continuous rotating at 4 °C overnight.
c) The mixture was centrifuged at 16,000 g for 30 minutes at 4 °C.
d) The supernatant was collected as the guanidine-soluble fraction and stored at -80 °C for the ELISA assays.

The detailed steps for ELISA assay of Aβ are as follows, according to the protocol provided by the company:

(1) Preparation of solutions

a) The Aβ40 standard reconstitution buffer was prepared by dissolving 2.31 g sodium bicarbonate in 500 ml deionized water and adjusting the pH to 9.0 to obtain a final cencentration of 55 mM $NaHCO_3$ buffer.

b) The wash buffer (1x) was prepared bei diluting the wash buffer concentrate (25x), provided in the kit, with deionized water.

(2) Dilution of standards

a) The human Aβ40 standard was reconstitued by serially diluting the human Aβ40 in reconstitution buffer at the following concentrations: 500, 250, 125, 62.5, 31.25, 15.63, 7.81, and 0 pg/ml.

b) The human Aβ42 standard was reconstitued by serially diluting the human Aβ42 in deionized water at the following concentrations: 1000, 500, 250, 125, 62.5, 31.25, 15.63, and 0 pg/ml.

(3) Sample preparation

a) The sample concentration was adjusted within the standard curve range by using standard diluting buffer provided in the kit.

b) In our study, we diluted the TBS-soluble fraction 1:1 (v/v), the TBS-T-soluble fraction 1:4 (v/v), and the guanidine-soluble fraction 1:100 (v/v).

(4) Binding antigen and adding detector

a) 50 µl of standards, controls or samples was added to the plate wells. The wells for chromogenic blanks were kept empty.

b) 50 µl of human Aβ40 or Aβ42 detection antibody solution was added in to each well, except the chromogenic blanks.

c) The solutions were mixed by taping the side of the plate, which was then covered with a plate cover and incubated at 4 °C overnight with shaking.

d) On the following day, the solution was thoroughly aspirated. The wells was washed 4 times with 1x wash buffer.

(5) Adding Anti-rabbit IgG HRP solution

a) The anti-rabbit IgG HRP solution was prepared by diluting the anti-rabbit IgG HRP concentrate (100x) with the HRP diluent provided in the kit to obtain a 1x solution. The solution was prepared 15 minutes before use.

b) 100 µl of anti-rabbit IgG HRP solution (1x) was added to each well, except the chromogenic blanks.

c) The plate was then covered with a plate cover and incubated at room temperature for 30 minutes.

d) The solution was thoroughly aspirated. The wells was washed 4 times with 1x wash buffer.

(6) Adding substrate solution
   a) 100 μL stabilized Chromogen was added to each well. The substrate solution began to turn blue.
   b) The plate was incubated for 30 minutes at room temperature in the dark.

(7) Adding stop solution
   a) 100 μL Stop Solution was added to each well. The solution were mixed by taping the side of the plate.
   b) The solution in the well changed from blue to yellow.

(8) Reading the plate and generating the standard curve
   a) The plate was read the absorbance at 450 nm within 2 hours after adding the Stop Solution.
   b) The curve-fitting software was used to generate the standard curve.
   c) The concentrations for unknown samples and controls were read from the standard curve. Value(s) obtained for sample(s) was multiplied by the appropriate factor to correct for the sample dilution.

The detailed steps for ELISA assay of Il-1β or Tnf-α are as follows, according to the protocol provided by the company:

(1) Plate Preparation
   a) The Capture Antibody was diluted to the working concentration in PBS without carrier protein. The 96-well microplate was immediately coated with 100 μL per well of the diluted Capture Antibody. The plate was sealed and incubated overnight at room temperature.
   b) Each well was aspirated and washed with Wash Buffer, 3 times.
   c) The plate was blocked by adding 300 μL of Reagent Diluent to each well and incubated at room temperature for a minimum of 1 hour.
   d) Each well was aspirated and washed with Wash Buffer, 3 times. The plate was then ready for sample addition.

(2) Assay Procedure
   a) 100 μL of sample or standards was added per well. The plate was covered with an adhesive strip and incubated 2 hours at room temperature.
   b) Each well was aspirated and washed with Wash Buffer, 3 times.

c) 100 µL of the Detection Antibody, diluted to working dilution by Reagent Diluent was added to each well. The plate was covered with a new adhesive strip and incubated 2 hours at room temperature.
d) Each well was aspirated and washed with Wash Buffer, 3 times.
e) 100 µL of the working dilution of Streptavidin-HRP was added to each
f) well. The plate was covered and incubated for 20 minutes at room temperature in dark
g) Each well was aspirated and washed with Wash Buffer, 3 times.
h) 100 µL of Substrate Solution was added to each well. The plate was incubated for 20 minutes at room temperature in dark.
i) 50 µL of Stop Solution was added to each well. The solutions were mixed by gently taping the plate.
j) The optical density of each well was determined immediately, using a microplate reader set to 450 nm.

5.3.14 Quantitative PCR for analysis of gene transcripts

Total RNA was isolated from mouse brains with TRIzol (Invitrogen) or from selected CD11b or CD4-positive cells with RNeasy Plus Mini Kit (Qiagen) and reverse-transcribed. Gene transcripts were quantified with established protocols (Liu, Liu et al. 2014, Hao, Decker et al. 2016) and Taqman gene expression assays of mouse *Tnf-α*, *Il-1β*, *Chemokine (C–C motif) ligand 2* (*Ccl-2*), *Il-10*, *Chitinase-like 3* (*Chi3l3*), *Mannose receptor C type 1* (*Mrc1*), *Apoe*, *Trem2*, *P2ry12*, *Cx3cr1*, *Lpl*, *Clec7a*, *Itgax*, *Il-17a*, *Ifn-γ*, *Il-4*, *Neprilysin* and *Insulin-degrading enzyme* (*Ide*), *Activity-regulated cytoskeleton-associated protein* (*Arc*), *Glutamate ionotropic receptor NMDA type subunit 1* (*Grin1*), *Brain derived neurotrophic factor* (*Bdnf*), and *Gapdh* (Thermo Fisher Scientific).

The steps to isolate total RNA from brain tissue are as follows, according to the protocol provided by the company:

(1) 0.5-mm-thick tissue slide sagittally excised from the right hemisphere (see above in Tissue Preparation section 5.3.2) was homogenized in 1 ml of TRIzol in a 2-ml tube.
(2) For complete dissociation of the nucleoprotein complex, the homogenized sample was frist incubated for 5 minutes ar toom temperature. Chloroform, 0.2 ml per ml

TRIzol used, was added into the tube, which was the closed tightly and shaked vigorously ba hand for 15 seconds. The sample was then incubated at room temperature for 3 minutes. The resulting mixture was centrifuged at 12,000 g for 15 minutes at 4 °C. The sample mixture was separated into 3 phases: a lower red oraganic phase (containing protein), an interphase (containing DNA), and a upper colourless aqueous phase (containing RNA).

(3) The colourless aqueous phase was transferred to a fresh tube and mixed with 0.5 ml isopropyl alcohol per ml TRIzol used before. The mixture was allowed to stand at room temperature for 10 minutes andcentrifuged at 12,000 g for 10 minutes at 4 °C. The RNA was precipitated to a gel-like pellet on the bottom of the tube.

(4) The supernatant was thoroughly removed and the RNA pellet was washed by adding 1 ml 75% ethanol. After votexing the mixture was centrifuged at 12,000 g for 5 minutes at 4 °C.

(5) The supernatant was agein thoroughly removed. The RNA precipitante was dryed briefly, and then dissolved in an appropriate volume of RNase-free water. For one sample of brain tissue 100 µl was typically needed.

The steps to isolate total RNA from selected cells are as follows, according to the protocol provided by the company:

(1) The selected cells were lysed in 700 µl Buffer RLT Plus and vortexed for 30 seconds.

(2) The homogenized lysate was tranfered to a gDNA eliminator spin column placed in a 2 ml collection tube. The lysate was centrifuged at 8,000 g for 30 seconds at 4 °C.

(3) The column was discharged. To the flow-through, 700 µl of 70% ethanol was added. The solution was mixing thoroughly by pipetting.

(4) The mixture, including any precipitate, was transferred to a RNeasy spin column placed in a 2 ml collection tube and centrifuged at 8,000 g for 30 seconds at 4 °C. The flow-through was discharged.

(5) 700 µl Buffer RPE was added to the RNeasy spin column in the 2 ml collection tube. The whole system was centrifuged at 8,000 g for 30 senconds at 4 °C. The flow-through was discharged.

(6) 500 µl Buffer RW1 was added to the RNeasy spin column in the 2 ml collection tube. The whole system was centrifuged at 8,000 g for 30 senconds at 4 °C. The flow-through was discharged. The step was repeated once to wash the spin column. After

discharge the flow-through for the second time, the whole system was centrifuged at 12,000 g for 1 minute at 4 °C to further dry the membrane.

(7) The RNeasy spin column was placed in anew 1.5 ml collection tube. 30 µl RNase-free water was directly added to the spin column membrane. The whole system was centrifuged at 8,000 g for 1 minutes at 4 °C to elute the RNA.

Genomic DNA was degradated prior to the RT-PCR by using the RQ1 Rnase-free Dnase (Promega, Mannheim Germany).

(1) The reaction was set up as follows:

Components	Volume/ 10µl reaction
RNA sample in water	8 µl
RQ 1 Rnase-free DNase 10x Reaction Buffer	1 µl
RQ 1 Rnase-free DNase	1 U/ µg RNA
Nuclease-free water	To a final volume of 10 µl

(2) The mixure was incubated at 37 °C for 30 minutes. The reaction was then terminated by adding 1 µl of RQ1 DNase Stop solution. DNase was inactived by heating at 65 °C for 10 minutes.

First-strand cDNA was synthesized by priming total RNA with hexamer random primers (Invitrogen) and using Maxima Reverse Transcriptase (ThermoFisher Scientific).

(1) The reaction was set up as follows:

Components	Volume/ 20µl reaction
Total RNA	3 µg
Random primer (250 ng/µl)	1 µl
dNTP mix (10 mM each)	1 µl
Nuclease-free water	To a final volume of 15 µl

(2) The mixure was incubated at 65 °C for 5 minutes and then cooled down on ice for 2 minutes.

(3) The reaction was further performed by adding 4 µl of 5x RT buffer und 1 µl (200U) Maxima H Minus reverse Transcriptase. The mixure was incubated at 25 °C for 10 minutes, followed by 30 minutes at 50 °C.

(4) The reaction was then terminated by heating at 85 °C for 5 minutes. The cDNA was then ready for use.

To quantify the gene transcription, real-time quantitative PCR with the Taqman® gene expression assay was performed using the 7500 Fast real-time PCR system (Applied Biosystems) with a DyNAmo™Flash Probe q PCR kit (Roche Applied Science).

(1) The reaction was set up as follows:

Components	Volume
2x DyNAmo™Flash Probe Master Mix	10 µl
Primer Mix (10 µM)	1 µl
50x ROX reference dye	0.06 µl
cDNA	1 µl
dd H_2O	To a final volume of 20 µl

(2) The reaction was performed as follows:

Steps	Temperature	Time	Cycles
Initial denaturation	95 °C	10 minutes	1
Denaturation	95 °C	10 seconds	45
Annealing and extension	60 °C	30 seconds	

(3) By detecting the free FAM dye cleaved from the Taqman® probe, the amount of double-strand PCR product generated in each cycle may be determined. The threshold dycle (Ct) value for each gene tested in the replicate PCR was normalized to the Ct value of the *gapdh* RNA control from the same cDNA preparations. The ratio of transcription of each gene was calculated as $2(\Delta Ct)$, where ΔCt is the difference Ct (*gapdh*) – Ct (test gene).

5.3.15 Statistical analysis

Data were presented as mean ± *SEM* and displayed using a scatter plot with a bar overlay in the figure, with the scatter plot representing individual data points. Means for two groups of cases were compared with two independent-samples Students *t*-test. The comparison of cerebral DNA levels of bacterial 16S rRNA gene between IL-17a-deficient and wild-type APP-transgenic mice with and without antibiotic treatment were conducted by Mann-Whitney-*U*-test, because the variables were apparently non-normally distributed. For multiple comparisons, we used one-way or two-way ANOVA followed by Bonferroni, Tukey, or Dunnett T3 *post hoc* test (dependent on the result of Levene's test to determine the equality of variances). All statistical analyses were performed with GraphPad Prism 8 version 8.0.2. for Windows (GraphPad Software, San Diego, USA) or SPSS software for Windows (Version 26.0, IBM, Armonk, USA). Other statistical methods in microbiome analysis offered by external companies have been described above. Statistical significance was set at $p < 0.05$.

6 RESULTS

6.1 Oral treatment with an antibiotic cocktail depletes almost all bacteria in the gut of APP-transgenic mice

To investigate the relationship between gut and brain, we treated 3-month-old APP-transgenic female littermate mice with and without an antibiotic cocktail in drinking water for 2 months. By quantifying gut bacterial *16S rRNA* gene with real-time PCR, we found that antibiotic treatment depleted almost all bacteria in the gut, as the number of remaining bacteria was only 0.08% of that of normal drinking water control mice (Fig. 6.1, A; ΔCt value: 10.34 in real-time PCR; *t* test, $p < 0.0001$), which was consistent with previous studies that have demonstrated the depletion of gut bacteria by anaerobic and aerobic culture of gut contents (Benjamin, Sumpter et al. 2013, Liu, da Cunha et al. 2016). Not surprisingly, the richness and diversity of the remaining bacteria in the gut of antibiotics-treated AD mice were dramatically reduced, as indicated by decreased Sobs, Ace, Chao, and Shannon indices and increased Simpson index in the α-diversity analysis (Fig. 6.1, B - F; *t* test, $p < 0.05$). Similarly, the β-diversity-based PCoA analysis clearly showed the difference in intestinal bacterial architecture between APP-transgenic mice with and without antibiotic treatment (Fig. 6.1, G; ANOSIM, R = 1.0000, $p = 0.008$). We further observed that the remaining antibiotic-resistant bacteria belonged almost exclusively to the genera *Escherichia-Shigella* and *Parasutterella* (Fig. 6.1, H; Wilcoxon rank-sum test, $p < 0.05$).

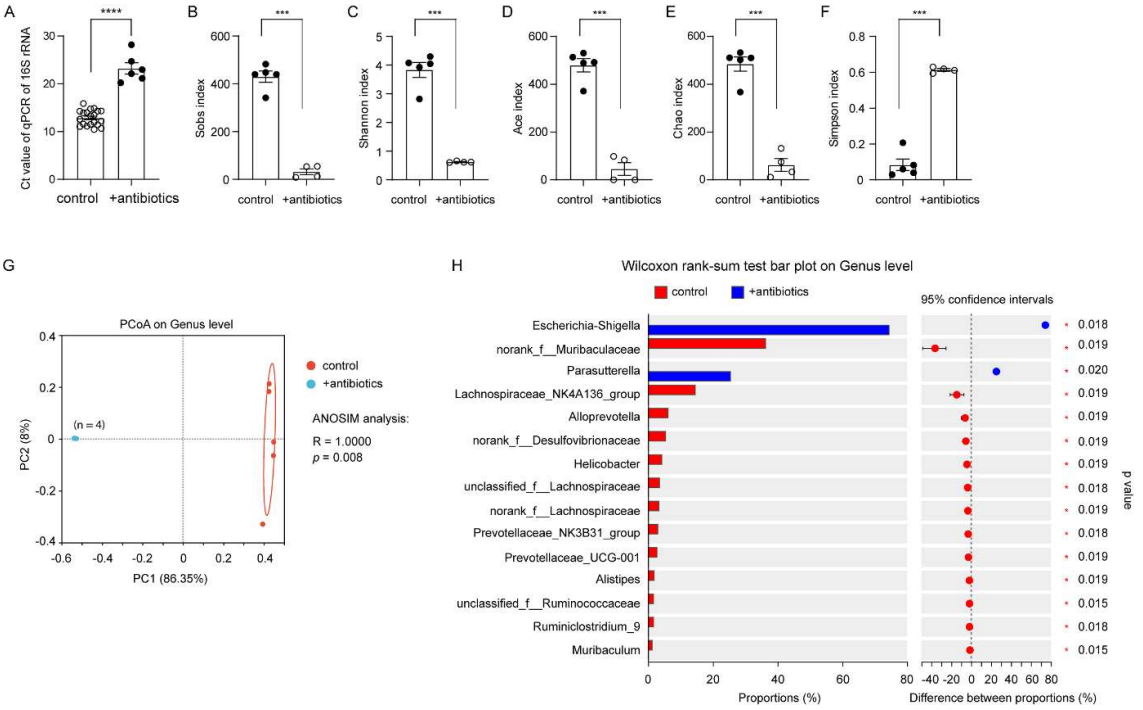

Fig.6.1, Antibiotic treatment successfully depletes the bacteria in the gut of APP-transgenic mice. Three-month-old APP-transgenic female mice were treated with and without antibiotics in drinking water for 2 months. Intestinal content (total 100mg) for the isolation of bacterial DNA was harvested from the appendix and neighboring colon. Bacterial DNA was first measured for the amount with real-time PCR (A; *t* test; $n = 20$ and 6 for mice receiving normal water and antibiotic supplement), and then sequenced for the V3-V4 region of 16S rRNA-encoding gene ($n = 5$ and 4 for control and antibiotic-treated mice, respectively). Using Sobs, Shannon, Ace, Chao and Simpson's indices, α-diversity analysis shows that treatment with an antibiotic cocktail significantly reduces bacterial richness and diversity within each mouse (B - F; *t* test). Principal coordinate analysis (PCoA) was used for β-diversity analysis of bacterial composition at the genus level in APP-transgenic mice with and without antibiotic treatment (G; each symbol represents the gut bacteria of an individual mouse). As expected, the structure of gut bacterial community of antibiotics-treated APP-transgenic mice differed significantly from those of APP-transgenic littermates with normal drinking water (H; ANOSIM analysis between +antibiotics and control mice). Bar plots depict abundance (% of total) of the indicated genera. Wilcoxon rank-sum tests show that antibiotic treatment increases the relative abudance of bacteria in the genera *Escherichia-Shigella* and *Parasutterella* (H). ***: $p < 0.001$ and ****: $p < 0.0001$.

6.2 Depletion of gut bacteria reduces IL-17a-expressing CD4-positive lymphocytes in APP-transgenic mice

Our recent study showed that IL-17a-expressing CD4-positive lymphocytes increase in the gut and spleen of APP-transgenic mice (Luo, Schnoder et al. 2022). We therefore selected CD4-positive cells with a magnetic beads-conjugated antibody from the spleen of antibiotics-treated APP-transgenic mice and quantified the transcripts of characteristic genes for Th1, Th2, Th17 and Treg lymphocytes. As shown in Fig. 6.2.1, A - D, depletion of gut bacteria significantly decreased the transcription of *Il-17a*, but increased the transcription of *Ifn-γ* and *Il-4* (*t* test, $p < 0.05$). We further treated 3-month-old APP-transgenic mice expressing IL-17a-eGFP reporter (Esplugues, Huber et al. 2011) with and without antibiotics, and observed that depletion of gut bacteria for 2 months significantly reduced eGFP-expressing CD4+ lymphocytes in both lamina propria and Peyer's patches of the gut compared to control AD mice with normal drinking water (Fig. 6.2.1, E - H; *t* test, $p < 0.05$). Therefore, depletion of intestinal bacteria leads to a significant reduction in IL-17a-expressing CD4-positive T lymphocytes in AD mice. We also found some IL-17a-eGFP-expressing CD4-negative cells in both lamina propria and Peyer's patches (see upper-left quadrant in Fig. 6.2.1, E and G); however, these cells could not form a clearly distinguishable population in both the antibiotics-treated and non-treated AD mice, which made it difficult to reliably quantify cells. Thus, our results do not exclude the possibility that depletion of gut bacteria also regulates IL-17a expression in other immune cells, such as lymphoid-tissue inducer-like cells, natural killer cells, and Paneth cells (Cua and Tato 2010). In our APP-transgenic animal models, expression of GFP was not detected in γδ T lymphocytes in the gut (Luo, Schnoder et al. 2022).

In additional experiments, we performed an immunohistochemical analysis of GFP in the brain of APP-transgenic mice and of EAE mice that were established in our previous study (Hao, Luo et al. 2021), both of which expressed IL-17a-eGFP. We could not detect GFP-expressing cells in the brain parenchyma of AD mice, but clearly saw GFP-positive cells surrounding blood vessels in the EAE model (Fig. 6.2.2). Similarly, we did not detect *Il-17a* gene transcripts in the brain tissue from APP-transgenic mice within 40 cycles of real-time PCR (data not shown). These results suggest that gut bacterial depletion alters brain pathology by regulating IL-17a-expressing cells outside the brain.

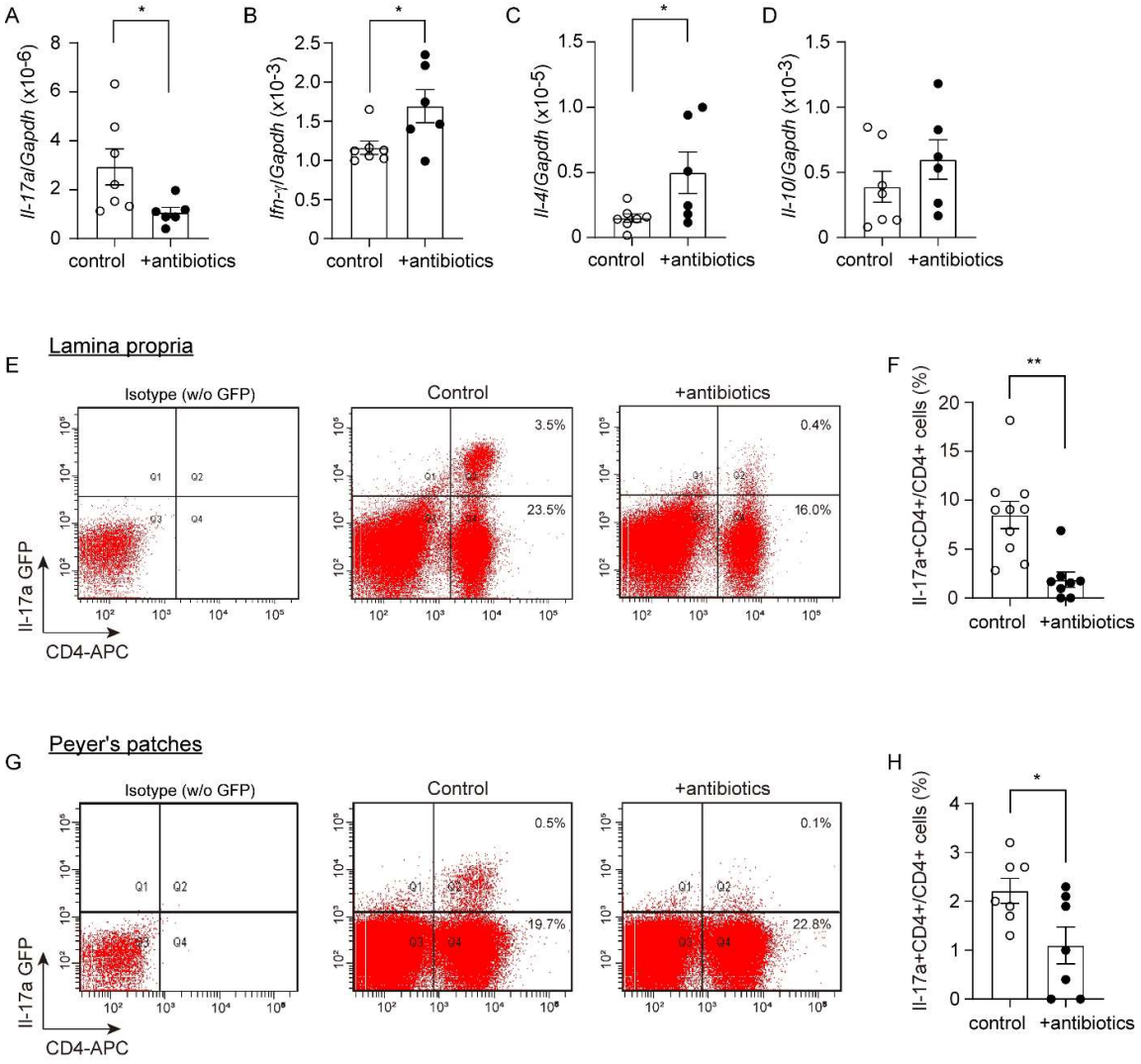

Fig. 6.2.1, Depletion of gut bacteria reduces IL-17a-expressing CD4-positive lymphocytes.

Three-month-old APP-transgenic female mice, expressing or not IL-17a-eGFP reporter, were treated with and without antibiotics in drinking water for 2 months. CD4-positive splenocytes were selected and detected for transcription of T lymphocyte marker genes. The transcription of *Il-17a* gene was significantly down-regulated by antibiotic treatment, while the transcription of *Ifn-γ* and *Il-4* genes was up-regulated in CD4+ splenocytes compared to APP-transgenic control mice with normal drinking water (A - C; *t* test, n = 6 - 7 per group). The transcription of *Il-10* gene in spleen cells was not changed by antibiotic treatment (E; *t* test, n = 6 - 7 per group). In addition, single cell suspensions were prepared from both lamina propria and Peyer's patches of 5-month-old IL-17a-eGFP-expressing APP-transgenic mice and analyzed by flow cytometry after fluorescent staining of CD4 (E and G). Intestinal cells prepared from APP-transgenic mice without expressing IL-17a-eGFP reporter were stained with APC-conjugated rat IgG2b as an isotype control (Isotype w/o GFP). The expression of IL-17a-associated eGFP was decreased in CD4+ lymphocytes in the intestine of APP-transgenic mice by antibiotic treatments (F and H; *t* test, n = 7 - 10 per group). *: $p < 0.05$; **: $p < 0.01$.

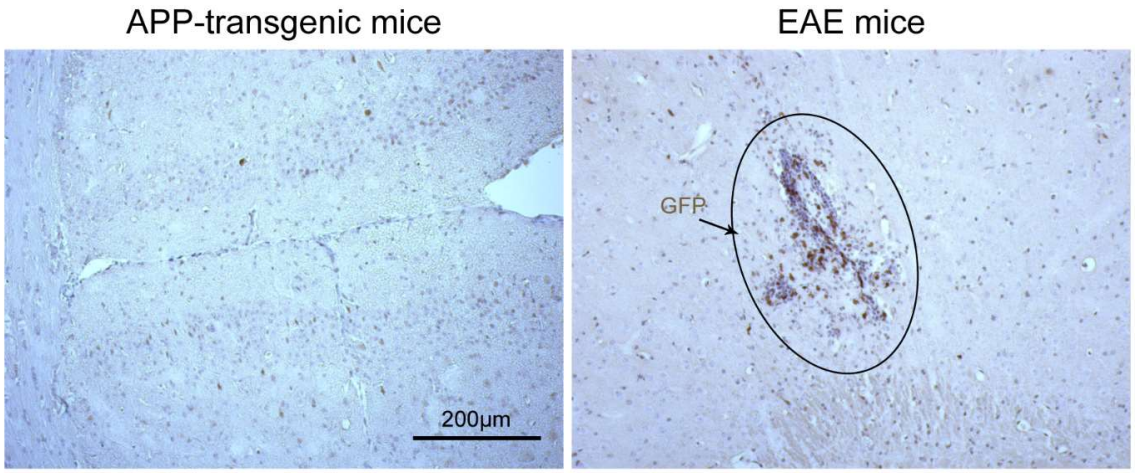

Fig. 6.2.2, IL-17a-eGFP expressing cells are detected in the brain of EAE mice but not in AD mice. Brain sections from 5-month-old APP-transgenic mice and EAE mice both expressing IL-17a-eGFP were detected for GFP protein with immunohistochemistry. Rabbit anti-GFP antibody (Cat.-No.: 600-901-215; Rockland Immunochemicals) was used. The staining was visualized with HRP/3,3'-diaminobenzidine in brown (DAB; Sigma).

6.3 Depletion of gut bacteria reduces bacterial DNA in the brain of APP-transgenic mice

Disruptions of the gut microbiome and altered gut permeability are associated with AD. Intestinal bacteria may release structural components into the blood that circulate to the brain, or the bacteria translocate via the vagus nerve to the brain but not to other organs like blood, lung, heart, kidney oder spleen (Dominy, Lynch et al. 2019, Thapa, Kumari et al. 2023). We then asked whether depletion of gut bacteria alters the potential presence of bacterial components in the brain. Since we observed that depletion of gut bacteria reduced the number of IL-17a-expressing lymphocytes, we asked whether IL-17a affected the amount of bacterial substance in the brain. We treated IL-17a-deficient and wild-type APP-transgenic female mice with antibiotics as described above. Both groups of mice after antibiotic treatment showed enlargement of the caeca and dark-colored cecal contents as shown in published studies (Erny, Hrabe de Angelis et al. 2015) (data not shown). Interestingly, antibiotic treatment significantly decreased the DNA level of the bacterial *16S rRNA* gene in the brains of both IL-17a-deficient and wild-type APP-transgenic mice (Fig. 6.3, A and B; Mann-Whitney-*U*-Test, $p < 0.05$). The DNA level of *16S rRNA* gene was significantly lower in IL-17a-deficient than in IL-17a-wild-type

APP-transgenic mice without antibiotic treatment (Fig. 6.3, A and B; *16S rRNA*/*Gapdh*: $2.99 \pm 0.49 \times 10^{-5}$ vs. $2.00 \pm 0.93 \times 10^{-3}$; Mann-Whitney-*U*-Test, $U = 4$, $p = 0.015$). After antibiotic treatment, the DNA level of the *16S rRNA* gene did not differ between IL-17a-deficient and wild-type AD mice (*16S rRNA*/*Gapdh*: $1.49 \pm 0.42 \times 10^{-5}$ [Il-17a-deficient] vs. $4.32 \pm 1.32 \times 10^{-5}$ [Il-17a-wild-type]); Mann-Whitney-*U*-Test, $U = 19$, $p = 0.102$). Thus, IL-17a deficiency potentially blocked the translocation of bacterial components from the intestine to the brain.

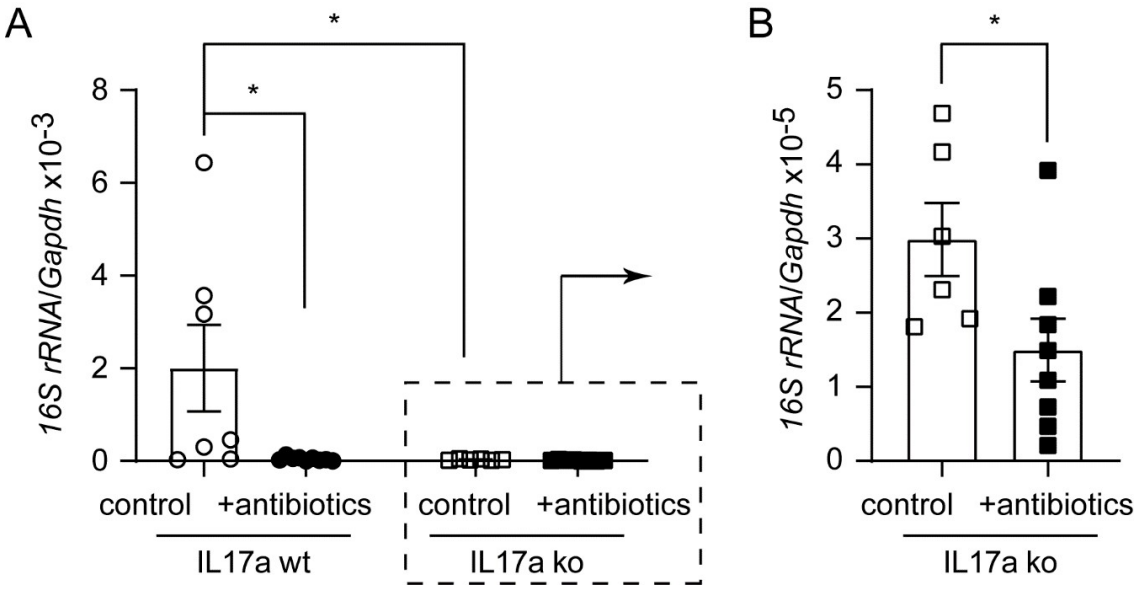

Fig. 6.3, Depletion of gut bacteria reduces bacterial DNA in the brains of both IL-17a-deficient and wild-type APP-transgenic mice.

Three-month-old IL-17a-deficient (ko) and wild-type (wt) APP-transgenic female mice received drinking water with and without supplement of antibiotics for 2 months. The hippocampus and cortex were collected and homogenized in Trizol for DNA isolation. The amount of bacterial DNA was evaluated by real-time PCR using mouse *Gapdh* gene as an internal control. Depletion of gut bacteria significantly decreased bacterial DNA in both IL-17a-deficient and wild-type APP-transgenic mice; interestingly, deficiency of IL-17a also reduced bacterial DNA in the brain compared wth IL-17a wild-type AD mice (A and B; Mann-Whitney-*U*-Test, n = 8 - 9 per group for IL-17a-wildtype mice and 6 - 8 per group for IL-17a-deficient mice). *, $p < 0.05$.

6.4 Depletion of intestinal bacteria inhibits proinflammatory activation in the brain of APP-transgenic mice, but not in IL-17a-deficient AD mice

Depletion of intestinal bacteria has been shown to suppress inflammation in the brain of APP-transgenic mice (Minter, Zhang et al. 2016, Harach, Marungruang et al. 2017). We did observe that intestinal antibiotic treatment for 2 months significantly reduced the number of Iba1-positive microglia in both the hippocampus and cortex of female APP-transgenic mice (Hippocampus: from $17.13 \pm 1.29 \times 10^3$ cells/mm^3 to $11.85 \pm 0.73 \times 10^3$ cells/mm^3, and Cortex: from $24.31 \pm 0.84 \times 10^3$ cells/mm^3 to $17.46 \pm 2.55 \times 10^3$ cells/mm^3; Fig. 6.4.1, A - C; *t* test, $p < 0.05$). Interestingly, in IL-17a-deficient APP-transgenic mice, depletion of gut bacteria did not alter the number of Iba-1-positive cells in the hippocampus (Fig. 6.4.1, D and E; $16.21 \pm 0.57 \times 10^3$ cells/mm^3 vs. $15.85 \pm 0.83 \times 10^3$ cells/mm^3; *t* test, $p > 0.05$). We measured transcripts of proinflammatory genes (*Tnf-α*, *Il-1β*, and *Ccl-2*) and anti-inflammatory genes (*Il-10*, *Chi3l3*, and *Mrc1*) in brains of APP-transgenic mice. As shown in Fig. 6.4.1, F, H and J - M, depletion of intestinal bacteria down-regulated the transcription of *Il-1β* and *Ccl-2*, but up-regulated *Il-10* transcription in IL-17a-wildtype APP-transgenic mice (*t* test, $p < 0.05$). Intestinal bacterial depletion did not change the transcription of *Tnf-α*, *Chi3l3* and *Mrc-1* in APP-transgenic mice (Fig. 6.4.1, F, L and M; *t* test, $p > 0.05$). In IL-17a-deficient AD mice, depletion of intestinal bacteria did not modulate the transcription of *Tnf-α*, *Il-1β*, *Ccl-2*, *Il-10*, and *Mrc-1* (Fig. 6.4.1, F, H, and J - M, and K; *t* test, $p > 0.05$), except decreasing the transcription of *Chi3l3* (Fig. 6.4.1, L; *t* test, $p < 0.05$). The results on antibiotics-induced transcriptional regulations of *Tnf-α* and *Il-1β* genes were confirmed by ELISA measurements of their protein levels, which showed that depletion of gut bacteria significantly decreased the Il-1β protein concentration (Fig. 6.4.1, I; *t* test, $p < 0.05$) and tended to reduce the amount of Tnf-α protein (Fig. 6.4.1, G; *t* test, $p = 0.075$) in brains of IL-17a-wildtype but not IL-17a-deficient mice.

In order to investigate whether the intestinal bacterial depletion-induced inflammatory inhibition was specific for mice with AD pathology, we treated 3 and 22-month-old female C57BL/6J mice with and without antibiotics for 2 months. Depletion of intestinal bacteria did not change transcription of all genes tested in 5-month-old C57BL/6J mice (*Tnf-α*, *Il-1β*, *Ccl-2*, *Il-10*, *Chi3l3*, and *Mrc1*; Fig. 6.4.1, N; *t* test, $p > 0.05$). In 24-month-

old C57BL/6J mice, depletion of intestinal bacteria increased *Tnf-α* transcription and decreased *Chi3l3* transcription (Fig. 6.4.1, O; *t* test, $p < 0.05$). These experiments also suggested that it was intestinal bacterial depletion instead of antibiotics themselves modifying the inflammatory activation in the brain of APP-transgenic mice.

In order to examine the off-target effects of oral treatment of antibiotics, we injected 5-month-old APP-transgenic mice daily for 7 days with the antibiotic cocktail (1.5 mg/kg/day vancomycin, 3 mg/kg/day ampicillin, neomycin and streptomycin) according to the published protocol (Bercik, Denou et al. 2011). We injected metronidazole at the maximal dose of 30 mg/kg/day, because it has a high oral bioavailability (Jensen and Gugler 1983). Intraperitoneal injection of the antibiotic cocktail did not change the transcription of proinflammatory genes, *Tnf-α*, *Il-1β*, and *Ccl-2* (Fig. 6.4.2, A - C; *t* test, $p > 0.05$); however, significantly decreased the transcription of anti-inflammatory genes, *Il-10*, and *Mrc1* (Fig. 6.4.2, D and F; *t* test, $p < 0.05$), and tended to inhibit *Chi3l3* gene transcription (Fig. 6.4.2, E; *t* test, $p = 0.055$). The pattern of transcriptional modification in the brain by intraperitoneal injection of antibiotic cocktail is obviously different from that in oral antibiotics-treated mice; therefore, the effects of oral antibiotic treatment were due to the depletion of bacteria in the gut and not the antibiotics themselves.

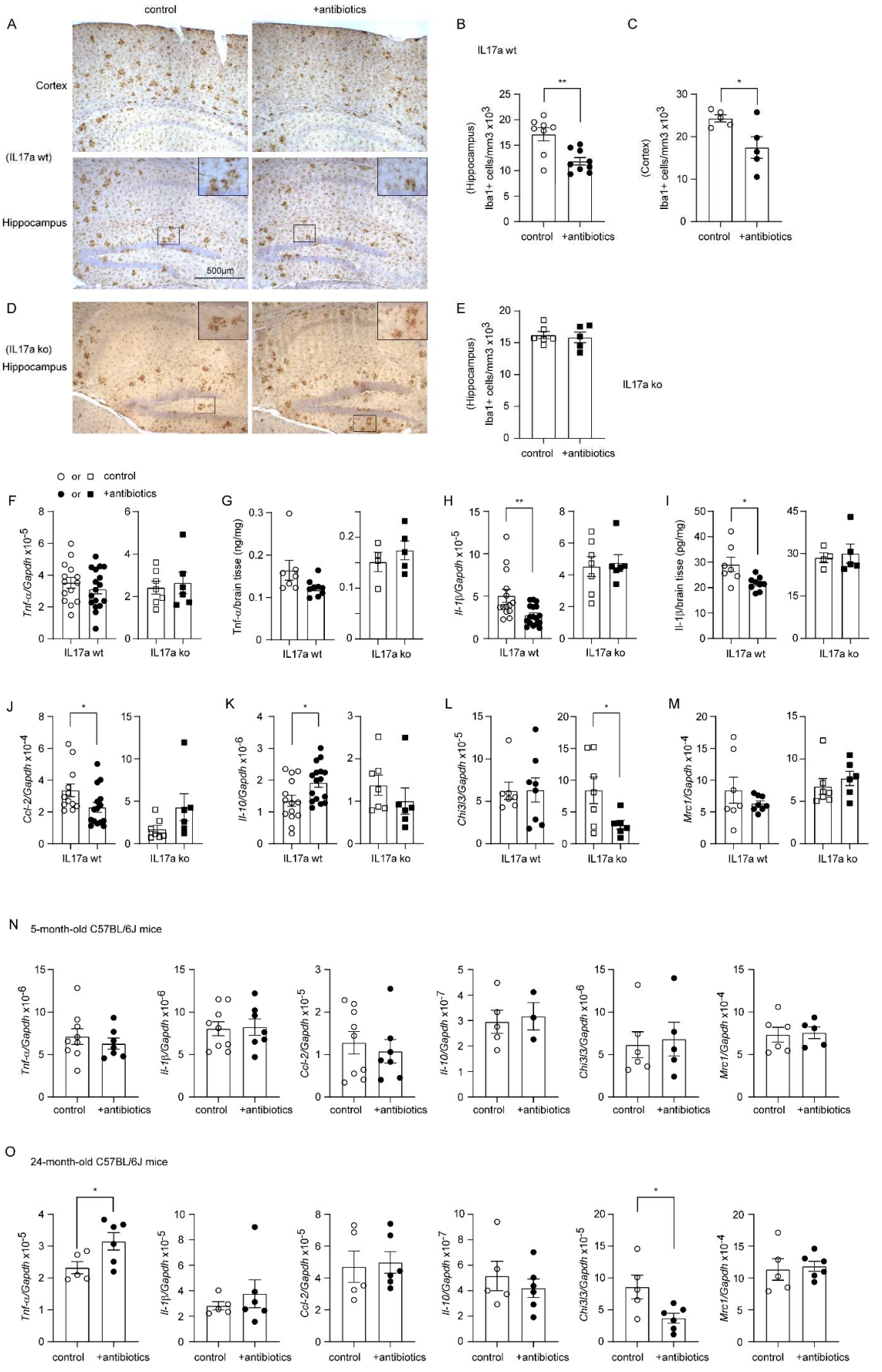
A
control
+antibiotics
Cortex
(IL17a wt)
Hippocampus
500µm
B
IL17a wt
(Hippocampus) Iba1+ cells/mm3 x10^3
control
+antibiotics
C
(Cortex) Iba1+ cells/mm3 x10^3
D
(IL17a ko)
Hippocampus
E
IL17a ko
F
○ or □ control
● or ■ +antibiotics
Tnf-α/Gapdh x10^-5
IL17a wt
IL17a ko
G
Tnf-α/brain tisse (ng/mg)
H
Il-1β/Gapdh x10^-5
I
Il-1β/brain tisse (pg/mg)
J
Ccl-2/Gapdh x10^-4
K
Il-10/Gapdh x10^-6
L
Chi3l3/Gapdh x10^-5
M
Mrc1/Gapdh x10^-4
N
5-month-old C57BL/6J mice
Tnf-α/Gapdh x10^-6
Il-1β/Gapdh x10^-6
Ccl-2/Gapdh x10^-5
Il-10/Gapdh x10^-7
Chi3l3/Gapdh x10^-6
Mrc1/Gapdh x10^-4
O
24-month-old C57BL/6J mice
Tnf-α/Gapdh x10^-5
Il-1β/Gapdh x10^-5
Ccl-2/Gapdh x10^-5
Il-10/Gapdh x10^-7
Chi3l3/Gapdh x10^-5
Mrc1/Gapdh x10^-4

Fig. 6.4.1, Depletion of gut bacteria reduces inflammatory activation in the brain of IL-17a-wildtype, but not Il17a-deficient APP-transgenic mice. Three-month-old APP-transgenic female mice with (ko) and without (wt) knockout of *Il-17a* gene, and 3 or 22-month-old C57B/L6 female mice were treated with and without antibiotics in drinking water for 2 months. Thereafter, brain tissues were sectioned and microglia were counted with stereological method, Optical Fractionator, after immunohistochemical staining of Iba1 (in brown color) (A - E), or homogenized for RNA isolation (F, H, and J - M) and measurement of inflammatory gene transcripts with real-time PCR, as well as for ELISA assays of Tnf-α and Il-1β concentrations (G and I; n = 4 - 9 per group). Depletion of gut bacteria significantly decreased Iba1-positive microglia in both the hippocampus and cortex of IL-17a-wildtype, but not in Il17a-deficient APP-transgenic mice (B, C and E; t test, n = 5 - 9 per group). Similarly, depletion of gut bacteria significantly reduced the transcripts of *Il-1β* and *Ccl-2*, and increased *Il-10* transcript in the brain of Il-17a-wildtype, but not in Il17a-deficient APP-transgenic mice (H, J, and K; t test, n = 6 - 17 per group). Transcriptional regulation in AD mice deleted of gut bacteria was confirmed by the reduction in protein levels of Il-1β but not Tnf-α in brain homogenate compared to APP mice receiving normal water (G and I; t test, n = 4 - 9 per group). However, depletion of gut bacteria significantly reduced the transcript of *Chi3l3* in the brain of Il17a-deficient APP-transgenic mice (L; t test, n = 6 - 7 per group). Moreover, depletion of gut bacteria did not change the transcription of various inflammatory genes (*Tnf-α*, *Il-1β*, *Ccl-2*, *Il-10*, *Chi3l3*, and *Mrc1*) in in the brain of 5-month-old C57BL/6J female mice (N; t test, n = 3 - 9 per group), however, significantly increased *Tnf-α* transcription and decreased *Chi3l3* transcription in 24-month-old C57B/L6 female mice (O; t test, n = 5 - 6 per group). *: $p < 0.05$; **: $p < 0.01$.

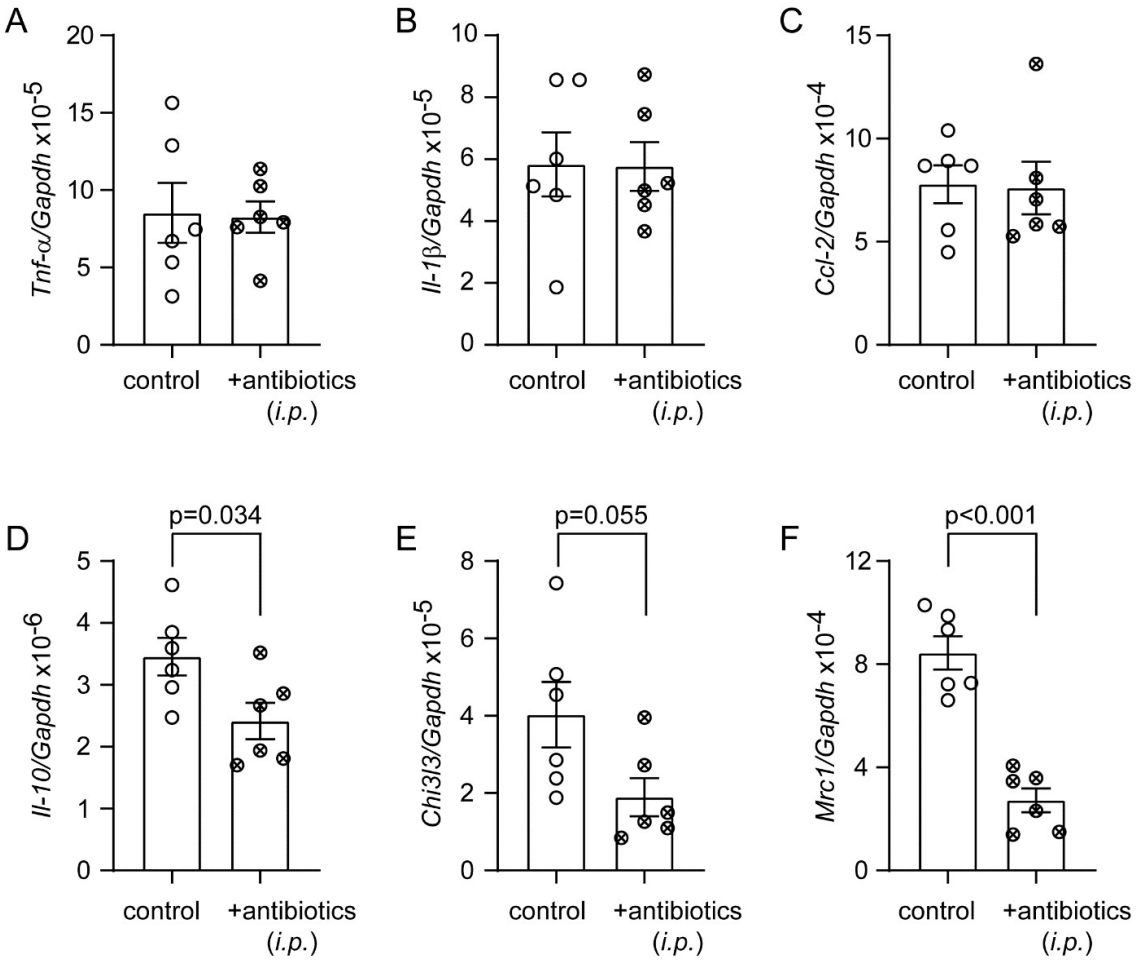

Fig. 6.4.2 Intraperitoneal injection of an antibiotic cocktail inhibits the transcription of anti-inflammatory but not proinflammatory genes in the brain of APP-transgenic mice. Five-month-old APP-transgenic mice were injected (*i.p.*) daily with an antibiotic cocktail (vancomycin, ampicillin, neomycin sulfate, streptomycin, and metronidazole; all from Sigma) for 7 days. Brain tissues were then homogenized in Trizol and total RNA was isolated. Transcripts of inflammatory genes (*Tnf-α*, *Il-1β*, *Ccl-2*, *Il-10*, *Chi3l3* and *Mrc1*) were measured with quantitative RT-PCR. Intraperitoneal injection of antibiotics does not alter the transcription of proinflammatory genes *Tnf-α*, *Il-1β*, and *Ccl-2* (A - C), but decreases the transcripts of antiinflammatory genes *Il-10*, *Chi3l3* and *Mrc1* (D - F). *t* test, n = 6 per group.

6.5 Depletion of intestinal bacteria inhibits microglial activation in the brain of APP-transgenic mice, which is abolished by knockout of *Il-17a* gene

To understand the mechanism, through which intestinal antibiotic treatment modified neuroinflammation in AD mice, we selected $CD11b^+$ brain cells from 5-month-old female APP-transgenic mice with and without 2-month treatments of antibiotics and detected transcripts of disease-associated microglia (DAM) signature genes (Keren-Shaul, Spinrad

et al. 2017). Depletion of intestinal bacteria significantly reduced transcription of *Il-1β* and *Ccl-2* genes (Fig. 6.5.1, B and C; *t* test, $p < 0.05$), and tended to decrease the transcription of *Tnf-α*, *Il-10* and *Itgax* genes (Fig. 6.5.1, A, D and K; *t* test, $0.05 < p < 0.10$) in cells derived from IL-17a-wildtype APP-transgenic mice, but not in cells from IL-17a-deficient control AD mice. Depletion of intestinal bacteria even increased transcription of *Il-10* gene in IL-17a-deficient APP-transgenic mice (Fig. 6.5.1, D; *t* test, $p < 0.05$). Gut bacterial depletion down-regulated transcription of *Apoe* gene in both Il17a-deficient and wild-type APP-transgenic mice (Fig. 6.5.1, E; *t* test, $p < 0.05$). Antibiotic treatment did not significantly change the transcription of other genes (*Trem2*, *Cx3cr1*, *P2ry12*, *Clec7a*, and *Lpl*) tested in both IL-17a-deficient and wild-type mice (Fig. 6.5.1, F - K; *t* test, $p > 0.05$).

In further experiments, we labelled microglia with Iba-1 antibodies and analyzed the morphology of microglia in the vicinity of Aβ deposits as we had done previously (Luo, Schnoder et al. 2022). Depletion of intestinal bacteria increased the total number and end points of branching microglial processes (Fig. 6.5.1, L - N; *t* test, $p < 0.05$), and tended to increase branch length (Fig. 6.5.1, O; *t* test, $p = 0.078$) in 5-month-old APP-transgenic mice, consistent with previous observations (Erny, Dokalis et al. 2021, Xie, Bruggeman et al. 2023). However, all changes in microglial morphology caused by gut bacteria depletion were absent in IL-17a-deficient AD mice (Fig. 6.5.1, M - O; *t* test, $p > 0.05$).

As we observed bacterial DNA in the brain, we further investigated whether IL-17a deficiency alters the response of microglia to bacterial components. We found that 5-month-old IL-17a-deficient and wild-type APP-transgenic mice without antibiotic treatment did not differ in the transcription of *Myd88*, *Cd14*, *Tlr1*, *Tlr2*, *Tlr4* and *Tlr9* (Fig. 6.5.2, A), suggesting that knockout of *Il-17a* gene does not change microglial reactivity to bacteria. Surprisingly, our additional experiments and a previous study showed that the lack of IL-17a did not reduce the transcription of inflammatory genes, *Tnf-α*, *Il-1β*, *Ccl-2* and *Il-10* in microglia (Fig. 6.5.2, B) and even activate microglia (Luo, Schnoder et al. 2022).

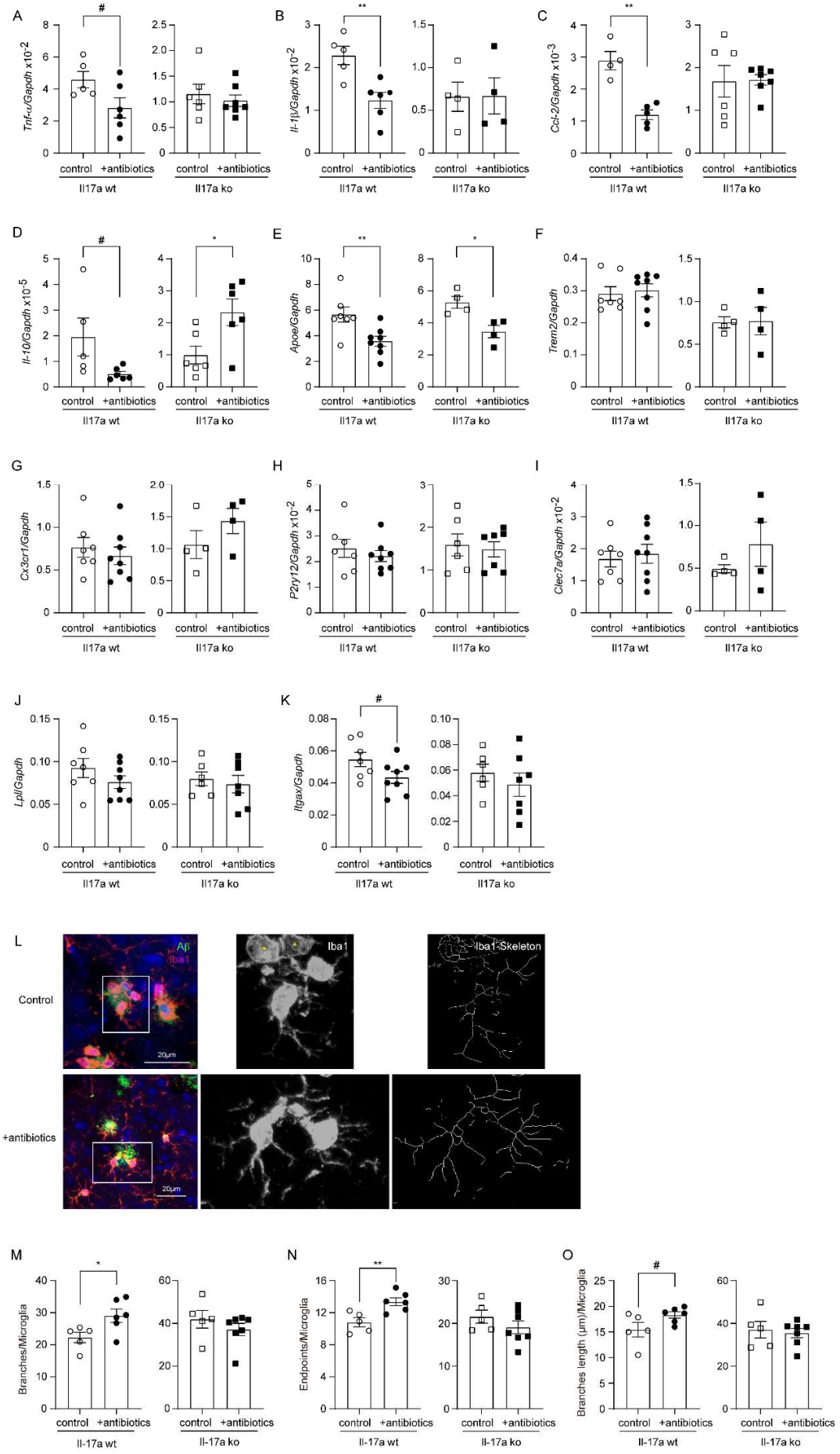
A
Tnf-α/Gapdh x10-2
B
Il-1β/Gapdh x10-2
C
Ccl-2/Gapdh x10-3
D
Il-10/Gapdh x10-5
E
Apoe/Gapdh
F
Trem2/Gapdh
G
Cx3cr1/Gapdh
H
P2ry12/Gapdh x10-2
I
Clec7a/Gapdh x10-2
J
Lpl/Gapdh
K
Itgax/Gapdh
control
+antibiotics
Il17a wt
Il17a ko
L
Control
+antibiotics
Aβ
Iba1
20μm
Iba1
Iba1-Skeleton
M
Branches/Microglia
N
Endpoints/Microglia
O
Branches length (μm)/Microglia
Il-17a wt
Il-17a ko

Fig. 6.5.1, Depletion of gut bacteria inhibits inflammatory activation in microglia in the brain of IL-17a-wildtype, but not Il17a-deficient APP-transgenic mice. Three-month-old APP-transgenic female mice with (ko) and without (wt) knockout of *Il-17a* gene were treated with and without antibiotics in drinking water for 2 months. CD11b-positive brain cells were selected and quantified for the transcription of DAM marker genes. Depletion of gut significantly decreased the transcription of *Il-1β*, and *Ccl-2* genes, and tended to down-regulate the transcription of *Tnf-α*, *Il-10*, and *Itgax* genes in the brain of IL-17a-wildtype, but not in Il17a-deficient APP-transgenic mice (A - D, and K; *t* test, n = 4 - 7 per group). Depletion of gut significantly reduced transcription of *Apoe* gene, but not *Trem2*, *Cx3cr1*, *P2ry12*, *Clec7a*, and *Lpl* genes in both IL-17a-wildtype and deficient APP-transgenic mice (E - J; *t* test, n = 4 - 8 per group). In the analysis of microglial morphology after immunofluorescent staining of Iba1 (L), depletion of gut bacteria increased the number of branches and endpoints of the processes of microglia in IL-17a-wildtype, but not in Il17a-deficient APP-transgenic mice (M - O; *t* test, n = 5 - 7 per group). The Iba1-positive celles marked with "*" without showing clear processes were excluded for analysis of microglial morphology (L). *: $p < 0.05$; **: $p < 0.01$; #: $0.05 < p < 0.10$.

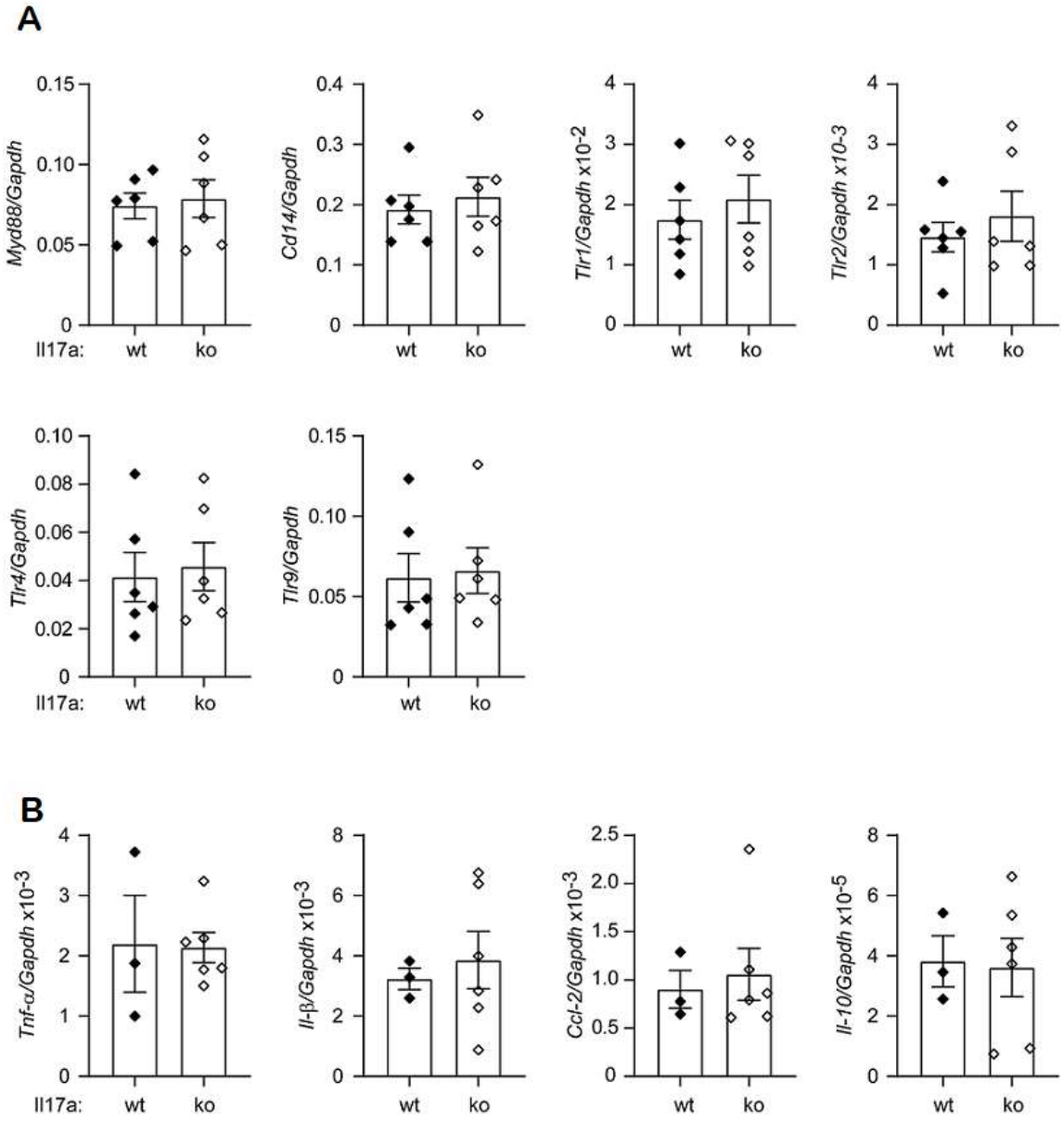

Fig.6.5.2 Deficiency of IL-17a does not change the transcription of innate immune receptors and inflammatory genes. CD11b-positive cells were selected from single cell preparations from brains of 5-month-old *Il-17a* gene-knocked out (ko) and wild-type (wt) APP-transgenic mice with magnetic beads-conjugated antibody (clone M1/70.15.11.5; Miltenyi Biotec) and detected for transcripts of various innate immune receptor genes (*Cd14*, *Tlr1*, *Tlr2* and *Tlr4*) and *Myd88*, as well as inflammatory genes (*Tnf-α*, *Il-1β*, *Ccl-2* and *Il-10*) with quantitative RT-PCR. *t* test, n = 3 - 6 per group, $p > 0.05$ for all tested genes.

6.6 Depletion of intestinal bacteria reduces cerebral Aβ in IL-17a-wildtype but not in IL-17a-deficient APP-transgenic mice

Extracellular Aβ plaques are a pathological hallmark of AD. Depletion of gut bacteria was reported to attenuate Aβ deposits in APP-transgenic mice (Minter, Zhang et al. 2016, Dodiya, Kuntz et al. 2019). We treated 3-month-old female APP-transgenic mice with an antibiotic cocktail for 2 months. As shown in Fig. 6.6, A - C, 2-month treatments with antibiotics significantly reduced immunoreactive Aβ density from 6.02% ± 0.32% to 4.42% ± 0.64% in the cortex and from 5.67 % ± 0.34 % to 4.16 % ± 0.58% in the hippocampus (*t* test, $p < 0.05$) of IL-17a-wildtype AD mice. In Il-17a-deficient APP-transgenic mice, treatment with antibiotics changed the density of Aβ in neither hippocampus nor cortex (Fig. 6.6, D - F; *t* test, $p > 0.05$). The brain section was also stained with methoxy-XO4 that typically binds to the β sheet structure of Aβ aggregates. Similarly, treatments with antibiotics significantly reduced Aβ deposits in the cortex (Fig. 6.6, G and H; *t* test, $p < 0.05$) and tended to decrease Aβ in the hippocampus (Fig. 6.6, G and I; *t* test, $p = 0.060$) of IL-17a-wildtype APP-transgenic mice, but did not change density of methoxy-XO4-stained Aβ deposits in IL-17a-deficient AD mice (Fig. 6.6, J - L; *t* test, $p > 0.05$).

We went on measuring Aβ in the brain homogenate with ELISA. In IL-17a wild-type APP-transgenic mice, antibiotic treatment significantly decreased the levels of both Aβ42 and Aβ40 in TBS- and TBS-T fractions (Fig. 6.6, M, N, P and Q; *t* test, $p < 0.05$), but not in guanidine-soluble fraction (Fig. 6.6, O and R; *t* test, $p > 0.05$). TBS-, TBS-T-, and guanidine-soluble brain homogenates are enriched with monomeric, oligomeric and high-molecular-weight aggregated Aβ, respectively (Liu, Walter et al. 2005). In IL-17a-deficient APP-transgenic mice, treatment with antibiotics did not reduce Aβ42 and Aβ40 in all three fractions of brain homogenates (Fig. 6.6, M - R). On the contrary, antibiotic treatment even increased the concentration of Aβ42 in TBS-soluble fraction of brain homogenate (Fig. 6.6, M; *t* test, $p < 0.05$).

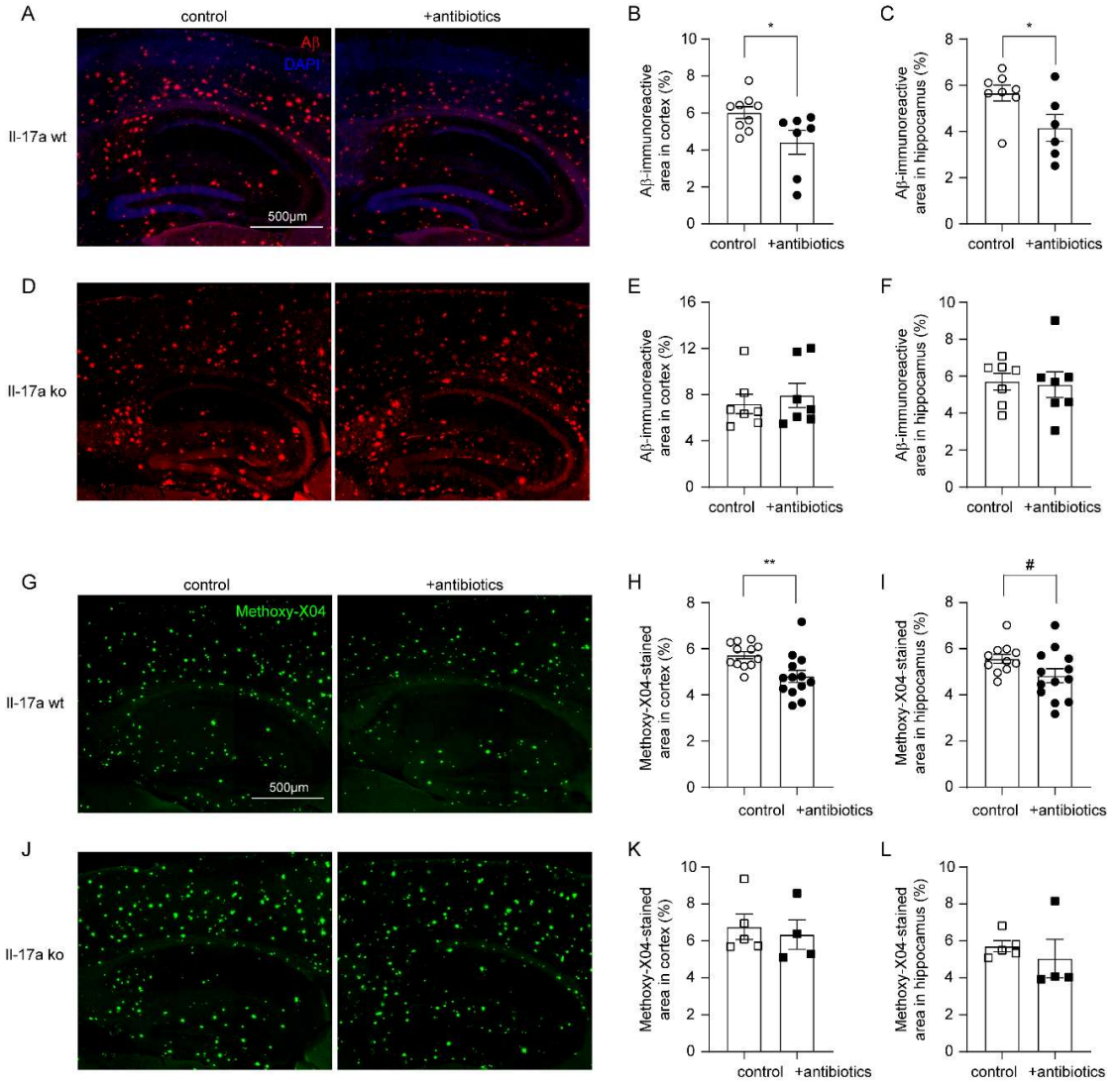
A
control
+antibiotics
Il-17a wt
Aβ
DAPI
500µm
B
Aβ-immunoreactive area in cortex (%)
control
+antibiotics
C
Aβ-immunoreactive area in hippocamus (%)
D
Il-17a ko
E
F
G
Methoxy-X04
H
Methoxy-X04-stained area in cortex (%)
I
Methoxy-X04-stained area in hippocamus (%)
J
K
L

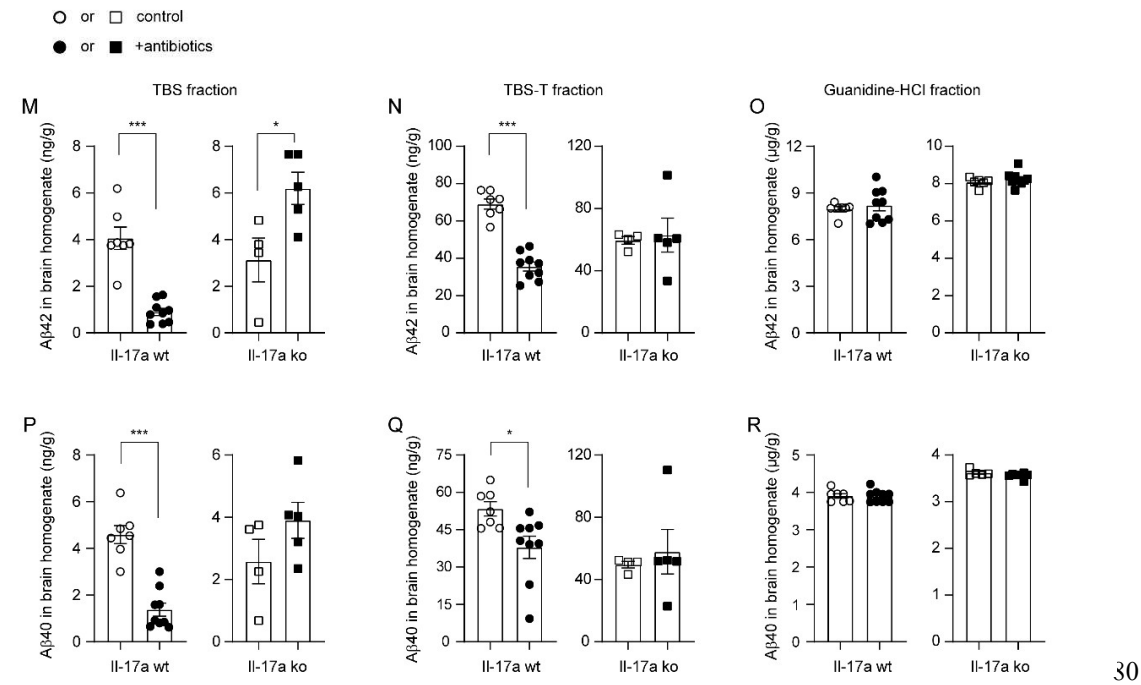
or control
or +antibiotics
TBS fraction
TBS-T fraction
Guanidine-HCl fraction
M
N
O
Aβ42 in brain homogenate (ng/g)
Aβ42 in brain homogenate (µg/g)
Il-17a wt
Il-17a ko
P
Q
R
Aβ40 in brain homogenate (ng/g)
Aβ40 in brain homogenate (µg/g)

Fig. 6.6, Depletion of gut bacteria reduces Aβ in the brain of IL-17a-wildtype, but not IL-17a-deficient APP-transgenic mice. Three-month-old APP-transgenic female mice with (ko) and without (wt) knockout of *Il-17a* gene were treated with and without antibiotics in drinking water for 2 months. Brain tissues were sectioned and stained with immunofluoresce-conjugated Aβ antibodies (A and D) and methoxy-XO4, a fluorescent dye for Aβ aggregates (G and J). Depletion of gut bacteria decreased Aβ deposits in both the hippocampus and cortex after staining of Aβ either with antibody or dye (B, C, H and I; *t* test, $n = 6$ - 13 per group). However, in the IL-17a-deficient AD mice, depletion of gut bacteria did not change the cerebral Aβ loads (E, F, K and L; *t* test, $n = 4$ - 7 per group). Brain tissues were also serially homogenized and extracted in TBS, TBS plus 1% Triton-100 (TBS-T) and guanidine-HCl, and then measured for Aβ40 and Aβ42 with ELISA (M - R). Depletion of gut bacteria decreased the concentrations of both Aβ40 and Aβ42 in TBS- and TBS-T-soluble brain fractions, but not in guanidine-HCl-soluble fraction of IL-17a-wildtype APP-transgenic mice (M - R; *t* test, $n = 7$ - 9 per group). Depletion of gut bacteria did not change the concentrations of Aβ40 and Aβ42 in various fractions of bran homogenates of IL-17a-deficient AD mice (N - R; *t* test, $n = 4$ - 5 per group), except that it significantly incrased the concentration of Aβ42 in TBS-soluble fraction (M). *: $p < 0.05$; **: $p < 0.01$; ***: $p < 0.001$; #: $0.05 < p < 0.10$.

6.7 Depletion of intestinal bacteria does not increase microglial Aβ phagocytosis and extracellular Aβ degradation, but potentially reduces Aβ production

In following experiments, we asked how depletion of intestinal bacteria attenuated the amyloid pathology in AD mice. First, we stained brain tissue with an antibody targeting the lysosomal protein CD68, a suggested marker of phagocytosis. As shown in Fig. 6.7, A - C, depletion of gut bacteria significantly decreased the density of CD68 immunofluorescence (*t* test, $p < 0.05$). We then conducted a flow cytometric analysis of brain cells after Aβ staining with methoxy-X04, in which depletion of intestinal bacteria remarkedly decreased both percentage of Aβ-positive CD11b+ brain cells and the mean fluorescence intensity (mFI) of CD11b+ cell population in APP-transgenic mice (Fig. 6.7, D - F; *t* test, $p < 0.05$), apparently indicating that microglial internalization of Aβ did not contribute to cerebral Aβ clearance in gut bacteria-depleted AD mice.

In the same APP-transgenic mouse strain as we used in this study, another group has reported that the absence of gut bacteria increased protein levels of Aβ-degrading enzymes neprilysin and Ide (Harach, Marungruang et al. 2017). However, our study showed that depletion of intestinal bacteria altered neither *Neprilysin* nor *Ide* gene transcription in the brains of IL-17a-deficient and wildtype APP-transgenic mice (Fig.

6.7, G - J; *t* test, $p > 0.05$), which suggested that extracellular degradation of Aβ was not the mechanism mediating Aβ reduction in our AD mice.

Our previous study has shown that inhibition of neuroinflammation inhibits β- and γ-secretase activity in the brain of AD mice (Quan, Luo et al. 2021). We found that depletion of intestinal bacteria slightly but significantly decreased β-, but not γ-secretase activity (Fig. 6.7, K and L; two-way ANOVA, antibiotic treatment vs. control, $p < 0.05$), as observed in a published study (Colombo, Sadler et al. 2021). It was not surprising that the same inhibitory effects of antibiotic treatment on β- and γ-secretase activity could not be seen in IL-17a-deficient APP-transgenic mice (Fig. 6.7, M and N; two-way ANOVA, antibiotic treatment vs. control, $p > 0.05$), as the antibiotic treatment did not change the inflammatory activation in the brain of IL-17a-deficient AD mice (see Fig. 6.4.1).

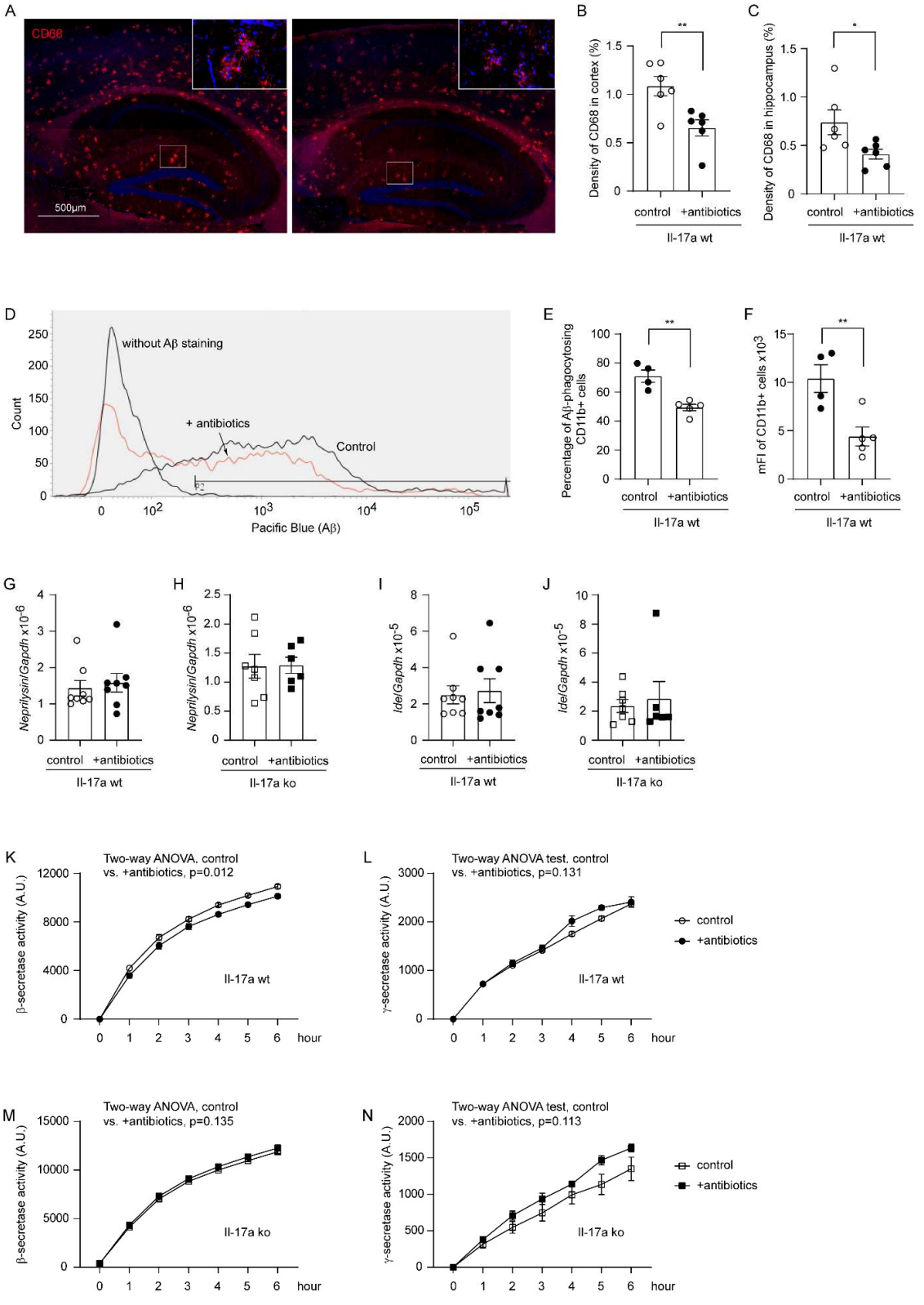

Fig. 6.7, Depletion of gut bacteria reduces β-secretase activity in the brain of IL-17a-wildtype, but not Il17a-deficient APP-transgenic mice. Three-month-old IL-17a-deficient (ko) and wild-type (wt) APP-transgenic female mice were treated with and without antibiotics in drinking water for 2 months. The

brain tissue was stained with Cy3-conjugated CD68 antibody (A). Antibiotic treatment significantly reduces the density of CD68-immunofluorescence in both cortex and hippocampus of APP-transgenic mice compared to AD mice drinking normal water (B and C; *t* test, $n = 6$ per group). APP-transgenic mice were also injected (*i.p.*) with methoxy-XO4 for the detection of Aβ-associated fluorescence in CD11b-positive brain cells by flow cytometry (D). Depletion of gut bacteria significantly decreased both the percentage of fluorescent cells among CD11b-positive brain cells, and the mean fluorescence intensity (mFI) of CD11b-positive cell population (E and F; *t* test, $n = 4$ - 5 per group). Brain tissues were further collected from AD mice for quantification of *Neprilysin* and *Ide* gene transcripts (G - J), and for β- and γ-secretase assays (K - N). Depletion of gut bacteria did not change the transcription of *Neprilysin* and *Ide* genes (G - J; *t* test, $n = 6$ - 8 per group); however, significantly inhibited the activity of β-secretase in the brain of IL-17a-wildtype but not IL-17a-deficient APP-transgenic mice (K and M; two-way ANOVA, $n = 6$ - 7 per group for IL-17a-wildtype mice, and $n = 4$ - 5 per group for IL-17a knockout mice). Depletion of gut bacteria did not change γ-secretase activity in AD mice (L and N; two-way ANOVA, $n = 6$ - 7 per group for IL-17a-wildtype mice, and $n = 4$ - 5 per group for IL-17a knockout mice). *: $p < 0.05$; **: $p < 0.01$.

6.8 Depletion of intestinal bacteria potentially increases Aβ efflux through blood-brain-barrier in APP-transgenic mice, which is driven by IL-17a inhibition

The transportation of Aβ from brain parenchyma to peripheral circulation is an efficient pathway for the cerebral Aβ clearance (Roberts, Elbert et al. 2014). LRP1 and ABCB1 are a couple of key transporters at the BBB that are responsible for Aβ efflux (Kuhnke, Jedlitschky et al. 2007, Shinohara, Tachibana et al. 2017). We found that the protein levels of ABCB1 and LRP1were significantly increased in 5-month-old APP-transgenic mice, which had been treated with antibiotics for 2 months (Fig. 6.8, A - C; *t* test, $p < 0.05$). Remarkably, the up-regulation of both LRP1 and ABCB1 in the brain homogenate by depletion of intestinal bacteria was again abolished by knockout of *Il-17a* gene (Fig. 6.8, D - F; *t* test, $p > 0.05$).

We also isolated blood vessels from 5-month-old APP-transgenic mice with and without treatments with antibiotics. We validated the results from the entire brain homogenate that treatments with antibiotics strongly elevated protein levels of ABCB1 and LRP1 at the BBB (Fig. 6.8, G - I; *t* test, $p < 0.05$). Notably, the protein level of claudin-5 in cerebral blood vessels did not differ between APP-transgenic mice with and without antibiotic treatment (Fig. 6.8, G and J; *t* test, $p > 0.05$). Similarly, we did not detect any mouse IgG in brain homogenates of antibiotics-treated AD mice with Western blot (data not shown),

which suggests that depletion of intestinal bacteria increased expression of ABCB1 and LRP1 at the BBB, but did not significantly impair the BBB.

In further experiments, we detected LRP1 and ABCB1 in the brain homogenates from 5-month-old APP-non-transgenic female mice with different expression of IL-17a. We observed that deficiency of IL-17a significantly increased the protein level of ABCB1, but not LRP1, in a gene dose-dependent way (Fig. 6.8, K - M; one-way ANOVA, $p < 0.05$). Similarly, we isolated blood vessels from IL-17a-deficient and wild-type APP-transgenic mice and observed that deficiency of IL-17a significantly increased both LRP1 and ABCB1 in the tissue lysate of blood vessels (Fig. 6.8, N - P; *t* test, $p < 0.05$), suggesting that depletion of intestinal bacteria potentially increases LRP1/ABCB1-mediated Aβ efflux through inhibiting IL-17a signaling.

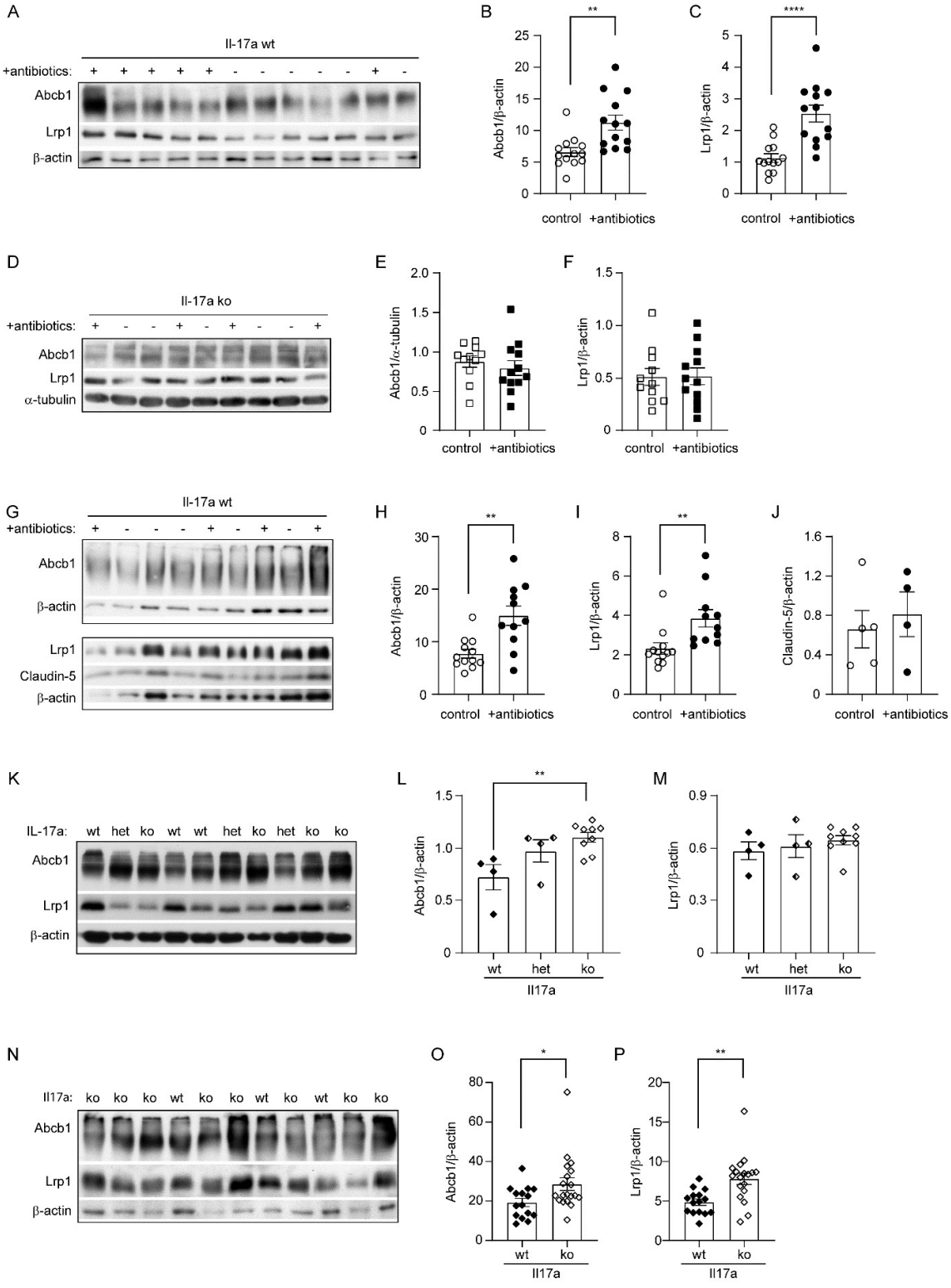

Fig. 6.8, Depletion of gut bacteria increases ABCB1 and LRP1 expression in the blood-brain-barrier of IL-17a-wildtype, but not IL-17a-deficient APP-transgenic mice. Three-month-old IL-17a-deficient (ko) and wild-type (wt) APP-transgenic female mice were treated with and without antibiotics in drinking water for 2 months. Brain homogenates were quantified for protein levels of ABCB1 and LRP1 with

Western blot (A and D). Depletion of gut bacteria significantly increased expression of ABCB1 and LRP1 in brains of IL-17a-wildtype (B and C), but not in IL-17a-deficient (E and F) APP-transgenic mice (*t* test, $n = 13$, and 11 - 12 per group for Il-17a wt and ko mice, respectively). Cerebral vessels were also isolated from Il17a-wildtype AD mice and detected for ABCB1 and LRP1 at the BBB (G). Depletion of gut bacteria significantly increased the expression of ABCB1 and LRP1 in blood vessels of APP-transgenic mice (H and I; *t* test, $n = 11$ - 12 per group); however, it did not change the protein level of claudin-5 (J; *t* test, $n = 4$ - 5 per group). In further experiments, ABCB1 and LRP1 were detected with quantitative Western blot in the brain homogenates from 5-month-old non-APP-transgenic female mice with different expression of IL-17a (K; wild-type [wt], heterozygote [het] and knockout [ko]), and in the isolated blood vessels from 5-month-old Il17a-wt and ko APP-transgenic female mice (N). Deficiency of IL-17a significantly inceased ABCB1 but not LRP1 in the non-APP-transgenic mouse brain in a gene dose-dependent manner (L and M; one-way ANOVA followed by Bonferroni *post-hoc* test, $n = 4$ - 9 per group), and increased protein levels of both ABCB1 and LRP1 in the blood vessels of APP-transgenic mice (O and P; *t* test, $n = 15$ - 19 per group). *: $p < 0.05$; **: $p < 0.01$; ****: $p < 0.0001$.

6.9 Depletion of intestinal bacteria potentially promotes synaptic plasticity in APP-transgenic mice, which is abolished by deficiency of IL-17a

After finding that gut bacterial depletion attenuated inflammatory activation and amyloid pathology in the brains of APP-transgenic mice, we performed a preliminary analysis of the neuroprotective effect of antibiotic treatment. Our previous study has shown that upregulated transcription of the immediate early gene *Arc* and the gene *Grin1*, which encodes subunit 1 of the NMDA-type ionotropic glutamate receptor, is associated with the improvement of cognitive function in APP-transgenic mice (Hao, Liu et al. 2011). BDNF plays an important role in the maintenance of synaptic plasticity in learning and memory (Gao, Zhang et al. 2022), the transcript of which is influenced by gut bacteria (Frohlich, Farzi et al. 2016). Therefore, we measured the transcripts of *Arc*, *Grin1* and *Bdnf* genes in brains of 5-month-old APP-transgenic mice with and without 2-month treatment with antibiotics. As shown in Fig. 6.9, A - C, treatment with the antibiotic cocktail significantly increased the transcription of *Arc*, but not *Grin1* and *Bdnf* genes in IL-17a-wildtype APP mice (*t* test, $p < 0.05$). Again, knockout of *Il-17a* gene abolished the neuroprotective effect of antibiotic treatment (Fig. 6.9, A - C; *t* test, $p < 0.05$). However, the neuroprotective effects of antibiotic treatment should be further investigated by other methods, such as behavioral tests and electrophysiological approaches, in older (e.g., 9-month-old) APP-transgenic mice as we did previously (Quan, Luo et al. 2021, Luo, Schnoder et al. 2022).

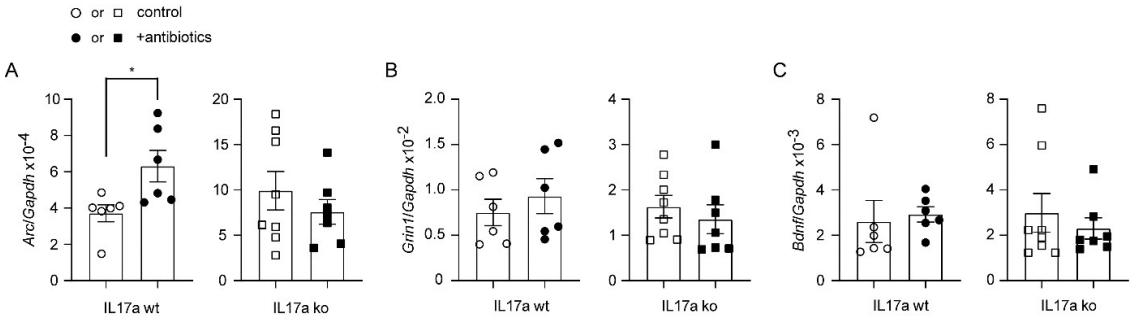

Fig. 6.9, Depletion of gut bacteria increases *Arc* transcription in the brain of IL-17a-wildtype, but not Il17a-deficient APP-transgenic mice. Three-month-old IL-17a-deficient (ko) and wild-type (wt) APP-transgenic female mice were treated with and without antibiotics in drinking water for 2 months. Thereafter, brain tissues were homogenized and measured for transcripts of *Arc*, *Grin1* and *Bdnf* genes. Antibiotic treatment significantly increased the transcription of *Arc* gene in IL-17a-wildtype, but not in IL-17a-deficient APP-transgenic mice (A; *t* test, n = 6 and 7 - 8 per group for IL-17a wt and ko mice, respectively). Antibiotic treatment did not change the transcription of *Grin1* and *Bdnf* genes (B and C; *t* test, n = 6 and 7 - 8 per group for IL-17a wt and ko mice, respectively). *: $p < 0.05$.

7 DISCUSSION

Gut bacteria contribute to AD development (Chandra, Sisodia et al. 2023), but how gut bacteria regulate brain pathology remains unclear. By using young female APP-transgenic mice with rapidly developing Aβ pathology, we found that depletion of gut bacteria decreased microglial inflammatory activation and Aβ levels, particularly soluble Aβ, and might promote synaptic plasticity in the brain. These effects were abolished by knockout of *Il-17a* gene. The attenuation of cerebral Aβ pathology by gut bacterial depletion may be attributed to the inhibition of β-secretase activity and the upregulation of Aβ efflux-related LRP1 and ABCB1 expression in the brain, which was also abrogated by IL-17a deficiency.

Bacterial phenotypes are potentially transferred between contacting mice (Zhang, Shen et al. 2023). We co-housed 4-6 IL-17a-deficient and wild-type female AD mice in the same cage for treatments with and without antibiotics, which reduced the variability caused by different housing conditions. Depletion of gut bacteria in APP-transgenic mice inhibited proinflammatory activation in the brain tissue as evidenced by reduction of microglial number, down-regulation of *Il-1β* and *Ccl-2* transcription and up-regulation of *Il-10* transcription, consistent with published studies (Harach, Marungruang et al. 2017, Minter, Hinterleitner et al. 2017, Colombo, Sadler et al. 2021). In individual microglia, depletion of gut bacteria decreased transcripts of both pro- (e.g., *Tnf-α*, *Il-1β*, *Ccl-2*) and anti-inflammatory (*Il-10*) genes, which is also in agreement with the published finding that the absence of gut bacteria leads to global defects in microglial activation (Erny, Hrabe de Angelis et al. 2015). The opposing regulation of *Il-10* transcription in microglia and brain tissue suggests that brain cells other than microglia, such as astrocytes, may also respond to gut bacteria (Chandra, Di Meco et al. 2023) and produce IL-10 in the brain.

We noted that intestinal bacterial depletion in 5-month-old C57BL/6J mice did not have the same effect on the inflammatory modulation as in AD mice, and even promoted inflammatory activation (e.g., transcriptional up-regulation of *Tnf-α*, and down-regulation of *Chi3l3*) in the brain of 24-month-old C57BL/6J mice. In fact, the mechanism leading

to inflammatory activation in the brain, and particularly in microglia, is not the same in AD and healthy ageing. For example, inflammation in ageing microglia may be due to a reduced ability to clear endogenous metabolites, whereas microglia in AD mice respond efficiently to exogenous Aβ. A transcriptomic study (Li, Li et al. 2023) identified 85 ageing-associated genes in female C57BL/6J mice, of which only 21 genes overlapped with DAM genes that were identified in APP-transgenic mouse model (Keren-Shaul, Spinrad et al. 2017), with the exception of the DAM-characteristic genes *Trem2* and *Apoe*. Thus, it stands to reason that a significant inflammatory modulation caused by gut bacterial depletion depends on the preactivated status and pattern of inflammatory brain cells (e.g., microglia).

Depletion of gut bacteria resulted in a significant reduction of IL-17a-expressing CD4-positive cells in the gut and spleen as well as bacterial DNA in brain tissue, suggesting that gut bacteria regulate brain pathology in AD mice via at least two pathways: 1) regulating peripheral IL-17a-expressing T lymphocytes and 2) directly modulating cells in the brain with bacterial components (not necessary living cells). Very interestingly, we also observed that deficiency of IL-17a reduces bacterial DNA in the brain of APP-transgenic mice. Due to our limited research resource, we have not yet succeeded in the microbiome analysis of brain tissues. The recent study detected *Streptococcus*, *Clostridium*, *Roseburia* and *Tyzzerella* in the brain of APP/PS1 mice (Thapa, Kumari et al. 2023). The bacteria from *Cutibacterium acnes* were found in the brain of AD patient and linked to AD pathogenesis (Mone, Earl et al. 2023). How the bacteria or their structural components enter the brain is unclear. It has been reported that deficiency of IL-17a alters the composition of gut bacteria, i.e., increases the abundance of *Barnesiella* genus bacteria, and hinders the development of EAE (Regen, Isaac et al. 2021). *Barnesiella* bacteria are the main source of hypoxanthine in the gut. Intestinal epithelial cells utilize hypoxanthine for energy balance and nucleotide biosynthesis (Lee, Wang et al. 2021). Thus, IL-17a deficiency may favor intestinal barrier function and lead to the reduction of bacterial DNA in the brain of APP-transgenic mice. Inhibition of IL-17a signaling, which can be achieved by administering IL-17a inhibitors or by depleting specific bacterial taxa in the gut that stimulate the development of IL-17a-producing T cells, therefore has the potential to avoid bacterial overload in the brain and prevent AD progression.

Exactly how the depletion of bacteria in the gut and subsequent IL-17a inhibition, in particular the reduction of Th17 cells, regulates microglial activity in our antibiotic-treated AD mice remains unclear. IL-17a inhibition itself does not appear to inhibit microglial activation. We have recently observed that knockout of *Il-17a* gene reduces microglial branches in APP-transgenic mice (Luo, Schnoder et al. 2022), suggesting activation of microglial inflammatory response (Madry, Kyrargyri et al. 2018). Our current study shows that IL-17a deficiency did not reduce the transcription of *Tnf-α*, *Il-1β*, *Ccl-2* and *Il-10* genes in isolated microglia (Fig. 6.5.2, B). The inhibition of inflammation in both brain tissue and microglia in our antibiotic-treated AD mice may be due to the depletion of bacteria other than IL-17a-promoting taxa in the gut. In IL-17a-deficient APP-transgenic mice, antibiotic treatment did not inhibit inflammatory activation in brain tissue and microglia, for which there are perhaps several reasons. Deficiency of IL-17a reduced soluble Aβ (discussed later) and bacterial DNA, minimizing the inflammatory priming of microglia as in 5-month-old C57B/L6 mice, limiting the capacity to further inhibit inflammation by depleting gut bacteria. However, we believe that there are other unknown mechanisms by which IL-17a inhibition maintains and even enhances microglial activity in the brain, which we will investigate in the future studies. To answer this question, it is helpful to identify the IL-17a signaling-promoting bacteria or their metabolites in the gut of AD mice. Unfortunately, the available relevant results for today are very limited or controversial. For example, the bacterial product valeric acid was reported to increase the concentrations of IL-17, IL-1β, and IL-6 in the blood and brain of mice with experimental stroke (Zeng, Li et al. 2023). However, treatment with valeric acid was also shown to reduce the concentrations of TNF-α and IL-6 in the blood of mice after irradiation (Li, Dong et al. 2020). In addition, activation of the valeric acid receptor Gpr43 inhibited neuroinflammation and improved cognitive function in APP-transgenic mice (Zhou, Xie et al. 2023).

It should be noted that microglial activation is a double-edged sword in AD pathogenesis: on the one side, it releases cytotoxic cytokines and reactive oxygen species, leading to neuronal damage; on the other side, it clears neurotoxic Aβ via microglial internalization, thereby safeguarding neurons (Heneka, Carson et al. 2015). In our recent study, p38α-MAPK deficiency in myeloid cells or IL-17a deficiency promotes microglial activation and Aβ clearance, which improves cognitive performance in APP-transgenic mice (Luo,

Schnoder et al. 2022). We and other groups have also shown that stimulation of TLR4 and TLR9 by injection of a low dose of LPS or synthetic oligodeoxynucleotides containing unmethylated CpG dinucleotides, similar to those found in bacterial DNA, induces mild and long-term microglial activation that facilitates the clearance of Aβ and hyperphosphorylated tau protein in human APP or tau-transgenic mice (Scholtzova, Kascsak et al. 2009, Michaud, Halle et al. 2013, Scholtzova, Chianchiano et al. 2014, Qin, Liu et al. 2016), and in squirrel monkeys (Patel, Nehete et al. 2021). Our present study has shown that general depletion of gut bacteria reduces microglial phagocytosis of Aβ in APP-transgenic mice, which is consistent with previous observations that gut bacteria are essential for microglial maturation, activation and Aβ phagocytosis (Erny, Hrabe de Angelis et al. 2015, Colombo, Sadler et al. 2021, Erny, Dokalis et al. 2021, Xie, Bruggeman et al. 2023). We would expect that specific depletion of IL-17a-promoting gut bacteria could maintain microglial activity and help clear the pathogenic Aβ molecules from the AD brain.

When studying the gut and brain, how gut bacteria modulate cerebral Aβ load is always an important question to answer. Our present study showed that microglia are not responsible for cerebral Aβ reduction in APP-transgenic mice after depletion of gut bacteria. Interestingly, we observed that depletion of gut bacteria increased the expression of LRP1 and ABCB1 in the BBB of APP-transgenic mice, which was reversed by knockout of *Il-17a* gene. Knocking out *Il-17a* gene completely mimicked the effects of gut bacteria depletion on the expression of LRP1 and ABCB1. LRP1 and ABCB1 are two important transporters responsible for Aβ efflux across the BBB (Kuhnke, Jedlitschky et al. 2007, Shinohara, Tachibana et al. 2017). Depletion or inhibition of endothelial LRP1 and ABCB1 leads to Aβ accumulation in the AD mouse brain (Cirrito, Deane et al. 2005, Storck, Meister et al. 2016). Since transportation of Aβ from brain parenchyma to peripheral plasma might contribute 25% of total clearance of cerebral Aβ (Roberts, Elbert et al. 2014), Aβ efflux represents a major pathway mediating the reduction of Aβ in the brain of AD mice following depletion of gut bacteria. It has been reported that the absence of ApoE retains less Aβ in the brain parenchyma and increases soluble Aβ in the interstitial fluid, possibly promoting the diffusion of soluble Aβ from the parenchyma into the perivascular space (DeMattos, Cirrito et al. 2004), which favors Aβ efflux. Notably, depletion of gut bacteria decreased *Apoe* gene transcription in microglia, as

observed in our study and by other scientists (Colombo, Sadler et al. 2021), which may indicate the cooperation between microglia and BBB in the clearance of cerebral Aβ.

Aβ is produced by β- (BACE1) and γ-secretases after serial digestions of APP. The published studies by our group and others have shown that the activity or protein level of β- and γ-secretases is regulated by inflammatory activation in the brain (He, Zhong et al. 2007, Hur, Frost et al. 2020, Quan, Luo et al. 2021). Not surprisingly, depletion of gut bacteria inhibited β-secretase activity in correlation with inflammatory inhibition in our APP-transgenic mice, which is consistent with the observation in germ-free AD mice (Colombo, Sadler et al. 2021). We did not detect an increase in the expression of neprilysin and Ide in our APP-transgenic mice after antibiotic treatment, suggesting that extracellular degradation of Aβ is not the key mechanism for Aβ clearance after gut bacterial depletion. This result differs from the observation in a study on germ-free AD mice (Harach, Marungruang et al. 2017).

Antibiotic therapy for AD patients has gained interest (Panza, Lozupone et al. 2019). In several studies, germ-free APP-transgenic mice show better cognitive function and lower cerebral Aβ levels than specific pathogen-free (SPF) AD mice (Mezo, Dokalis et al. 2020, Colombo, Sadler et al. 2021). Our study supports antibiotic therapy, as gut bacterial depletion reduced Aβ burden in AD mice and, in particular, increased Aβ efflux-associated ABCB1 and LRP1 across the BBB. Depletion of gut bacteria also up-regulated the transcription of *Arc* gene in the brain, which is associated with synaptic plasticity and cognitive improvement in APP-transgenic mice (Bramham, Worley et al. 2008, Hao, Liu et al. 2011). However, as discussed above, the general depletion of gut bacteria inhibits the activation of microglia, which decreases the efficiency of Aβ clearance. In addition, gut bacteria have also been shown to promote the development of cognitive performance (Cerdo, Ruiz-Rodriguez et al. 2023). Adult germ-free mice transplanted with fecal microbiota from 2-3-month-old mice perform better cognitively than mice transplanted with fecal microbiota from 18-20-month-old mice (Lee, Venna et al. 2020). Treatment with broad-spectrum antibiotics can deplete as well the taxa of gut bacteria that favor learning and memory. Our study also indicated that bacteria belonging to the genera *Escherichia-Shigella* and *Parasutterella* were more resistant to antibiotic treatment. The possible expansion of these bacteria, especially *Escherichia Shigella* bacteria, after long-

term antibiotic treatment could increase inflammatory activation in the brain and accelerate the progression of AD. The combination of our results and the literature indicates that it is important to manipulate a specific bacterial taxon, e.g. by reducing the bacteria that stimulate immune cells to produce IL-17a. Currently, antibiotic therapy targeting specific bacterial taxa is still a major challenge for AD patients.

A limitation of our study is that the direct anti-inflammatory effects of antibiotics orally used to deplete gut bacteria could not be excluded. Although oral vancomycin, neomycin, streptomycin and ampicillin have low systemic absorption (Frohlich, Farzi et al. 2016), the oral bioavailability of metronidazole is high (98.9%) (Jensen and Gugler 1983). Metronidazole must not be omitted from the antibiotic cocktail as it decimates anaerobic bacteria in the gut. Metronidazole has the potential to suppress the activity of both innate and acquired immune systems (Shakir, Javeed et al. 2011). We observed that intraperitoneal injection of the antibiotic cocktail inhibited inflammatory gene transcription in the brain; however, the affected genes were mainly limited to anti-inflammatory *Il-10* and *Mrc1* genes (see Figure 6.4.2), with a pattern different from the inflammatory regulation caused by oral treatment of antibiotics. We also observed that oral antibiotic treatment decreased *Il-17a* transcription but increased transcription of *Ifn-γ* and *Il-4* genes in CD4-positive spleen cells in APP-transgenic mice and promoted inflammatory activation in the brains of 24-month-old mice. Indeed, oral antibiotic (amoxicillin/clavulanate) treatment of mice with antibiotic-sensitive and -resistant bacteria in the gut has shown that depletion of sensitive gut bacteria inhibits the development of IL-17a-expressing γδ T cells (Benakis, Brea et al. 2016). Therefore, we have reason to believe that the inhibition of neuroinflammation and Th17 development in our AD animal models was not due to the direct effects of antibiotics, but was a consequence of the depletion of gut bacteria. The potential inhibitory effect of antibiotics on immune cells is a common pitfall in antibiotic-treated mice in many gut and brain studies (Erny, Hrabe de Angelis et al. 2015, Dodiya, Kuntz et al. 2019, Xie, Bruggeman et al. 2023).

Over the recent decades, growing evidence has suggest a role of infection in the AD pathogenesis. Multiple studies on post-mortem AD brain have reported that diverse pathogens are present, ranging from bacteria to fungi to viruses (Lathe, Schultek et al.

2023). However, a pathogen contamination might be possible during the sampling and proceeding. This awaits further confirmation. The most employed techniques to detect bacteria in AD brain are based on ribosomal RNA (rRNA) or rDNA analysis and metagenomics. No AD-specific bacteria have been directly detected in the brain. Furthermore, brain biopsy is unfeasible, with the exception of patients undergoing neurosurgery for other reasons. A sample from peripheral organ is needed, which may be representative of the bacteria profile in AD brain (Lathe, Schultek et al. 2023, Mone, Earl et al. 2023) .

In summary, our results are consistent with published observations that depletion of gut bacteria attenuates microglial inflammatory activation and Aβ pathology in the brain of APP-transgenic mice; however, we further elucidated the possible mechanisms mediating the gut-brain axis in AD pathogenesis: 1) depletion of gut bacteria reduces peripherally circulating IL-17a-expressing T lymphocytes and translocation of bacterial components from the gut to the brain. IL-17a deficiency inhibits this bacterial translocation; 2) inhibition of IL-17a possibly maintains and even enhances microglial activity; 3) inhibition of IL-17a upregulates the expression of LRP1 and ABCB1 in the BBB, possibly promoting Aβ efflux and Aβ clearance in the brain; and 4) depletion of gut bacteria has the potential to improve neuronal plasticity. Our study supports antibiotic therapy for AD patients; however, precise therapy targeting specific bacterial taxa is still a huge challenge.

New methods and future work are needed to characterize the AD-specific microbiome profile in the gut. Particular attention should be paid to how IL-17a-associated intestinal bacteria can be manipulated. Recent studies have shown, that specific microRNA, a small non-coding RNA molecule released from intestinal epithelial cells, is associated with the alteration of the gut bacterial profile in several diseases. We performed the preliminary experiments und observed that the temporal depletion of microRNA could alter the component of gut bacteria in AD mice. Our future work will be focused on the identifying of the AD-specific microRNA, which may provide a method to modify the specific group of gut bacteria that stimulate IL-17a-expressing T lymphocytes. Detailed preliminary data are described in the section ‘PERSPECTIVES AND FUTURE RESEARCH PLAN’.

8 PERSPECTIVES AND FUTURE RESEARCH PLAN

Modification of the gut bacteria through depletion or transplantation of the gut bacteria in animal models has shown that there is an important link between the gut and the AD brain. However, the AD-associated profile of gut microbiome has not been defined. At the family and genus levels, the results about changes in gut bacteria of AD patients are highly variable between various studies; for example, a consistent decrease in butyrate-producing bacteria of the genus *Butyricicoccus* or *Coprococcus* or an increase in the genera *Escherichia/Shigella* (three genera are not changed in the same study) in AD patients is only found in two out of twenty independent studies (Zhang, Gao et al. 2023). The variable changes in gut microbiome also exist in APP-transgenic AD mice compared to their corresponding wild-type controls (Zhang, Gao et al. 2023). A limited number of reports have investigated which specific bacteria that are related to aging and AD pathology (Fang, Kazmi et al. 2020, Wasen, Beauchamp et al. 2024). Therefore, a potential precision therapy for each AD patient that targets potential AD-associated bacterial taxa in the gut should be considered. Our study suggests that depletion of a specific group of gut bacteria that stimulate IL-17a-expressing T lymphocytes may be able to prevent AD progression in APP-transgenic mice. A flexible method to efficiently and specifically modify the microbiome in AD patients and animal models is desirable.

Intestinal epithelial cells have been shown to release microRNA (miRNA), a small non-coding RNA molecule, which enters intestinal bacteria, post-transcriptionally modifies bacterial protein expression and subsequently alters bacterial proliferation and metabolism (Liu, da Cunha et al. 2016). Intenstinal epithelial-miRNA-deficient mice exhibit uncontrolled gut microbiota and exacerbated colitis with an increase in IL-17a expression, and transplantation with fecal miRNA from wild-type mice restores fecal microbiota and ameliorates colitis (Liu, da Cunha et al. 2016). A recent study has demonstrated the association between specific miRNA expressions and key gut bacteria at different stages of Crohn's diease in pediatric patients (Lv, Zhen et al. 2024). Oral administration of miR-30d that is enriched in the feces of untreated multiple sclerosis patients and mice with experimental autoimmune encephalomyelitis (EAE) at the peak disease was reported to attenuate symptoms of EAE mice by increasing *Akkermansia*

muciniphila bacteria and the population of regulatory T cells in the gut (Liu, Rezende et al. 2019). Therefore, we hypothesize that oral treatment with a specific miRNA in AD mice could provide a strategy to manipulate the specific group of gut bacteria that stimulate IL-17a-expressing T lymphocytes.

We have started preliminary experiments for the following studies on gut miRNA and AD. Intestinal epithelial cells are the major source of miRNA in the intestinal lumen (Liu, da Cunha et al. 2016). We established $App^{NL\text{-}G\text{-}F}$ knock-in AD mice (Saito, Matsuba et al. 2014) with and without expression of Dicer1, an essential enzyme in miRNA production, in epithelial cells of the intestine ($App^{ki/ki}Dicer1^{del}$ and $App^{ki/ki}Dicer1^{wt}$) by crossing $App^{ki/ki}$ mice with *Dicer1*-floxed mice (Cobb, Nesterova et al. 2005) and Villin-Cre mice over-expressing CreERT2 under control of the *Villin* gene promoter (el Marjou, Janssen et al. 2004) to obtain the genotypes $App^{ki/ki}/Dicer1^{fl/fl}/Cre^{tg}$ and $App^{ki/ki}/Dicer1^{fl/fl}/Cre^{wt}$, followed by feeding littermate AD mice with tamoxifen. Interestingly, 2 months after tamoxifen induction, the number of bacteria as shown by the level of bacterial 16S rRNA was significantly reduced in cecum contents of 9-month-old $App^{ki/ki}Dicer1^{del}$ mice compared with $App^{ki/ki}Dicer1^{wt}$ littermates (Fig. 8, A; *t* test, $p < 0.05$), despite the fact that gut epithelial cells are known to renew continuously and rapidly (Barker 2014).

In α-diversity analysis of bacterial species, we found that the Sobs, Ace, Chao, and Shannon indexes were significantly smaller in $App^{ki/ki}Dicer1^{del}$ mice than in $App^{ki/ki}Dicer1^{wt}$ littermates (Fig. 8, B - E; *t* test, $p < 0.05$). The Simpson index was not altered (Fig. 8, F). The Sobs, Chao, Ace were used to describe the bacterial species richness, i.e., the number of operational taxonomic units (OUT). The Shannon index and Simpson indexes were used to describe community diversity, including species richness and species evenness. Therefore, deletion of epithelial Dicer1 reduces gut bacterial richness and diversity in AD mice.

In the β-diversity-based principal coordinate analysis (PCoA), we clearly observed the difference in the architecture of gut bacteria between $App^{ki/ki}Dicer1^{del}$ and $App^{ki/ki}Dicer1^{wt}$ mice (Fig. 8, G; ANOSIM, R = 0.8850, $p = 0.002$), which was in line with the observation in mice with constitutive knockout of *Dicer1* gene in intestinal epithelial cells (Liu, da Cunha et al. 2016). At the genus level, the abundance of

Helicobacter, *Parasutterella*, *Bacteroides* and *Lachnoclostrium* increased, while that of *Prevotellaceas*, *Muribaculaceae*, and *Lachnospiraceae* decreased in $App^{ki/ki}Dicer1^{del}$ mice compared with $App^{ki/ki}Dicer1^{wt}$ controls (Fig. 8, H; Wilcoxon rank-sum test, $p < 0.01$).

To investigate the impact of miRNA deficiency on the brain, we used the PICRUSt2 software (Douglas, Maffei et al. 2020) and annotated the metagenomic reads on the KEGG database (Kanehisa and Goto 2000) to predict the function of changed microbiota. Deletion of gut miRNA had the potential to influence various pathophysiological functions of the host. Notably, deletion of Dicer1 in epithelial cells of gut might promote neurodegenerative disease and adversely affect the nervous system compared with Dicer1 wild-type AD mice (Fig. 8, I; Wilcoxon rank-sum test, $p < 0.05$), although the underlying mechanism remains to be investigated.

Our preliminary experiments clearly showed that a temporal (for one month) depletion of miRNA is able to change the components of bacteria in the gut for a long term (the following two months). In our future work we would compare miRNA expression in feces from AD mice and healthy controls to identify the specific miRNA for AD. Then we would investigate the changes of the gut bacteria by oral administration of synthesized miRNA, which may provide a method to identify the specific group of gut bacteria that stimulate IL-17a-expressing T lymphocytes. The AD-specific miRNA may also have the potential to modify the gut bacteria and serve therapeutic effects in AD mice, perhaps also in AD patients.

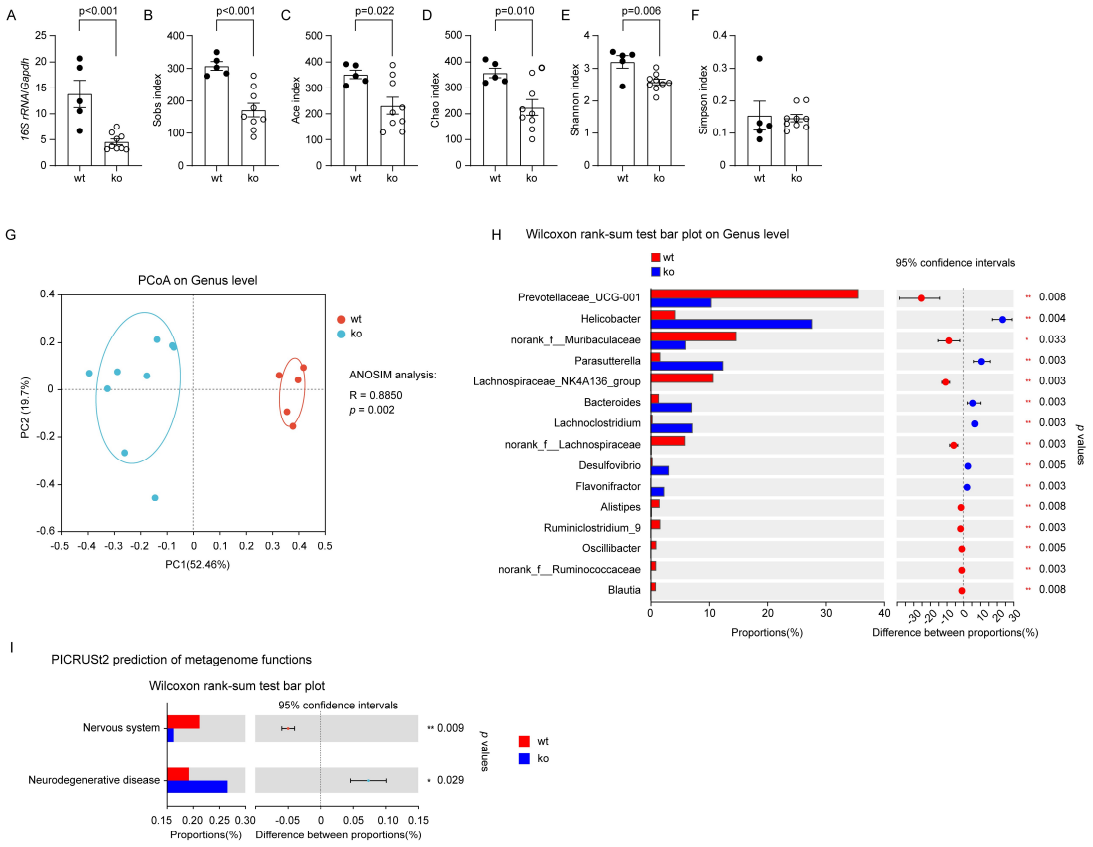

Figure 8. Deletion of dicer1 in gut epithelial cells changed the composition of gut bacteria in App-knock-in mice. Nine-month-old App-knock-in mice with (ko, n = 9) and without (wt, n = 5) deletion of dicer1 in gut epithelial cells were analyzed for the composition of gut bacteria. Intestinal content for the isolation of bacterial DNA was harvested from the appendix and neighboring colon. Bacterial DNA was first measured for the amount with real-time PCR (A; *t* test), and then sequenced for the V3-V4 region of 16S rRNA-encoding gene. Deletion of dicer1 significantly decreased Sobs, Ace, Chao and Shannon, but not Simpson's indices (B - F; *t* test), indicating the reduction of bacterial richness and diversity. Principal coordinate analysis (PCoA) was used for β-diversity analysis of bacterial composition at the genus level in App-knock-in mice with and without deletion of dicer1 (G; Each symbol represents the gut bacteria of an individual mouse). As expected, the structure of gut bacterial community differed significantly between these two mouse groups (G; ANOSIM analysis). Bar plots depict abundance (% of total) of the indicated genera. Wilcoxon rank-sum tests show that deletion of dicer1 in epithelial cells changed the relative abundance of bacteria in various genera, e.g., *Prevotellaceae*, *Helicobacter* and *Parasutterella* (H). Finally, the PICRUSt2 software was used to predict the function of gut bacteria, which showed that deletion of dicer1 potentially contributes to neurodegenerative disorders (I; Wilcoxon rank-sum tests).

9 APPENDIX

GUT MICROBES
2024, VOL. 16, NO. 1, 2363014
https://doi.org/10.1080/19490976.2024.2363014

Taylor & Francis
Taylor & Francis Group

RESEARCH PAPER

OPEN ACCESS Check for updates

Modulation of Alzheimer's disease brain pathology in mice by gut bacterial depletion: the role of IL-17a

Wenlin Hao[a,b], Qinghua Luo[a,b,c], Inge Tomic[a,b], Wenqiang Quan[a,b,d], Tobias Hartmann[b,e], Michael D. Menger[f], Klaus Fassbender[a,b], and Yang Liu[a,b]

[a]Department of Neurology, Saarland University, Homburg/Saar, Germany; [b]German Institute for Dementia Prevention (DIDP), Saarland University, Homburg/Saar, Germany; [c]Department of Neurology, The second affiliated hospital of Nanchang University, Nanchang, China; [d]Department of Clinical Laboratory, Tongji Hospital, Tongji University Medical School, Shanghai, China; [e]Department of Experimental Neurology, Saarland University, Homburg/Saar, Germany; [f]Department of Experimental Surgery, Saarland University, Homburg/Saar, Germany

ABSTRACT

Gut bacteria regulate brain pathology of Alzheimer's disease (AD) patients and animal models; however, the underlying mechanism remains unclear. In this study, 3-month-old APP-transgenic female mice with and without knock-out of *Il-17a* gene were treated with antibiotics-supplemented or normal drinking water for 2 months. The antibiotic treatment eradicated almost all intestinal bacteria, which led to a reduction in Il-17a-expressing CD4-positive T lymphocytes in the spleen and gut, and to a decrease in bacterial DNA in brain tissue. Depletion of gut bacteria inhibited inflammatory activation in both brain tissue and microglia, lowered cerebral Aβ levels, and promoted transcription of *Arc* gene in the brain of APP-transgenic mice, all of which effects were abolished by deficiency of Il-17a. As possible mechanisms regulating Aβ pathology, depletion of gut bacteria inhibited β-secretase activity and increased the expression of Abcb1 and Lrp1 in the brain or at the blood-brain barrier, which were also reversed by the absence of Il-17a. Interestingly, a crossbreeding experiment between APP-transgenic mice and *Il-17a* knockout mice further showed that deficiency of Il-17a had already increased Abcb1 and Lrp1 expression at the blood-brain barrier. Thus, depletion of gut bacteria attenuates inflammatory activation and amyloid pathology in APP-transgenic mice via Il-17a-involved signaling pathways. Our study contributes to a better understanding of the gut-brain axis in AD pathophysiology and highlights the therapeutic potential of Il-17a inhibition or specific depletion of gut bacteria that stimulate the development of Il-17a-expressing T cells.

ARTICLE HISTORY
Received 7 December 2023
Revised 23 April 2024
Accepted 29 May 2024

KEYWORDS
Alzheimer's disease; gut microbiome; microglia; amyloid pathology; and Il-17a

Introduction

The microbial composition in the gut undergoes alterations in both Alzheimer's disease (AD) patients and mouse models.[1-4] A prospective study of cognitively healthy individuals revealed that a decrease in butyrate-producing bacterial species (e.g., *Roseburia inulinivorans* and *R. faecis*) or an increase in pro-inflammatory bacteria (e.g., *Veillonella dispar* and *V. atypica*) correlates with subjective cognitive decline over a follow-up period of 2 to 4 years[5]). Transplantation of gut bacteria from AD patients to gut bacteria-depleted rats results in impaired neurogenesis and cognitive function.[6] Gut bacteria-free Alzheimer's precursor protein (APP)-transgenic or $App^{NL\text{-}G\text{-}F}$ knock-in AD mice also exhibit reduced amyloid β peptide (Aβ) deposition and microgliosis in the brain.[7-11] Consequently, gut bacteria play an important role in AD pathogenesis, though the mechanism of how gut bacteria impact brain pathology in AD remains to be investigated.

However, the specific profile of intestinal bacteria associated with AD has not yet been defined. There is often a decrease in bacterial abundance in *Firmicutes* phylum, an increase in *Proteobacteria* phylum, and both a decrease and an increase in the proportion of *Bacteroidetes* bacteria.[1,4,12,13] At the family and genus levels, the variability of results regarding AD-specific bacterial changes is even greater across different studies. For example, a consistent decrease in bacteria of the genus *Butyricicoccus* or *Coprococcus* or an increase in the genera *Escherichia/Shigella* (three genera are

CONTACT Yang Liu a.liu@mx.uni-saarland.de Department of Neurology, Saarland University, Kirrberger Straße, Homburg/Saar 66421, Germany
Supplemental data for this article can be accessed online at https://doi.org/10.1080/19490976.2024.2363014

not changed in the same study) in AD patients is only found in two out of twenty independent studies.[4] *Butyricicoccus* and *Coprococcus* produce butyrate, which prevents excessive inflammation in the gut,[14,15] while *Escherichia/Shigella* releases toxins and promotes inflammatory activation in the human body.[14] The variability in research findings also exists in AD animals.[4] It is a challenge to investigate the precise role of different bacterial taxa in AD pathogenesis. Germ-free or broad-spectrum antibiotic-treated mice are still often used to study the molecular mechanisms by which gut bacteria influence brain pathology in AD.

An important mechanism mediating the brain-gut axis is that gut bacteria produce short-chain free fatty acids (SCFAs, i.e., acetate, butyrate and propionate) that promote the maturation of microglia, innate immune responses and energy metabolism in a homeostatic state.[16,17] Administration of SCFAs to germ-free or antibiotic-treated AD mice restores microglial proliferation and inflammatory activation; however, the effects on Aβ phagocytosis and Aβ accumulation in the brain are inconsistent between different studies.[16,18,19] Whether SCFAs act directly on microglia also remains unclear. We found that SCFA receptors, G protein-coupled receptor (Gpr) 41 and Gpr43 are absent in murine microglia[20]; however, deficiency of Gpr41 and Gpr43 likely inhibits microglial maturation under physiological conditions[17] and increases microglial density and Aβ deposits in the brain of APP-transgenic mice.[21] Deficiency of the butyrate receptor Gpr109a, which is highly expressed in microglia,[20] has limited effects on microglial activation.[21] Since the SCFAs produced by intestinal bacteria activate Gpr41, Gpr43 and Gpr109a, promote anti-inflammatory properties and regulate the development of interleukin (Il)-17a or Il-10 producing T cells in the gut,[21–23] we hypothesized that gut bacteria alter microglial activation and brain pathology through circulating T lymphocytes.

Germ-free mice generate fewer Il-17a-producing CD4(+) T help (Th17) lymphocytes but more CD4(+)CD25(+)Foxp3(+) regulatory T (Treg) cells in the gut and spinal cord, which is associated with resistance to experimental autoimmune encephalomyelitis (EAE) in mice.[24] Depletion of intestinal bacteria by antibiotics reduces the accumulation of Il-17a-producing γδ T cells in the leptomeninges and ameliorates brain injury in a stroke mouse model.[25] In APP-transgenic mice, reductions in cerebral Aβ deposition and microglia after gut antibiotic treatments correlate with increased levels of Foxp3+ Treg cells in blood and brain.[10] However, transient depletion of Treg cells was shown to regulate microglia or/and infiltrated macrophages with differential effects on Aβ clearance and cognitive protection in two studies.[26,27] Our recent study showed that deficiency of p38α-MAPK in peripheral myeloid cells decreases Th17 cells, which possibly increases microglial activation and Aβ clearance in AD mice.[28] Therefore, we asked whether Il-17a-expressing cells mediate the effects of gut bacteria on AD pathology.

Intestinal bacteria may also release structural components into the blood and bacteria themselves may even spread in the brain, both of which can directly activate microglia. Blood concentrations of lipopolysaccharide (LPS) together with inflammatory cytokines, e.g., IL-1β and tumor necrosis factor (TNF)-α, are increased in AD patients compared to non-AD individuals with and without cognitive impairment.[29] Components of *Porphyromonas gingivalis*, a bacterium often existing in chronic periodontitis, were found in the brains of AD patients.[30] We have observed that bacterial receptors CD14 and Toll-like receptor (TLR)-2 are receptors for aggregated Aβ,[31–33] implying that Aβ and bacterial components share receptors on microglia in the brain. MyD88 is an adaptor protein that is down-stream of most TLRs.[34] Our previous studies showed that deficiency of CD14, TLR2, TLR4, or MyD88 inhibits inflammatory activation of microglia, reduces cerebral Aβ and improves cognitive function in APP-transgenic mice.[20,32,33,35,36] Antibiotic therapy for AD patients has attracted interest.[37] A large cohort study suggests that sporadic use of antibiotics in older adults may decrease the risk of dementia.[38] Long-term antibiotic exposure reduces Th17 cells in the gut.[39] The question arises as to whether inhibition of Il-17a signaling mediates the efficacy of potential antibiotic therapy in AD.

AD pathology is more likely to lead to clinical dementia in women than in men. It is also believed that the prevalence or incidence of AD is higher in women than in men. The difference is not only due to the longer life expectancy of women, but also to

bovine serum albumin (Sigma-Aldrich) and filtered with 20 μm-mesh. The blood vessel fragments were collected on the top of filter and stored at −80° C for biochemical analysis.

Intestinal bacterial collection and 16S rRNA sequencing

Bacterial DNA was extracted from intestinal bacteria (100 mg) in the frozen cecum and colon with QIAamp Fast DNA Stool Mini Kit (Qiagen, Hilden, Germany). The amount of bacteria was evaluated by quantifying 16S rRNA with SYBR Green-based real-time PCR using the universal bacterial r16S gene primers (16S-V2-101F: 5-AGYGGCGIACGGGTGAGTAA-3, and 16S-V2-361 R: 5-CYIACTGCTGCCTCCCGTAG-3) as it was conducted in a published study.[25] The V3 -V4 region of the 16S rRNA-encoding gene was then amplified with the barcode fusion primers (338F: 5-ACTCCTACGGGAGGCAGCAG-3, and 806 R: 5-GGACTACHVGGGTWTCTAAT-3). After purification, PCR products were used for constructing libraries and sequenced on the Illumina MiSeq platform at Majorbio Co. Ltd. (Shanghai, China). The raw data was processed on Qiime2 (https://qiime2.org/.), reducing sequencing and PCR errors, and denoising to get the operational taxonomic unit (OTU) consensus sequences, which were mapped to the 16S Mothur-Silva SEED r119 database (http://www.mothur.org/). Alpha diversity including Sobs, Shannon, Ace, Chao and Simpson indexes were used for the analysis of bacterial richness and diversity in a single mouse. Principal coordinate analysis (PCoA) and analysis of similarity (ANOSIM) were used for β-diversity analysis to compare bacterial compositions on genus level between APP-transgenic mice with and without antibiotic treatments. The difference of bacterial compositions on genus level between these two groups were also compared with Wilcoxon rank sum test. All the analysis was performed using cloud-based tools with default analysis parameters (https://cloud.majorbio.com/page/tools.html).

Quantification of bacterial DNA in the brain tissue

DNA was extracted from the brain tissue using TRIzol (Thermo Fisher Scientific) according to the protocol provided by the company. To assess the presence and extent of bacterial dissemination into the brain, real-time PCR was conducted using universal bacterial 16S rRNA gene primers (16S-V2-101F and 16S-V2-361 R), and primers targeted mouse *Gapdh* gene (sense, 5'-*ACAACTTTGGCATTGTGGAA*-3' and antisense, 5'-*GATGCAGGGATGATGTTCTG*-3') as an internal control.

Positive selection of CD11b-positive and CD4-positive cells from the brain and spleen, respectively

The brain tissue (hippocampus and cortex) and spleen of 5-month-old APP-transgenic mice with and without treatments with antibiotics were prepared for single-cell suspensions using Neural Tissue Dissociation Kit (papain-based) and Spleen Dissociation Kit (mouse), respectively (Miltenyi Biotec GmbH, Bergisch Gladbach, Germany). After blocking with 50 μg/ml CD16/CD32 antibody (clone 2.4G2; BioXCell, Lebanon, USA), CD11b-positive brain cells were selected from the brain with microbeads-conjugated CD11b antibody (clone M1/70.15.11.5; Miltenyi Biotec) and CD4-positive spleen cells from the spleen with Dynabeads magnetic beads-conjugated CD4 antibody (clone L3T4; Thermo Fisher Scientific). Lysis buffer was immediately added to selected cells and total RNA was isolated using RNeasy Plus Mini Kit (Qiagen).

Microglial Aβ phagocytosis assay

Five-month-old APP-transgenic mice received an intraperitoneal injection of 10 mg/kg methoxy-XO4 (Bio-Techne GmbH, Wiesbaden-Nordenstadt, Germany) (2 mg/ml in a 1:1 mixture of DMSO and 0.9% NaCl [pH 12] (v/v)) after treatment with and without antibiotics according to a published protocol.[47] Methoxy-XO4 binds to β-sheet secondary structure of Aβ aggregates. Three hours later, a single cell suspension from the hippocampus and cortex was prepared using Neural Tissue Dissociation Kit (papain-based) (Miltenyi Biotec GmbH). After blocking with CD16/CD32 antibody (clone 2.4G2; BioXCell) and subsequent staining with PE-Cy5-conjugated CD11b antibody (clone M1/70; Thermo Fisher Scientific), fibrillar Aβ-containing CD11b-positive

brain cells were detected by BD FACSVerse™ flow cytometry (BD Biosciences; Heidelberg, Germany).

Flow cytometric detection of Il17a-eGFP reporter in intestinal cells

A published protocol[48] was used to prepare single cell suspensions from both lamina propria and Peyer's patches of the small intestine of 5-month-old $APP^{tg}/Il17a^{GFP/wt}$ mice with and without two months of antibiotic treatment. After staining with APC-conjugated rat anti-CD4 monoclonal antibody (clone: GK1.5; Thermo Fisher Scientific), eGFP-expressing CD4-positive cells were detected by BD FACSCanto™ II flow cytometry (BD Biosciences).

Histological analysis

Serial 50-µm-thick sagittal sections were cut from the paraffin-embedded hemisphere. Four neighboring sections with 300 µm of interval were deparaffinized, labeled with rabbit anti-ionized calcium-binding adapter molecule (Iba)-1 antibody (Wako Chemicals, Neuss, Germany) and VectaStain *Elite* ABC-HRP kit (Cat.-No.: PK-6100, Vector Laboratories, Burlingame, USA), and visualized with diaminobenzidine (Sigma-Aldrich). Iba-1-positive microglia/brain macrophages were counted with Optical Fractionator in the hippocampus and cortex on a Zeiss AxioImager.Z2 microscope (Carl Zeiss Microscopy GmbH, Göttingen, Germany) equipped with a Stereo Investigator system (MBF Bioscience, Williston), as we did previously.[49]

To evaluate the cerebral Aβ level, after deparaffinization, 4 serial brain sections from each animal were stained with rabbit anti-human Aβ antibody (clone D12B2; Cell Signaling Technology Europe, Frankfurt am Main, Germany) and Cy3-conjugated goat anti-rabbit IgG (Jackson ImmunoResearch Europe Ltd. Cambridge, UK), or with methoxy-XO4 (Bio-Techne GmbH). After mounting, the whole section including hippocampus and cortex was imaged with Microlucida (MBF Bioscience) and merged. The positive staining and brain region analyzed were measured for the area with Image J tool "Analyse Particles" (https://imagej.nih.gov/ij/). The threshold for all compared samples was manually set and kept constantly. The percentage of Aβ coverage in the brain was calculated.

To determine the density of CD68-positive microglia, serial brain sections were stained with rabbit anti-CD68 antibody (clone E3O7V; Cell Signaling Technology Europe) and Cy3-conjugated goat anti-rabbit IgG (Jackson ImmunoResearch Europe Ltd.). Since the single CD68-positive cell could not be clearly recognized (see Figure 7a) and reliably counted, the percentage of CD68 coverage in the brain was calculated as for Aβ.

Analysis of microglial morphology

For the analysis of microglial morphology, our established protocol and Fiji Image J were used.[28] Paraffin-embedded 50-µm sagittal brain sections were used as described above. After fluorescent co-staining with Iba-1 and Aβ antibodies, total 10 Aβ plaques/mouse were randomly selected from the cortex dorsal to hippocampus and imaged under 40× objective with Z-stack scanning with 1 µm of interval. The serial images were Z-projected with maximal intensity, 8-bit grayscale transformed, Unsharp-Mask filter and despeckle-treated, and binarized to obtain a black and white image. The cells with complete nucleus and branches and without overlapping with neighboring cells were chosen for analysis. The single-pixel background noise was eliminated and the gaps along processes were filled under the view of the original image of the cell. The processed image was skeletonized and analyzed with the plugin Analyze Skeleton (2D/3D) (http://imagej.net/AnalyzeSkeleton) for the total number of primary branches, length of all branches, and the number of branch endpoints of each microglia. The whole analysis was done blinded to genotypes.

Western blot analysis

Frozen brain tissues and blood vessel isolates were homogenized in RIPA buffer (50 mM Tris [pH 8.0], 150 mM NaCl, 0.1% SDS, 0.5% sodiumdeoxy-cholate, 1% NP-40, and 5 mM EDTA) supplemented with protease inhibitor cocktail (Roche Applied Science, Mannheim, Germany) on ice. The proteins were separated by 10% or 12% Tris-glycine SDS/PAGE. Before loading on PAGE gel, vessel preparations

were sonicated. Western blots were performed using rabbit monoclonal antibody against Abcb1 (clone E1Y7S) and rabbit polyclonal antibody against Lrp1 (Cat.-No.: 64099) (both antibodies were bought from Cell Signaling Technology), as well as rabbit polyclonal antibody against claudin-5 (Cat.-No.: GTX49370; GeneTex, Hsinchu, China). The detected proteins were visualized via the Plus-ECL method (PerkinElmer, Waltham, USA). To quantify proteins of interest, rabbit monoclonal antibody against β-actin (clone 13E5) or rabbit polyclonal antibody against α-tubulin (Cat.-No.: 2144) (both antibodies were from Cell Signaling Technology) was used as a protein loading control. Densitometric analysis of band densities was performed with Image-Pro Plus software version 6.0.0.260 (Media Cybernetics, Rockville, MD, USA). For each sample, the protein level was calculated as a ratio of target protein/loading control per sample.

Brain homogenates and ELISA assays of Aβ and Il-1β and Tnf-α

The frozen brain hemispheres were homogenized and extracted serially in Tris-buffered saline (TBS), TBS plus 1% Triton X-100 (TBS-T), guanidine buffer (5 M guanidine HCl/50 mM Tris, pH 8.0) as described in our previous study.[49] Aβ concentrations in three separate fractions of brain homogenates were determined by Invitrogen™ Amyloid β 42 and 40 Human ELISA kits (Cat.-No.: KHB3441 and KHB3481, respectively; both from Thermo Fisher Scientific). Results were normalized on the basis of the sample's protein concentration.

We measured concentrations of Il-1β and Tnf-α in TBS-soluble brain homogenates with ELISA kits (Cat.-No.: DY401 and DY410, respectively, from R&D systems, Minneapolis, USA). The results were also adjusted by the protein concentration in the same sample.

Quantitative PCR for analysis of gene transcripts

Total RNA was isolated from mouse brains with TRIzol or from selected CD11b or CD4-positive cells with RNeasy Plus Mini Kit (Qiagen) and reverse-transcribed. Gene transcripts were quantified with established protocols[49,50] and TaqMan gene expression assays of mouse *Tnf-α*, *Il-1β*, *Chemokine (C – C motif) ligand 2* (*Ccl-2*), *Il-10*, *Chitinase-like 3* (*Chi3l3*), *Mannose receptor C type 1* (*Mrc1*), *Apolipoprotein e* (*Apoe*), *Triggering receptor expressed on myeloid cells 2* (*Trem2*), *Purinergic receptor P2Y, G-protein coupled 12* (*P2ry12*), *C-X3-C motif chemokine receptor 1* (*Cx3cr1*), *Lipoprotein lipase* (*Lpl*), *C-type lectin domain family 7, member a* (*Clec7a*), *Integrin alpha X* (*Itgax*), *Il-17a*, *Interferon γ* (*Ifn-γ*), *Il-4*, *Neprilysin* and *Insulin-degrading enzyme* (*Ide*), *Activity-regulated cytoskeleton-associated protein* (*Arc*), *Glutamate ionotropic receptor NMDA type subunit 1* (*Grin1*), *Brain derived neurotrophic factor* (*Bdnf*), and *Gapdh* (Thermo Fisher Scientific).

Statistical analysis

Data were presented as mean ± *SEM* and displayed using a scatter plot with a bar overlay in the figure, with the scatter plot representing individual data points. Means for two groups of cases were compared with two independent-samples Students *t*-test. The comparison of cerebral DNA levels of bacterial 16S rRNA gene between Il-17a-deficient and wild-type APP-transgenic mice with and without antibiotic treatment were conducted by Mann-Whitney-*U*-test, because the variables were apparently non-normally distributed. For multiple comparisons, we used one-way or two-way ANOVA followed by Bonferroni, Tukey, or Dunnett T3 *post hoc* test (dependent on the result of Levene's test to determine the equality of variances). All statistical analyses were performed with GraphPad Prism 8 version 8.0.2. for Windows (GraphPad Software, San Diego, USA) or SPSS software for Windows (Version 26.0, IBM, Armonk, USA). Other statistical methods in microbiome analysis offered by external companies have been described above. Statistical significance was set at $p < 0.05$.

Results

Oral treatment with an antibiotic cocktail depletes almost all bacteria in the gut of APP-transgenic mice

To investigate the relationship between gut and brain, we treated 3-month-old APP-transgenic

female littermate mice with and without an antibiotic cocktail in drinking water for 2 months. By quantifying gut bacterial *16S rRNA* gene with real-time PCR, we found that antibiotic treatment depleted almost all bacteria in the gut, as the number of remaining bacteria was only 0.08% of that of normal drinking water control mice (Figure 1a; ΔCt value: 10.34 in real-time PCR; *t* test, $p < 0.0001$), which was consistent with previous studies that have demonstrated the depletion of gut bacteria by anaerobic and aerobic culture of gut contents.[44,51] Not surprisingly, the richness and diversity of the remaining bacteria in the gut of antibiotics-treated AD mice were dramatically reduced, as indicated by decreased Sobs, Ace, Chao, and Shannon indices and increased Simpson index in the α-diversity analysis (Figure 1b–f; *t* test, $p < 0.05$). Similarly, the β-diversity-based PCoA analysis clearly showed the difference in intestinal bacterial architecture between APP-transgenic mice with and without antibiotic treatment (Figure 1g; ANOSIM, $R = 1.0000$, $p = 0.008$). We further observed that the remaining antibiotic-resistant bacteria belonged almost exclusively to the genera *Escherichia-Shigella* and *Parasutterella* (Figure 1h; Wilcoxon rank-sum test, $p < 0.05$).

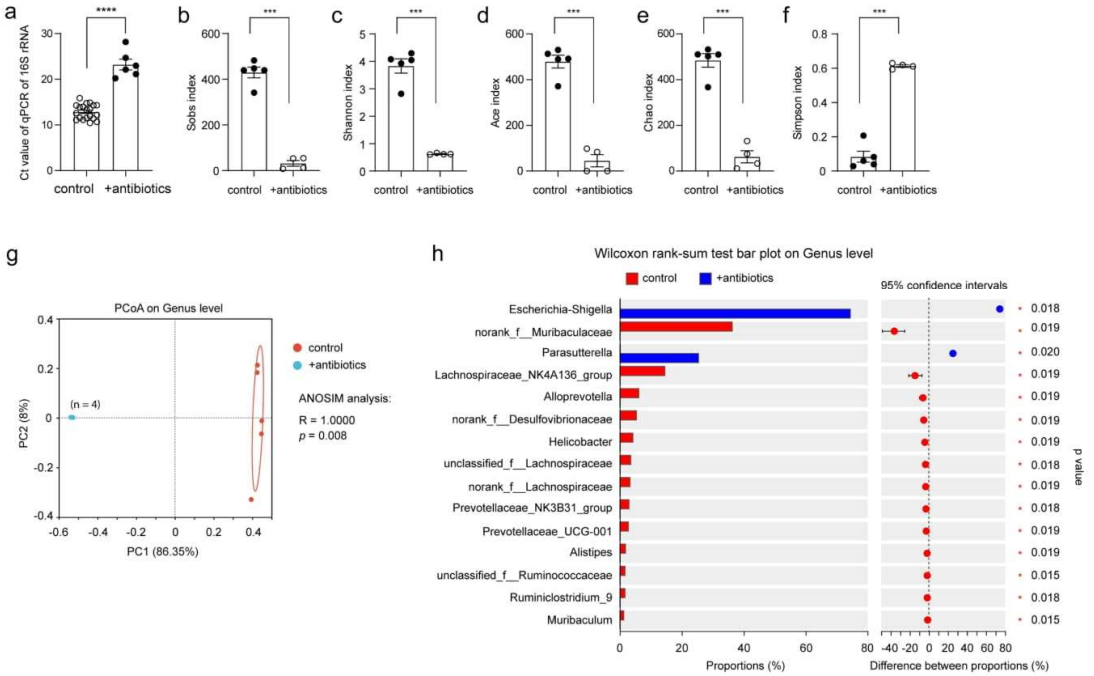

Figure 1. Antibiotic treatment successfully depletes the bacteria in the gut of APP-transgenic mice. Three-month-old APP-transgenic female mice were treated with and without antibiotics in drinking water for 2 months. Intestinal content (total 100 mg) for the isolation of bacterial DNA was harvested from the appendix and neighboring colon. Bacterial DNA was first measured for the amount with real-time PCR (a; *t* test; $n = 20$ and 6 for mice receiving normal water and antibiotic supplement), and then sequenced for the V3-V4 region of 16S rRNA-encoding gene ($n = 5$ and 4 for control and antibiotic-treated mice, respectively). Using Sobs, Shannon, Ace, Chao and Simpson's indices, α-diversity analysis shows that treatment with an antibiotic cocktail significantly reduces bacterial richness and diversity within each mouse (b–f; *t* test). Principal coordinate analysis (PCoA) was used for β-diversity analysis of bacterial composition at the genus level in APP-transgenic mice with and without antibiotic treatment (g; Each symbol represents the gut bacteria of an individual mouse). As expected, the structure of gut bacterial community of antibiotics-treated APP-transgenic mice differed significantly from those of APP-transgenic littermates with normal drinking water (g; ANOSIM analysis between +antibiotics and control mice). Bar plots depict abundance (% of total) of the indicated genera. Wilcoxon rank-sum tests show that antibiotic treatment increases the relative abundance of bacteria in the genera *Escherichia-Shigella* and *Parasutterella* (h). ***: $p < 0.001$ and ****: $p < 0.0001$.

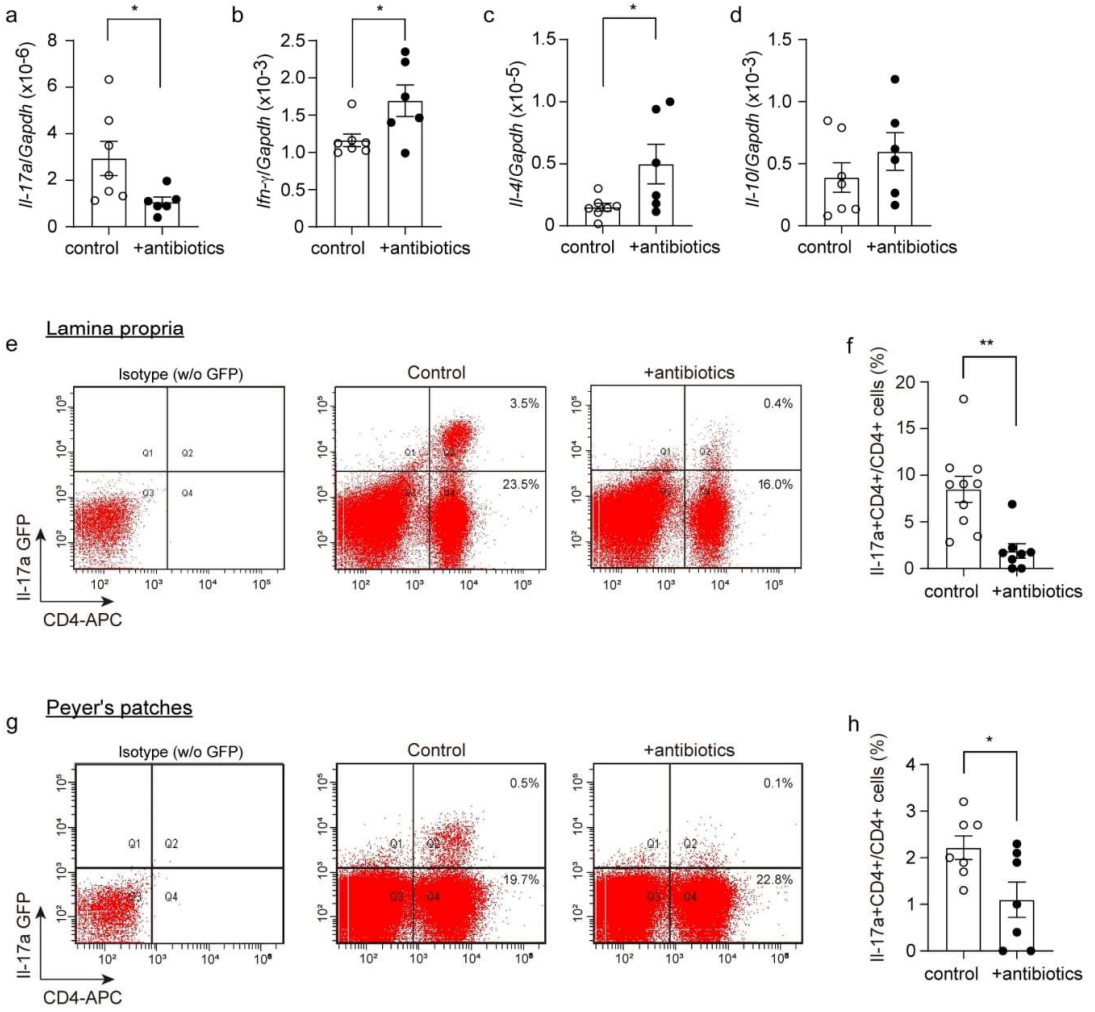

Figure 2. Depletion of gut bacteria reduces Il-17a-expressing CD4-positive lymphocytes. Three-month-old APP-transgenic female mice, expressing or not Il-17a-eGFP reporter, were treated with and without antibiotics in drinking water for 2 months. CD4-positive splenocytes were selected and detected for transcription of T lymphocyte marker genes. The transcription of *Il-17a* gene was significantly down-regulated by antibiotic treatment, while the transcription of *Ifn-γ* and *Il-4* genes was up-regulated in CD4+ splenocytes compared to APP-transgenic control mice with normal drinking water (a–c; *t* test, $n = 6$ - 7 per group). The transcription of *Il-10* gene in spleen cells was not changed by antibiotic treatment (d; *t* test, $n = 6$ - 7 per group). In addition, single cell suspensions were prepared from both lamina propria and Peyer's patches of 5-month-old Il-17a-eGFP-expressing APP-transgenic mice and analyzed by flow cytometry after fluorescent staining of CD4 (e and g). Intestinal cells prepared from APP-transgenic mice without expressing Il-17a-eGFP reporter were stained with APC-conjugated rat IgG2b as an isotype control (Isotype w/o GFP). The expression of IL-17a-associated eGFP was decreased in CD4+ lymphocytes in the intestine of APP-transgenic mice by antibiotic treatments (f and h; *t* test, $n = 7$ - 10 per group). $^*p < 0.05$; $^{**}p < 0.01$.

Depletion of gut bacteria reduces Il-17a-expressing CD4-positive lymphocytes in APP-transgenic mice

Our recent study showed that Il-17a-expressing CD4-positive lymphocytes increase in the gut and spleen of APP-transgenic mice.[28] We therefore selected CD4-positive cells with a magnetic beads-conjugated antibody from the spleen of antibiotics-treated APP-transgenic mice and quantified the transcripts of characteristic genes for Th1, Th2, Th17 and Treg lymphocytes. As shown in Figure 2a–d, depletion of gut bacteria significantly decreased the transcription of *Il-*

17a, but increased the transcription of *Ifn-γ* and *Il-4* (*t* test, $p < 0.05$). We further treated 3-month-old APP-transgenic mice expressing Il-17a-eGFP reporter[43] with and without antibiotics, and observed that depletion of gut bacteria for 2 months significantly reduced eGFP-expressing CD4+ lymphocytes in both lamina propria and Peyer's patches of the gut compared to control AD mice with normal drinking water (Figure 2e–h; *t* test, $p < 0.05$). Therefore, depletion of intestinal bacteria leads to a significant reduction in Il-17a-expressing CD4-positive T lymphocytes in AD mice. We also found some Il-17a-eGFP-expressing CD4-negative cells in both lamina propria and Peyer's patches (see upper-left quadrant in Figure 2e and g); however, these cells could not form a clearly distinguishable population in both the antibiotics-treated and non-treated AD mice, which made it difficult to reliably quantify cells. Thus, our results do not exclude the possibility that depletion of gut bacteria also regulates Il-17a expression in other immune cells, such as lymphoid-tissue inducer-like cells, natural killer cells, and Paneth cells.[52] In our APP-transgenic animal models, expression of GFP was not detected in γδ T lymphocytes in the gut.[28]

In additional experiments, we performed an immunohistochemical analysis of GFP in the brain of APP-transgenic mice and of EAE mice that were established in our previous study,[53] both of which expressed Il-17a-eGFP. We could not detect GFP-expressing cells in the brain parenchyma of AD mice, but clearly saw GFP-positive cells surrounding blood vessels in the EAE model (Supplementary Fig. S1, A). Similarly, we did not detect *Il-17a* gene transcripts in the brain tissue from APP-transgenic mice within 40 cycles of real-time PCR (data not shown). These results suggest that gut bacterial depletion alters brain pathology by regulating Il-17a-expressing cells outside the brain.

Depletion of gut bacteria reduces bacterial DNA in the brain of APP-transgenic mice

Intestinal bacteria may release structural components into the blood that circulate to the brain, or the bacteria spread directly to the brain.[30,54] We then asked whether depletion of gut bacteria alters the potential presence of bacterial components in the brain. Since we observed that depletion of gut bacteria reduced the number of Il-17a-expressing lymphocytes, we asked whether Il-17a affected the amount of bacterial substance in the brain. We treated Il-17a-deficient and wild-type APP-transgenic female mice with antibiotics as described

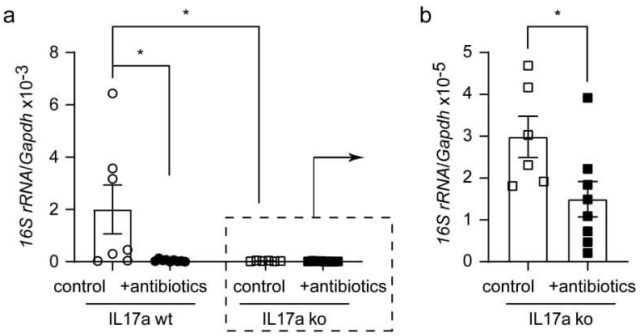

Figure 3. Depletion of gut bacteria reduces bacterial DNA in the brains of both Il-17a-deficient and wild-type APP-transgenic mice. Three-month-old Il-17a-deficient (ko) and wild-type (wt) APP-transgenic female mice received drinking water with and without supplement of antibiotics for 2 months. The hippocampus and cortex were collected and homogenized in Trizol for DNA isolation. The amount of bacterial DNA was evaluated by real-time PCR using mouse *Gapdh* gene as an internal control. Depletion of gut bacteria significantly decreased bacterial DNA in both Il-17a-deficient and wild-type APP-transgenic mice; interestingly, deficiency of Il-17a also reduced bacterial DNA in the brain compared with Il-17a wild-type AD mice (a and b; Mann-Whitney-*U*-Test, $n = 8$ - 9 per group for Il-17a-wildtype mice and 6 - 8 per group for Il-17a-deficient mice). *, $p < 0.05$.

above. Both groups of mice after antibiotic treatment showed enlargement of the ceca and dark-colored cecal contents as shown in published studies[17] (data not shown). Interestingly, antibiotic treatment significantly decreased the DNA level of the bacterial *16S rRNA* gene in the brains of both Il-17a-deficient and wild-type APP-transgenic mice (Figure 3a and b; Mann-Whitney-*U*-Test, $p < 0.05$). The DNA level of *16S rRNA* gene was significantly lower in Il-17a-deficient than in Il-17a-wild-type APP-transgenic mice without antibiotic treatment (Figure 3a and b; *16S rRNA*/*Gapdh*: $2.99 \pm 0.49 \times 10^{-5}$ vs. $2.00 \pm 0.93 \times 10^{-3}$; Mann-Whitney-*U*-Test, $U = 4$, $p = 0.015$). After antibiotic treatment, the DNA level of the *16S rRNA* gene did not differ between Il-17a-deficient and wild-type AD mice (*16S rRNA*/*Gapdh*: $1.49 \pm 0.42 \times 10^{-5}$ [Il-17a-deficient] vs. $4.32 \pm 1.32 \times 10^{-5}$ [Il-17a-wild-type]); Mann-Whitney-*U*-Test, $U = 19$, $p = 0.102$). Thus, Il-17a deficiency potentially blocked the translocation of bacterial components from the intestine to the brain.

Depletion of intestinal bacteria inhibits proinflammatory activation in the brain of APP-transgenic mice, but not in Il-17a-deficient AD mice

Depletion of intestinal bacteria has been shown to suppress inflammation in the brain of APP-transgenic mice.[8,11] We did observe that intestinal antibiotic treatment for 2 months significantly reduced the number of Iba1-positive microglia in both the hippocampus and cortex of female APP-transgenic mice (Hippocampus: from $17.13 \pm 1.29 \times 10^3$ cells/mm^3 to $11.85 \pm 0.73 \times 10^3$ cells/mm^3, and Cortex: from $24.31 \pm 0.84 \times 10^3$ cells/mm^3 to $17.46 \pm 2.55 \times 10^3$ cells/mm^3; Figure 4, a – c; *t* test, $p < 0.05$). Interestingly, in Il-17a-deficient APP-transgenic mice, depletion of gut bacteria did not alter the number of Iba-1-positive cells in the hippocampus (Figure 4, d and e; $16.21 \pm 0.57 \times 10^3$ cells/mm^3 vs. $15.85 \pm 0.83 \times 10^3$ cells/mm^3; *t* test, $p > 0.05$). We measured transcripts of proinflammatory genes (*Tnf-α*, *Il-1β*, and *Ccl-2*) and anti-inflammatory genes (*Il-10*, *Chi3l3*, and *Mrc1*) in brains of APP-transgenic mice. As shown in Figure 4, f, h and j – m, depletion of intestinal bacteria down-regulated the transcription of *Il-1β* and *Ccl-2*, but up-regulated *Il-10* transcription in Il-17a-wildtype APP-transgenic mice (*t* test, $p < 0.05$). Intestinal bacterial depletion did not change the transcription of *Tnf-α*, *Chi3l3* and *Mrc-1* in APP-transgenic mice (Figure 4, f, l and m; *t* test, $p > 0.05$). In Il-17a-deficient AD mice, depletion of intestinal bacteria did not modulate the transcription of *Tnf-α*, *Il-1β*, *Ccl-2*, *Il-10*, and *Mrc-1* (Figure 4, f, h, j, k and m; *t* test, $p > 0.05$), except decreasing the transcription of *Chi3l3* (Figure 4, l; *t* test, $p < 0.05$). The results on antibiotics-induced transcriptional regulations of *Tnf-α* and *Il-1β* genes were confirmed by ELISA measurements of their protein levels, which showed that depletion of gut bacteria significantly decreased the Il-1β protein concentration (Figure 4, i; *t* test, $p < 0.05$) and tended to reduce the amount of Tnf-α protein (Figure 4, g; *t* test, $p = 0.075$) in brains of Il-17a-wildtype but not Il-17a-deficient mice.

In order to investigate whether the intestinal bacterial depletion-induced inflammatory inhibition was specific for mice with AD pathology, we treated 3 and 22-month-old female C57BL/6J mice with and without antibiotics for 2 months. Depletion of intestinal bacteria did not change transcription of all genes tested in 5-month-old C57BL/6J mice (*Tnf-α*, *Il-1β*, *Ccl-2*, *Il-10*, *Chi3l3*, and *Mrc1*; Figure 4, n; *t* test, $p > 0.05$). In 24-month-old C57BL/6J mice, depletion of intestinal bacteria increased *Tnf-α* transcription and decreased *Chi3l3* transcription (Figure 4, o; *t* test, $p < 0.05$). These experiments also suggested that it was intestinal bacterial depletion instead of antibiotics themselves modifying the inflammatory activation in the brain of APP-transgenic mice.

In order to examine the off-target effects of oral treatment of antibiotics, we injected 5-month-old APP-transgenic mice daily for 7 days with the antibiotic cocktail (1.5 mg/kg/day vancomycin, 3 mg/kg/day ampicillin, neomycin and streptomycin) according to the published protocol.[45] We injected metronidazole at the maximal dose of 30 mg/kg/day, because it has a high oral bioavailability.[46] Intraperitoneal injection of the

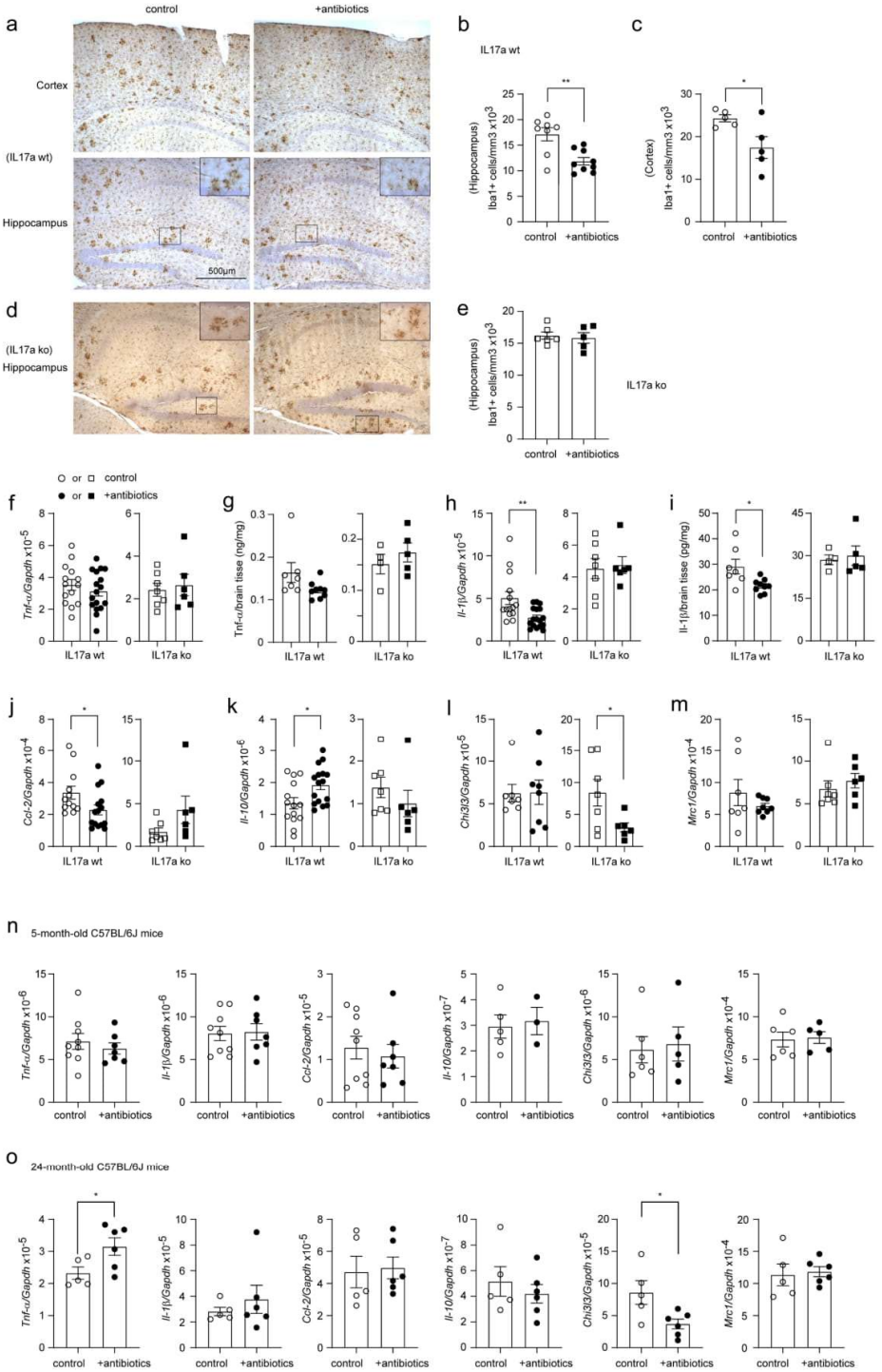

Figure 4. Depletion of gut bacteria reduces inflammatory activation in the brain of Il-17a-wildtype, but not Il17a-deficient APP-transgenic mice. Three-month-old APP-transgenic female mice with (ko) and without (wt) knockout of *Il-17a* gene, and 3 or 22-month-old C57BL/6J female mice were treated with and without antibiotics in drinking water for 2 months. Thereafter, brain tissues were

antibiotic cocktail did not change the transcription of proinflammatory genes, *Tnf-α*, *Il-1β*, and *Ccl-2* (Supplementary Fig. S2, A – C; *t* test, $p > 0.05$); however, significantly decreased the transcription of anti-inflammatory genes, *Il-10*, and *Mrc1* (Supplementary Fig. S2, D and F; *t* test, $p < 0.05$), and tended to inhibit *Chi3l3* gene transcription (Supplementary Fig. S2, E; *t* test, $p = 0.055$). The pattern of transcriptional modification in the brain by intraperitoneal injection of antibiotic cocktail is obviously different from that in oral antibiotics-treated mice; therefore, the effects of oral antibiotic treatment were due to the depletion of bacteria in the gut and not the antibiotics themselves.

Depletion of intestinal bacteria inhibits microglial activation in the brain of APP-transgenic mice, which is abolished by knockout of Il-17a gene

To understand the mechanism, through which intestinal antibiotic treatment modified neuroinflammation in AD mice, we selected $CD11b^+$ brain cells from 5-month-old female APP-transgenic mice with and without 2-month treatments of antibiotics and detected transcripts of disease-associated microglia (DAM) signature genes.[55] Depletion of intestinal bacteria significantly reduced transcription of *Il-1β* and *Ccl-2* genes (Figure 5, b and c; *t* test, $p < 0.05$), and tended to decrease the transcription of *Tnf-α*, *Il-10* and *Itgax* genes (Figure 5, a, d and k; *t* test, $0.05 < p < 0.10$) in cells derived from Il-17a-wildtype APP-transgenic mice, but not in cells from Il-17a-deficient AD mice. Depletion of intestinal bacteria even increased transcription of *Il-10* gene in Il-17a-deficient APP-transgenic mice (Figure 5, d; *t* test, $p < 0.05$). Gut bacterial depletion down-regulated transcription of *Apoe* gene in both Il17a-deficient and wild-type APP-transgenic mice (Figure 5, e; *t* test, $p < 0.05$). Antibiotic treatment did not significantly change the transcription of other genes (*Trem2*, *Cx3cr1*, *P2ry12*, *Clec7a*, and *Lpl*) tested in both Il-17a-deficient and wild-type mice (Figure 5, f – k; *t* test, $p > 0.05$).

In further experiments, we labeled microglia with Iba-1 antibodies and analyzed the morphology of microglia in the vicinity of Aβ deposits as we had done previously.[28] Depletion of intestinal bacteria increased the total number and end points of branching microglial processes (Figure 5, l – n; *t* test, $p < 0.05$), and tended to increase branch length (Figure 5, o; *t* test, $p = 0.078$) in 5-month-old APP-transgenic mice, consistent with previous observations.[16,19] However, all changes in microglial morphology caused by gut bacteria depletion were absent in Il-17a-deficient AD mice (Figure 5, m – o; *t* test, $p > 0.05$).

As we observed bacterial DNA in the brain, we further investigated whether Il-17a deficiency alters the response of microglia to bacterial components. We found that 5-month-old Il-17a-deficient and wild-type APP-transgenic mice without antibiotic treatment did not differ in the transcription of *Myd88*, *Cd14*, *Tlr1*, *Tlr2*, *Tlr4* and *Tlr9* (Supplementary Fig. S1, B), suggesting that knockout of *Il-17a* gene does not change microglial reactivity to bacteria. Surprisingly, our additional experiments and a previous study showed that the lack of Il-17a did not reduce the transcription of inflammatory genes, *Tnf-α*, *Il-1β*, *Ccl-2* and *Il-10* in microglia (Supplementary Fig. S1, C) and even activate microglia.[28]

sectioned and microglia were counted with stereological method, Optical Fractionator, after immunohistochemical staining of Iba1 (in brown color) (a–e), or homogenized for RNA isolation (f, h, and j–m) and measurement of inflammatory gene transcripts with real-time PCR, as well as for ELISA assays of Tnf-α and Il-1β concentrations (g and i). Depletion of gut bacteria significantly decreased Iba1-positive microglia in both the hippocampus and cortex of Il-17a-wildtype, but not in Il17a-deficient APP-transgenic mice (b, c and e; *t* test, $n = 5$ - 9 per group). Similarly, depletion of gut bacteria significantly reduced the transcripts of *Il-1β* and *Ccl-2*, and increased *Il-10* transcript in the brain of Il-17a-wildtype, but not in Il17a-deficient APP-transgenic mice (h, j, and k; *t* test, $n = 6$ - 17 per group). Transcriptional regulation in AD mice deleted of gut bacteria was confirmed by the reduction in protein levels of Il-1β but not Tnf-α in brain homogenate compared to APP mice receiving normal water (g and i; *t* test, $n = 4$ - 9 per group). However, depletion of gut bacteria significantly reduced the transcript of *Chi3l3* in the brain of Il17a-deficient APP-transgenic mice (l; *t* test, $n = 6$ - 7 per group). Moreover, depletion of gut bacteria did not change the transcription of various inflammatory genes (*Tnf-a*, *Il-1β*, *Ccl-2*, *Il-10*, *Chi3l3*, and *Mrc1*) in in the brain of 5-month-old C57BL/6J female mice (n; *t* test, $n = 3$ - 9 per group), however, significantly increased *Tnf-a* transcription and decreased *Chi3l3* transcription in 24-month-old C57BL/6J female mice (O; *t* test, $n = 5$ - 6 per group). *: $p < 0.05$; **: $p < 0.01$.

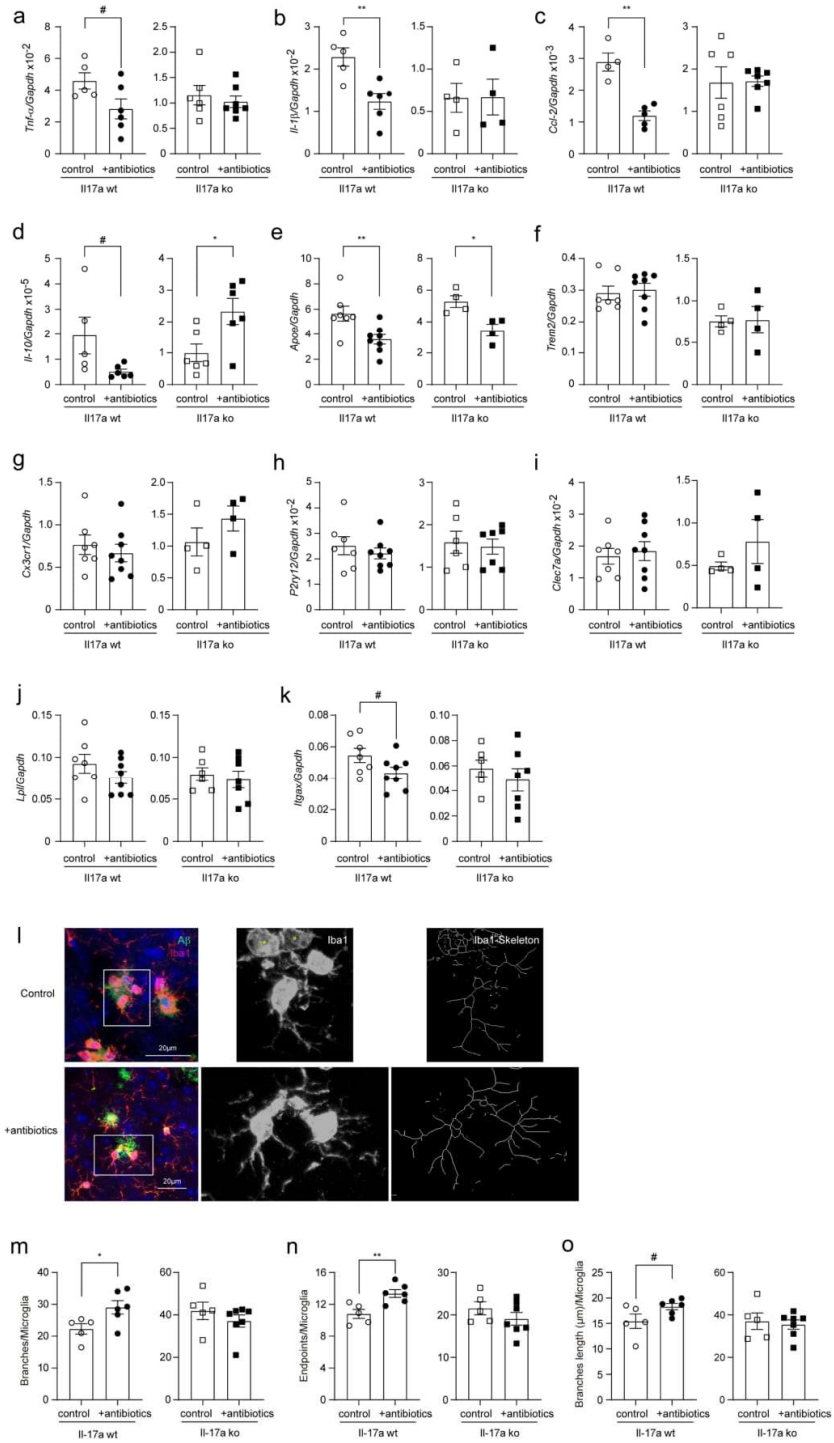

Figure 5. Depletion of gut bacteria inhibits inflammatory activation in microglia in the brain of Il-17a-wildtype, but not Il17a-deficient APP-transgenic mice. Three-month-old APP-transgenic female mice with (ko) and without (wt) knockout of *Il-17a* gene were treated with and without antibiotics in drinking water for 2 months. CD11b-positive brain cells were selected and quantified for the

Depletion of intestinal bacteria reduces cerebral Aβ in Il-17a-wildtype but not in Il-17a-deficient APP-transgenic mice

Extracellular Aβ plaques are a pathological hallmark of AD. Depletion of gut bacteria was reported to attenuate Aβ deposits in APP-transgenic mice.[7,11] We treated 3-month-old female APP-transgenic mice with an antibiotic cocktail for 2 months. As shown in Figure 6, a–c, 2-month treatments with antibiotics significantly reduced immunoreactive Aβ density from 6.02% ± 0.32% to 4.42% ± 0.64% in the cortex and from 5.67% ± 0.34% to 4.16% ± 0.58% in the hippocampus (*t* test, $p < 0.05$) of Il-17a-wildtype AD mice. In Il-17a-deficient APP-transgenic mice, treatment with antibiotics changed the density of Aβ in neither hippocampus nor cortex (Figure 6, d – f; *t* test, $p > 0.05$). The brain section was also stained with methoxy-XO4 that typically binds to the β sheet structure of Aβ aggregates. Similarly, treatments with antibiotics significantly reduced Aβ deposits in the cortex (Figure 6, g and h; *t* test, $p < 0.05$) and tended to decrease Aβ in the hippocampus (Figure 6, g and i; *t* test, $p = 0.060$) of Il-17a-wildtype APP-transgenic mice, but did not change density of methoxy-XO4-stained Aβ deposits in Il-17a-deficient AD mice (Figure 6, j – l; *t* test, $p > 0.05$).

We went on measuring Aβ in the brain homogenate with ELISA. In Il-17a wild-type APP-transgenic mice, antibiotic treatment significantly decreased the levels of both Aβ42 and Aβ40 in TBS- and TBS-T fractions (Figure 6, m, n, p and q; *t* test, $p < 0.05$), but not in guanidine-soluble fraction (Figure 6, o and r; *t* test, $p > 0.05$). TBS-, TBS-T-, and guanidine-soluble brain homogenates are enriched with monomeric, oligomeric and high-molecular-weight aggregated Aβ, respectively.[33] In Il-17a-deficient APP-transgenic mice, treatment with antibiotics did not reduce Aβ42 and Aβ40 in all three fractions of brain homogenates (Figure 6, m – r). On the contrary, antibiotic treatment even increased the concentration of Aβ42 in TBS-soluble fraction of brain homogenate (Figure 6, m; *t* test, $p < 0.05$).

Depletion of intestinal bacteria does not increase microglial Aβ phagocytosis and extracellular Aβ degradation, but potentially reduces Aβ production

In following experiments, we asked how depletion of intestinal bacteria attenuated the amyloid pathology in AD mice. First, we stained brain tissue with an antibody targeting the lysosomal protein CD68, a suggested marker of phagocytosis. As shown in Figure 7, a–c, depletion of gut bacteria significantly decreased the density of CD68 immunofluorescence (*t* test, $p < 0.05$). We then conducted a flow cytometric analysis of brain cells after Aβ staining with methoxy-X04, in which depletion of intestinal bacteria remarkedly decreased both percentage of Aβ-positive CD11b+ brain cells and the mean fluorescence intensity (mFI) of CD11b+ cell population in APP-transgenic mice (Figure 7, d – f; *t* test, $p < 0.05$), apparently indicating that microglial internalization of Aβ did not contribute to cerebral Aβ clearance in gut bacteria-depleted AD mice.

In the same APP-transgenic mouse strain as we used in this study, another group has reported that the absence of gut bacteria increased protein levels of Aβ-degrading enzymes neprilysin and Ide.[8] However, our study showed that depletion of intestinal bacteria altered neither *Neprilysin* nor *Ide* gene transcription in the brains of Il-17a-deficient and wildtype APP-transgenic mice (Figure 7, g–j; *t* test, $p > 0.05$), which suggested that extracellular

transcription of DAM marker genes. Depletion of gut significantly decreased the transcription of *Il-1β*, and *Ccl-2* genes, and tended to down-regulate the transcription of *Tnf-a*, *Il-10*, and *Itgax* genes in the brain of Il-17a-wildtype, but not in Il17a-deficient APP-transgenic mice (a–d, and k; *t* test, $n = 4 – 7$ per group). Depletion of gut bacteria significantly reduced transcription of *Apoe* gene, but not *Trem2*, *Cx3cr1*, *P2ry12*, *Clec7a*, and *Lpl* genes in both Il-17a-wildtype and deficient APP-transgenic mice (e–j; *t* test, $n = 4$ - 8 per group). In the analysis of microglial morphology after immunofluorescent staining of Iba1 (l), depletion of gut bacteria increased the number of branches and endpoints of the processes of microglia in Il-17a-wildtype, but not in Il17a-deficient APP-transgenic mice (m – o; *t* test, $n = 5$-7 per group). The Iba1-positive cells marked with "*" without showing clear processes were excluded for analysis of microglial morphology (l). *: $p < 0.05$; **: $p < 0.01$; #: $0.05 < p < 0.10$.

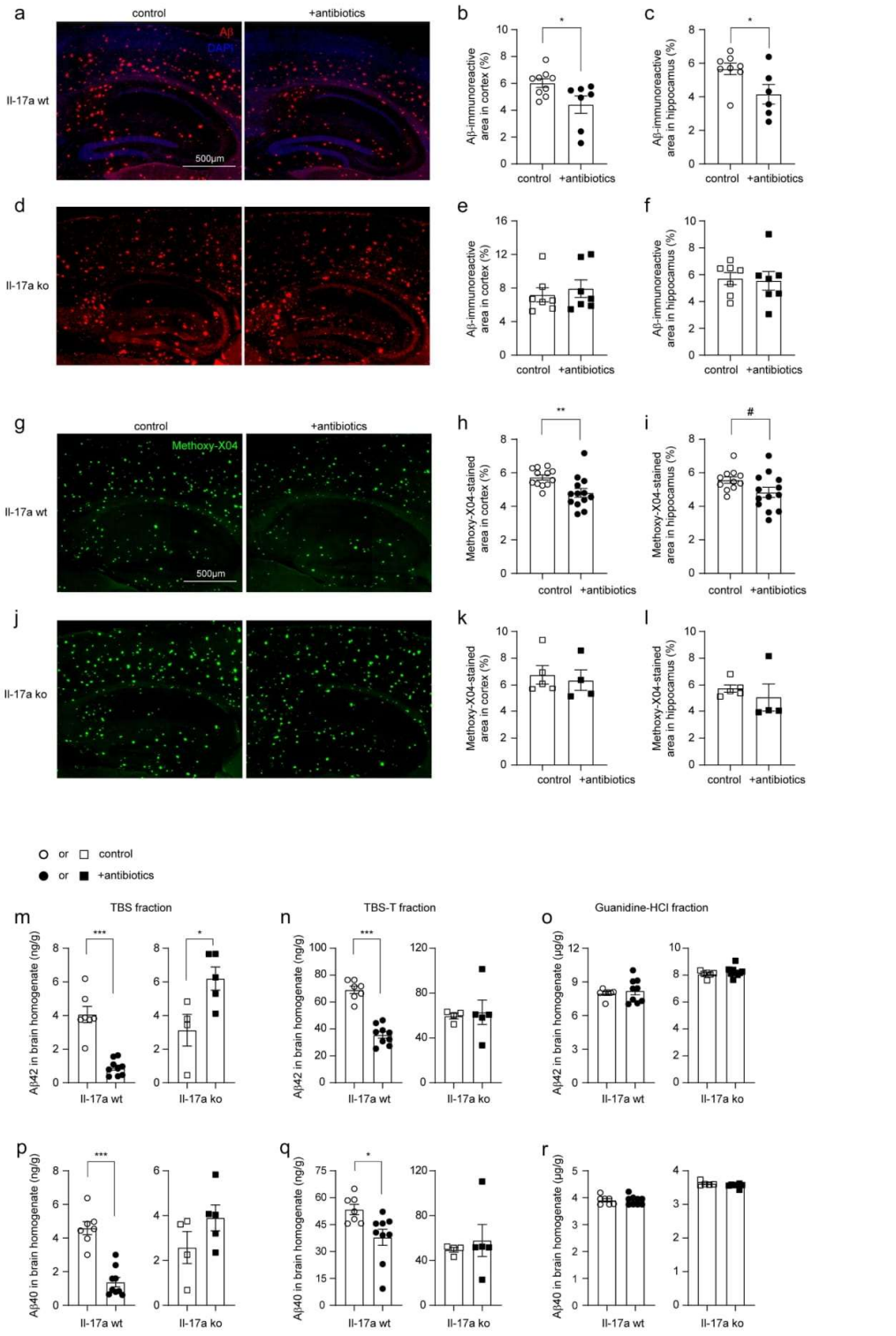

Figure 6. Depletion of gut bacteria reduces Aβ in the brain of Il-17a-wildtype, but not Il17a-deficient APP-transgenic mice. Three-month-old APP-transgenic female mice with (ko) and without (wt) knockout of *Il-17a* gene were treated with and without antibiotics in drinking water for 2 months. Brain tissues were sectioned and stained with immunofluoresce-conjugated Aβ antibodies (a and d)

degradation of Aβ was not the mechanism mediating Aβ reduction in our AD mice.

Our previous study has shown that inhibition of neuroinflammation inhibits β- and γ-secretase activity in the brain of AD mice.[20] We found that depletion of intestinal bacteria slightly but significantly decreased β-, but not γ-secretase activity (Figure 7, k and l; two-way ANOVA, antibiotic treatment vs. control, $p < 0.05$), as observed in a published study.[18] It was not surprising that the same inhibitory effects of antibiotic treatment on β- and γ-secretase activity could not be seen in Il-17a-deficient APP-transgenic mice (Figure 7, m and n; two-way ANOVA, antibiotic treatment vs. control, $p > 0.05$), as the antibiotic treatment did not change the inflammatory activation in the brain of Il-17a-deficient AD mice (see Figure 4).

Depletion of intestinal bacteria potentially increases Aβ efflux through blood-brain-barrier in APP-transgenic mice, which is driven by Il-17a inhibition

The transportation of Aβ from brain parenchyma to peripheral circulation is an efficient pathway for the cerebral Aβ clearance.[56] LRP1 and ABCB1 are a couple of key transporters at the BBB that are responsible for Aβ efflux.[57,58] We found that the protein levels of Abcb1 and Lrp1 were significantly increased in 5-month-old APP-transgenic mice, which had been treated with antibiotics for 2 months (Figure 8, a–c; *t* test, $p < 0.05$). Remarkably, the up-regulation of both Lrp1 and Abcb1 in the brain homogenate by depletion of intestinal bacteria was again abolished by knockout of Il-17a gene (Figure 8, d–f; *t* test, $p > 0.05$).

We also isolated blood vessels from 5-month-old APP-transgenic mice with and without treatments with antibiotics. We validated the results from the entire brain homogenate that treatments with antibiotics strongly elevated protein levels of Abcb1 and Lrp1 at the BBB (Figure 8, g–i; *t* test, $p < 0.05$). Notably, the protein level of claudin-5 in cerebral blood vessels did not differ between APP-transgenic mice with and without antibiotic treatment (Figure 8, g and j; *t* test, $p > 0.05$). Similarly, we did not detect any mouse IgG in brain homogenates of antibiotics-treated AD mice with Western blot (data not shown), which suggests that depletion of intestinal bacteria increased expression of Abcb1 and Lrp1 at the BBB, but did not significantly impair the BBB.

In further experiments, we detected Lrp1 and Abcb1 in the brain homogenates from 5-month-old APP-non-transgenic female mice with different expression of Il-17a. We observed that deficiency of Il-17a significantly increased the protein level of Abcb1, but not Lrp1, in a gene dose-dependent way (Figure 8, k–m; one-way ANOVA, $p < 0.05$). Similarly, we isolated blood vessels from Il-17a-deficient and wild-type APP-transgenic mice and observed that deficiency of Il-17a significantly increased both Lrp1 and Abcb1 in the tissue lysate of blood vessels (Figure 8, n–p; *t* test, $p < 0.05$), suggesting that depletion of intestinal bacteria potentially increases Lrp1/Abcb1-mediated Aβ efflux through inhibiting Il-17a signaling.

Depletion of intestinal bacteria potentially promotes synaptic plasticity in APP-transgenic mice, which is abolished by deficiency of Il-17a

After finding that gut bacterial depletion attenuated inflammatory activation and amyloid pathology in the brains of APP-transgenic mice, we performed a preliminary analysis of the neuroprotective effect of antibiotic treatment. Our previous study has shown that upregulated transcription of

and methoxy-XO4, a fluorescent dye for Aβ aggregates (g and j). Depletion of gut bacteria decreased Aβ deposits in both the hippocampus and cortex after staining of Aβ either with antibody or dye (b, c, h and i; *t* test, $n = 6$ - 13 per group). However, in the Il17a-deficient AD mice, depletion of gut bacteria did not change the cerebral Aβ loads (e, f, k and l; *t* test, $n = 4$-7 per group). Brain tissues were also serially homogenized and extracted in TBS, TBS plus 1% Triton-100 (TBS-T) and guanidine-HCl, and then measured for Aβ40 and Aβ42 with ELISA (m–r). Depletion of gut bacteria decreased the concentrations of both Aβ40 and Aβ42 in TBS- and TBS-T-soluble brain fractions, but not in guanidine-HCl-soluble fraction of Il-17a-wildtype APP-transgenic mice (m–r; *t* test, $n = 7$-9 per group). Depletion of gut bacteria did not change the concentrations of Aβ40 and Aβ42 in various fractions of brain homogenates of Il-17a-deficient AD mice (n–r; *t* test, $n = 4$ - 5 per group), except that it significantly increased the concentration of Aβ42 in TBS-soluble fraction (m). *: $p < 0.05$; **: $p < 0.01$; ***: $p < 0.001$; #: $0.05 < p < 0.10$.

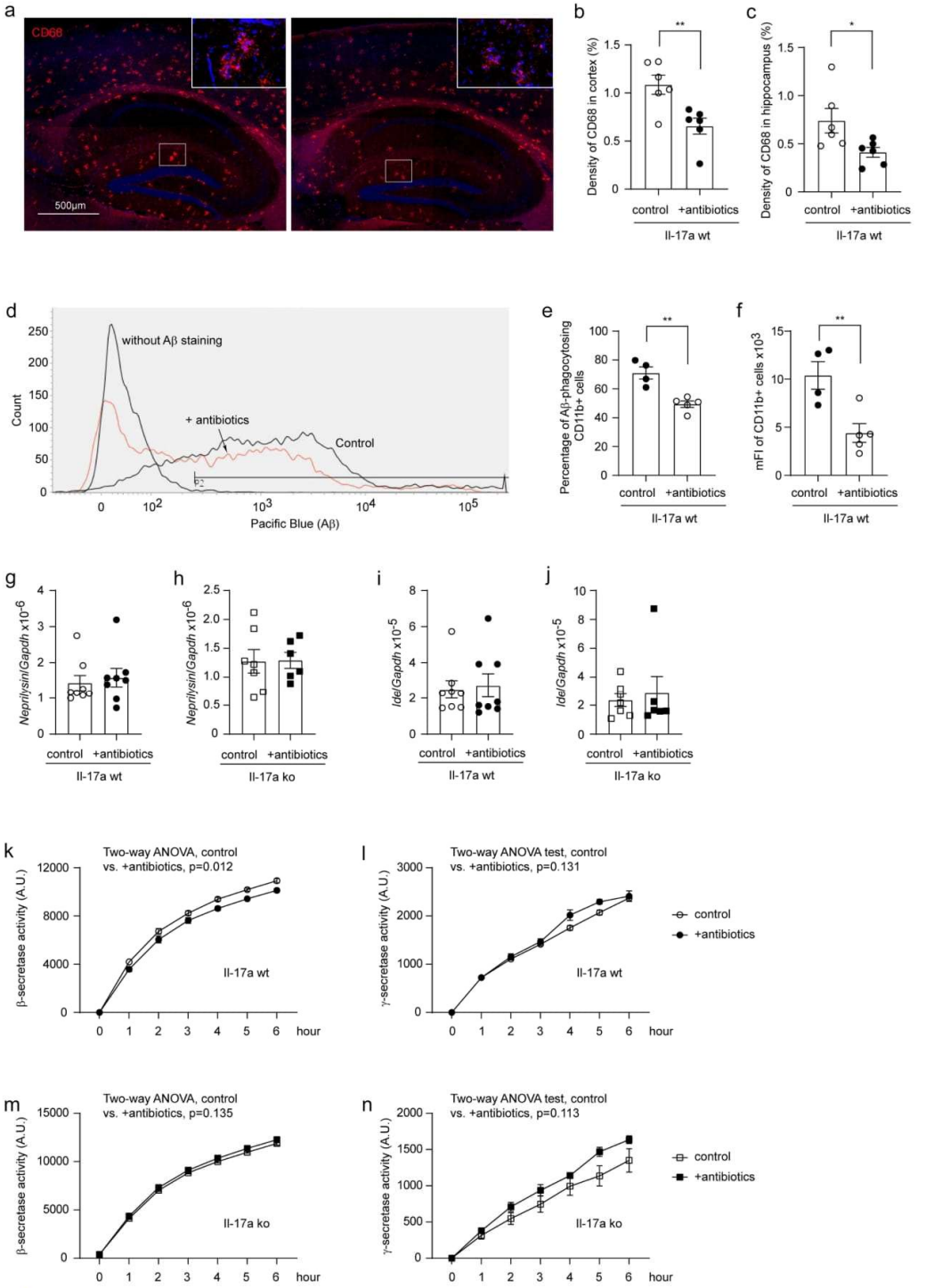

Figure 7. Depletion of gut bacteria reduces β-secretase activity in the brain of Il-17a-wildtype, but not Il17a-deficient APP-transgenic mice. Three-month-old Il-17a-deficient (ko) and wild-type (wt) APP-transgenic female mice were treated with and without antibiotics in drinking water for 2 months. The brain tissue was stained with Cy3-conjugated CD68 antibody (a). Antibiotic treatment significantly

the immediate early gene *Arc* and the gene *Grin1*, which encodes subunit 1 of the NMDA-type ionotropic glutamate receptor, is associated with the improvement of cognitive function in APP-transgenic mice.[35] BDNF plays an important role in the maintenance of synaptic plasticity in learning and memory,[59] the transcript of which is influenced by gut bacteria.[60] Therefore, we measured the transcripts of *Arc*, *Grin1* and *Bdnf* genes in brains of 5-month-old APP-transgenic mice with and without 2-month treatment of antibiotics. As shown in Figure 9, a–c, treatment with the antibiotic cocktail significantly increased the transcription of *Arc*, but not *Grin1* and *Bdnf* genes in Il-17a-wildtype APP mice (*t* test, $p < 0.05$). Again, knockout of *Il-17a* gene abolished the neuroprotective effect of antibiotic treatment (Figure 9, a–c; *t* test, $p > 0.05$). However, the neuroprotective effects of antibiotic treatment should be further investigated by other methods, such as behavioral tests and electrophysiological approaches, in older (e.g., 9-month-old) APP-transgenic mice as we did previously.[20,28]

Discussion

Gut bacteria contribute to AD development,[61] but how gut bacteria regulate brain pathology remains unclear. By using young female APP-transgenic mice with rapidly developing Aβ pathology, we found that depletion of gut bacteria decreased microglial inflammatory activation and Aβ levels, particularly soluble Aβ, and might promote synaptic plasticity in the brain. These effects were abolished by knockout of *Il-17a* gene. The attenuation of cerebral Aβ pathology by gut bacterial depletion may be attributed to the inhibition of β-secretase activity and the upregulation of Aβ efflux-related Lrp1 and Abcb1 expression in the brain, which was also abrogated by Il-17a deficiency.

Bacterial phenotypes are potentially transferred between contacting mice.[86] We co-housed 4–6 Il-17a-deficient and wild-type female AD mice in the same cage for treatments with and without antibiotics, which reduced the variability caused by different housing conditions. Depletion of gut bacteria in APP-transgenic mice inhibited proinflammatory activation in the brain tissue as evidenced by reduction of microglial number, down-regulation of *Il-1β* and *Ccl-2* transcription and up-regulation of *Il-10* transcription, consistent with published studies.[8,10,18] In individual microglia, depletion of gut bacteria decreased transcripts of both pro- (e.g., *Tnf-α*, *Il-1β*, *Ccl-2*) and anti-inflammatory (*Il-10*) genes, which is also in agreement with the published finding that the absence of gut bacteria leads to global defects in microglial activation.[17] The opposing regulation of *Il-10* transcription in microglia and brain tissue suggests that brain cells other than microglia, such as astrocytes, may also respond to gut bacteria[62] and produce Il-10 in the brain.

We noted that intestinal bacterial depletion in 5-month-old C57BL/6J mice did not have the same effect on the inflammatory modulation as in AD mice, and even promoted inflammatory activation (e.g., transcriptional up-regulation of *Tnf-α*, and down-regulation of *Chi3l3*) in the brain of 24-month-old C57BL/6J mice. In fact, the mechanism leading to inflammatory activation in the brain, and particularly in microglia, is not the same in AD and healthy aging. For example, inflammation in aging microglia may be due to a reduced ability to clear endogenous metabolites, whereas microglia in AD mice respond efficiently to exogenous Aβ. A transcriptomic study[63] identified 85 aging-associated genes in female C57BL/6J mice, of which only 21 genes overlapped with DAM genes that were

reduces the density of CD68-immunofluorescence in both cortex and hippocampus of APP-transgenic mice compared to AD mice drinking normal water (b and c; *t* test, $n = 6$ per group). APP-transgenic mice were also injected (*i.p.*) with methoxy-XO4 for the detection of Aβ-associated fluorescence in CD11b-positive brain cells by flow cytometry (d). Depletion of gut bacteria significantly decreased both the percentage of fluorescent cells among CD11b-positive brain cells, and the mean fluorescence intensity (mFI) of CD11b-positive cell population (e and f; *t* test, $n = 4$ - 5 per group). Brain tissues were further collected from AD mice for quantification of *Neprilysin* and *Ide* gene transcripts (g–j), and for β- and γ-secretase assays (k – n). Depletion of gut bacteria did not change the transcription of *Neprilysin* and *Ide* genes (g–j; *t* test, $n = 6$-8 per group); however, significantly inhibited the activity of β-secretase in the brain of Il-17a-wildtype but not Il17a-deficient APP-transgenic mice (k and m; two-way ANOVA, $n = 6$-7 per group for Il-17a-wildtype mice, and $n = 4$-5 per group for Il-17a knockout mice). Depletion of gut bacteria did not change γ-secretase activity in AD mice (l and n; two-way ANOVA, $n = 6$-7 per group for Il-17a-wildtype mice, and $n = 4$-5 per group for Il-17a knockout mice). *: $p < 0.05$; **: $p < 0.01$.

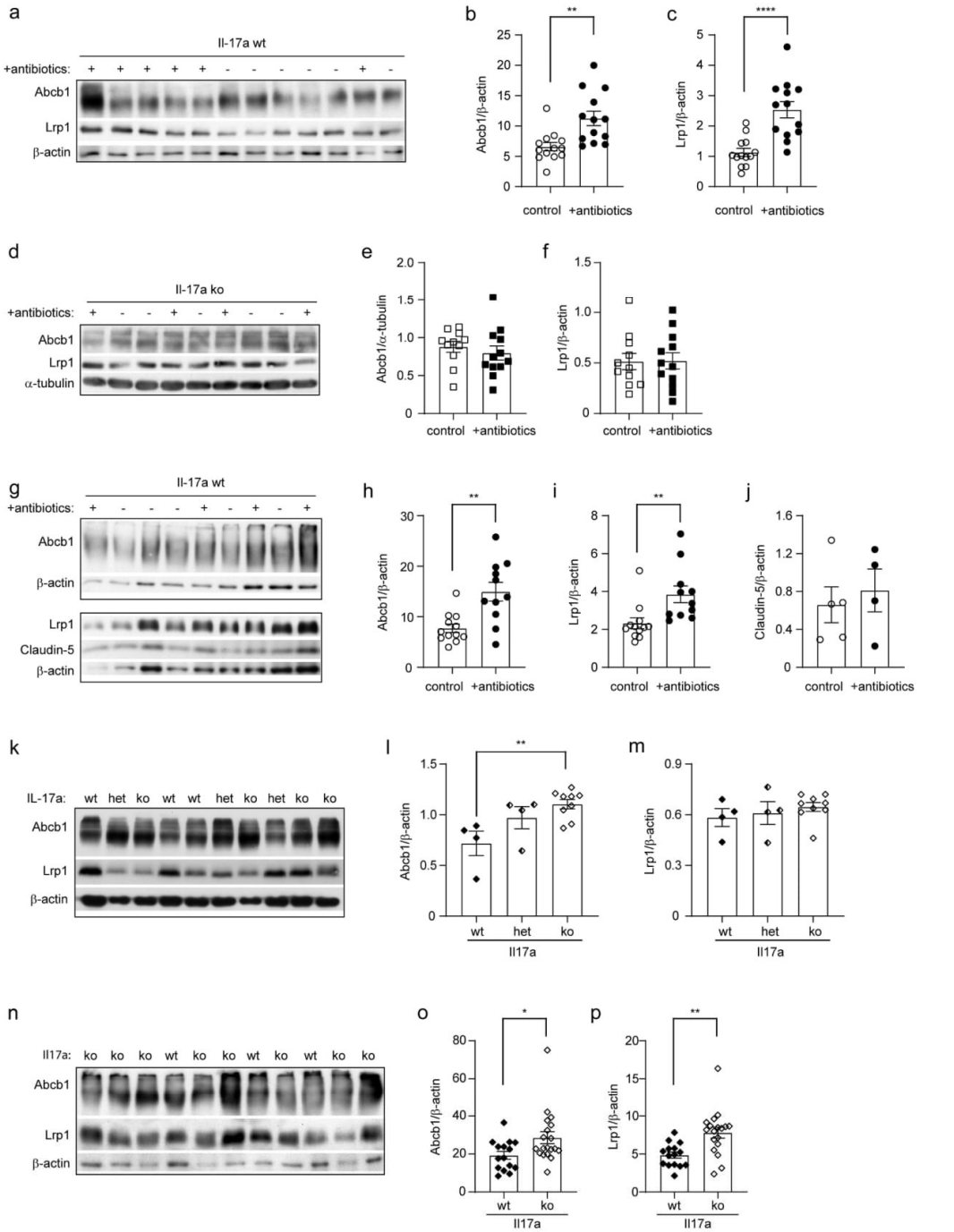

Figure 8. Depletion of gut bacteria increases Abcb1 and Lrp1 expression in the blood-brain-barrier of Il-17a-wildtype, but not Il17a-deficient APP-transgenic mice. Three-month-old Il-17a-deficient (ko) and wild-type (wt) APP-transgenic female mice were treated with and without antibiotics in drinking water for 2 months. Brain homogenates were quantified for protein levels of Abcb1 and Lrp1 with Western blot (a and d). Depletion of gut bacteria significantly increased expression of Abcb1 and Lrp1 in brains of Il-17a-wildtype (b and c), but not in Il-17a-deficient (e and f) APP-transgenic mice (*t* test, $n = 13$, and 11 - 12 per group for Il-17a wt and ko mice, respectively). Cerebral vessels were also isolated from Il17a-wildtype AD mice and detected for Abcb1 and Lrp1 at the BBB (g).

identified in APP-transgenic mouse model,[55] with the exception of the DAM-characteristic genes *Trem2* and *Apoe*. Thus, it stands to reason that a significant inflammatory modulation caused by gut bacterial depletion depends on the preactivated status and pattern of inflammatory brain cells (e.g., microglia).

Depletion of gut bacteria resulted in a significant reduction of Il-17a-expressing CD4-positive cells in the gut and spleen as well as bacterial DNA in brain tissue, suggesting that gut bacteria regulate brain pathology in AD mice via at least two pathways: 1) regulating peripheral Il-17a-expressing T lymphocytes and 2) directly modulating cells in the brain with bacterial components (not necessary living cells). Very interestingly, we also observed that deficiency of Il-17a reduces bacterial DNA in the brain of APP-transgenic mice. Due to our limited research resource, we have not yet succeeded in the microbiome analysis of brain tissues. The recent study detected *Streptococcus*, *Clostridium*, *Roseburia* and *Tyzzerella* in the brain of APP/PS1 mice.[54] The bacteria from *Cutibacterium acnes* were found in the brain of AD patient and linked to AD pathogenesis.[64] How the bacteria or their structural components enter the brain is unclear. It has been reported that deficiency of Il-17a alters the composition of gut bacteria, i.e., increases the abundance of *Barnesiella* genus bacteria, and hinders the development of EAE.[65] *Barnesiella* bacteria are the main source of hypoxanthine in the gut. Intestinal epithelial cells utilize hypoxanthine for energy balance and nucleotide biosynthesis.[66] Thus, Il-17a deficiency may favor intestinal barrier function and lead to the reduction of bacterial DNA in the brain of APP-transgenic mice. Inhibition of Il-17a signaling, which can be achieved by administering Il-17a inhibitors or by depleting specific bacterial taxa in the gut that stimulate the development of Il-17a-producing T cells, therefore has the potential to avoid bacterial overload in the brain and prevent AD progression.

Exactly how the depletion of bacteria in the gut and subsequent Il-17a inhibition, in particular the reduction of Th17 cells, regulates microglial activity in our antibiotic-treated AD mice remains unclear. Il-17a inhibition itself does not appear to inhibit microglial activation. We have recently observed that knockout of *Il-17a* gene reduces microglial branches in APP-transgenic mice,[28] suggesting activation of microglial inflammatory response.[67] Our current study shows that Il-17a deficiency did not reduce the transcription of *Tnf-α*, *Il-1β*, *Ccl-2* and *Il-10* genes in isolated microglia (Supplementary Fig. S1, C). The inhibition of inflammation in both brain tissue and microglia in our antibiotic-treated AD mice may be due to the depletion of bacteria other than Il-17a-promoting taxa in the gut. In Il-17a-deficient APP-transgenic mice, antibiotic treatment did not inhibit inflammatory activation in brain tissue and microglia, for which there are perhaps several reasons. Deficiency of Il-17a reduced soluble Aβ (discussed later) and bacterial DNA, minimizing the inflammatory priming of microglia as in 5-month-old C57BL/6J mice, limiting the capacity to further inhibit inflammation by depleting gut bacteria. However, we believe that there are other unknown mechanisms by which Il-17a inhibition maintains and even enhances microglial activity in the brain, which we will investigate in the future studies. To answer this question, it is helpful to identify the Il-17a signaling-promoting bacteria or their metabolites in the gut of AD mice. Unfortunately, the available relevant results for today are very limited or controversial. For example, the bacterial product valeric acid was reported to increase the concentrations of Il-17, Il-1β, and Il-6 in the blood and brain of mice with experimental stroke.[68] However, treatment with valeric acid was also shown to reduce the

Depletion of gut bacteria significantly increased the expression of Abcb1 and Lrp1 in blood vessels of APP-transgenic mice (h and l; *t* test, $n = 11$-12 per group); however, it did not change the protein level of claudin-5 (j; *t* test, $n = 4$-5 per group). In further experiments, Abcb1 and Lrp1 were detected with quantitative Western blot in the brain homogenates from 5-month-old non-APP-transgenic female mice with different expression of Il-17a (k; wild-type [wt], heterozygote [het] and knockout [ko]), and in the isolated blood vessels from 5-month-old Il17a-wt and ko APP-transgenic female mice (n). Deficiency of Il-17a significantly increased Abcb1 but not Lrp1 in the non-APP-transgenic mouse brain in a gene dose-dependent manner (l and m; one-way ANOVA followed by Bonferroni *post-hoc* test, $n = 4$-9 per group), and increased protein levels of both Abcb1 and Lrp1 in the blood vessels of APP-transgenic mice (o and p; *t* test, $n = 15$ - 19 per group). *: $p < 0.05$; **: $p < 0.01$; ****: $p < 0.0001$.

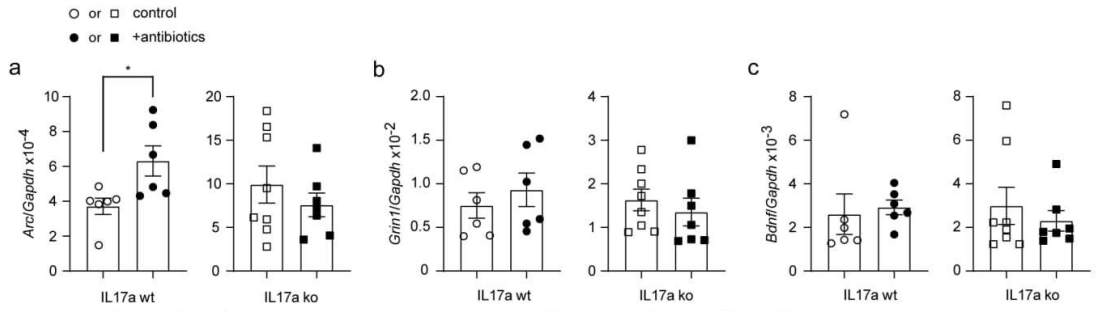

Figure 9. Depletion of gut bacteria increases Arc transcription in the brain of Il-17a-wildtype, but not Il17a-deficient APP-transgenic mice. Three-month-old Il-17a-deficient (ko) and wild-type (wt) APP-transgenic female mice were treated with and without antibiotics in drinking water for 2 months. Thereafter, brain tissues were homogenized and measured for transcripts of *Arc*, *Grin1* and *Bdnf* genes. Antibiotic treatment significantly increased the transcription of *Arc* gene in Il-17a-wildtype, but not in Il17a-deficient APP-transgenic mice (a; *t* test, $n = 6$ and 7 - 8 per group for Il-17a wt and ko mice, respectively). Antibiotic treatment did not change the transcription of *Grin1* and *Bdnf* genes (b and c; *t* test, $n = 6$ and 7 - 8 per group for Il-17a wt and ko mice, respectively). *: $p < 0.05$.

concentrations of Tnf-α and Il-6 in the blood of mice after irradiation.[69] In addition, activation of the valeric acid receptor Gpr43 inhibited neuroinflammation and improved cognitive function in APP-transgenic mice.[21]

It should be noted that microglial activation is a double-edged sword in AD pathogenesis: on the one side, it releases cytotoxic cytokines and reactive oxygen species, leading to neuronal damage; on the other side, it clears neurotoxic Aβ via microglial internalization, thereby safeguarding neurons.[70] In our recent study, p38α-MAPK deficiency in myeloid cells or Il-17a deficiency promotes microglial activation and Aβ clearance, which improves cognitive performance in APP-transgenic mice.[28] We and other groups have also shown that stimulation of TLR4 and TLR9 by injection of a low dose of LPS or synthetic oligodeoxynucleotides containing unmethylated CpG dinucleotides, similar to those found in bacterial DNA, induces mild and long-term microglial activation that facilitates the clearance of Aβ and hyperphosphorylated tau protein in human APP or tau -transgenic mice,[71–74] and in squirrel monkeys.[75] Our present study has shown that general depletion of gut bacteria reduces microglial phagocytosis of Aβ in APP-transgenic mice, which is consistent with previous observations that gut bacteria are essential for microglial maturation, activation and Aβ phagocytosis.[16–19] We would expect that specific depletion of Il-17a-promoting gut bacteria could maintain microglial activity and help clear the pathogenic Aβ molecules from the AD brain.

When studying the gut and brain, how gut bacteria modulate cerebral Aβ load is always an important question to answer. Our present study showed that microglia are not responsible for cerebral Aβ reduction in APP-transgenic mice after depletion of gut bacteria. Interestingly, we observed that depletion of gut bacteria increased the expression of Lrp1 and Abcb1 in the BBB of APP-transgenic mice, which was reversed by knockout of *Il-17a* gene. Knocking out *Il-17a* gene completely mimicked the effects of gut bacteria depletion on the expression of Lrp1 and Abcb1. Lrp1 and Abcb1 are two important transporters responsible for Aβ efflux across the BBB.[57,58] Depletion or inhibition of endothelial Lrp1 and Abcb1 leads to Aβ accumulation in the AD mouse brain.[76,77] Since transportation of Aβ from brain parenchyma to peripheral plasma might contribute 25% of total clearance of cerebral Aβ,[56] Aβ efflux represents a major pathway mediating the reduction of Aβ in the brain of AD mice following depletion of gut bacteria. It has been reported that the absence of ApoE retains less Aβ in the brain parenchyma and increases soluble Aβ in the interstitial fluid, possibly promoting the diffusion of soluble Aβ from the parenchyma into the perivascular space,[78] which favors Aβ efflux. Notably, depletion of gut bacteria decreased *Apoe* gene transcription in microglia, as observed in our study and by other scientists,[18] which may indicate the cooperation between microglia and BBB in the clearance of cerebral Aβ.

Aβ is produced by β- (BACE1) and γ-secretases after serial digestions of APP. The published

studies by our group and others have shown that the activity or protein level of β- and γ-secretases is regulated by inflammatory activation in the brain.[20,79,80] Not surprisingly, depletion of gut bacteria inhibited β-secretase activity in correlation with inflammatory inhibition in our APP-transgenic mice, which is consistent with the observation in germ-free AD mice.[18] We did not detect an increase in the expression of neprilysin and Ide in our APP-transgenic mice after antibiotic treatment, suggesting that extracellular degradation of Aβ is not the key mechanism for Aβ clearance after gut bacterial depletion. This result differs from the observation in a study on germ-free AD mice.[8]

Antibiotic therapy for AD patients has gained interest.[37] In several studies, germ-free APP-transgenic mice show better cognitive function and lower cerebral Aβ levels than specific pathogen-free (SPF) AD mice.[18,81] Our study supports antibiotic therapy, as gut bacterial depletion reduced Aβ burden in AD mice and, in particular, increased Aβ efflux-associated Abcb1 and Lrp1 across the BBB. Depletion of gut bacteria also up-regulated the transcription of *Arc* gene in the brain, which is associated with synaptic plasticity and cognitive improvement in APP-transgenic mice.[35,82] However, as discussed above, the general depletion of gut bacteria inhibits the activation of microglia, which decreases the efficiency of Aβ clearance. In addition, gut bacteria have also been shown to promote the development of cognitive performance.[83] Adult germ-free mice transplanted with fecal microbiota from 2–3-month-old mice perform better cognitively than mice transplanted with fecal microbiota from 18–20-month-old mice.[84] Treatment with broad-spectrum antibiotics can deplete as well the taxa of gut bacteria that favor learning and memory. Our study also indicated that bacteria belonging to the genera *Escherichia-Shigella* and *Parasutterella* were more resistant to antibiotic treatment. The possible expansion of these bacteria, especially *Escherichia-Shigella* bacteria, after long-term antibiotic treatment could increase inflammatory activation in the brain and accelerate the progression of AD. The combination of our results and the literature indicates that it is important to manipulate a specific bacterial taxon, e.g. by reducing the bacteria that stimulate immune cells to produce Il-17a. Currently, antibiotic therapy targeting specific bacterial taxa is still a major challenge for AD patients.

A limitation of our study is that the direct anti-inflammatory effects of antibiotics orally used to deplete gut bacteria could not be excluded. Although oral vancomycin, neomycin, streptomycin and ampicillin have low systemic absorption,[60] the oral bioavailability of metronidazole is high (98.9%).[46] Metronidazole must not be omitted from the antibiotic cocktail as it decimates anaerobic bacteria in the gut. Metronidazole has the potential to suppress the activity of both innate and acquired immune systems.[85] We observed that intraperitoneal injection of the antibiotic cocktail inhibited inflammatory gene transcription in the brain; however, the affected genes were mainly limited to anti-inflammatory *Il-10* and *Mrc1* genes (see Supplementary Figure S2), with a pattern different from the inflammatory regulation caused by oral treatment of antibiotics. We also observed that oral antibiotic treatment decreased *Il-17a* transcription but increased transcription of *Ifn-γ* and *Il-4* genes in CD4-positive spleen cells in APP-transgenic mice and promoted inflammatory activation in the brains of 24-month-old C57BL/6J mice. Indeed, oral antibiotic (amoxicillin/clavulanate) treatment of mice with antibiotic-sensitive and -resistant bacteria in the gut has shown that depletion of sensitive gut bacteria inhibits the development of Il-17a-expressing γδ T cells.[25] Therefore, we have reason to believe that the inhibition of neuroinflammation and Th17 development in our AD animal models was not due to the direct effects of antibiotics, but was a consequence of the depletion of gut bacteria. The potential inhibitory effect of antibiotics on immune cells is a common pitfall in antibiotic-treated mice in many gut and brain studies.[7,17,19]

In summary, our results are consistent with published observations that depletion of gut bacteria attenuates microglial inflammatory activation and Aβ pathology in the brain of APP-transgenic mice; however, we further elucidated the possible mechanisms mediating the gut-brain axis in AD pathogenesis: 1) depletion of gut bacteria reduces peripherally circulating Il-17a-expressing T lymphocytes and translocation of

bacterial components from the gut to the brain. Il-17a deficiency inhibits this bacterial translocation; 2) inhibition of Il-17a possibly maintains and even enhances microglial activity; 3) inhibition of Il-17a upregulates the expression of Lrp1 and Abcb1 in the BBB, possibly promoting Aβ efflux and Aβ clearance in the brain; and 4) depletion of gut bacteria has the potential to improve neuronal plasticity. Our study supports antibiotic therapy for AD patients; however, precise therapy targeting specific bacterial taxa is still a huge challenge. New methods and future work are needed to characterize the AD-specific microbiome profile in the gut. Particular attention should be paid to how Il-17a-associated intestinal bacteria can be manipulated.

Acknowledgments

We thank Prof. M. Jucker (Hertie Institute for Clinical Brain Research, Tübingen) for providing APP/PS1-transgenic mice, Prof. Y. Iwakura (Tokyo University of Science) for Il-17a knockout mice and Prof. R. Flavell (Yale University) for Il-17a-eGFP reporter mice. We appreciate Elisabeth Gluding and Kati Jordan for their excellent technical assistance.

Disclosure statement

No potential conflict of interest was reported by the author(s).

Funding

This work was supported by Alzheimer Forschung Initiative e.V. (Project #18009, and Publication Grant #P2405; to Y.L.), Saarland University through HOMFOR 2016 and 2019 (to Y.L.) and Anschubfinanzierung 2021 and 2023 (to Y.L.).

ORCID

Yang Liu http://orcid.org/0000-0002-7614-4233

Author contributions

Y.L. conceptualized and designed the study, acquired funding, conducted experiments, acquired and analyzed data, and wrote the manuscript. W.H., Q.L., I.T., and W.Q. conducted experiments, acquired data and analyzed data. T.H. provided resource and discussed study design. M.M. provided an animal facility and supervised animal experiments. K.F. provided a research laboratory and supervised the laboratory work. All authors contributed to the article and approved the submitted version.

Data availability statement

Our study has not generated new datasets. All data generated or analyzed during this study are included in this published article and its supplementary information files.

References

1. Vogt NM, Kerby RL, Dill-McFarland KA, Harding SJ, Merluzzi AP, Johnson SC, Carlsson CM, Asthana S, Zetterberg H, Blennow K. et al. Gut microbiome alterations in Alzheimer's disease. Sci Rep. 2017;7(1):13537. doi:10.1038/s41598-017-13601-y.
2. Dunham SJB, McNair KA, Adams ED, Avelar-Barragan J, Forner S, Mapstone M, Whiteson KL, Huffnagle GB. Longitudinal analysis of the microbiome and metabolome in the 5xfAD Mouse Model of Alzheimer's Disease. mBio. 2022;13(6):e0179422. doi:10.1128/mbio.01794-22.
3. Meyer K, Lulla A, Debroy K, Shikany JM, Yaffe K, Meirelles O, Launer LJ. Association of the gut microbiota with cognitive function in midlife. JAMA Netw Open. 2022;5(2):e2143941. doi:10.1001/jamanetworkopen.2021.43941.
4. Zhang T, Gao G, Kwok LY, Sun Z. Gut microbiome-targeted therapies for Alzheimer's disease. Gut Microbes. 2023;15(2):2271613. doi:10.1080/19490976.2023.2271613.
5. Ma C, Li Y, Mei Z, Yuan C, Kang JH, Grodstein F, Ascherio A, Willett WC, Chan AT, Huttenhower C. et al. Association between bowel movement pattern and cognitive function: Prospective cohort study and a metagenomic analysis of the gut microbiome. Neurology. 2023;101(20):e2014–e2025. doi:10.1212/WNL.0000000000207849.
6. Grabrucker S, Marizzoni M, Silajdzic E, Lopizzo N, Mombelli E, Nicolas S, Dohm-Hansen S, Scassellati C, Moretti DV, Rosa M. et al. Microbiota from Alzheimer's patients induce deficits in cognition and hippocampal neurogenesis. Brain. 2023;146(12):4916–4934. doi:10.1093/brain/awad303.
7. Dodiya HB, Kuntz T, Shaik SM, Baufeld C, Leibowitz J, Zhang X, Gottel N, Zhang X, Butovsky O, Gilbert JA. et al. Sex-specific effects of microbiome perturbations on cerebral Abeta amyloidosis and microglia phenotypes. J Exp Med. 2019;216(7):1542–1560. doi:10.1084/jem.20182386.
8. Harach T, Marungruang N, Duthilleul N, Cheatham V, Mc Coy KD, Frisoni G, Neher JJ, Fak F, Jucker M, Lasser T. et al. Reduction of Abeta amyloid pathology in APPPS1 transgenic mice in the absence of gut microbiota. Sci Rep. 2017;7(1):41802. doi:10.1038/srep41802 .

9. Kaur H, Nookala S, Singh S, Mukundan S, Nagamoto-Combs K, Combs CK. Sex-dependent effects of intestinal microbiome manipulation in a mouse model of alzheimer's disease. Cells. 2021;10(9):2370. doi:10.3390/cells10092370.
10. Minter MR, Hinterleitner R, Meisel M, Zhang C, Leone V, Zhang X, Oyler-Castrillo P, Zhang X, Musch MW, Shen X. et al. Antibiotic-induced perturbations in microbial diversity during post-natal development alters amyloid pathology in an aged APPSWE/PS1DeltaE9 murine model of Alzheimer's disease. Sci Rep. 2017;7(1):10411. doi:10.1038/s41598-017-11047-w.
11. Minter MR, Zhang C, Leone V, Ringus DL, Zhang X, Oyler-Castrillo P, Musch MW, Liao F, Ward JF, Holtzman DM. et al. Antibiotic-induced perturbations in gut microbial diversity influences neuro-inflammation and amyloidosis in a murine model of Alzheimer's disease. Sci Rep. 2016;6(1):30028. doi:10.1038/srep30028.
12. Liu P, Wu L, Peng G, Han Y, Tang R, Ge J, Zhang L, Jia L, Yue S, Zhou K. et al. Altered microbiomes distinguish Alzheimer's disease from amnestic mild cognitive impairment and health in a Chinese cohort. Brain Behav Immun. 2019;80:633–643. doi:10.1016/j.bbi.2019.05.008.
13. Murray ER, Kemp M, Nguyen TT. The microbiota-gut-brain axis in alzheimer's disease: A review of taxonomic alterations and potential avenues for Interventions. Arch Clin Neuropsychol. 2022;37(3):595–607. doi:10.1093/arclin/acac008.
14. Cattaneo A, Cattane N, Galluzzi S, Provasi S, Lopizzo N, Festari C, Ferrari C, Guerra UP, Paghera B, Muscio C. et al. Association of brain amyloidosis with pro-inflammatory gut bacterial taxa and peripheral inflammation markers in cognitively impaired elderly. Neurobiol Aging. 2017;49:60–68. doi:10.1016/j.neurobiolaging.2016.08.019.
15. Vital M, Karch A, Pieper DH, Shade A. Colonic Butyrate-Producing Communities in Humans: an overview using omics data. mSystems. 2017;2(6). doi:10.1128/mSystems.00130-17.
16. Erny D, Dokalis N, Mezo C, Castoldi A, Mossad O, Staszewski O, Frosch M, Villa M, Fuchs V, Mayer A. et al. Microbiota-derived acetate enables the metabolic fitness of the brain innate immune system during health and disease. Cell Metab. 2021;33(11):2260–2276 e2267. doi:10.1016/j.cmet.2021.10.010.
17. Erny D, Hrabe de Angelis AL, Jaitin D, Wieghofer P, Staszewski O, David E, Keren-Shaul H, Mahlakoiv T, Jakobshagen K, Buch T. et al. Host microbiota constantly control maturation and function of microglia in the CNS. Nat Neurosci. 2015;18(7):965–977. doi:10.1038/nn.4030.
18. Colombo AV, Sadler RK, Llovera G, Singh V, Roth S, Heindl S, Sebastian Monasor L, Verhoeven A, Peters F, Parhizkar S. et al. Microbiota-derived short chain fatty acids modulate microglia and promote Abeta plaque deposition. Elife. 2021;10:e59826. doi:10.7554/eLife.59826.
19. Xie J, Bruggeman A, De Nolf C, Vandendriessche C, Van Imschoot G, Van Wonterghem E, Vereecke L, Vandenbroucke RE. Gut microbiota regulates blood-cerebrospinal fluid barrier function and Abeta pathology. Embo J. 2023;42(17):e111515. doi:10.15252/embj.2022111515 .
20. Quan W, Luo Q, Hao W, Tomic I, Furihata T, Schulz-Schaffer W, Menger MD, Fassbender K, Liu Y. Haploinsufficiency of microglial MyD88 ameliorates Alzheimer's pathology and vascular disorders in APP/PS1-transgenic mice. Glia. 2021;69(8):1987–2005. doi:10.1002/glia.24007.
21. Zhou Y, Xie L, Schroder J, Schuster IS, Nakai M, Sun G, Sun YBY, Marino E, Degli-Esposti MA, Marques FZ. et al. Dietary fiber and microbiota metabolite receptors enhance cognition and alleviate disease in the 5xFAD Mouse model of alzheimer's disease. J Neurosci. 2023;43(37):6460–6475. doi:10.1523/JNEUROSCI.0724-23.2023.
22. Dupraz L, Magniez A, Rolhion N, Richard ML, Da Costa G, Touch S, Mayeur C, Planchais J, Agus A, Danne C. et al. Gut microbiota-derived short-chain fatty acids regulate IL-17 production by mouse and human intestinal γδ T cells. Cell Rep. 2021;36(1):109332. doi:10.1016/j.celrep.2021.109332.
23. Singh N, Gurav A, Sivaprakasam S, Brady E, Padia R, Shi H, Thangaraju M, Prasad PD, Manicassamy S, Munn DH. et al. Activation of Gpr109a, receptor for niacin and the commensal metabolite butyrate, suppresses colonic inflammation and carcinogenesis. Immunity. 2014;40(1):128–139. doi:10.1016/j.immuni.2013.12.007.
24. Lee YK, Menezes JS, Umesaki Y, Mazmanian SK. Proinflammatory T-cell responses to gut microbiota promote experimental autoimmune encephalomyelitis. Proc Natl Acad Sci USA. 2011;108 Suppl 1(supplement_1):4615–4622. doi:10.1073/pnas.1000082107.
25. Benakis C, Brea D, Caballero S, Faraco G, Moore J, Murphy M, Sita G, Racchumi G, Ling L, Pamer EG. et al. Commensal microbiota affects ischemic stroke outcome by regulating intestinal gammadelta T cells. Nat Med. 2016;22(5):516–523. doi:10.1038/nm.4068.
26. Baruch K, Rosenzweig N, Kertser A, Deczkowska A, Sharif AM, Spinrad A, Tsitsou-Kampeli A, Sarel A, Cahalon L, Schwartz M. Breaking immune tolerance by targeting Foxp3+ regulatory T cells mitigates Alzheimer's disease pathology. Nat Commun. 2015;6(1):7967. doi:10.1038/ncomms8967.
27. Dansokho C, Ait Ahmed D, Aid S, Toly-Ndour C, Chaigneau T, Calle V, Cagnard N, Holzenberger M, Piaggio E, Aucouturier P. et al. Regulatory T cells delay disease progression in Alzheimer-like pathology. Brain. 2016;139(Pt 4):1237–1251. doi:10.1093/brain/awv408.
28. Luo Q, Schnoder L, Hao W, Litzenburger K, Decker Y, Tomic I, Menger MD, Liu Y, Fassbender K. p38alpha-MAPK-deficient myeloid cells ameliorate symptoms and

pathology of APP-transgenic Alzheimer's disease mice. Aging Cell. 2022;21(8):e13679. doi:10.1111/acel.13679.
29. Marizzoni M, Mirabelli P, Mombelli E, Coppola L, Festari C, Lopizzo N, Luongo D, Mazzelli M, Naviglio D, Blouin JL. et al. A peripheral signature of Alzheimer's disease featuring microbiota-gut-brain axis markers. Alzheimers Res Ther. 2023;15(1):101. doi:10.1186/s13195-023-01218-5.
30. Dominy SS, Lynch C, Ermini F, Benedyk M, Marczyk A, Konradi A, Nguyen M, Haditsch U, Raha D, Griffin C. et al. Porphyromonas gingivalis in Alzheimer's disease brains: Evidence for disease causation and treatment with small-molecule inhibitors. Sci Adv. 2019;5(1):eaau3333. doi:10.1126/sciadv.aau3333.
31. Fassbender K, Walter S, Kuhl S, Landmann R, Ishii K, Bertsch T, Stalder AK, Muehlhauser F, Liu Y, Ulmer AJ. et al. The LPS receptor (CD14) links innate immunity with Alzheimer's disease. FASEB J. 2004;18(1):203–205. doi:10.1096/fj.03-0364fje.
32. Liu S, Liu Y, Hao W, Wolf L, Kiliaan AJ, Penke B, Rube CE, Walter J, Heneka MT, Hartmann T. et al. TLR2 is a primary receptor for Alzheimer's amyloid beta peptide to trigger neuroinflammatory activation. J Immunol. 2012;188(3):1098–1107. doi:10.4049/jimmunol.1101121.
33. Liu Y, Walter S, Stagi M, Cherny D, Letiembre M, Schulz-Schaeffer W, Heine H, Penke B, Neumann H, Fassbender K. LPS receptor (CD14): a receptor for phagocytosis of Alzheimer's amyloid peptide. Brain. 2005;128(Pt 8):1778–1789. doi:10.1093/brain/awh531.
34. O'Neill LA, Golenbock D, Bowie AG. The history of Toll-like receptors - redefining innate immunity. Nat Rev Immunol. 2013;13(6):453–460. doi:10.1038/nri3446.
35. Hao W, Liu Y, Liu S, Walter S, Grimm MO, Kiliaan AJ, Penke B, Hartmann T, Rube CE, Menger MD. et al. Myeloid differentiation factor 88-deficient bone marrow cells improve Alzheimer's disease-related symptoms and pathology. Brain. 2011;134(Pt 1):278–292. doi:10.1093/brain/awq325.
36. Walter S, Letiembre M, Liu Y, Heine H, Penke B, Hao W, Bode B, Manietta N, Walter J, Schulz-Schuffer W. et al. Role of the toll-like receptor 4 in neuroinflammation in Alzheimer's disease. Cell Physiol Biochem. 2007;20(6):947–956. doi:10.1159/000110455.
37. Panza F, Lozupone M, Solfrizzi V, Watling M, Imbimbo BP. Time to test antibacterial therapy in Alzheimer's disease. Brain. 2019;142(10):2905–2929. doi:10.1093/brain/awz244.
38. Rakusa E, Fink A, Tamguney G, Heneka MT, Doblhammer G. Sporadic use of antibiotics in older adults and the risk of dementia: a nested case-control study based on German health claims data. J Alzheimers Dis. 2023;93(4):1329–1339. doi:10.3233/JAD-221153.
39. Drummond RA, Desai JV, Ricotta EE, Swamydas M, Deming C, Conlan S, Quinones M, Matei-Rascu V, Sherif L, Lecky D. et al. Long-term antibiotic exposure promotes mortality after systemic fungal infection by driving lymphocyte dysfunction and systemic escape of commensal bacteria. Cell Host Microbe. 2022;30(7):1020–1033 e1026. doi:10.1016/j.chom.2022.04.013.
40. Nebel RA, Aggarwal NT, Barnes LL, Gallagher A, Goldstein JM, Kantarci K, Mallampalli MP, Mormino EC, Scott L, Yu WH. et al. Understanding the impact of sex and gender in Alzheimer's disease: A call to action. Alzheimers Dement. 2018;14(9):1171–1183. doi:10.1016/j.jalz.2018.04.008.
41. Radde R, Bolmont T, Kaeser SA, Coomaraswamy J, Lindau D, Stoltze L, Calhoun ME, Jaggi F, Wolburg H, Gengler S. et al. Abeta42-driven cerebral amyloidosis in transgenic mice reveals early and robust pathology. EMBO Rep. 2006;7(9):940–946. doi:10.1038/sj.embor.7400784.
42. Nakae S, Komiyama Y, Nambu A, Sudo K, Iwase M, Homma I, Sekikawa K, Asano M, Iwakura Y. Antigen-specific T cell sensitization is impaired in IL-17-deficient mice, causing suppression of allergic cellular and humoral responses. Immunity. 2002;17(3):375–387. doi:10.1016/S1074-7613(02)00391-6.
43. Esplugues E, Huber S, Gagliani N, Hauser AE, Town T, Wan YY, O'Connor W Jr., Rongvaux A, Van Rooijen N, Haberman AM. et al. Control of TH17 cells occurs in the small intestine. Nature. 2011;475(7357):514–518. doi:10.1038/nature10228.
44. Liu S, da Cunha AP, Rezende RM, Cialic R, Wei Z, Bry L, Comstock LE, Gandhi R, Weiner HL. The host shapes the gut microbiota via fecal MicroRNA. Cell Host Microbe. 2016;19(1):32–43. doi:10.1016/j.chom.2015.12.005.
45. Bercik P, Denou E, Collins J, Jackson W, Lu J, Jury J, Deng Y, Blennerhassett P, Macri J, Kd M. et al. The intestinal microbiota affect central levels of brain-derived neurotropic factor and behavior in mice. Gastroenterology. 2011;141(2):599–609, 609 e591–593. doi:10.1053/j.gastro.2011.04.052.
46. Jensen JC, Gugler R. Single- and multiple-dose metronidazole kinetics. Clin Pharmacol Ther. 1983;34(4):481–487. doi:10.1038/clpt.1983.201.
47. Lau SF, Wu W, Seo H, Aky F, Ip NY. Quantitative in vivo assessment of amyloid-beta phagocytic capacity in an Alzheimer's disease mouse model. STAR Protoc. 2021;2(1):100265. doi:10.1016/j.xpro.2020.100265.
48. Couter CJ, Surana NK. Isolation and flow cytometric characterization of murine small intestinal lymphocytes. JoVE (J Visualized Exp). 2016;111:e54114.
49. Liu Y, Liu X, Hao W, Decker Y, Schomburg R, Fulop L, Pasparakis M, Menger MD, Fassbender K. IKKbeta deficiency in myeloid cells ameliorates Alzheimer's disease-related symptoms and pathology. J Neurosci. 2014;34(39):12982–12999. doi:10.1523/JNEUROSCI.1348-14.2014.
50. Hao W, Decker Y, Schnoder L, Schottek A, Li D, Menger MD, Fassbender K, Liu Y. Deficiency of IkappaB kinase beta in myeloid cells reduces severity of experimental

autoimmune encephalomyelitis. Am J Pathol. 2016;186 (5):1245–1257. doi:10.1016/j.ajpath.2016.01.004.
51. Benjamin JL, Sumpter R Jr., Levine B, Hooper LV. Intestinal epithelial autophagy is essential for host defense against invasive bacteria. Cell Host Microbe. 2013;13(6):723–734. doi:10.1016/j.chom.2013.05.004.
52. Cua DJ, Tato CM. Innate IL-17-producing cells: the sentinels of the immune system. Nat Rev Immunol. 2010;10(7):479–489. doi:10.1038/nri2800.
53. Hao W, Luo Q, Menger MD, Fassbender K, Liu Y. Treatment with CD52 antibody protects neurons in experimental autoimmune encephalomyelitis mice during the recovering phase. Front Immunol. 2021;12:792465. doi:10.3389/fimmu.2021.792465.
54. Thapa M, Kumari A, Chin C-Y, Choby JE, Jin F, Bogati B, Chopyk DM, Koduri N, Pahnke A, Elrod EJ. et al. Translocation of gut commensal bacteria to the brain. bioRxiv. 2023;2023.08.30:555630. doi: 10.1101/2023.08.30.555630.
55. Keren-Shaul H, Spinrad A, Weiner A, Matcovitch-Natan O, Dvir-Szternfeld R, Ulland TK, David E, Baruch K, Lara-Astaiso D, Toth B. et al. A unique microglia type associated with restricting development of alzheimer's disease. Cell. 2017;169(7):1276–1290 e1217. doi:10.1016/j.cell.2017.05.018.
56. Roberts KF, Elbert DL, Kasten TP, Patterson BW, Sigurdson WC, Connors RE, Ovod V, Munsell LY, Mawuenyega KG, Miller-Thomas MM. et al. Amyloid-β efflux from the central nervous system into the plasma. Ann Neurol. 2014;76(6):837–844. doi:10.1002/ana.24270.
57. Kuhnke D, Jedlitschky G, Grube M, Krohn M, Jucker M, Mosyagin I, Cascorbi I, Walker LC, Kroemer HK, Warzok RW. et al. MDR1-P-Glycoprotein (ABCB1) mediates transport of Alzheimer's amyloid-beta peptides–implications for the mechanisms of Abeta clearance at the blood-brain barrier. Brain Pathol. 2007;17 (4):347–353. doi:10.1111/j.1750-3639.2007.00075.x.
58. Shinohara M, Tachibana M, Kanekiyo T, Bu G. Role of LRP1 in the pathogenesis of Alzheimer's disease: evidence from clinical and preclinical studies. J Lipid Res. 2017;58(7):1267–1281. doi:10.1194/jlr.R075796.
59. Gao L, Zhang Y, Sterling K, Song W. Brain-derived neurotrophic factor in Alzheimer's disease and its pharmaceutical potential. Transl Neurodegener. 2022;11 (1):4. doi:10.1186/s40035-022-00279-0.
60. Frohlich EE, Farzi A, Mayerhofer R, Reichmann F, Jacan A, Wagner B, Zinser E, Bordag N, Magnes C, Frohlich E. et al. Cognitive impairment by antibiotic-induced gut dysbiosis: analysis of gut microbiota-brain communication. Brain Behav Immun. 2016;56:140–155. doi:10.1016/j.bbi.2016.02.020.
61. Chandra S, Sisodia SS, Vassar RJ. The gut microbiome in Alzheimer's disease: what we know and what remains to be explored. Mol Neurodegener. 2023;18 (1):9. doi:10.1186/s13024-023-00595-7.
62. Chandra S, Di Meco A, Dodiya HB, Popovic J, Cuddy LK, Weigle IQ, Zhang X, Sadleir K, Sisodia SS, Vassar R. The gut microbiome regulates astrocyte reaction to Abeta amyloidosis through microglial dependent and independent mechanisms. Mol Neurodegener. 2023;18 (1):45. doi:10.1186/s13024-023-00635-2.
63. Li X, Li Y, Jin Y, Zhang Y, Wu J, Xu Z, Huang Y, Cai L, Gao S, Liu T. et al. Transcriptional and epigenetic decoding of the microglial aging process. Nat Aging. 2023;3 (10):1288–1311. doi:10.1038/s43587-023-00479-x.
64. Mone Y, Earl JP, Krol JE, Ahmed A, Sen B, Ehrlich GD, Lapides JR. Evidence supportive of a bacterial component in the etiology for Alzheimer's disease and for a temporal-spatial development of a pathogenic microbiome in the brain. Front Cell Infect Microbiol. 2023;13:1123228. doi:10.3389/fcimb.2023.1123228.
65. Regen T, Isaac S, Amorim A, Núñez NG, Hauptmann J, Shanmugavadivu A, Klein M, Sankowski R, Mufazalov IA, Yogev N. et al. IL-17 controls central nervous system autoimmunity through the intestinal microbiome. Sci Immunol. 2021;6(56):eaaz6563. doi:10.1126/sciimmunol.aaz6563.
66. Lee JS, Wang RX, Alexeev EE, Colgan SP. Intestinal Inflammation as a dysbiosis of energy procurement: New Insights into an old topic. Gut Microbes. 2021;13 (1):1–20. doi:10.1080/19490976.2021.1880241.
67. Madry C, Kyrargyri V, Arancibia-Carcamo IL, Jolivet R, Kohsaka S, Bryan RM, Attwell D. Microglial Ramification, surveillance, and interleukin-1beta release are regulated by the two-pore domain K(+) channel THIK-1. Neuron. 2018;97(2):299–312 e296. doi:10.1016/j.neuron.2017.12.002.
68. Zeng X, Li J, Shan W, Lai Z, Zuo Z. Gut microbiota of old mice worsens neurological outcome after brain ischemia via increased valeric acid and IL-17 in the blood. Microbiome. 2023;11(1):204. doi:10.1186/s40168-023-01648-1.
69. Li Y, Dong J, Xiao H, Zhang S, Wang B, Cui M, Fan S. Gut commensal derived-valeric acid protects against radiation injuries. Gut Microbes. 2020;11(4):789–806. doi:10.1080/19490976.2019.1709387.
70. Heneka MT, Carson MJ, El Khoury J, Landreth GE, Brosseron F, Feinstein DL, Jacobs AH, Wyss-Coray T, Vitorica J, Ransohoff RM. et al. Neuroinflammation in Alzheimer's disease. Lancet Neurol. 2015;14(4):388–405. doi:10.1016/S1474-4422(15)70016-5.
71. Michaud JP, Halle M, Lampron A, Theriault P, Prefontaine P, Filali M, Tribout-Jover P, Lanteigne AM, Jodoin R, Cluff C. et al. Toll-like receptor 4 stimulation with the detoxified ligand monophosphoryl lipid a improves Alzheimer's disease-related pathology. Proc Natl Acad Sci USA. 2013;110(5):1941–1946. doi:10.1073/pnas.1215165110.
72. Qin Y, Liu Y, Hao W, Decker Y, Tomic I, Menger MD, Liu C, Fassbender K. Stimulation of TLR4 attenuates alzheimer's disease-related symptoms and pathology in

tau-transgenic mice. J Immunol. 2016;197(8):3281–3292. doi:10.4049/jimmunol.1600873.
73. Scholtzova H, Chianchiano P, Pan J, Sun Y, Goni F, Mehta PD, Wisniewski T. Amyloid ß and Tau Alzheimer's disease related pathology is reduced by toll-like receptor 9 stimulation. Acta Neuropathol Commun. 2014;2(1):101. doi:10.1186/PREACCEPT-2151623761356337.
74. Scholtzova H, Kascsak RJ, Bates KA, Boutajangout A, Kerr DJ, Meeker HC, Mehta PD, Spinner DS, Wisniewski T. Induction of toll-like receptor 9 signaling as a method for ameliorating Alzheimer's disease-related pathology. J Neurosci. 2009;29(6):1846–1854. doi:10.1523/JNEUROSCI.5715-08.2009.
75. Patel AG, Nehete PN, Krivoshik SR, Pei X, Cho EL, Nehete BP, Ramani MD, Shao Y, Williams LE, Wisniewski T. et al. Innate immunity stimulation via CpG oligodeoxynucleotides ameliorates Alzheimer's disease pathology in aged squirrel monkeys. Brain. 2021;144(7):2146–2165. doi:10.1093/brain/awab129.
76. Cirrito JR, Deane R, Fagan AM, Spinner ML, Parsadanian M, Finn MB, Jiang H, Prior JL, Sagare A, Bales KR. et al. P-glycoprotein deficiency at the blood-brain barrier increases amyloid-beta deposition in an Alzheimer disease mouse model. J Clin Invest. 2005;115(11):3285–3290. doi:10.1172/JCI25247.
77. Storck SE, Meister S, Nahrath J, Meissner JN, Schubert N, Di Spiezio A, Baches S, Vandenbroucke RE, Bouter Y, Prikulis I. et al. Endothelial LRP1 transports amyloid-beta(1-42) across the blood-brain barrier. J Clin Invest. 2016;126(1):123–136. doi:10.1172/JCI81108.
78. DeMattos RB, Cirrito JR, Parsadanian M, May PC, O'Dell MA, Taylor JW, Harmony JA, Aronow BJ, Bales KR, Paul SM. et al. ApoE and clusterin cooperatively suppress Abeta levels and deposition: evidence that ApoE regulates extracellular Abeta metabolism in vivo. Neuron. 2004;41(2):193–202. doi:10.1016/S0896-6273(03)00850-X.
79. He P, Zhong Z, Lindholm K, Berning L, Lee W, Lemere C, Staufenbiel M, Li R, Shen Y. Deletion of tumor necrosis factor death receptor inhibits amyloid beta generation and prevents learning and memory deficits in Alzheimer's mice. J Cell Biol. 2007;178(5):829–841. doi:10.1083/jcb.200705042.
80. Hur J-Y, Frost GR, Wu X, Crump C, Pan SJ, Wong E, Barros M, Li T, Nie P, Zhai Y. et al. The innate immunity protein IFITM3 modulates γ-secretase in Alzheimer's disease. Nature. 2020;586(7831):735–740. doi:10.1038/s41586-020-2681-2.
81. Mezo C, Dokalis N, Mossad O, Staszewski O, Neuber J, Yilmaz B, Schnepf D, de Aguero MG, Ganal-Vonarburg SC, Macpherson AJ. et al. Different effects of constitutive and induced microbiota modulation on microglia in a mouse model of Alzheimer's disease. Acta Neuropathol Commun. 2020;8(1):119. doi:10.1186/s40478-020-00988-5.
82. Bramham CR, Worley PF, Moore MJ, Guzowski JF. The immediate early gene arc/arg3.1: regulation, mechanisms, and function. J Neurosci. 2008;28(46):11760–11767. doi:10.1523/JNEUROSCI.3864-08.2008.
83. Cerdo T, Ruiz-Rodriguez A, Acuna I, Torres-Espinola FJ, Menchen-Marquez S, Gamiz F, Gallo M, Jehmlich N, Haange SB, von Bergen M. et al. 1974. Infant gut microbiota contributes to cognitive performance in mice. Cell Host Microbe. 2023;31(12):1974–1988 e. doi:10.1016/j.chom.2023.11.004.
84. Lee J, Venna VR, Durgan DJ, Shi H, Hudobenko J, Putluri N, Petrosino J, Ld M, Bryan RM. Young versus aged microbiota transplants to germ-free mice: increased short-chain fatty acids and improved cognitive performance. Gut Microbes. 2020;12(1):1–14. doi:10.1080/19490976.2020.1814107.
85. Shakir L, Javeed A, Ashraf M, Riaz A. Metronidazole and the immune system. Pharmazie. 2011;66(6):393–398.
86. Zhang Y, Shen Y, Liufu N, Liu L, Li W, Shi Z, Zheng H, Mei X, Chen CY, Jiang Z. et al. Transmission of Alzheimer's disease-associated microbiota dysbiosis and its impact on cognitive function: evidence from mice and patients. Mol Psychiatry. 2023;28(10):4421–4437. doi:10.1038/s41380-023-02216-7.

10 REFERENCES

Amatya, N., A. V. Garg and S. L. Gaffen (2017). "IL-17 Signaling: The Yin and the Yang." Trends Immunol **38**(5): 310-322.

Arbel-Ornath, M., E. Hudry, J. R. Boivin, T. Hashimoto, S. Takeda, K. V. Kuchibhotla, S. Hou, C. R. Lattarulo, A. M. Belcher, N. Shakerdge, P. B. Trujillo, A. Muzikansky, R. A. Betensky, B. T. Hyman and B. J. Bacskai (2017). "Soluble oligomeric amyloid-beta induces calcium dyshomeostasis that precedes synapse loss in the living mouse brain." Mol Neurodegener **12**(1): 27.

Aspelund, A., S. Antila, S. T. Proulx, T. V. Karlsen, S. Karaman, M. Detmar, H. Wiig and K. Alitalo (2015). "A dural lymphatic vascular system that drains brain interstitial fluid and macromolecules." J Exp Med **212**(7): 991-999.

Barker, N. (2014). "Adult intestinal stem cells: critical drivers of epithelial homeostasis and regeneration." Nat Rev Mol Cell Biol **15**(1): 19-33.

Baruch, K., N. Rosenzweig, A. Kertser, A. Deczkowska, A. M. Sharif, A. Spinrad, A. Tsitsou-Kampeli, A. Sarel, L. Cahalon and M. Schwartz (2015). "Breaking immune tolerance by targeting Foxp3(+) regulatory T cells mitigates Alzheimer's disease pathology." Nat Commun **6**: 7967.

Bell, R. D., A. P. Sagare, A. E. Friedman, G. S. Bedi, D. M. Holtzman, R. Deane and B. V. Zlokovic (2007). "Transport pathways for clearance of human Alzheimer's amyloid beta-peptide and apolipoproteins E and J in the mouse central nervous system." J Cereb Blood Flow Metab **27**(5): 909-918.

Benakis, C., D. Brea, S. Caballero, G. Faraco, J. Moore, M. Murphy, G. Sita, G. Racchumi, L. Ling, E. G. Pamer, C. Iadecola and J. Anrather (2016). "Commensal microbiota affects ischemic stroke outcome by regulating intestinal gammadelta T cells." Nat Med **22**(5): 516-523.

Benjamin, J. L., R. Sumpter, Jr., B. Levine and L. V. Hooper (2013). "Intestinal epithelial autophagy is essential for host defense against invasive bacteria." Cell Host Microbe **13**(6): 723-734.

Bercik, P., E. Denou, J. Collins, W. Jackson, J. Lu, J. Jury, Y. Deng, P. Blennerhassett, J. Macri, K. D. McCoy, E. F. Verdu and S. M. Collins (2011). "The intestinal microbiota affect central levels of brain-derived neurotropic factor and behavior in mice." Gastroenterology **141**(2): 599-609, 609 e591-593.

Bramham, C. R., P. F. Worley, M. J. Moore and J. F. Guzowski (2008). "The immediate early gene arc/arg3.1: regulation, mechanisms, and function." J Neurosci **28**(46): 11760-11767.

Bruttger, J., K. Karram, S. Wortge, T. Regen, F. Marini, N. Hoppmann, M. Klein, T. Blank, S. Yona, Y. Wolf, M. Mack, E. Pinteaux, W. Muller, F. Zipp, H. Binder, T. Bopp, M. Prinz, S. Jung and A. Waisman (2015). "Genetic Cell Ablation Reveals Clusters of Local Self-Renewing Microglia in the Mammalian Central Nervous System." Immunity **43**(1): 92-106.

Bulloj, A., M. C. Leal, H. Xu, E. M. Castano and L. Morelli (2010). "Insulin-degrading enzyme sorting in exosomes: a secretory pathway for a key brain amyloid-beta degrading protease." J Alzheimers Dis **19**(1): 79-95.

Burokas, A., R. D. Moloney, T. G. Dinan and J. F. Cryan (2015). "Microbiota regulation of the Mammalian gut-brain axis." Adv Appl Microbiol **91**: 1-62.

Busche, M. A., G. Eichhoff, H. Adelsberger, D. Abramowski, K. H. Wiederhold, C. Haass, M. Staufenbiel, A. Konnerth and O. Garaschuk (2008). "Clusters of hyperactive neurons near amyloid plaques in a mouse model of Alzheimer's disease." Science **321**(5896): 1686-1689.

Caccamo, A., V. De Pinto, A. Messina, C. Branca and S. Oddo (2014). "Genetic reduction of mammalian target of rapamycin ameliorates Alzheimer's disease-like cognitive and pathological deficits by restoring hippocampal gene expression signature." J Neurosci **34**(23): 7988-7998.

Caccamo, A., S. Oddo, M. C. Sugarman, Y. Akbari and F. M. LaFerla (2005). "Age- and region-dependent alterations in Abeta-degrading enzymes: implications for Abeta-induced disorders." Neurobiol Aging **26**(5): 645-654.

Caponio, D., K. Veverova, S. Q. Zhang, L. Shi, G. Wong, M. Vyhnalek and E. F. Fang (2022). "Compromised autophagy and mitophagy in brain ageing and Alzheimer's diseases." Aging Brain **2**: 100056.

Carare, R. O., M. Bernardes-Silva, T. A. Newman, A. M. Page, J. A. Nicoll, V. H. Perry and R. O. Weller (2008). "Solutes, but not cells, drain from the brain parenchyma along basement membranes of capillaries and arteries: significance for cerebral amyloid angiopathy and neuroimmunology." Neuropathol Appl Neurobiol **34**(2): 131-144.

Casali, B. T., K. P. MacPherson, E. G. Reed-Geaghan and G. E. Landreth (2020). "Microglia depletion rapidly and reversibly alters amyloid pathology by modification of plaque compaction and morphologies." Neurobiol Dis **142**: 104956.

Cattaneo, A., N. Cattane, S. Galluzzi, S. Provasi, N. Lopizzo, C. Festari, C. Ferrari, U. P. Guerra, B. Paghera, C. Muscio, A. Bianchetti, G. D. Volta, M. Turla, M. S. Cotelli, M. Gennuso, A. Prelle, O. Zanetti, G. Lussignoli, D. Mirabile, D. Bellandi, S. Gentile, G. Belotti, D. Villani, T. Harach, T. Bolmont, A. Padovani, M. Boccardi, G. B. Frisoni and I.-F. Group (2017). "Association of brain amyloidosis with pro-inflammatory gut bacterial taxa and peripheral inflammation markers in cognitively impaired elderly." Neurobiol Aging **49**: 60-68.

Cerdo, T., A. Ruiz-Rodriguez, I. Acuna, F. J. Torres-Espinola, S. Menchen-Marquez, F. Gamiz, M. Gallo, N. Jehmlich, S. B. Haange, M. von Bergen, C. Campoy and A. Suarez (2023). "Infant gut microbiota contributes to cognitive performance in mice." Cell Host Microbe **31**(12): 1974-1988 e1974.

Chandra, S., A. Di Meco, H. B. Dodiya, J. Popovic, L. K. Cuddy, I. Q. Weigle, X. Zhang, K. Sadleir, S. S. Sisodia and R. Vassar (2023). "The gut microbiome regulates astrocyte reaction to Abeta amyloidosis through microglial dependent and independent mechanisms." Mol Neurodegener **18**(1): 45.

Chandra, S., S. S. Sisodia and R. J. Vassar (2023). "The gut microbiome in Alzheimer's disease: what we know and what remains to be explored." Mol Neurodegener **18**(1): 9.

Chen, J., X. Liu and Y. Zhong (2020). "Interleukin-17A: The Key Cytokine in Neurodegenerative Diseases." Front Aging Neurosci **12**: 566922.

Chen, J. M., G. X. Jiang, Q. W. Li, Z. M. Zhou and Q. Cheng (2014). "Increased serum levels of interleukin-18, -23 and -17 in Chinese patients with Alzheimer's disease." Dement Geriatr Cogn Disord **38**(5-6): 321-329.

Chung, D. R., D. L. Kasper, R. J. Panzo, T. Chitnis, M. J. Grusby, M. H. Sayegh and A. O. Tzianabos (2003). "CD4+ T cells mediate abscess formation in intra-abdominal sepsis by an IL-17-dependent mechanism." J Immunol **170**(4): 1958-1963.

Chung, K. M., N. Hernandez, A. A. Sproul and W. H. Yu (2019). "Alzheimer's disease and the autophagic-lysosomal system." Neurosci Lett **697**: 49-58.

Cirrito, J. R., R. Deane, A. M. Fagan, M. L. Spinner, M. Parsadanian, M. B. Finn, H. Jiang, J. L. Prior, A. Sagare, K. R. Bales, S. M. Paul, B. V. Zlokovic, D. Piwnica-Worms and D. M. Holtzman (2005). "P-glycoprotein deficiency at the blood-brain barrier increases amyloid-beta deposition in an Alzheimer disease mouse model." J Clin Invest **115**(11): 3285-3290.

Cobb, B. S., T. B. Nesterova, E. Thompson, A. Hertweck, E. O'Connor, J. Godwin, C. B. Wilson, N. Brockdorff, A. G. Fisher, S. T. Smale and M. Merkenschlager (2005). "T cell lineage choice and differentiation in the absence of the RNase III enzyme Dicer." J Exp Med **201**(9): 1367-1373.

Colombo, A. V., R. K. Sadler, G. Llovera, V. Singh, S. Roth, S. Heindl, L. Sebastian Monasor, A. Verhoeven, F. Peters, S. Parhizkar, F. Kamp, M. Gomez de Aguero, A. J. MacPherson, E. Winkler, J. Herms, C. Benakis, M. Dichgans, H. Steiner, M. Giera, C. Haass, S. Tahirovic and A. Liesz (2021). "Microbiota-derived short chain fatty acids modulate microglia and promote Abeta plaque deposition." Elife **10**: e59826.

Colombo, A. V., R. K. Sadler, G. Llovera, V. Singh, S. Roth, S. Heindl, L. Sebastian Monasor, A. Verhoeven, F. Peters, S. Parhizkar, F. Kamp, M. Gomez de Aguero, A. J. MacPherson, E. Winkler, J. Herms, C. Benakis, M. Dichgans, H. Steiner, M. Giera, C. Haass, S. Tahirovic and A. Liesz (2021). "Microbiota-derived short chain fatty acids modulate microglia and promote Abeta plaque deposition." Elife **10**.

Condello, C., P. Yuan, A. Schain and J. Grutzendler (2015). "Microglia constitute a barrier that prevents neurotoxic protofibrillar Abeta42 hotspots around plaques." Nat Commun **6**: 6176.

Cook, D. G., J. B. Leverenz, P. J. McMillan, J. J. Kulstad, S. Ericksen, R. A. Roth, G. D. Schellenberg, L. W. Jin, K. S. Kovacina and S. Craft (2003). "Reduced hippocampal insulin-degrading enzyme in late-onset Alzheimer's disease is associated with the apolipoprotein E-epsilon4 allele." Am J Pathol **162**(1): 313-319.

Couter, C. J. and N. K. Surana (2016). "Isolation and Flow Cytometric Characterization of Murine Small Intestinal Lymphocytes." J Vis Exp(111).

Crossgrove, J. S., G. J. Li and W. Zheng (2005). "The choroid plexus removes beta-amyloid from brain cerebrospinal fluid." Exp Biol Med (Maywood) **230**(10): 771-776.

Cua, D. J. and C. M. Tato (2010). "Innate IL-17-producing cells: the sentinels of the immune system." Nat Rev Immunol **10**(7): 479-489.

Damkier, H. H., P. D. Brown and J. Praetorius (2013). "Cerebrospinal fluid secretion by the choroid plexus." Physiol Rev **93**(4): 1847-1892.

Dansokho, C., D. Ait Ahmed, S. Aid, C. Toly-Ndour, T. Chaigneau, V. Calle, N. Cagnard, M. Holzenberger, E. Piaggio, P. Aucouturier and G. Dorothee (2016). "Regulatory T cells delay disease progression in Alzheimer-like pathology." Brain **139**(Pt 4): 1237-1251.

Davidson, L., J. van den Reek, M. Bruno, F. van Hunsel, R. M. C. Herings, V. Matzaraki, C. K. Boahen, V. Kumar, H. M. M. Groenewoud, F. L. van de Veerdonk, M. G. Netea, E. de Jong and B. J. Kullberg (2022). "Risk of candidiasis associated with interleukin-17 inhibitors: A real-world observational study of multiple independent sources." Lancet Reg Health Eur **13**: 100266.

DeKosky, S. T. and S. W. Scheff (1990). "Synapse loss in frontal cortex biopsies in Alzheimer's disease: correlation with cognitive severity." Ann Neurol **27**(5): 457-464.

DeMattos, R. B., J. R. Cirrito, M. Parsadanian, P. C. May, M. A. O'Dell, J. W. Taylor, J. A. Harmony, B. J. Aronow, K. R. Bales, S. M. Paul and D. M. Holtzman (2004). "ApoE and clusterin cooperatively suppress Abeta levels and deposition: evidence that ApoE regulates extracellular Abeta metabolism in vivo." Neuron **41**(2): 193-202.

Dodiya, H. B., T. Kuntz, S. M. Shaik, C. Baufeld, J. Leibowitz, X. Zhang, N. Gottel, X. Zhang, O. Butovsky, J. A. Gilbert and S. S. Sisodia (2019). "Sex-specific effects of microbiome perturbations on cerebral Abeta amyloidosis and microglia phenotypes." J Exp Med **216**(7): 1542-1560.

Doecke, J. D., S. M. Laws, N. G. Faux, W. Wilson, S. C. Burnham, C. P. Lam, A. Mondal, J. Bedo, A. I. Bush, B. Brown, K. De Ruyck, K. A. Ellis, C. Fowler, V. B. Gupta, R. Head, S. L. Macaulay, K. Pertile, C. C. Rowe, A. Rembach, M. Rodrigues, R. Rumble, C. Szoeke, K. Taddei, T. Taddei, B. Trounson, D. Ames, C. L. Masters, R. N. Martins, I. Alzheimer's Disease Neuroimaging, B. Australian Imaging and G. Lifestyle Research (2012). "Blood-based protein biomarkers for diagnosis of Alzheimer disease." Arch Neurol **69**(10): 1318-1325.

Dominguez-Bello, M. G., E. K. Costello, M. Contreras, M. Magris, G. Hidalgo, N. Fierer and R. Knight (2010). "Delivery mode shapes the acquisition and structure of the initial microbiota across multiple body habitats in newborns." Proc Natl Acad Sci U S A **107**(26): 11971-11975.

Dominy, S. S., C. Lynch, F. Ermini, M. Benedyk, A. Marczyk, A. Konradi, M. Nguyen, U. Haditsch, D. Raha, C. Griffin, L. J. Holsinger, S. Arastu-Kapur, S. Kaba, A. Lee, M. I. Ryder, B. Potempa, P. Mydel, A. Hellvard, K. Adamowicz, H. Hasturk, G. D. Walker, E. C. Reynolds, R. L. M. Faull, M. A. Curtis, M. Dragunow and J. Potempa (2019). "Porphyromonas gingivalis in Alzheimer's disease brains: Evidence for disease causation and treatment with small-molecule inhibitors." Sci Adv **5**(1): eaau3333.

Douglas, G. M., V. J. Maffei, J. R. Zaneveld, S. N. Yurgel, J. R. Brown, C. M. Taylor, C. Huttenhower and M. G. I. Langille (2020). "PICRUSt2 for prediction of metagenome functions." Nature Biotechnology **38**(6): 685-688.

Douzandeh-Mobarrez, B. and A. Kariminik (2019). "Gut Microbiota and IL-17A: Physiological and Pathological Responses." Probiotics Antimicrob Proteins **11**(1): 1-10.

Drummond, R. A., J. V. Desai, E. E. Ricotta, M. Swamydas, C. Deming, S. Conlan, M. Quinones, V. Matei-Rascu, L. Sherif, D. Lecky, C. R. Lee, N. M. Green, N. Collins, A.

M. Zelazny, D. R. Prevots, D. Bending, D. Withers, Y. Belkaid, J. A. Segre and M. S. Lionakis (2022). "Long-term antibiotic exposure promotes mortality after systemic fungal infection by driving lymphocyte dysfunction and systemic escape of commensal bacteria." Cell Host Microbe **30**(7): 1020-1033 e1026.

Dunham, S. J. B., K. A. McNair, E. D. Adams, J. Avelar-Barragan, S. Forner, M. Mapstone and K. L. Whiteson (2022). "Longitudinal Analysis of the Microbiome and Metabolome in the 5xfAD Mouse Model of Alzheimer's Disease." mBio **13**(6): e0179422.

Dupraz, L., A. Magniez, N. Rolhion, M. L. Richard, G. Da Costa, S. Touch, C. Mayeur, J. Planchais, A. Agus, C. Danne, C. Michaudel, M. Spatz, F. Trottein, P. Langella, H. Sokol and M. L. Michel (2021). "Gut microbiota-derived short-chain fatty acids regulate IL-17 production by mouse and human intestinal gammadelta T cells." Cell Rep **36**(1): 109332.

el Marjou, F., K. P. Janssen, B. H. Chang, M. Li, V. Hindie, L. Chan, D. Louvard, P. Chambon, D. Metzger and S. Robine (2004). "Tissue-specific and inducible Cre-mediated recombination in the gut epithelium." Genesis **39**(3): 186-193.

Erny, D., N. Dokalis, C. Mezo, A. Castoldi, O. Mossad, O. Staszewski, M. Frosch, M. Villa, V. Fuchs, A. Mayer, J. Neuber, J. Sosat, S. Tholen, O. Schilling, A. Vlachos, T. Blank, M. Gomez de Aguero, A. J. Macpherson, E. J. Pearce and M. Prinz (2021). "Microbiota-derived acetate enables the metabolic fitness of the brain innate immune system during health and disease." Cell Metab **33**(11): 2260-2276 e2267.

Erny, D., A. L. Hrabe de Angelis, D. Jaitin, P. Wieghofer, O. Staszewski, E. David, H. Keren-Shaul, T. Mahlakoiv, K. Jakobshagen, T. Buch, V. Schwierzeck, O. Utermohlen, E. Chun, W. S. Garrett, K. D. McCoy, A. Diefenbach, P. Staeheli, B. Stecher, I. Amit and M. Prinz (2015). "Host microbiota constantly control maturation and function of microglia in the CNS." Nat Neurosci **18**(7): 965-977.

Esplugues, E., S. Huber, N. Gagliani, A. E. Hauser, T. Town, Y. Y. Wan, W. O'Connor, Jr., A. Rongvaux, N. Van Rooijen, A. M. Haberman, Y. Iwakura, V. K. Kuchroo, J. K. Kolls, J. A. Bluestone, K. C. Herold and R. A. Flavell (2011). "Control of TH17 cells occurs in the small intestine." Nature **475**(7357): 514-518.

Fabi, J. P. (2024). "The connection between gut microbiota and its metabolites with neurodegenerative diseases in humans." Metab Brain Dis **39**(5): 967-984.

Fabi, J. P. (2024). "The connection between gut microbiota and its metabolites with neurodegenerative diseases in humans." Metab Brain Dis.

Fang, P., S. A. Kazmi, K. G. Jameson and E. Y. Hsiao (2020). "The Microbiome as a Modifier of Neurodegenerative Disease Risk." Cell Host Microbe **28**(2): 201-222.

Farris, W., S. Mansourian, M. A. Leissring, E. A. Eckman, L. Bertram, C. B. Eckman, R. E. Tanzi and D. J. Selkoe (2004). "Partial loss-of-function mutations in insulin-degrading enzyme that induce diabetes also impair degradation of amyloid beta-protein." Am J Pathol **164**(4): 1425-1434.

Fassbender, K., S. Walter, S. Kuhl, R. Landmann, K. Ishii, T. Bertsch, A. K. Stalder, F. Muehlhauser, Y. Liu, A. J. Ulmer, S. Rivest, A. Lentschat, E. Gulbins, M. Jucker, M. Staufenbiel, K. Brechtel, J. Walter, G. Multhaup, B. Penke, Y. Adachi, T. Hartmann and

K. Beyreuther (2004). "The LPS receptor (CD14) links innate immunity with Alzheimer's disease." FASEB J **18**(1): 203-205.

Fishman, R. A. (2002). "The cerebrospinal fluid production rate is reduced in dementia of the Alzheimer's type." Neurology **58**(12): 1866; author reply 1866.

Frohlich, E. E., A. Farzi, R. Mayerhofer, F. Reichmann, A. Jacan, B. Wagner, E. Zinser, N. Bordag, C. Magnes, E. Frohlich, K. Kashofer, G. Gorkiewicz and P. Holzer (2016). "Cognitive impairment by antibiotic-induced gut dysbiosis: Analysis of gut microbiota-brain communication." Brain Behav Immun **56**: 140-155.

Fruhwurth, S., H. Zetterberg and S. R. Paludan (2024). "Microglia and amyloid plaque formation in Alzheimer's disease - Evidence, possible mechanisms, and future challenges." J Neuroimmunol **390**: 578342.

Fujino, S., A. Andoh, S. Bamba, A. Ogawa, K. Hata, Y. Araki, T. Bamba and Y. Fujiyama (2003). "Increased expression of interleukin 17 in inflammatory bowel disease." Gut **52**(1): 65-70.

Gao, L., Y. Zhang, K. Sterling and W. Song (2022). "Brain-derived neurotrophic factor in Alzheimer's disease and its pharmaceutical potential." Translational Neurodegeneration **11**(1): 4.

Gautam, A. S., C. B. Pulivarthi and R. K. Singh (2023). "Proinflammatory IL-17 levels in serum/cerebrospinal fluid of patients with neurodegenerative diseases: a meta-analysis study." Naunyn Schmiedebergs Arch Pharmacol **396**(3): 577-588.

Goulay, R., L. Mena Romo, E. M. Hol and R. M. Dijkhuizen (2020). "From Stroke to Dementia: a Comprehensive Review Exposing Tight Interactions Between Stroke and Amyloid-beta Formation." Transl Stroke Res **11**(4): 601-614.

Grabrucker, S., M. Marizzoni, E. Silajdzic, N. Lopizzo, E. Mombelli, S. Nicolas, S. Dohm-Hansen, C. Scassellati, D. V. Moretti, M. Rosa, K. Hoffmann, J. F. Cryan, O. F. O'Leary, J. A. English, A. Lavelle, C. O'Neill, S. Thuret, A. Cattaneo and Y. M. Nolan (2023). "Microbiota from Alzheimer's patients induce deficits in cognition and hippocampal neurogenesis." Brain **146**(12): 4916-4934.

Haass, C. and D. J. Selkoe (2007). "Soluble protein oligomers in neurodegeneration: lessons from the Alzheimer's amyloid beta-peptide." Nat Rev Mol Cell Biol **8**(2): 101-112.

Haass, C. and M. Willem (2019). "Secreted APP Modulates Synaptic Activity: A Novel Target for Therapeutic Intervention?" Neuron **101**(4): 557-559.

Hamada, H., L. Garcia-Hernandez Mde, J. B. Reome, S. K. Misra, T. M. Strutt, K. K. McKinstry, A. M. Cooper, S. L. Swain and R. W. Dutton (2009). "Tc17, a unique subset of CD8 T cells that can protect against lethal influenza challenge." J Immunol **182**(6): 3469-3481.

Hamby, M. E. and M. V. Sofroniew (2010). "Reactive astrocytes as therapeutic targets for CNS disorders." Neurotherapeutics **7**(4): 494-506.

Hao, W., Y. Decker, L. Schnoder, A. Schottek, D. Li, M. D. Menger, K. Fassbender and Y. Liu (2016). "Deficiency of IkappaB Kinase beta in Myeloid Cells Reduces Severity of Experimental Autoimmune Encephalomyelitis." Am J Pathol **186**(5): 1245-1257.

Hao, W., Y. Liu, S. Liu, S. Walter, M. O. Grimm, A. J. Kiliaan, B. Penke, T. Hartmann, C. E. Rube, M. D. Menger and K. Fassbender (2011). "Myeloid differentiation factor 88-deficient bone marrow cells improve Alzheimer's disease-related symptoms and pathology." Brain **134**(Pt 1): 278-292.

Hao, W., Q. Luo, M. D. Menger, K. Fassbender and Y. Liu (2021). "Treatment With CD52 Antibody Protects Neurons in Experimental Autoimmune Encephalomyelitis Mice During the Recovering Phase." Front Immunol **12**: 792465.

Harach, T., N. Marungruang, N. Duthilleul, V. Cheatham, K. D. Mc Coy, G. Frisoni, J. J. Neher, F. Fak, M. Jucker, T. Lasser and T. Bolmont (2017). "Reduction of Abeta amyloid pathology in APPPS1 transgenic mice in the absence of gut microbiota." Sci Rep **7**: 41802.

He, P., Z. Zhong, K. Lindholm, L. Berning, W. Lee, C. Lemere, M. Staufenbiel, R. Li and Y. Shen (2007). "Deletion of tumor necrosis factor death receptor inhibits amyloid beta generation and prevents learning and memory deficits in Alzheimer's mice." J Cell Biol **178**(5): 829-841.

Heckmann, B. L., B. J. W. Teubner, B. Tummers, E. Boada-Romero, L. Harris, M. Yang, C. S. Guy, S. S. Zakharenko and D. R. Green (2019). "LC3-Associated Endocytosis Facilitates beta-Amyloid Clearance and Mitigates Neurodegeneration in Murine Alzheimer's Disease." Cell **178**(3): 536-551 e514.

Heneka, M. T., M. J. Carson, J. El Khoury, G. E. Landreth, F. Brosseron, D. L. Feinstein, A. H. Jacobs, T. Wyss-Coray, J. Vitorica, R. M. Ransohoff, K. Herrup, S. A. Frautschy, B. Finsen, G. C. Brown, A. Verkhratsky, K. Yamanaka, J. Koistinaho, E. Latz, A. Halle, G. C. Petzold, T. Town, D. Morgan, M. L. Shinohara, V. H. Perry, C. Holmes, N. G. Bazan, D. J. Brooks, S. Hunot, B. Joseph, N. Deigendesch, O. Garaschuk, E. Boddeke, C. A. Dinarello, J. C. Breitner, G. M. Cole, D. T. Golenbock and M. P. Kummer (2015). "Neuroinflammation in Alzheimer's disease." Lancet Neurol **14**(4): 388-405.

Hickman, S. E., E. K. Allison and J. El Khoury (2008). "Microglial dysfunction and defective beta-amyloid clearance pathways in aging Alzheimer's disease mice." J Neurosci **28**(33): 8354-8360.

Huang, J. Y., D. M. Hafez, B. D. James, D. A. Bennett and R. A. Marr (2012). "Altered NEP2 expression and activity in mild cognitive impairment and Alzheimer's disease." J Alzheimers Dis **28**(2): 433-441.

Huang, W., L. Na, P. L. Fidel and P. Schwarzenberger (2004). "Requirement of interleukin-17A for systemic anti-Candida albicans host defense in mice." J Infect Dis **190**(3): 624-631.

Hur, J.-Y., G. R. Frost, X. Wu, C. Crump, S. J. Pan, E. Wong, M. Barros, T. Li, P. Nie, Y. Zhai, J. C. Wang, J. Tcw, L. Guo, A. McKenzie, C. Ming, X. Zhou, M. Wang, Y. Sagi, A. E. Renton, B. T. Esposito, Y. Kim, K. R. Sadleir, I. Trinh, R. A. Rissman, R. Vassar, B. Zhang, D. S. Johnson, E. Masliah, P. Greengard, A. Goate and Y.-M. Li (2020). "The innate immunity protein IFITM3 modulates γ-secretase in Alzheimer's disease." Nature **586**(7831): 735-740.

Iliff, J. J., M. Wang, Y. Liao, B. A. Plogg, W. Peng, G. A. Gundersen, H. Benveniste, G. E. Vates, R. Deane, S. A. Goldman, E. A. Nagelhus and M. Nedergaard (2012). "A paravascular pathway facilitates CSF flow through the brain parenchyma and the

clearance of interstitial solutes, including amyloid beta." Sci Transl Med **4**(147): 147ra111.

Ito, S., S. Ohtsuki, J. Kamiie, Y. Nezu and T. Terasaki (2007). "Cerebral clearance of human amyloid-beta peptide (1-40) across the blood-brain barrier is reduced by self-aggregation and formation of low-density lipoprotein receptor-related protein-1 ligand complexes." J Neurochem **103**(6): 2482-2490.

Iwata, N., S. Tsubuki, Y. Takaki, K. Shirotani, B. Lu, N. P. Gerard, C. Gerard, E. Hama, H. J. Lee and T. C. Saido (2001). "Metabolic regulation of brain Abeta by neprilysin." Science **292**(5521): 1550-1552.

Jensen, J. C. and R. Gugler (1983). "Single- and multiple-dose metronidazole kinetics." Clin Pharmacol Ther **34**(4): 481-487.

Ji, X. R., K. C. Cheng, Y. R. Chen, T. Y. Lin, C. H. A. Cheung, C. L. Wu and H. C. Chiang (2018). "Dysfunction of different cellular degradation pathways contributes to specific beta-amyloid42-induced pathologies." FASEB J **32**(3): 1375-1387.

Kanehisa, M. and S. Goto (2000). "KEGG: kyoto encyclopedia of genes and genomes." Nucleic Acids Res **28**(1): 27-30.

Kang, D. E., C. U. Pietrzik, L. Baum, N. Chevallier, D. E. Merriam, M. Z. Kounnas, S. L. Wagner, J. C. Troncoso, C. H. Kawas, R. Katzman and E. H. Koo (2000). "Modulation of amyloid beta-protein clearance and Alzheimer's disease susceptibility by the LDL receptor-related protein pathway." J Clin Invest **106**(9): 1159-1166.

Kant, S., E. G. Stopa, C. E. Johanson, A. Baird and G. D. Silverberg (2018). "Choroid plexus genes for CSF production and brain homeostasis are altered in Alzheimer's disease." Fluids Barriers CNS **15**(1): 34.

Kaur, H., S. Nookala, S. Singh, S. Mukundan, K. Nagamoto-Combs and C. K. Combs (2021). "Sex-Dependent Effects of Intestinal Microbiome Manipulation in a Mouse Model of Alzheimer's Disease." Cells **10**(9).

Keller, J. N., K. B. Hanni and W. R. Markesbery (2000). "Impaired proteasome function in Alzheimer's disease." J Neurochem **75**(1): 436-439.

Keren-Shaul, H., A. Spinrad, A. Weiner, O. Matcovitch-Natan, R. Dvir-Szternfeld, T. K. Ulland, E. David, K. Baruch, D. Lara-Astaiso, B. Toth, S. Itzkovitz, M. Colonna, M. Schwartz and I. Amit (2017). "A Unique Microglia Type Associated with Restricting Development of Alzheimer's Disease." Cell **169**(7): 1276-1290 e1217.

Kierdorf, K., D. Erny, T. Goldmann, V. Sander, C. Schulz, E. G. Perdiguero, P. Wieghofer, A. Heinrich, P. Riemke, C. Holscher, D. N. Muller, B. Luckow, T. Brocker, K. Debowski, G. Fritz, G. Opdenakker, A. Diefenbach, K. Biber, M. Heikenwalder, F. Geissmann, F. Rosenbauer and M. Prinz (2013). "Microglia emerge from erythromyeloid precursors via Pu.1- and Irf8-dependent pathways." Nat Neurosci **16**(3): 273-280.

Knopman, D. S., H. Amieva, R. C. Petersen, G. Chetelat, D. M. Holtzman, B. T. Hyman, R. A. Nixon and D. T. Jones (2021). "Alzheimer disease." Nat Rev Dis Primers **7**(1): 33.

Krohn, M., C. Lange, J. Hofrichter, K. Scheffler, J. Stenzel, J. Steffen, T. Schumacher, T. Bruning, A. S. Plath, F. Alfen, A. Schmidt, F. Winter, K. Rateitschak, A. Wree, J. Gsponer, L. C. Walker and J. Pahnke (2011). "Cerebral amyloid-beta proteostasis is

regulated by the membrane transport protein ABCC1 in mice." J Clin Invest **121**(10): 3924-3931.

Krzyzanowska, A. and E. Carro (2012). "Pathological alteration in the choroid plexus of Alzheimer's disease: implication for new therapy approaches." Front Pharmacol **3**: 75.

Kuhnke, D., G. Jedlitschky, M. Grube, M. Krohn, M. Jucker, I. Mosyagin, I. Cascorbi, L. C. Walker, H. K. Kroemer, R. W. Warzok and S. Vogelgesang (2007). "MDR1-P-Glycoprotein (ABCB1) Mediates Transport of Alzheimer's amyloid-beta peptides--implications for the mechanisms of Abeta clearance at the blood-brain barrier." Brain Pathol **17**(4): 347-353.

Lathe, R., N. M. Schultek, B. J. Balin, G. D. Ehrlich, L. A. Auber, G. Perry, E. B. Breitschwerdt, D. B. Corry, R. L. Doty, R. A. Rissman, P. L. Nara, R. Itzhaki, W. A. Eimer, R. E. Tanzi and C. Intracell Research Group Consortium (2023). "Establishment of a consensus protocol to explore the brain pathobiome in patients with mild cognitive impairment and Alzheimer's disease: Research outline and call for collaboration." Alzheimers Dement **19**(11): 5209-5231.

Lau, S. F., W. Wu, H. Seo, A. K. Y. Fu and N. Y. Ip (2021). "Quantitative in vivo assessment of amyloid-beta phagocytic capacity in an Alzheimer's disease mouse model." STAR Protoc **2**(1): 100265.

Lee, J., V. R. Venna, D. J. Durgan, H. Shi, J. Hudobenko, N. Putluri, J. Petrosino, L. D. McCullough and R. M. Bryan (2020). "Young versus aged microbiota transplants to germ-free mice: increased short-chain fatty acids and improved cognitive performance." Gut Microbes **12**(1): 1-14.

Lee, J. S., R. X. Wang, E. E. Alexeev and S. P. Colgan (2021). "Intestinal Inflammation as a Dysbiosis of Energy Procurement: New Insights into an Old Topic." Gut Microbes **13**(1): 1-20.

Lee, Y. K., J. S. Menezes, Y. Umesaki and S. K. Mazmanian (2011). "Proinflammatory T-cell responses to gut microbiota promote experimental autoimmune encephalomyelitis." Proc Natl Acad Sci U S A **108 Suppl 1**(Suppl 1): 4615-4622.

Leissring, M. A., W. Farris, A. Y. Chang, D. M. Walsh, X. Wu, X. Sun, M. P. Frosch and D. J. Selkoe (2003). "Enhanced proteolysis of beta-amyloid in APP transgenic mice prevents plaque formation, secondary pathology, and premature death." Neuron **40**(6): 1087-1093.

Leng, F. and P. Edison (2021). "Neuroinflammation and microglial activation in Alzheimer disease: where do we go from here?" Nat Rev Neurol **17**(3): 157-172.

Li, X., Y. Li, Y. Jin, Y. Zhang, J. Wu, Z. Xu, Y. Huang, L. Cai, S. Gao, T. Liu, F. Zeng, Y. Wang, W. Wang, T. F. Yuan, H. Tian, Y. Shu, F. Guo, W. Lu, Y. Mao, X. Mei, Y. Rao and B. Peng (2023). "Transcriptional and epigenetic decoding of the microglial aging process." Nat Aging **3**(10): 1288-1311.

Li, Y., J. Dong, H. Xiao, S. Zhang, B. Wang, M. Cui and S. Fan (2020). "Gut commensal derived-valeric acid protects against radiation injuries." Gut Microbes **11**(4): 789-806.

Liu, P., L. Wu, G. Peng, Y. Han, R. Tang, J. Ge, L. Zhang, L. Jia, S. Yue, K. Zhou, L. Li, B. Luo and B. Wang (2019). "Altered microbiomes distinguish Alzheimer's disease from amnestic mild cognitive impairment and health in a Chinese cohort." Brain Behav Immun **80**: 633-643.

Liu, S., A. P. da Cunha, R. M. Rezende, R. Cialic, Z. Wei, L. Bry, L. E. Comstock, R. Gandhi and H. L. Weiner (2016). "The Host Shapes the Gut Microbiota via Fecal MicroRNA." Cell Host Microbe **19**(1): 32-43.

Liu, S., Y. Liu, W. Hao, L. Wolf, A. J. Kiliaan, B. Penke, C. E. Rube, J. Walter, M. T. Heneka, T. Hartmann, M. D. Menger and K. Fassbender (2012). "TLR2 is a primary receptor for Alzheimer's amyloid beta peptide to trigger neuroinflammatory activation." J Immunol **188**(3): 1098-1107.

Liu, S., R. M. Rezende, T. G. Moreira, S. K. Tankou, L. M. Cox, M. Wu, A. Song, F. H. Dhang, Z. Wei, G. Costamagna and H. L. Weiner (2019). "Oral Administration of miR-30d from Feces of MS Patients Suppresses MS-like Symptoms in Mice by Expanding Akkermansia muciniphila." Cell Host Microbe **26**(6): 779-794 e778.

Liu, Y., X. Liu, W. Hao, Y. Decker, R. Schomburg, L. Fulop, M. Pasparakis, M. D. Menger and K. Fassbender (2014). "IKKbeta deficiency in myeloid cells ameliorates Alzheimer's disease-related symptoms and pathology." J Neurosci **34**(39): 12982-12999.

Liu, Y., S. Walter, M. Stagi, D. Cherny, M. Letiembre, W. Schulz-Schaeffer, H. Heine, B. Penke, H. Neumann and K. Fassbender (2005). "LPS receptor (CD14): a receptor for phagocytosis of Alzheimer's amyloid peptide." Brain **128**(Pt 8): 1778-1789.

Loeffler, D. A. (2024). "Approaches for Increasing Cerebral Efflux of Amyloid-beta in Experimental Systems." J Alzheimers Dis.

Loeffler, D. A. (2024). "Enhancing of cerebral Abeta clearance by modulation of ABC transporter expression: a review of experimental approaches." Front Aging Neurosci **16**: 1368200.

Long, J. M. and D. M. Holtzman (2019). "Alzheimer Disease: An Update on Pathobiology and Treatment Strategies." Cell **179**(2): 312-339.

Lu, Y., P. Zhang, F. Xu, Y. Zheng and H. Zhao (2023). "Advances in the study of IL-17 in neurological diseases and mental disorders." Front Neurol **14**: 1284304.

Lucin, K. M., C. E. O'Brien, G. Bieri, E. Czirr, K. I. Mosher, R. J. Abbey, D. F. Mastroeni, J. Rogers, B. Spencer, E. Masliah and T. Wyss-Coray (2013). "Microglial beclin 1 regulates retromer trafficking and phagocytosis and is impaired in Alzheimer's disease." Neuron **79**(5): 873-886.

Luo, Q., L. Schnoder, W. Hao, K. Litzenburger, Y. Decker, I. Tomic, M. D. Menger, Y. Liu and K. Fassbender (2022). "p38alpha-MAPK-deficient myeloid cells ameliorate symptoms and pathology of APP-transgenic Alzheimer's disease mice." Aging Cell **21**(8): e13679.

Lv, Y., C. Zhen, A. Liu, Y. Hu, G. Yang, C. Xu, Y. Lou, Q. Cheng, Y. Luo, J. Yu, Y. Fang, H. Zhao, K. Peng, Y. Yu, J. Lou, J. Chen and Y. Ni (2024). "Profiles and interactions of gut microbiome and intestinal microRNAs in pediatric Crohn's disease." mSystems **9**(9): e0078324.

Ma, C., Y. Li, Z. Mei, C. Yuan, J. H. Kang, F. Grodstein, A. Ascherio, W. C. Willett, A. T. Chan, C. Huttenhower, M. J. Stampfer and D. D. Wang (2023). "Association Between Bowel Movement Pattern and Cognitive Function: Prospective Cohort Study and a Metagenomic Analysis of the Gut Microbiome." Neurology **101**(20): e2014-e2025.

Madry, C., V. Kyrargyri, I. L. Arancibia-Carcamo, R. Jolivet, S. Kohsaka, R. M. Bryan and D. Attwell (2018). "Microglial Ramification, Surveillance, and Interleukin-1beta Release Are Regulated by the Two-Pore Domain K(+) Channel THIK-1." Neuron **97**(2): 299-312 e296.

Majumder, S. and M. J. McGeachy (2021). "IL-17 in the Pathogenesis of Disease: Good Intentions Gone Awry." Annu Rev Immunol **39**: 537-556.

Marizzoni, M., P. Mirabelli, E. Mombelli, L. Coppola, C. Festari, N. Lopizzo, D. Luongo, M. Mazzelli, D. Naviglio, J. L. Blouin, M. Abramowicz, M. Salvatore, M. Pievani, A. Cattaneo and G. B. Frisoni (2023). "A peripheral signature of Alzheimer's disease featuring microbiota-gut-brain axis markers." Alzheimers Res Ther **15**(1): 101.

Marr, R. A., E. Rockenstein, A. Mukherjee, M. S. Kindy, L. B. Hersh, F. H. Gage, I. M. Verma and E. Masliah (2003). "Neprilysin gene transfer reduces human amyloid pathology in transgenic mice." J Neurosci **23**(6): 1992-1996.

Meyer, K., A. Lulla, K. Debroy, J. M. Shikany, K. Yaffe, O. Meirelles and L. J. Launer (2022). "Association of the Gut Microbiota With Cognitive Function in Midlife." JAMA Netw Open **5**(2): e2143941.

Mezo, C., N. Dokalis, O. Mossad, O. Staszewski, J. Neuber, B. Yilmaz, D. Schnepf, M. G. de Aguero, S. C. Ganal-Vonarburg, A. J. Macpherson, M. Meyer-Luehmann, P. Staeheli, T. Blank, M. Prinz and D. Erny (2020). "Different effects of constitutive and induced microbiota modulation on microglia in a mouse model of Alzheimer's disease." Acta Neuropathol Commun **8**(1): 119.

Michaud, J. P., M. Halle, A. Lampron, P. Theriault, P. Prefontaine, M. Filali, P. Tribout-Jover, A. M. Lanteigne, R. Jodoin, C. Cluff, V. Brichard, R. Palmantier, A. Pilorget, D. Larocque and S. Rivest (2013). "Toll-like receptor 4 stimulation with the detoxified ligand monophosphoryl lipid A improves Alzheimer's disease-related pathology." Proc Natl Acad Sci U S A **110**(5): 1941-1946.

Mills, K. H. G. (2023). "IL-17 and IL-17-producing cells in protection versus pathology." Nat Rev Immunol **23**(1): 38-54.

Minter, M. R., R. Hinterleitner, M. Meisel, C. Zhang, V. Leone, X. Zhang, P. Oyler-Castrillo, X. Zhang, M. W. Musch, X. Shen, B. Jabri, E. B. Chang, R. E. Tanzi and S. S. Sisodia (2017). "Antibiotic-induced perturbations in microbial diversity during post-natal development alters amyloid pathology in an aged APP(SWE)/PS1(DeltaE9) murine model of Alzheimer's disease." Sci Rep **7**(1): 10411.

Minter, M. R., R. Hinterleitner, M. Meisel, C. Zhang, V. Leone, X. Zhang, P. Oyler-Castrillo, X. Zhang, M. W. Musch, X. Shen, B. Jabri, E. B. Chang, R. E. Tanzi and S. S. Sisodia (2017). "Antibiotic-induced perturbations in microbial diversity during post-natal development alters amyloid pathology in an aged APPSWE/PS1DeltaE9 murine model of Alzheimer's disease." Sci Rep **7**(1): 10411.

Minter, M. R., C. Zhang, V. Leone, D. L. Ringus, X. Zhang, P. Oyler-Castrillo, M. W. Musch, F. Liao, J. F. Ward, D. M. Holtzman, E. B. Chang, R. E. Tanzi and S. S. Sisodia (2016). "Antibiotic-induced perturbations in gut microbial diversity influences neuro-inflammation and amyloidosis in a murine model of Alzheimer's disease." Sci Rep **6**: 30028.

Mone, Y., J. P. Earl, J. E. Krol, A. Ahmed, B. Sen, G. D. Ehrlich and J. R. Lapides (2023). "Evidence supportive of a bacterial component in the etiology for Alzheimer's disease and for a temporal-spatial development of a pathogenic microbiome in the brain." Front Cell Infect Microbiol **13**: 1123228.

Morris, A. W., R. O. Carare, S. Schreiber and C. A. Hawkes (2014). "The Cerebrovascular Basement Membrane: Role in the Clearance of beta-amyloid and Cerebral Amyloid Angiopathy." Front Aging Neurosci **6**: 251.

Muller, U. C., T. Deller and M. Korte (2017). "Not just amyloid: physiological functions of the amyloid precursor protein family." Nat Rev Neurosci **18**(5): 281-298.

Murray, E. R., M. Kemp and T. T. Nguyen (2022). "The Microbiota-Gut-Brain Axis in Alzheimer's Disease: A Review of Taxonomic Alterations and Potential Avenues for Interventions." Arch Clin Neuropsychol **37**(3): 595-607.

Nakae, S., Y. Komiyama, A. Nambu, K. Sudo, M. Iwase, I. Homma, K. Sekikawa, M. Asano and Y. Iwakura (2002). "Antigen-specific T cell sensitization is impaired in IL-17-deficient mice, causing suppression of allergic cellular and humoral responses." Immunity **17**(3): 375-387.

Nalivaeva, N. N., N. D. Belyaev, C. Kerridge and A. J. Turner (2014). "Amyloid-clearing proteins and their epigenetic regulation as a therapeutic target in Alzheimer's disease." Front Aging Neurosci **6**: 235.

Nalivaeva, N. N., N. D. Belyaev, I. A. Zhuravin and A. J. Turner (2012). "The Alzheimer's amyloid-degrading peptidase, neprilysin: can we control it?" Int J Alzheimers Dis **2012**: 383796.

Nalivaevaa, N. N., L. Fisk, E. G. Kochkina, S. A. Plesneva, I. A. Zhuravin, E. Babusikova, D. Dobrota and A. J. Turner (2004). "Effect of hypoxia/ischemia and hypoxic preconditioning/reperfusion on expression of some amyloid-degrading enzymes." Ann N Y Acad Sci **1035**: 21-33.

O'Neill, L. A., D. Golenbock and A. G. Bowie (2013). "The history of Toll-like receptors - redefining innate immunity." Nat Rev Immunol **13**(6): 453-460.

Olmos-Alonso, A., S. T. Schetters, S. Sri, K. Askew, R. Mancuso, M. Vargas-Caballero, C. Holscher, V. H. Perry and D. Gomez-Nicola (2016). "Pharmacological targeting of CSF1R inhibits microglial proliferation and prevents the progression of Alzheimer's-like pathology." Brain **139**(Pt 3): 891-907.

Ortega, M. A., M. A. Alvarez-Mon, C. Garcia-Montero, O. Fraile-Martinez, J. Monserrat, L. Martinez-Rozas, R. Rodriguez-Jimenez, M. Alvarez-Mon and G. Lahera (2023). "Microbiota-gut-brain axis mechanisms in the complex network of bipolar disorders: potential clinical implications and translational opportunities." Mol Psychiatry **28**(7): 2645-2673.

Osgood, D., M. C. Miller, A. A. Messier, L. Gonzalez and G. D. Silverberg (2017). "Aging alters mRNA expression of amyloid transporter genes at the blood-brain barrier." Neurobiol Aging **57**: 178-185.

Panza, F., M. Lozupone, V. Solfrizzi, M. Watling and B. P. Imbimbo (2019). "Time to test antibacterial therapy in Alzheimer's disease." Brain **142**(10): 2905-2929.

Parums, D. V. (2024). "A Review of the Current Status of Disease-Modifying Therapies and Prevention of Alzheimer's Disease." Med Sci Monit **30**: e945091.

Patel, A. G., P. N. Nehete, S. R. Krivoshik, X. Pei, E. L. Cho, B. P. Nehete, M. D. Ramani, Y. Shao, L. E. Williams, T. Wisniewski and H. Scholtzova (2021). "Innate immunity stimulation via CpG oligodeoxynucleotides ameliorates Alzheimer's disease pathology in aged squirrel monkeys." Brain **144**(7): 2146-2165.

Preston, S. D., P. V. Steart, A. Wilkinson, J. A. Nicoll and R. O. Weller (2003). "Capillary and arterial cerebral amyloid angiopathy in Alzheimer's disease: defining the perivascular route for the elimination of amyloid beta from the human brain." Neuropathol Appl Neurobiol **29**(2): 106-117.

Puel, A., S. Cypowyj, J. Bustamante, J. F. Wright, L. Liu, H. K. Lim, M. Migaud, L. Israel, M. Chrabieh, M. Audry, M. Gumbleton, A. Toulon, C. Bodemer, J. El-Baghdadi, M. Whitters, T. Paradis, J. Brooks, M. Collins, N. M. Wolfman, S. Al-Muhsen, M. Galicchio, L. Abel, C. Picard and J. L. Casanova (2011). "Chronic mucocutaneous candidiasis in humans with inborn errors of interleukin-17 immunity." Science **332**(6025): 65-68.

Qin, Y., Y. Liu, W. Hao, Y. Decker, I. Tomic, M. D. Menger, C. Liu and K. Fassbender (2016). "Stimulation of TLR4 Attenuates Alzheimer's Disease-Related Symptoms and Pathology in Tau-Transgenic Mice." J Immunol **197**(8): 3281-3292.

Qosa, H., B. S. Abuasal, I. A. Romero, B. Weksler, P. O. Couraud, J. N. Keller and A. Kaddoumi (2014). "Differences in amyloid-beta clearance across mouse and human blood-brain barrier models: kinetic analysis and mechanistic modeling." Neuropharmacology **79**: 668-678.

Quan, W., Q. Luo, W. Hao, I. Tomic, T. Furihata, W. Schulz-Schaffer, M. D. Menger, K. Fassbender and Y. Liu (2021). "Haploinsufficiency of microglial MyD88 ameliorates Alzheimer's pathology and vascular disorders in APP/PS1-transgenic mice." Glia **69**(8): 1987-2005.

Quigley, E. M. M. (2017). "Microbiota-Brain-Gut Axis and Neurodegenerative Diseases." Curr Neurol Neurosci Rep **17**(12): 94.

Radde, R., T. Bolmont, S. A. Kaeser, J. Coomaraswamy, D. Lindau, L. Stoltze, M. E. Calhoun, F. Jaggi, H. Wolburg, S. Gengler, C. Haass, B. Ghetti, C. Czech, C. Holscher, P. M. Mathews and M. Jucker (2006). "Abeta42-driven cerebral amyloidosis in transgenic mice reveals early and robust pathology." EMBO Rep **7**(9): 940-946.

Rakusa, E., A. Fink, G. Tamguney, M. T. Heneka and G. Doblhammer (2023). "Sporadic Use of Antibiotics in Older Adults and the Risk of Dementia: A Nested Case-Control Study Based on German Health Claims Data." J Alzheimers Dis **93**(4): 1329-1339.

Redzic, Z. B., J. E. Preston, J. A. Duncan, A. Chodobski and J. Szmydynger-Chodobska (2005). "The choroid plexus-cerebrospinal fluid system: from development to aging." Curr Top Dev Biol **71**: 1-52.

Regen, T., S. Isaac, A. Amorim, N. G. Nunez, J. Hauptmann, A. Shanmugavadivu, M. Klein, R. Sankowski, I. A. Mufazalov, N. Yogev, J. Huppert, F. Wanke, M. Witting, A. Grill, E. J. C. Galvez, A. Nikolaev, M. Blanfeld, I. Prinz, P. Schmitt-Kopplin, T. Strowig, C. Reinhardt, M. Prinz, T. Bopp, B. Becher, C. Ubeda and A. Waisman (2021). "IL-17

controls central nervous system autoimmunity through the intestinal microbiome." Sci Immunol **6**(56).

Regen, T., S. Isaac, A. Amorim, N. G. Núñez, J. Hauptmann, A. Shanmugavadivu, M. Klein, R. Sankowski, I. A. Mufazalov, N. Yogev, J. Huppert, F. Wanke, M. Witting, A. Grill, E. J. C. Gálvez, A. Nikolaev, M. Blanfeld, I. Prinz, P. Schmitt-Kopplin, T. Strowig, C. Reinhardt, M. Prinz, T. Bopp, B. Becher, C. Ubeda and A. Waisman (2021). "IL-17 controls central nervous system autoimmunity through the intestinal microbiome." Science Immunology **6**(56): eaaz6563.

Ren, W., J. Yin, H. Xiao, S. Chen, G. Liu, B. Tan, N. Li, Y. Peng, T. Li, B. Zeng, W. Li, H. Wei, Z. Yin, G. Wu, P. R. Hardwidge and Y. Yin (2016). "Intestinal Microbiota-Derived GABA Mediates Interleukin-17 Expression during Enterotoxigenic Escherichia coli Infection." Front Immunol **7**: 685.

Rennels, M. L., T. F. Gregory, O. R. Blaumanis, K. Fujimoto and P. A. Grady (1985). "Evidence for a 'paravascular' fluid circulation in the mammalian central nervous system, provided by the rapid distribution of tracer protein throughout the brain from the subarachnoid space." Brain Res **326**(1): 47-63.

Roberts, K. F., D. L. Elbert, T. P. Kasten, B. W. Patterson, W. C. Sigurdson, R. E. Connors, V. Ovod, L. Y. Munsell, K. G. Mawuenyega, M. M. Miller-Thomas, C. J. Moran, D. T. Cross, 3rd, C. P. Derdeyn and R. J. Bateman (2014). "Amyloid-beta efflux from the central nervous system into the plasma." Ann Neurol **76**(6): 837-844.

Rouvier, E., M. F. Luciani, M. G. Mattei, F. Denizot and P. Golstein (1993). "CTLA-8, cloned from an activated T cell, bearing AU-rich messenger RNA instability sequences, and homologous to a herpesvirus saimiri gene." J Immunol **150**(12): 5445-5456.

Ruan, W., M. A. Engevik, J. K. Spinler and J. Versalovic (2020). "Healthy Human Gastrointestinal Microbiome: Composition and Function After a Decade of Exploration." Dig Dis Sci **65**(3): 695-705.

Saito, T., Y. Matsuba, N. Mihira, J. Takano, P. Nilsson, S. Itohara, N. Iwata and T. C. Saido (2014). "Single App knock-in mouse models of Alzheimer's disease." Nat Neurosci **17**(5): 661-663.

Salter, M. W. and B. Stevens (2017). "Microglia emerge as central players in brain disease." Nat Med **23**(9): 1018-1027.

Sato, K., H. Yamamoto, T. Nomura, J. Kasamatsu, T. Miyasaka, D. Tanno, I. Matsumoto, T. Kagesawa, A. Miyahara, T. Zong, A. Oniyama, K. Kawamura, R. Yokoyama, Y. Kitai, S. Ishizuka, E. Kanno, H. Tanno, H. Suda, M. Morita, M. Yamamoto, Y. Iwakura, K. Ishii and K. Kawakami (2020). "Production of IL-17A at Innate Immune Phase Leads to Decreased Th1 Immune Response and Attenuated Host Defense against Infection with Cryptococcus deneoformans." J Immunol **205**(3): 686-698.

Scheltens, P., B. De Strooper, M. Kivipelto, H. Holstege, G. Chetelat, C. E. Teunissen, J. Cummings and W. M. van der Flier (2021). "Alzheimer's disease." Lancet **397**(10284): 1577-1590.

Scholtzova, H., P. Chianchiano, J. Pan, Y. Sun, F. Goni, P. D. Mehta and T. Wisniewski (2014). "Amyloid beta and Tau Alzheimer's disease related pathology is reduced by Toll-like receptor 9 stimulation." Acta Neuropathol Commun **2**: 101.

Scholtzova, H., R. J. Kascsak, K. A. Bates, A. Boutajangout, D. J. Kerr, H. C. Meeker, P. D. Mehta, D. S. Spinner and T. Wisniewski (2009). "Induction of toll-like receptor 9 signaling as a method for ameliorating Alzheimer's disease-related pathology." J Neurosci **29**(6): 1846-1854.

Serot, J. M., M. C. Bene, B. Foliguet and G. C. Faure (2000). "Morphological alterations of the choroid plexus in late-onset Alzheimer's disease." Acta Neuropathol **99**(2): 105-108.

Shakir, L., A. Javeed, M. Ashraf and A. Riaz (2011). "Metronidazole and the immune system." Pharmazie **66**(6): 393-398.

Shi, Q., R. A. Gutierrez and M. A. Bhat (2024). "Microglia, Trem2, and Neurodegeneration." Neuroscientist: 10738584241254118.

Shinohara, M., M. Tachibana, T. Kanekiyo and G. Bu (2017). "Role of LRP1 in the pathogenesis of Alzheimer's disease: evidence from clinical and preclinical studies." J Lipid Res **58**(7): 1267-1281.

Shirotani, K., S. Tsubuki, N. Iwata, Y. Takaki, W. Harigaya, K. Maruyama, S. Kiryu-Seo, H. Kiyama, H. Iwata, T. Tomita, T. Iwatsubo and T. C. Saido (2001). "Neprilysin degrades both amyloid beta peptides 1-40 and 1-42 most rapidly and efficiently among thiorphan- and phosphoramidon-sensitive endopeptidases." J Biol Chem **276**(24): 21895-21901.

Silva, M. V. F., C. M. G. Loures, L. C. V. Alves, L. C. de Souza, K. B. G. Borges and M. D. G. Carvalho (2019). "Alzheimer's disease: risk factors and potentially protective measures." J Biomed Sci **26**(1): 33.

Silverberg, G. D., M. Mayo, T. Saul, E. Rubenstein and D. McGuire (2003). "Alzheimer's disease, normal-pressure hydrocephalus, and senescent changes in CSF circulatory physiology: a hypothesis." Lancet Neurol **2**(8): 506-511.

Singh, N., A. Gurav, S. Sivaprakasam, E. Brady, R. Padia, H. Shi, M. Thangaraju, P. D. Prasad, S. Manicassamy, D. H. Munn, J. R. Lee, S. Offermanns and V. Ganapathy (2014). "Activation of Gpr109a, receptor for niacin and the commensal metabolite butyrate, suppresses colonic inflammation and carcinogenesis." Immunity **40**(1): 128-139.

Spangenberg, E., P. L. Severson, L. A. Hohsfield, J. Crapser, J. Zhang, E. A. Burton, Y. Zhang, W. Spevak, J. Lin, N. Y. Phan, G. Habets, A. Rymar, G. Tsang, J. Walters, M. Nespi, P. Singh, S. Broome, P. Ibrahim, C. Zhang, G. Bollag, B. L. West and K. N. Green (2019). "Sustained microglial depletion with CSF1R inhibitor impairs parenchymal plaque development in an Alzheimer's disease model." Nat Commun **10**(1): 3758.

Spires-Jones, T. L. and B. T. Hyman (2014). "The intersection of amyloid beta and tau at synapses in Alzheimer's disease." Neuron **82**(4): 756-771.

Spires, T. L., M. Meyer-Luehmann, E. A. Stern, P. J. McLean, J. Skoch, P. T. Nguyen, B. J. Bacskai and B. T. Hyman (2005). "Dendritic spine abnormalities in amyloid precursor protein transgenic mice demonstrated by gene transfer and intravital multiphoton microscopy." J Neurosci **25**(31): 7278-7287.

Stamatovic, S. M., A. M. Johnson, R. F. Keep and A. V. Andjelkovic (2016). "Junctional proteins of the blood-brain barrier: New insights into function and dysfunction." Tissue Barriers **4**(1): e1154641.

Storck, S. E., A. M. S. Hartz, J. Bernard, A. Wolf, A. Kachlmeier, A. Mahringer, S. Weggen, J. Pahnke and C. U. Pietrzik (2018). "The concerted amyloid-beta clearance of LRP1 and ABCB1/P-gp across the blood-brain barrier is linked by PICALM." Brain Behav Immun **73**: 21-33.

Storck, S. E., S. Meister, J. Nahrath, J. N. Meissner, N. Schubert, A. Di Spiezio, S. Baches, R. E. Vandenbroucke, Y. Bouter, I. Prikulis, C. Korth, S. Weggen, A. Heimann, M. Schwaninger, T. A. Bayer and C. U. Pietrzik (2016). "Endothelial LRP1 transports amyloid-beta(1-42) across the blood-brain barrier." J Clin Invest **126**(1): 123-136.

Sun, Y., H. Zhang, X. Zhang, W. Wang, Y. Chen, Z. Cai, Q. Wang, J. Wang and Y. Shi (2023). "Promotion of astrocyte-neuron glutamate-glutamine shuttle by SCFA contributes to the alleviation of Alzheimer's disease." Redox Biol **62**: 102690.

Thapa, M., A. Kumari, C.-Y. Chin, J. E. Choby, F. Jin, B. Bogati, D. M. Chopyk, N. Koduri, A. Pahnke, E. J. Elrod, E. M. Burd, D. S. Weiss and A. Grakoui (2023). "Translocation of gut commensal bacteria to the brain." bioRxiv: 2023.2008.2030.555630.

Thinakaran, G. and E. H. Koo (2008). "Amyloid precursor protein trafficking, processing, and function." J Biol Chem **283**(44): 29615-29619.

Tseng, B. P., K. N. Green, J. L. Chan, M. Blurton-Jones and F. M. LaFerla (2008). "Abeta inhibits the proteasome and enhances amyloid and tau accumulation." Neurobiol Aging **29**(11): 1607-1618.

Vital, M., A. Karch and D. H. Pieper (2017). "Colonic Butyrate-Producing Communities in Humans: an Overview Using Omics Data." mSystems **2**(6).

Vogt, N. M., R. L. Kerby, K. A. Dill-McFarland, S. J. Harding, A. P. Merluzzi, S. C. Johnson, C. M. Carlsson, S. Asthana, H. Zetterberg, K. Blennow, B. B. Bendlin and F. E. Rey (2017). "Gut microbiome alterations in Alzheimer's disease." Sci Rep **7**(1): 13537.

Walter, S., M. Letiembre, Y. Liu, H. Heine, B. Penke, W. Hao, B. Bode, N. Manietta, J. Walter, W. Schulz-Schuffer and K. Fassbender (2007). "Role of the toll-like receptor 4 in neuroinflammation in Alzheimer's disease." Cell Physiol Biochem **20**(6): 947-956.

Wang, L., S. Chen and K. Xu (2011). "IL-17 expression is correlated with hepatitis B-related liver diseases and fibrosis." Int J Mol Med **27**(3): 385-392.

Wang, S. and M. Colonna (2019). "Microglia in Alzheimer's disease: A target for immunotherapy." J Leukoc Biol **106**(1): 219-227.

Wang, S., R. Wang, L. Chen, D. A. Bennett, D. W. Dickson and D. S. Wang (2010). "Expression and functional profiling of neprilysin, insulin-degrading enzyme, and endothelin-converting enzyme in prospectively studied elderly and Alzheimer's brain." J Neurochem **115**(1): 47-57.

Wang, X., W. Yuan, C. Yang, Z. Wang, J. Zhang, D. Xu, X. Sun and W. Sun (2024). "Emerging role of gut microbiota in autoimmune diseases." Front Immunol **15**: 1365554.

Wang, Y., Y. An, W. Ma, H. Yu, Y. Lu, X. Zhang, Y. Wang, W. Liu, T. Wang and R. Xiao (2020). "27-Hydroxycholesterol contributes to cognitive deficits in APP/PS1 transgenic mice through microbiota dysbiosis and intestinal barrier dysfunction." J Neuroinflammation **17**(1): 199.

Wasen, C., L. C. Beauchamp, J. Vincentini, S. Li, D. S. LeServe, C. Gauthier, J. R. Lopes, T. G. Moreira, M. N. Ekwudo, Z. Yin, P. da Silva, R. K. Krishnan, O. Butovsky, L. M. Cox and H. L. Weiner (2024). "Bacteroidota inhibit microglia clearance of amyloid-beta and promote plaque deposition in Alzheimer's disease mouse models." Nat Commun **15**(1): 3872.

Weller, R. O., E. Djuanda, H. Y. Yow and R. O. Carare (2009). "Lymphatic drainage of the brain and the pathophysiology of neurological disease." Acta Neuropathol **117**(1): 1-14.

Wijesuriya, H. C., J. Y. Bullock, R. L. Faull, S. B. Hladky and M. A. Barrand (2010). "ABC efflux transporters in brain vasculature of Alzheimer's subjects." Brain Res **1358**: 228-238.

Wu, J., L. Tang, Y. Ma, Y. Li, D. Zhang, Q. Li, H. Mei and Y. Hu (2021). "Immunological Profiling of COVID-19 Patients with Pulmonary Sequelae." mBio **12**(5): e0159921.

Xie, J., A. Bruggeman, C. De Nolf, C. Vandendriessche, G. Van Imschoot, E. Van Wonterghem, L. Vereecke and R. E. Vandenbroucke (2023). "Gut microbiota regulates blood-cerebrospinal fluid barrier function and Abeta pathology." EMBO J **42**(17): e111515.

Xie, K., Y. Liu, W. Hao, S. Walter, B. Penke, T. Hartmann, M. Schachner and K. Fassbender (2013). "Tenascin-C deficiency ameliorates Alzheimer's disease-related pathology in mice." Neurobiol Aging **34**(10): 2389-2398.

Xu, Y. J., N. P. B. Au and C. H. E. Ma (2022). "Functional and Phenotypic Diversity of Microglia: Implication for Microglia-Based Therapies for Alzheimer's Disease." Front Aging Neurosci **14**: 896852.

Yang, X., Q. Zeng, E. Goktas, K. Gopal, L. Al-Aswad, D. M. Blumberg, G. A. Cioffi, J. M. Liebmann and G. Tezel (2019). "T-Lymphocyte Subset Distribution and Activity in Patients With Glaucoma." Invest Ophthalmol Vis Sci **60**(4): 877-888.

Yasojima, K., H. Akiyama, E. G. McGeer and P. L. McGeer (2001). "Reduced neprilysin in high plaque areas of Alzheimer brain: a possible relationship to deficient degradation of beta-amyloid peptide." Neurosci Lett **297**(2): 97-100.

Zeng, X., J. Li, W. Shan, Z. Lai and Z. Zuo (2023). "Gut microbiota of old mice worsens neurological outcome after brain ischemia via increased valeric acid and IL-17 in the blood." Microbiome **11**(1): 204.

Zhang, B., C. Gaiteri, L. G. Bodea, Z. Wang, J. McElwee, A. A. Podtelezhnikov, C. Zhang, T. Xie, L. Tran, R. Dobrin, E. Fluder, B. Clurman, S. Melquist, M. Narayanan, C. Suver, H. Shah, M. Mahajan, T. Gillis, J. Mysore, M. E. MacDonald, J. R. Lamb, D. A. Bennett, C. Molony, D. J. Stone, V. Gudnason, A. J. Myers, E. E. Schadt, H. Neumann, J. Zhu and V. Emilsson (2013). "Integrated systems approach identifies genetic nodes and networks in late-onset Alzheimer's disease." Cell **153**(3): 707-720.

Zhang, H., X. Li, X. Wang, J. Xu, F. Elefant and J. Wang (2023). "Cellular response to beta-amyloid neurotoxicity in Alzheimer's disease and implications in new therapeutics." Animal Model Exp Med **6**(1): 3-9.

Zhang, J., K. F. Ke, Z. Liu, Y. H. Qiu and Y. P. Peng (2013). "Th17 cell-mediated neuroinflammation is involved in neurodegeneration of abeta1-42-induced Alzheimer's disease model rats." PLoS One **8**(10): e75786.

Zhang, T., G. Gao, L. Y. Kwok and Z. Sun (2023). "Gut microbiome-targeted therapies for Alzheimer's disease." Gut Microbes **15**(2): 2271613.

Zhang, Y., X. Chen, Y. Zhao, M. Ponnusamy and Y. Liu (2017). "The role of ubiquitin proteasomal system and autophagy-lysosome pathway in Alzheimer's disease." Rev Neurosci **28**(8): 861-868.

Zhang, Y., Y. Shen, N. Liufu, L. Liu, W. Li, Z. Shi, H. Zheng, X. Mei, C. Y. Chen, Z. Jiang, S. Abtahi, Y. Dong, F. Liang, Y. Shi, L. L. Cheng, G. Yang, J. X. Kang, J. E. Wilkinson and Z. Xie (2023). "Transmission of Alzheimer's disease-associated microbiota dysbiosis and its impact on cognitive function: evidence from mice and patients." Mol Psychiatry **doi: 10.1038/s41380-023-02216-7.**

Zhou, Y., L. Xie, J. Schroder, I. S. Schuster, M. Nakai, G. Sun, Y. B. Y. Sun, E. Marino, M. A. Degli-Esposti, F. Z. Marques, A. Grubman, J. M. Polo and C. R. Mackay (2023). "Dietary Fiber and Microbiota Metabolite Receptors Enhance Cognition and Alleviate Disease in the 5xFAD Mouse Model of Alzheimer's Disease." J Neurosci **43**(37): 6460-6475.

11 LIST OF FIGURES AND COOPERATIONS

Fig. 5.3.2	**Schematic diagram of the preparation of brain sample sections.** Kindly provided by Qinghua Luo
Fig. 6.1	**Antibiotic treatment successfully depletes the bacteria in the gut of APP-transgenic mice.** Realtime-PCR: Wenlin Hao; Data analyse: Yang Liu
Fig. 6.2.1	**Depletion of gut bacteria reduces IL-17a-expressing CD4-positive lymphocytes.** Isolation of CD4-positive splenocyte: Qinghua Luo; Real time-PCR, flow cytometry and data analysis: Wenlin Hao
Fig. 6.2.2	**IL-17a-eGFP expressing cells are detected in the brain of EAE mice but not in AD mice.** Immunohistochemistry: Wenlin Hao
Fig. 6.3	**Depletion of gut bacteria reduces bacterial DNA in the brains of both IL-17a-deficient and wild-type APP-transgenic mice.** Real time-PCR and data analysis: Wenlin Hao
Fig. 6.4.1	**Depletion of gut bacteria reduces inflammatory activation in the brain of IL-17a-wildtype, but not IL-17a-deficient APP-transgenic mice.** Immunohistochemistry, real time-PCR and ELISA: Wenlin Hao; data analysis: Yang Liu
Fig. 6.4.2	**Intraperitoneal injection of an antibiotic cocktail inhibits the transcription of anti-inflammatory but not proinflammatory genes in the brain of APP-transgenic mice.** Real time-PCR and data analysis: Wenlin Hao
Fig. 6.5.1	**Depletion of gut bacteria inhibits inflammatory activation in microglia in the brain of IL-17a-wildtype, but not Il17a-deficient APP-transgenic mice.** Real time-PCR, immunohistochemistry: Wenlin Hao; microglia morphology analysis and data analysis: Yang Liu
Fig. 6.5.2	**Deficiency of IL-17a does not change the transcription of innate immune receptors and inflammatory genes.** Real time-PCR and data analysis: Wenlin Hao
Fig. 6.6	**Depletion of gut bacteria reduces Aβ in the brain of IL-17a-wildtype, but not IL-17a-deficient APP-transgenic mice.** Immunohistochemistry and ELISA: Wenlin Hao; data analysis: Yang Liu
Fig. 6.7	**Depletion of gut bacteria reduces β-secretase activity in the brain of IL-17a-wildtype, but not IL-17a-deficient APP-transgenic mice.** Immunohistochemistry and real time-PCR: Wenlin Hao; β- and γ-secretase assays: Yang Liu
Fig. 6.8	**Depletion of gut bacteria increases ABCB1 and LRP1 expression in the blood-brain-barrier of IL-17a-wildtype, but not IL-17a-deficient APP-transgenic mice.** Westenblot: Inge Tomic; data analysis: Wenlin Hao
Fig. 6.9	**Depletion of gut bacteria increases *Arc* transcription in the brain of IL-17a-wildtype, but not IL-17a-deficient APP-transgenic mice.** Real time PCR and data analysis: Wenlin Hao
Fig. 8	**Deletion of dicer1 in gut epithelial cells changed the composition of gut bacteria in App-knock-in mice.** Realtime-PCR: Wenlin Hao and Ilona Magdalena Szabo; Data analyse: Yang Liu

12 PUBLICATIONS

1. **Hao W,** Luo Q, Tomic I, Quan W, Hartmann T, Menger MD, Fassbender K, Liu Y. (2024) Modulation of Alzheimer's disease brain pathology in mice by gut bacterial depletion: the role of IL-17a. Gut Microbes 2024 Jan-Dec;16(1):2363014.
2. Luo Q, Schnöder L, **Hao W (Co-first author)**, Litzenburger K, Decker Y, Tomic I, Menger MD, Liu Y, Fassbender K (2022) p38α-MAPK-deficient myeloid cells ameliorate symptoms and pathology of APP-transgenic Alzheimer's disease mice. Aging Cell. 2022 Aug;21(8):e13679.
3. **Hao W**, Luo Q, Menger MD, Fassbender K, Liu Y (2021) Treatment With CD52 Antibody Protects Neurons in Experimental Autoimmune Encephalomyelitis Mice During the Recovering Phase. Front Immunol. 2021 Dec 16;12:792465.
4. **Hao W**, Decker Y, Schnöder L, Schottek A, Li D, Menger MD, Fassbender K, Liu Y (2016) Deficiency of IκB Kinase β in Myeloid Cells Reduces Severity of Experimental Autoimmune Encephalomyelitis. Am J Pathol. 2016 May;186(5):1245-57.
5. **Hao W (Co-first author)**, Liu Y, Liu S, Walter S, Grimm MO, Kiliaan AJ, Penke B, Hartmann T, Rübe CE, Menger MD, Fassbender K (2011) Myeloid differentiation factor 88-deficient bone marrow cells improve Alzheimer's disease-related symptoms and pathology. Brain. 2011 Jan;134(Pt 1):278-92.
6. Letiembre M, **Hao W (Co-first author)**, Liu Y, Walter S, Mihaljevic I, Rivest S, Hartmann T, Fassbender K (2007) Innate immune receptor expression in normal brain aging. Neuroscience. 2007 Apr 25;146(1):248-54.
7. Liu Y, **Hao W (Co-first author)**, Letiembre M, Walter S, Kulanga M, Neumann H, Fassbender K (2006) Suppression of microglial inflammatory activity by myelin phagocytosis: role of p47-PHOX-mediated generation of reactive oxygen species. J Neurosci. 2006 Dec 13;26(50):12904-13.
8. Schnöder L, Quan W, Yu Y, Tomic I, Luo Q, **Hao W**, Peng G, Li D, Fassbender K, Liu Y (2023) Deficiency of IKKβ in neurons ameliorates Alzheimer's disease pathology in APP- and tau-transgenic mice. FASEB J. 2023 Feb;37(2):e22778.
9. Quan W, Luo Q, **Hao W**, Tomic I, Furihata T, Schulz-Schäffer W, Menger MD, Fassbender K, Liu Y (2021) Haploinsufficiency of microglial MyD88 ameliorates Alzheimer's pathology and vascular disorders in APP/PS1-transgenic mice. Glia. 2021 Aug;69(8):1987-2005.
10. Qin Y, Zhang Y, Tomic I, **Hao W**, Menger MD, Liu C, Fassbender K, Liu Y (2018) Ginkgo biloba Extract EGb 761 and Its Specific Components Elicit Protective Protein Clearance Through the Autophagy-Lysosomal Pathway in Tau-Transgenic Mice and Cultured Neurons. J Alzheimers Dis. 2018;65(1):243-263.
11. Qin Y, Liu Y, **Hao W**, Decker Y, Tomic I, Menger MD, Liu C, Fassbender K (2016) Stimulation of TLR4 Attenuates Alzheimer's Disease-Related Symptoms and Pathology in Tau-Transgenic Mice. J Immunol. 2016 Oct 15;197(8):3281-3292.
12. Schnöder L, **Hao W**, Qin Y, Liu S, Tomic I, Liu X, Fassbender K, Liu Y (2016) Deficiency of Neuronal p38α MAPK Attenuates Amyloid Pathology in Alzheimer

Disease Mouse and Cell Models through Facilitating Lysosomal Degradation of BACE1. J Biol Chem. 2016 Jan 29;291(5):2067-79.

13. Liu X, **Hao W**, Qin Y, Decker Y, Wang X, Burkart M, Schötz K, Menger MD, Fassbender K, Liu Y (2015) Long-term treatment with Ginkgo biloba extract EGb 761 improves symptoms and pathology in a transgenic mouse model of Alzheimer's disease. Brain Behav Immun. 2015 May;46:121-31.
14. Liu Y, Liu X, **Hao W**, Decker Y, Schomburg R, Fülöp L, Pasparakis M, Menger MD, Fassbender K (2014) IKKβ deficiency in myeloid cells ameliorates Alzheimer's disease-related symptoms and pathology. J Neurosci. 2014 Sep 24;34(39):12982-99.
15. Xie K, Liu Y, **Hao W**, Walter S, Penke B, Hartmann T, Schachner M, Fassbender K (2013) Tenascin-C deficiency ameliorates Alzheimer's disease-related pathology in mice. Neurobiol Aging. 2013 Oct;34(10):2389-98.
16. Liu Y, Zhang M, **Hao W**, Mihaljevic I, Liu X, Xie K, Walter S, Fassbender K (2013) Matrix metalloproteinase-12 contributes to neuroinflammation in the aged brain. Neurobiol Aging. 2013 Apr;34(4):1231-9.
17. Liu S, Liu Y, **Hao W**, Wolf L, Kiliaan AJ, Penke B, Rübe CE, Walter J, Heneka MT, Hartmann T, Menger MD, Fassbender K (2012) TLR2 is a primary receptor for Alzheimer's amyloid β peptide to trigger neuroinflammatory activation. J Immunol. 2012 Feb 1;188(3):1098-107
18. Liu Y, **Hao W**, Dawson A, Liu S, Fassbender K (2009) Expression of amyotrophic lateral sclerosis-linked SOD1 mutant increases the neurotoxic potential of microglia via TLR2. J Biol Chem. 2009 Feb 6;284(6):3691-9.
19. Schwarting S, Litwak S, **Hao W**, Bähr M, Weise J, Neumann H (2008) Hematopoietic stem cells reduce postischemic inflammation and ameliorate ischemic brain injury. Stroke. 2008 Oct;39(10):2867-75.
20. Walter S, Letiembre M, Liu Y, Heine H, Penke B, **Hao W**, Bode B, Manietta N, Walter J, Schulz-Schuffer W, Fassbender K (2007) Role of the toll-like receptor 4 in neuroinflammation in Alzheimer's disease. Cell Physiol Biochem. 2007;20(6):947-56.
21. Letiembre M, Liu Y, Walter S, **Hao W**, Pfander T, Wrede A, Schulz-Schaeffer W, Fassbender K. (2007) Screening of innate immune receptors in neurodegenerative diseases: a similar pattern. Neurobiol Aging. 2009 May;30(5):759-68. Epub 2007 Oct 1.
22. Walter S, Doering A, Letiembre M, Liu Y, **Hao W**, Diem R, Bernreuther C, Glatzel M, Engelhardt B, Fassbender K (2006) The LPS receptor, CD14, in experimental autoimmune encephalomyelitis and multiple sclerosis. Cell Physiol Biochem. 2006;17(3-4):167-72.

13 ACKNOWLEDGEMENTS

This thesis would not have been possible without the guidance and the help of several individuals who in one way or another contributed and extended their valuable assistance in the preparation und completion of this study, it is a pleasure to thank those who made it a possibility.

I am indebted to my three supervisors whose guidance, support and expertise have enabled me to complete the study. I would like to thank PD Dr. Yang Liu, who supervised the entire project. His rigorous scientific approach and attention to detail has enabled me to become a much improved scientist and writer for which I am extremely grateful. I would like to express my deepest gratitude to Professor Hartmann for his guidance and encouragement throughout my candidature and the study. His expertise and knowledge were invaluable during this research. Last, but certainly not least, I would like to thank Professor Fassbender for providing me the opportunity to work both as a scientist and as a clinician. Without his longtime support I can not become who I am today.

The conclusion of the thesis would have been as compelling without the people I have worked with in our Lab. I am deeply thankful to my colleagues, Andrea Schottek and Inge Tomic, for their technical assistance and moral support. Further thanks extend to Dr. Qinghua Luo for her helpful suggestions in writing the thesis.

Without the ongoing support of a few special people in my life, completing a MD/PhD would have seemed unattainable. I must acknowledge my hunsband und my son for their unwavering love and encouragement. The most significant acknowlegment is reserved for my parents, it is the love and support, which they have provided to me, has enabled me to achieve everything that I have. It is with a feeling of immense accomplishment that I dedicate this thesis to my mum and dad.

14 CURRICULUM VITAE

Aus datenschutzrechtlichen Gründen wird der Lebenslauf in der elektronischen Fassung der Dissertation nicht veröffentlicht